Quantum criticality, the cuprate superconductors, and the AdS/CFT correspondence

Talk online: sachdev.physics.harvard.edu

PHYSICS

VE RI TAS

HARVARD

Lars Fritz, Harvard
Victor Galitski, Maryland
Ribhu Kaul, Kentucky
Max Metlitski, Harvard
Eun Gook Moon, Harvard
Markus Mueller, Trieste
Joerg Schmalian, Iowa
Yang Qi, Harvard
Cenke Xu, Harvard

Frederik Denef, Harvard
Sean Hartnoll, Harvard
Christopher Herzog, Princeton
Pavel Kovtun, Victoria
Dam Son, Washington

PHYSICS

HARVARD

The cuprate superconductors

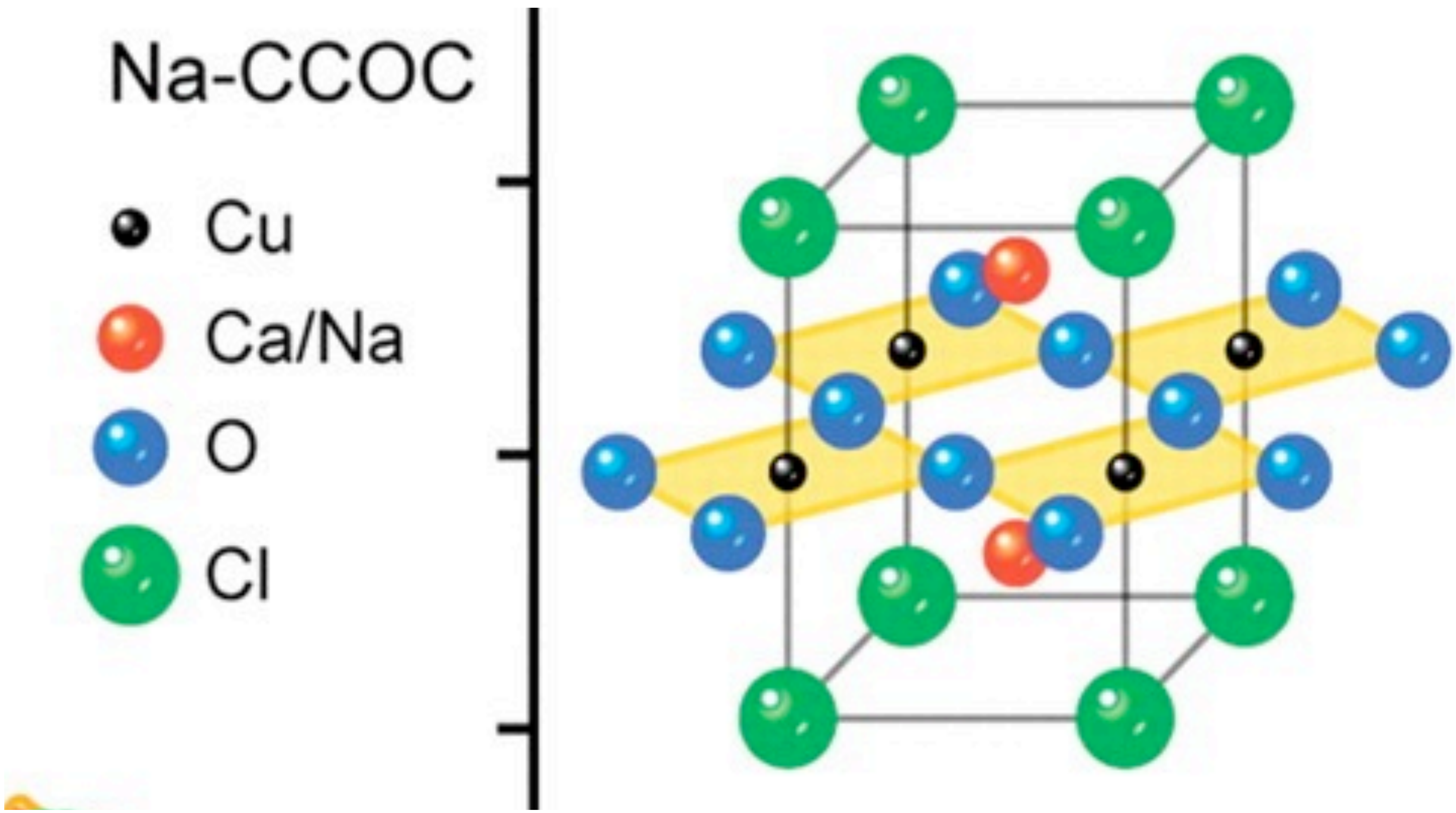

Square lattice antiferromagnet

$$H = \sum_{\langle ij \rangle} J_{ij} \vec{S}_i \cdot \vec{S}_j$$

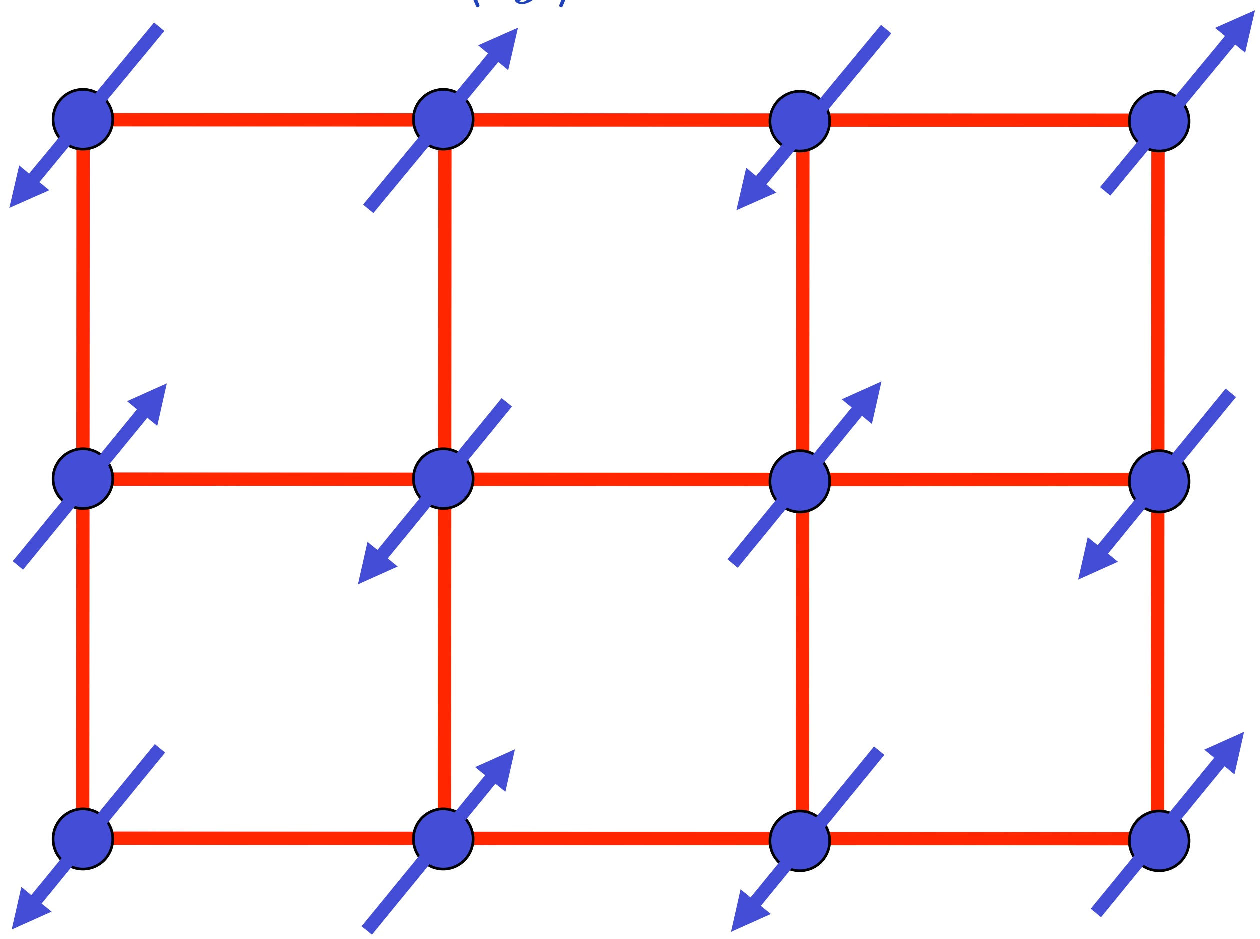

Ground state has long-range Néel order

Order parameter is a single vector field $\vec{\varphi} = \eta_i \vec{S}_i$

$\eta_i = \pm 1$ on two sublattices

$\langle \vec{\varphi} \rangle \neq 0$ in Néel state.

Central ingredients in cuprate phase diagram: antiferromagnetism, superconductivity, and change in Fermi surface

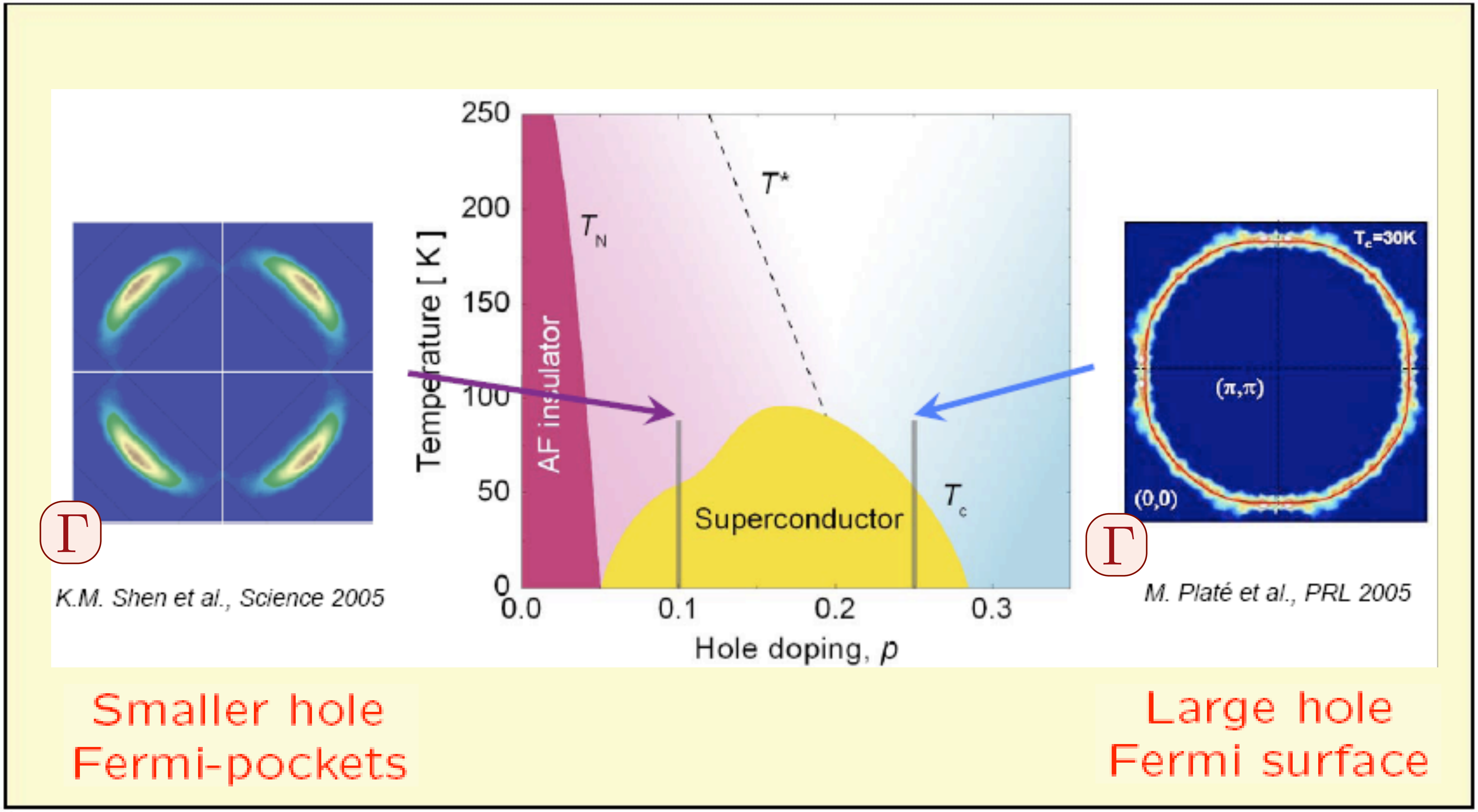

Antiferro-
magnetism

d-wave
supercon-
ductivity

Fermi
surface

Crossovers in transport properties of hole-doped cuprates

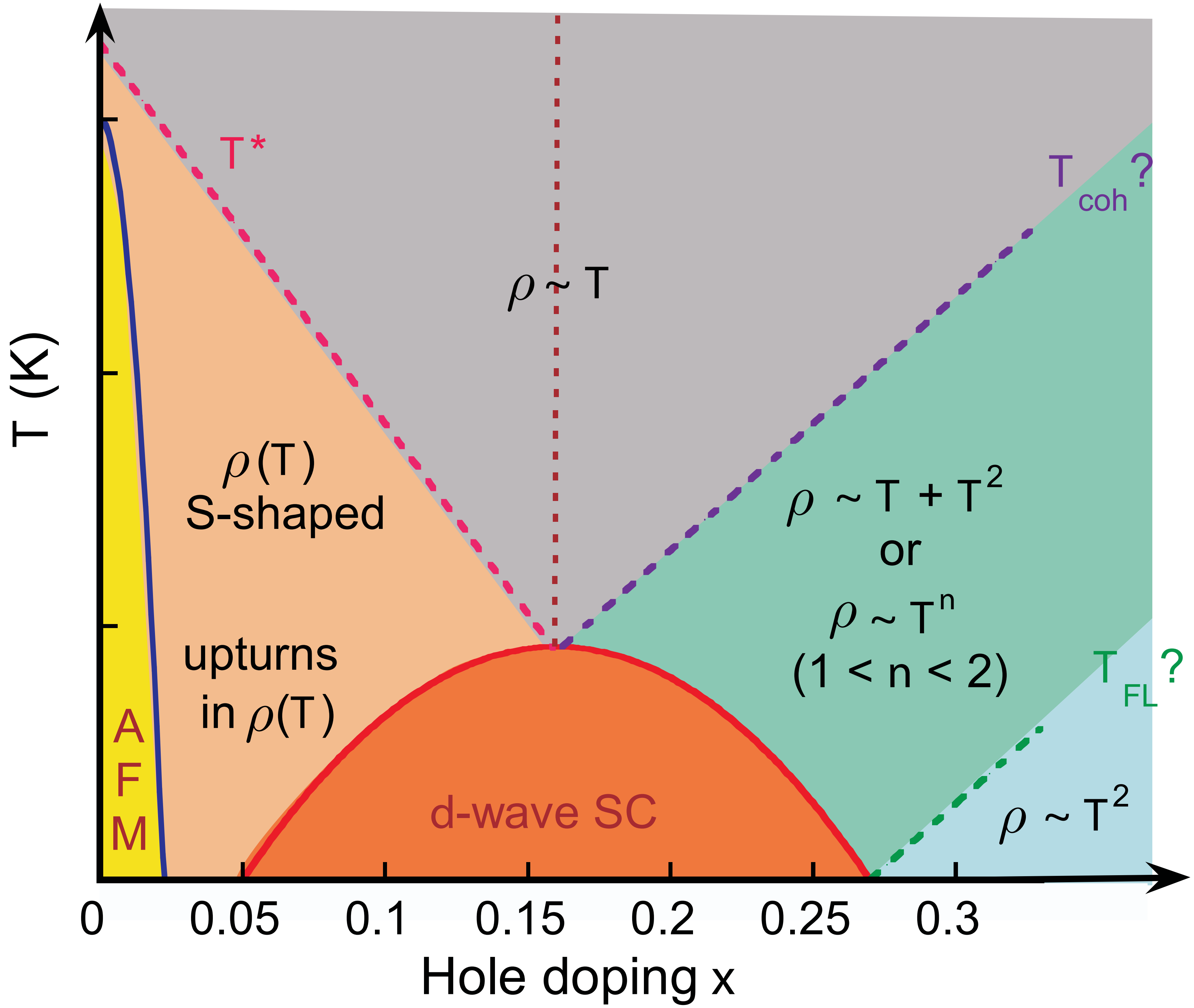

N. E. Hussey, *J. Phys: Condens. Matter* **20**, 123201 (2008)

Crossovers in transport properties of hole-doped cuprates

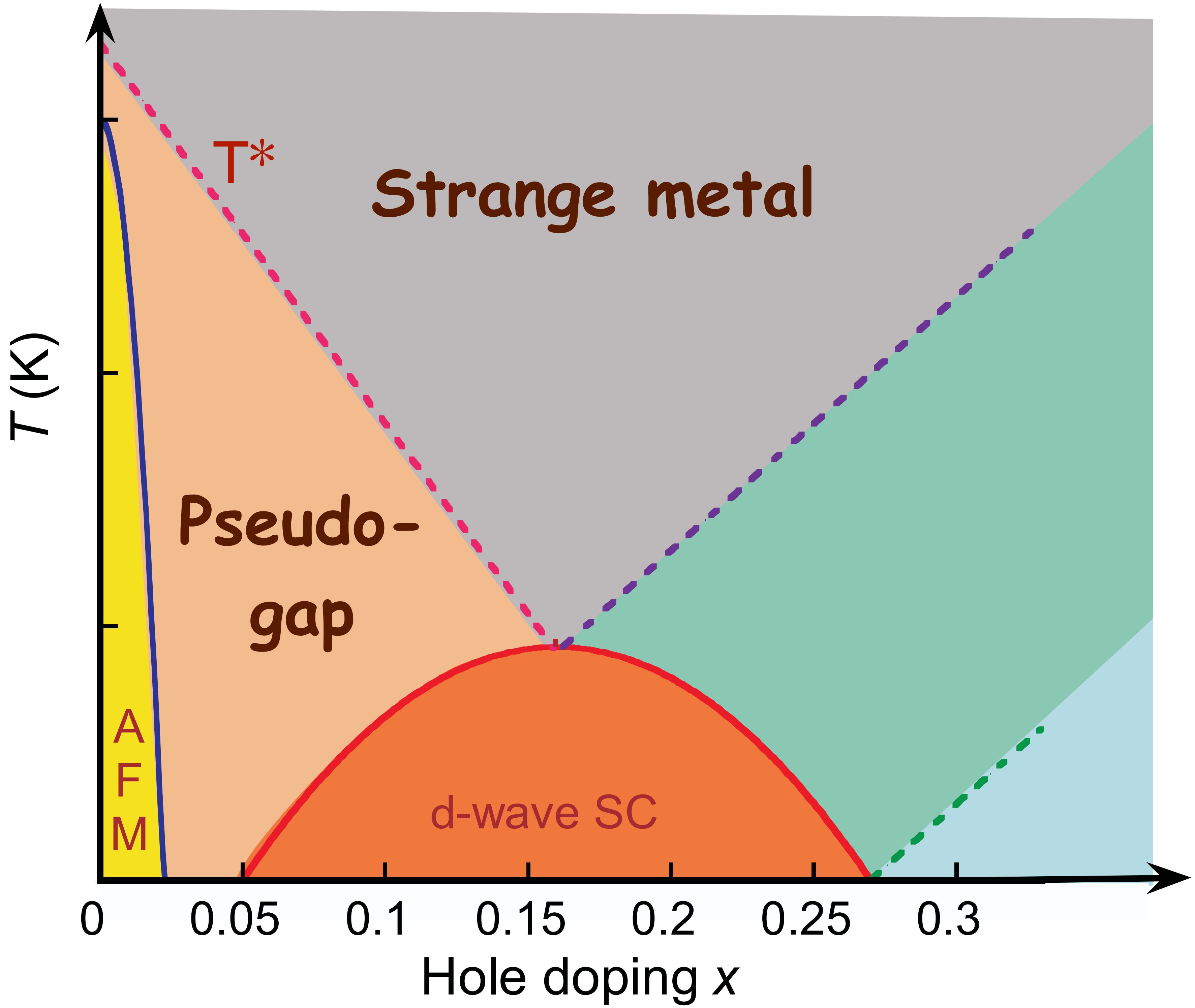

N. E. Hussey, *J. Phys: Condens. Matter* **20**, 123201 (2008)

Outline

1. Coupled dimer antiferromagnets

   Introduction to quantum criticality

2. Phase diagram of the cuprates

   Quantum criticality of the competition between antiferromagnetism and superconductivity

3. Theory of Ising-nematic ordering in a metal

   Strongly-coupled field theory

4. The AdS/CFT correspondence

   Phases of finite density quantum matter at strong coupling

Outline

1. Coupled dimer antiferromagnets

   Introduction to quantum criticality

2. Phase diagram of the cuprates

   Quantum criticality of the competition between antiferromagnetism and superconductivity

3. Theory of Ising-nematic ordering in a metal

   Strongly-coupled field theory

4. The AdS/CFT correspondence

   Phases of finite density quantum matter at strong coupling

Antiferro-
magnetism

d-wave
supercon-
ductivity

Fermi
surface

Antiferro-
magnetism

d-wave
supercon-
ductivity

Fermi
surface

$TlCuCl_3$

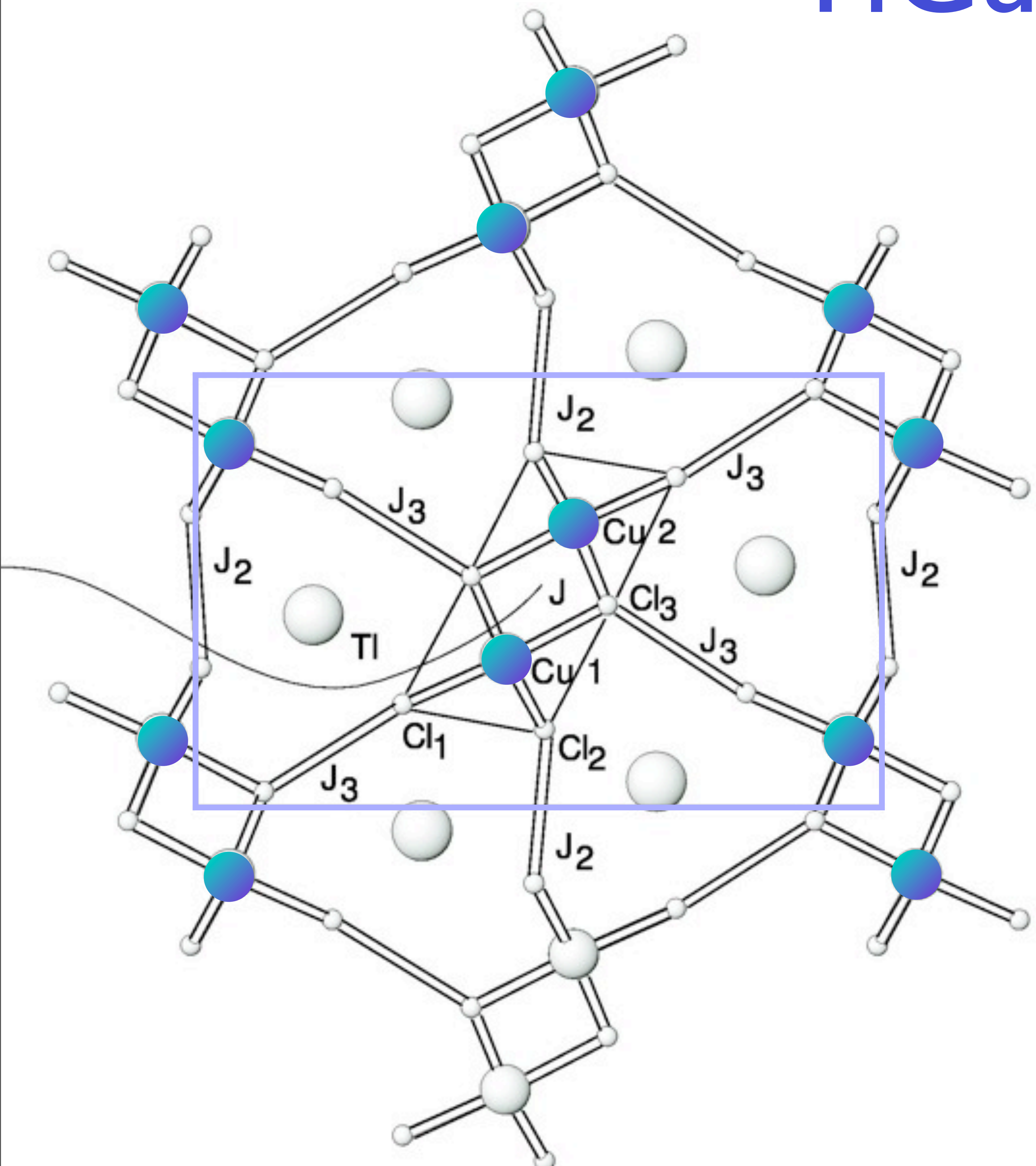
J2
J3
J2
J3
Cu 2
J2
J
Cl3
Tl
J3
Cu 1
Cl1
Cl2
J3
J2

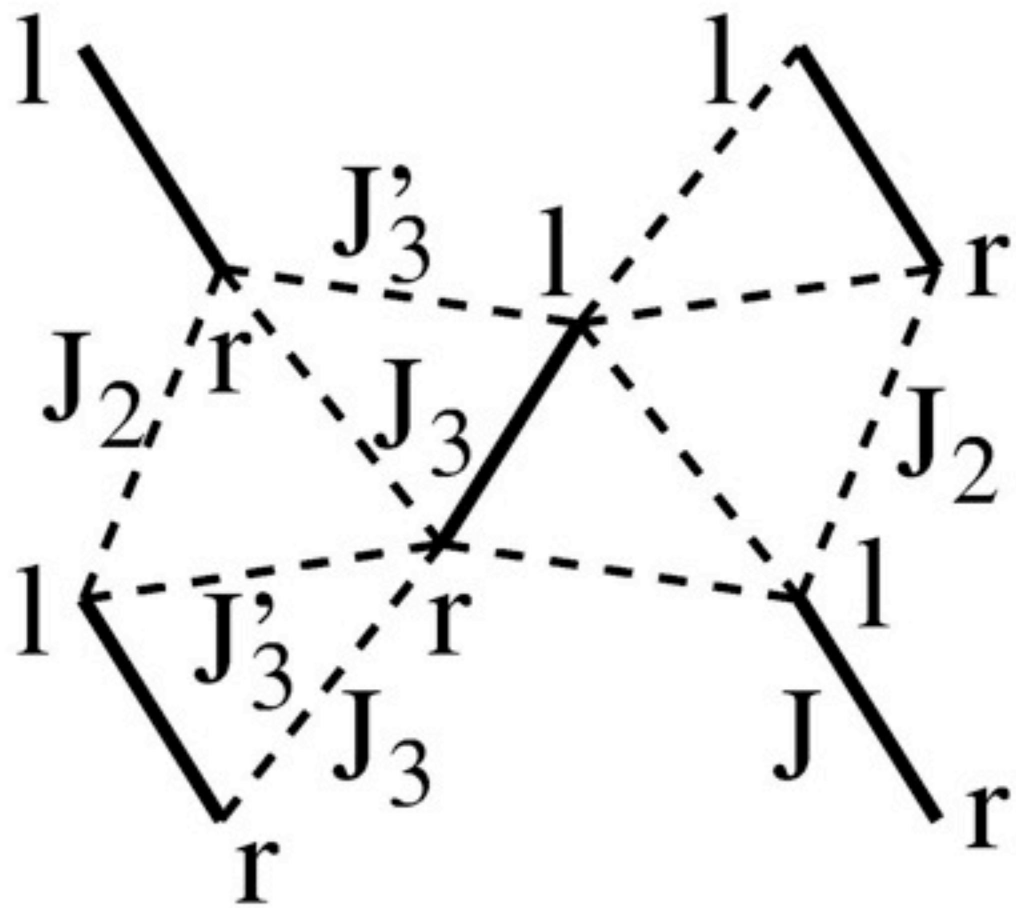
l
l
J'3
l
r
J2
r
J3
J2
l
r
l
J'3
J3
J
r
r

$TlCuCl_3$

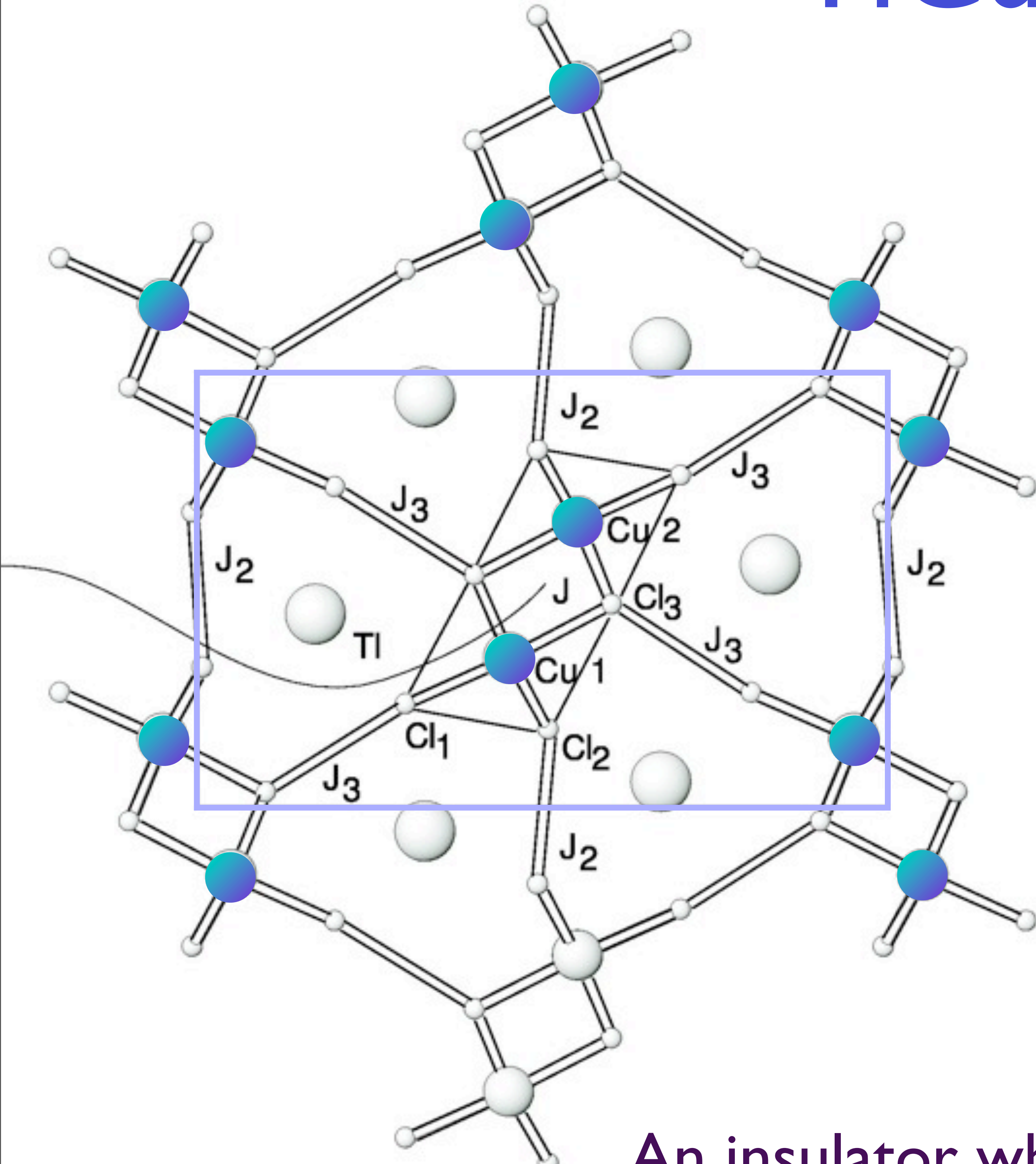

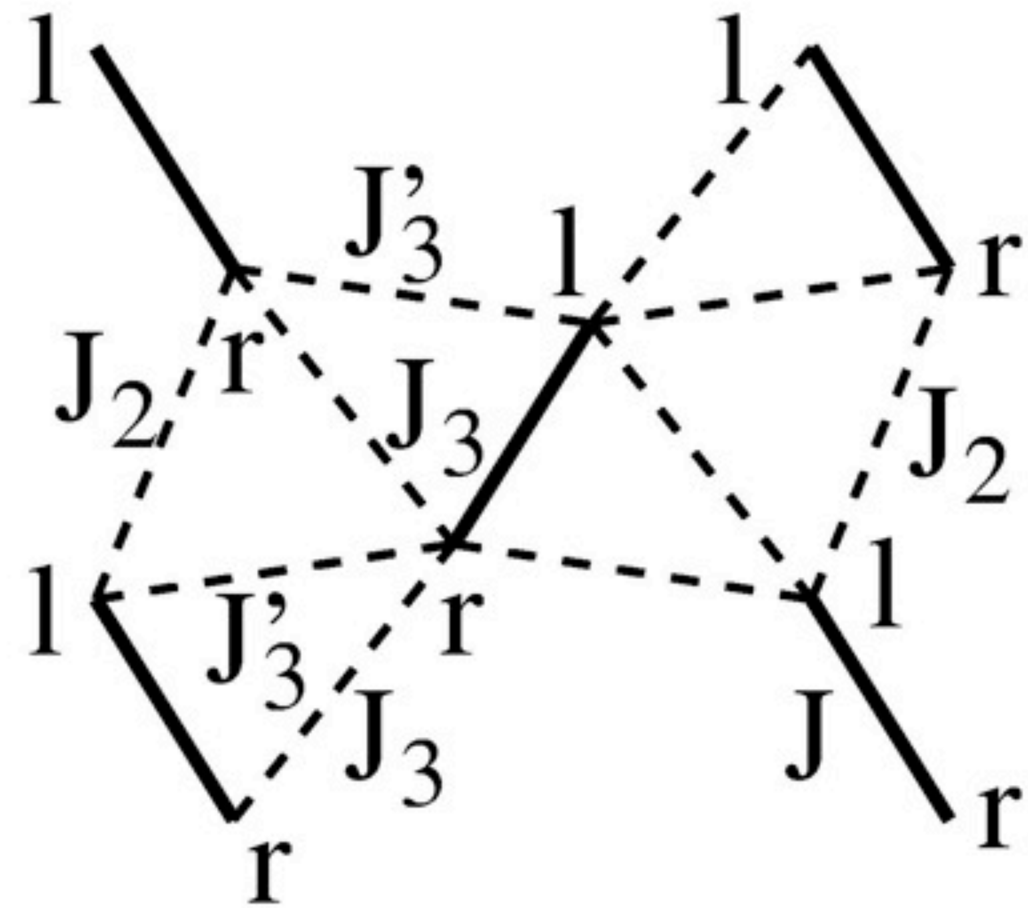

An insulator whose spin susceptibility vanishes exponentially as the temperature T tends to zero.

Square lattice antiferromagnet

$$H = \sum_{\langle ij \rangle} J_{ij} \vec{S}_i \cdot \vec{S}_j$$

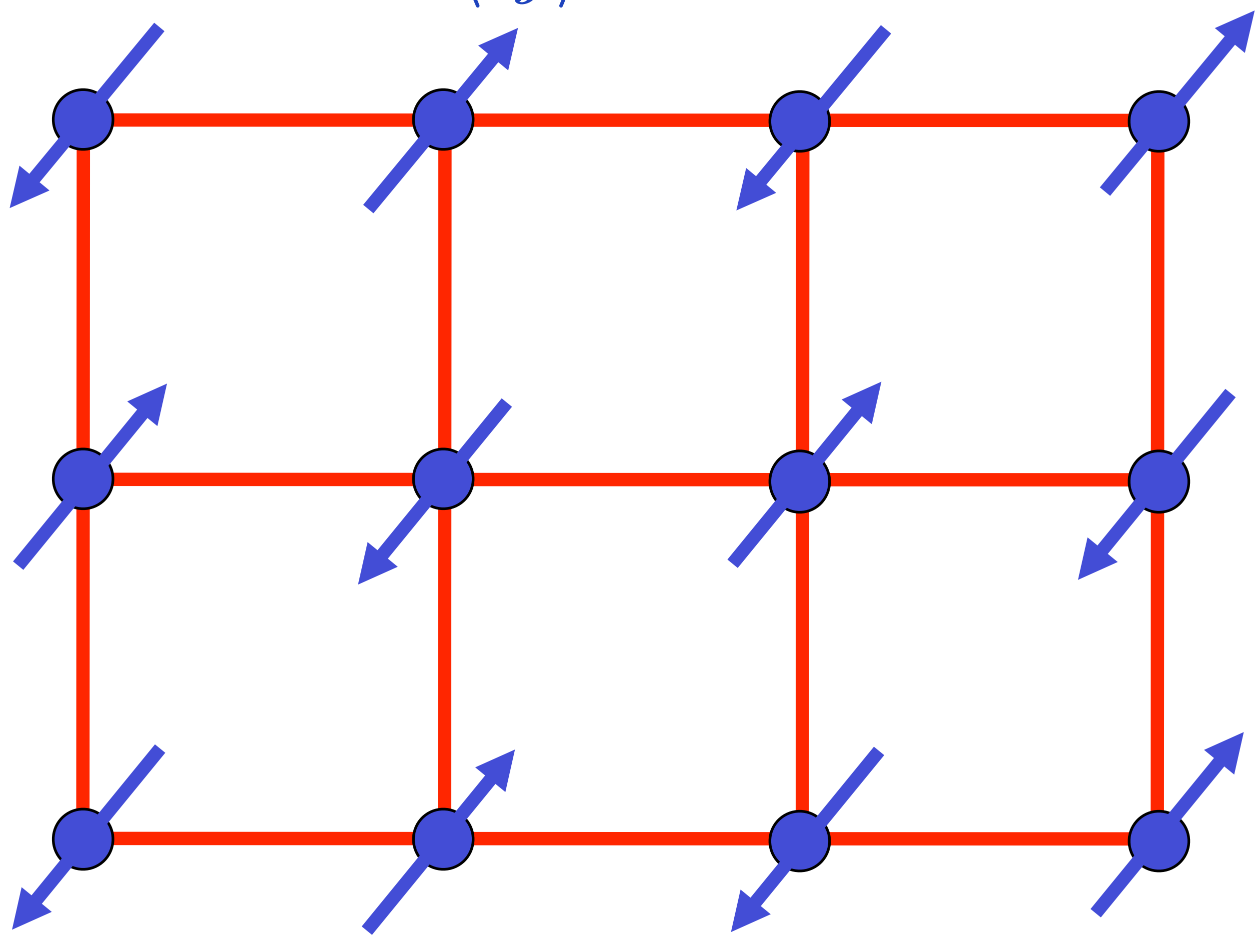

Ground state has long-range Néel order

Order parameter is a single vector field $\vec{\varphi} = \eta_i \vec{S}_i$

$\eta_i = \pm 1$ on two sublattices

$\langle \vec{\varphi} \rangle \neq 0$ in Néel state.

Square lattice antiferromagnet

$$H = \sum_{\langle ij \rangle} J_{ij} \vec{S}_i \cdot \vec{S}_j$$

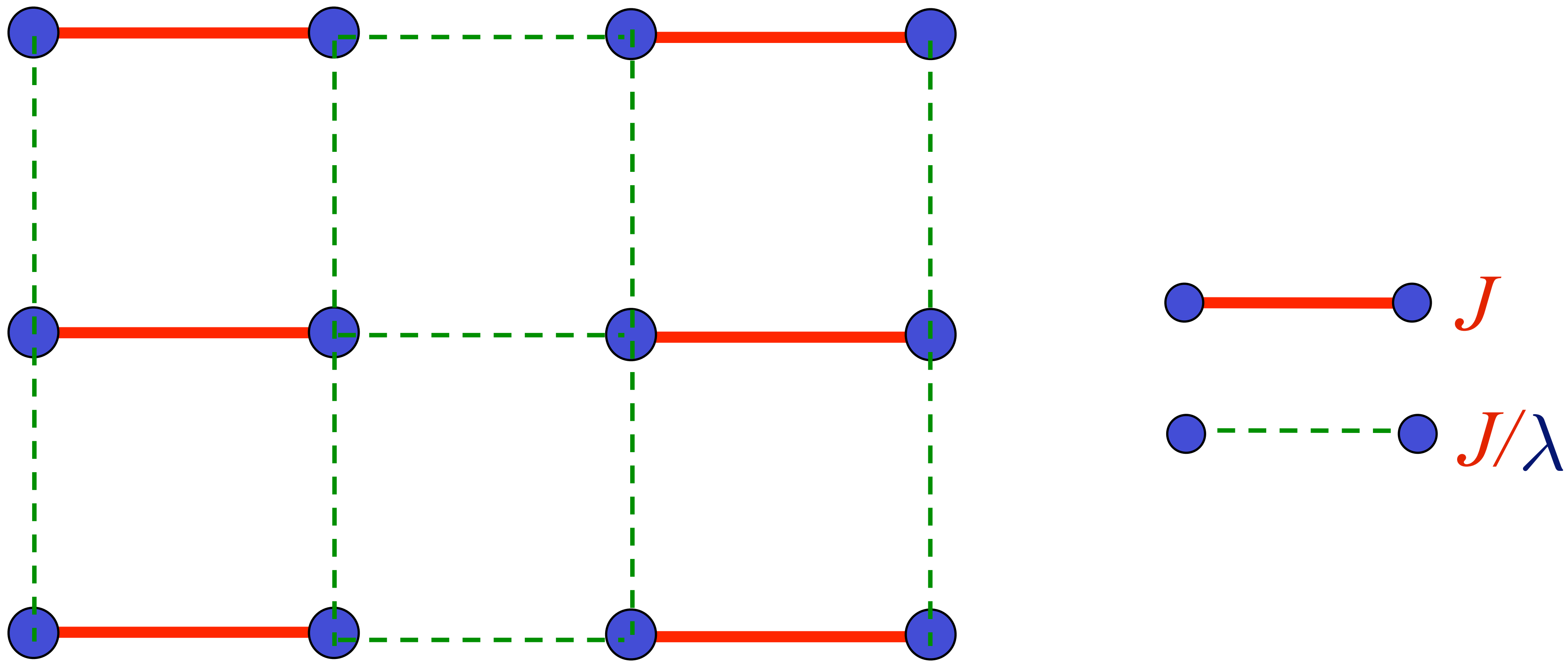

Weaken some bonds to induce spin entanglement in a new quantum phase

Square lattice antiferromagnet

$$H = \sum_{\langle ij \rangle} J_{ij} \vec{S}_i \cdot \vec{S}_j$$

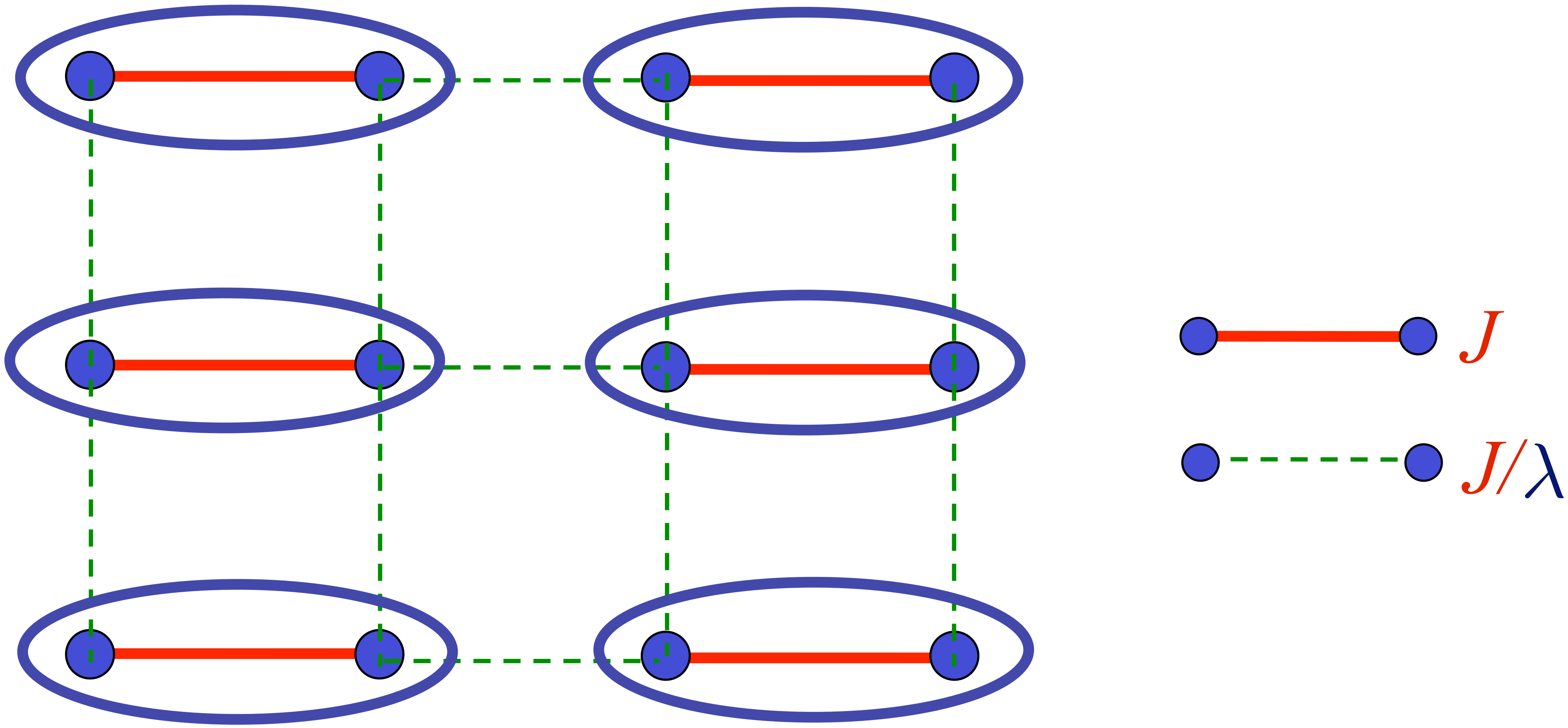

Ground state is a "quantum paramagnet" with spins locked in valence bond singlets

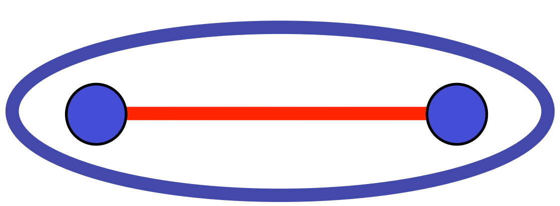

$$= \frac{1}{\sqrt{2}} \Big(\left| \uparrow\downarrow \right\rangle - \left| \downarrow\uparrow \right\rangle \Big)$$

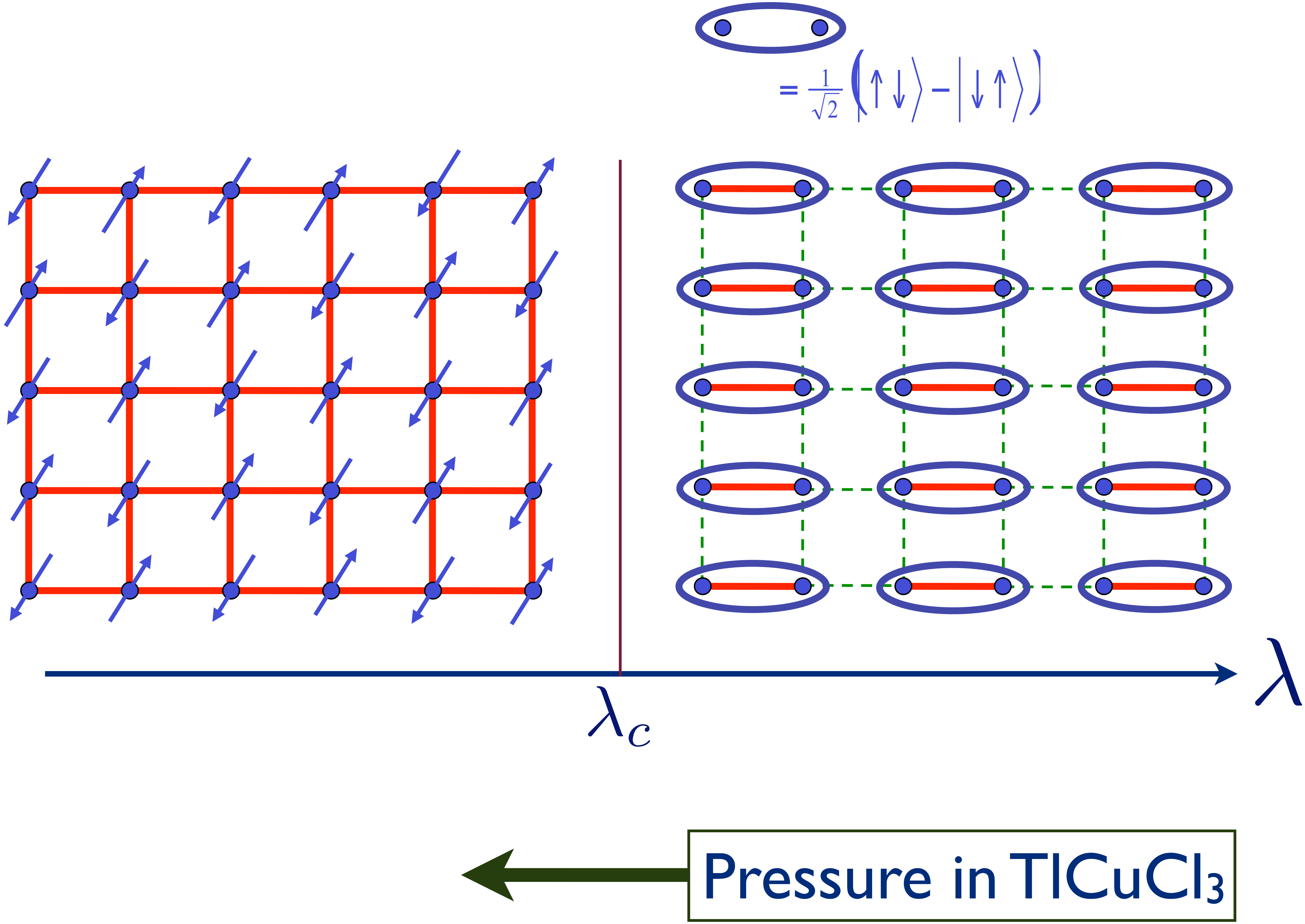

$= \frac{1}{\sqrt{2}} \left(|\uparrow\downarrow\rangle - |\downarrow\uparrow\rangle \right)$
λ
λ_c
Pressure in $TlCuCl_3$

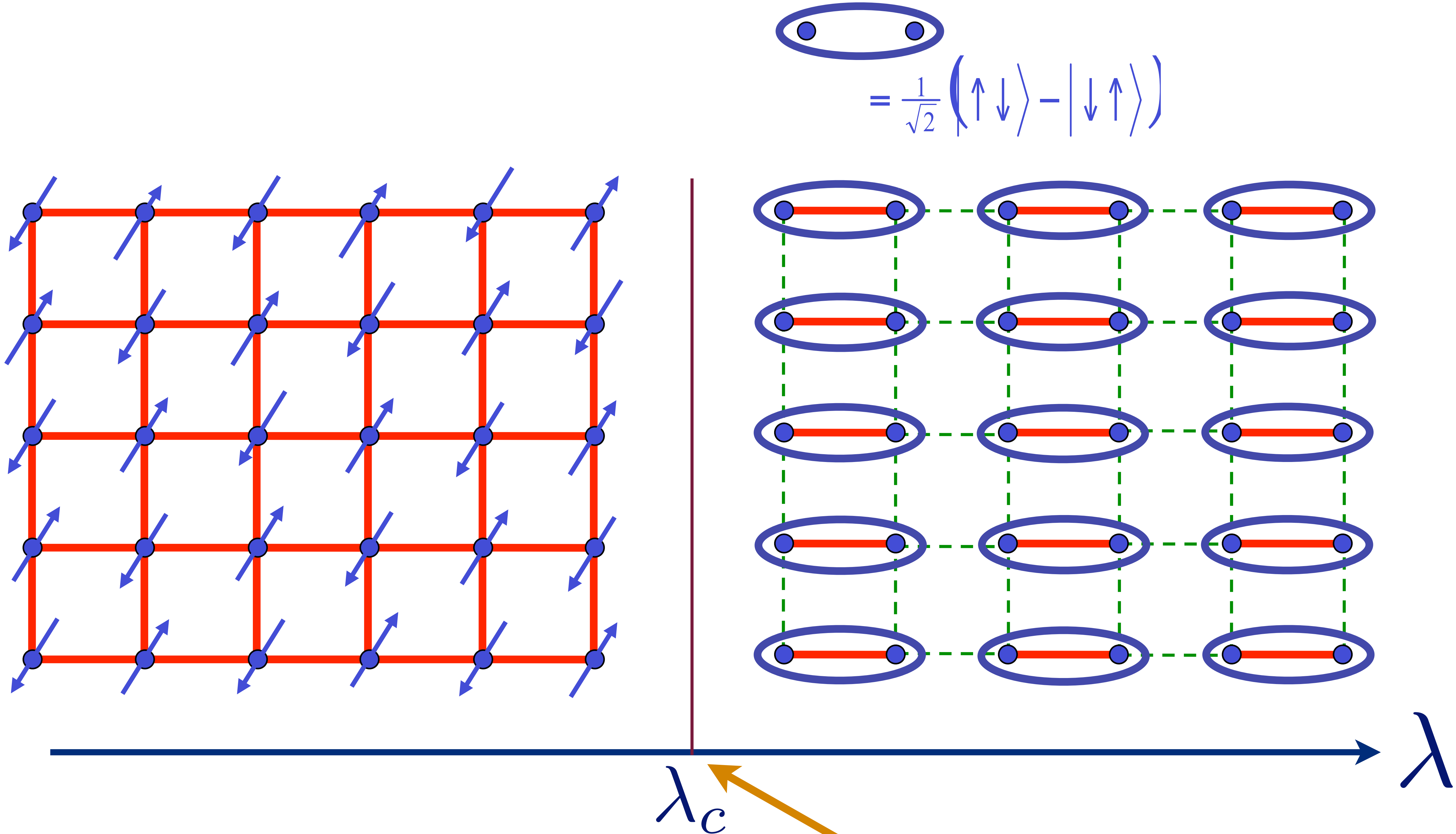

Quantum critical point with non-local entanglement in spin wavefunction

Description using Landau-Ginzburg field theory

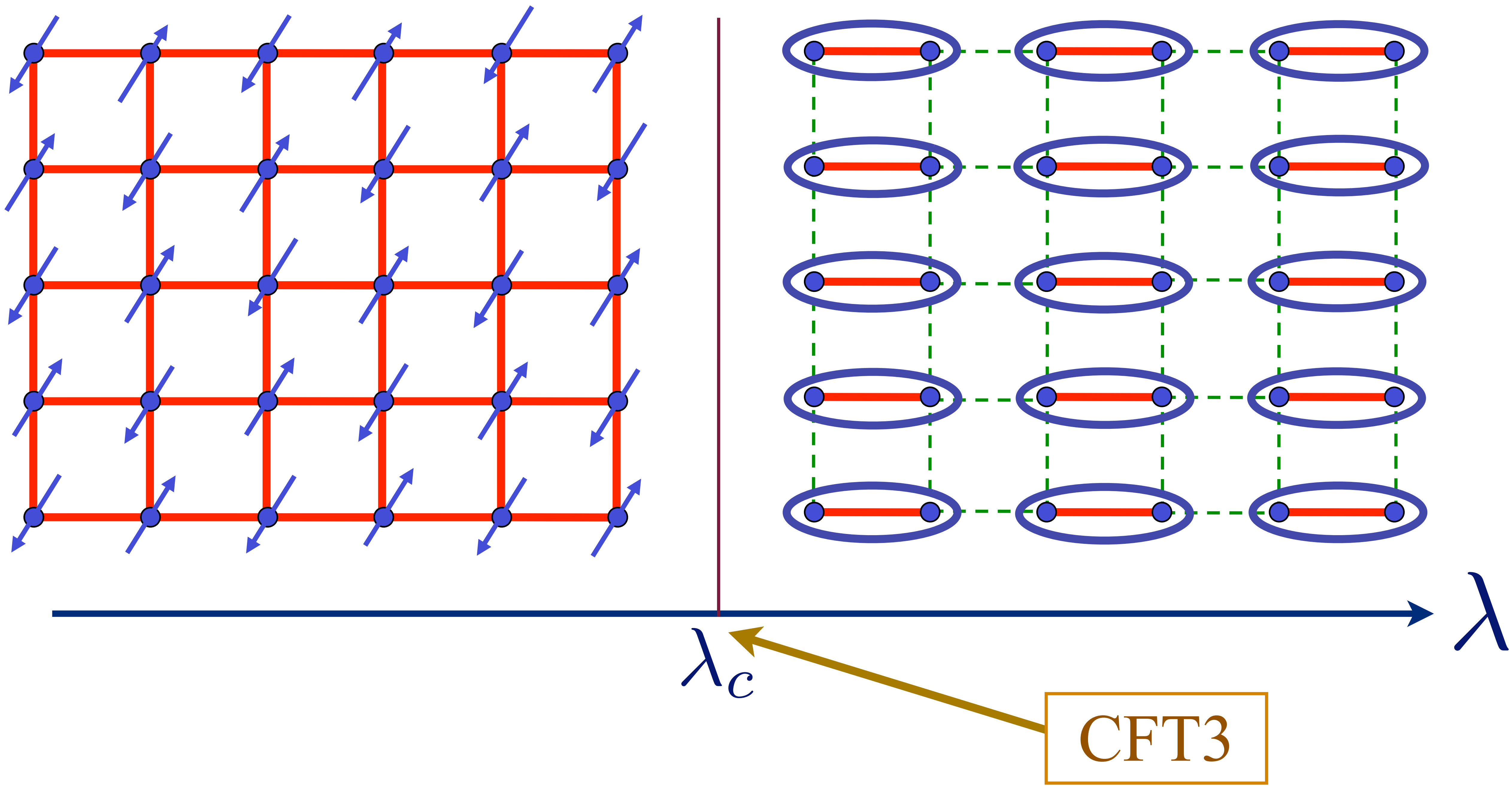

O(3) order parameter $\vec{\varphi}$

$$\mathcal{S} = \int d^2r d\tau \left[(\partial_\tau \varphi)^2 + c^2 (\nabla_r \vec{\varphi})^2 + (\lambda - \lambda_c)\vec{\varphi}^2 + u\left(\vec{\varphi}^2\right)^2 \right]$$

Excitation spectrum in the paramagnetic phase

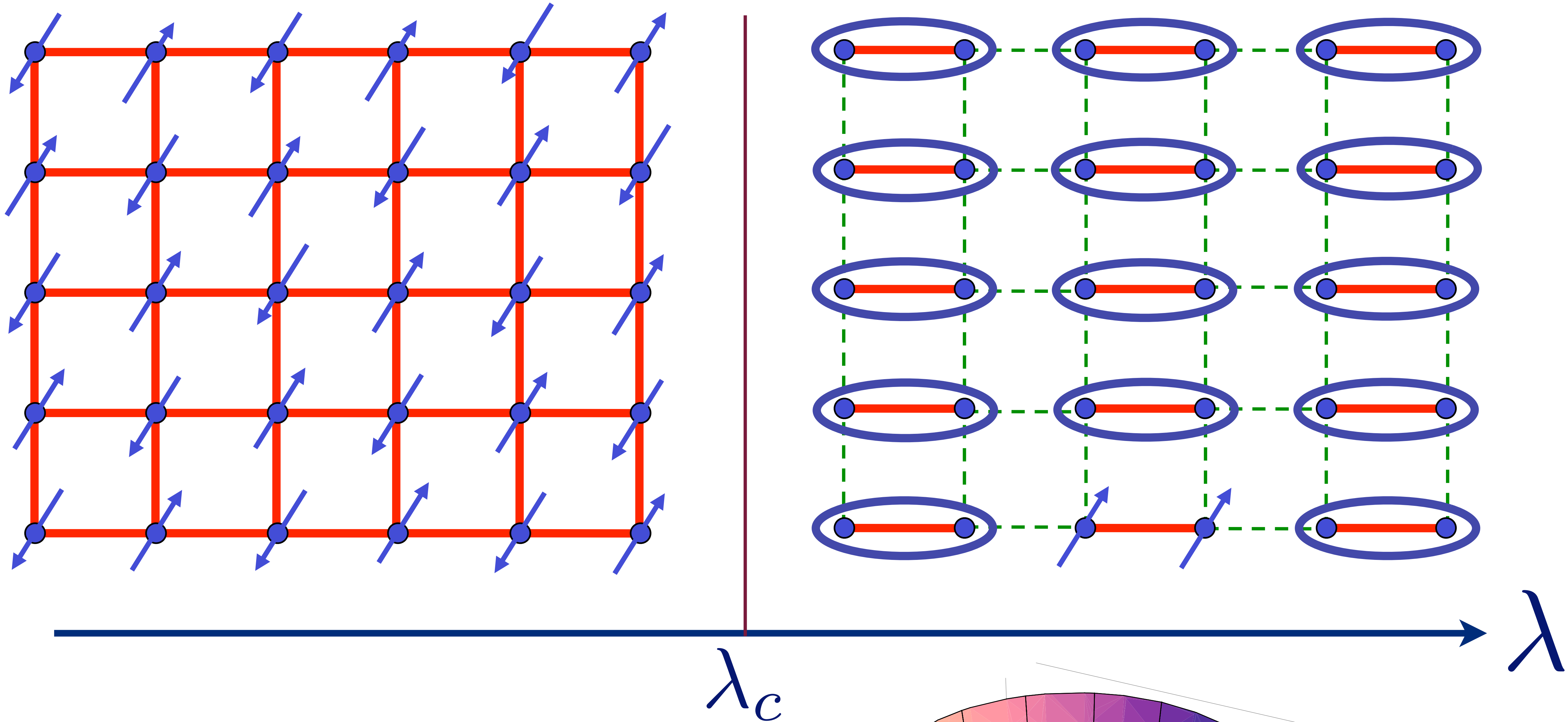

$$V(\vec{\varphi}) = (\lambda - \lambda_c)\vec{\varphi}^2 + u\left(\vec{\varphi}^2\right)^2$$

$$\lambda > \lambda_c$$

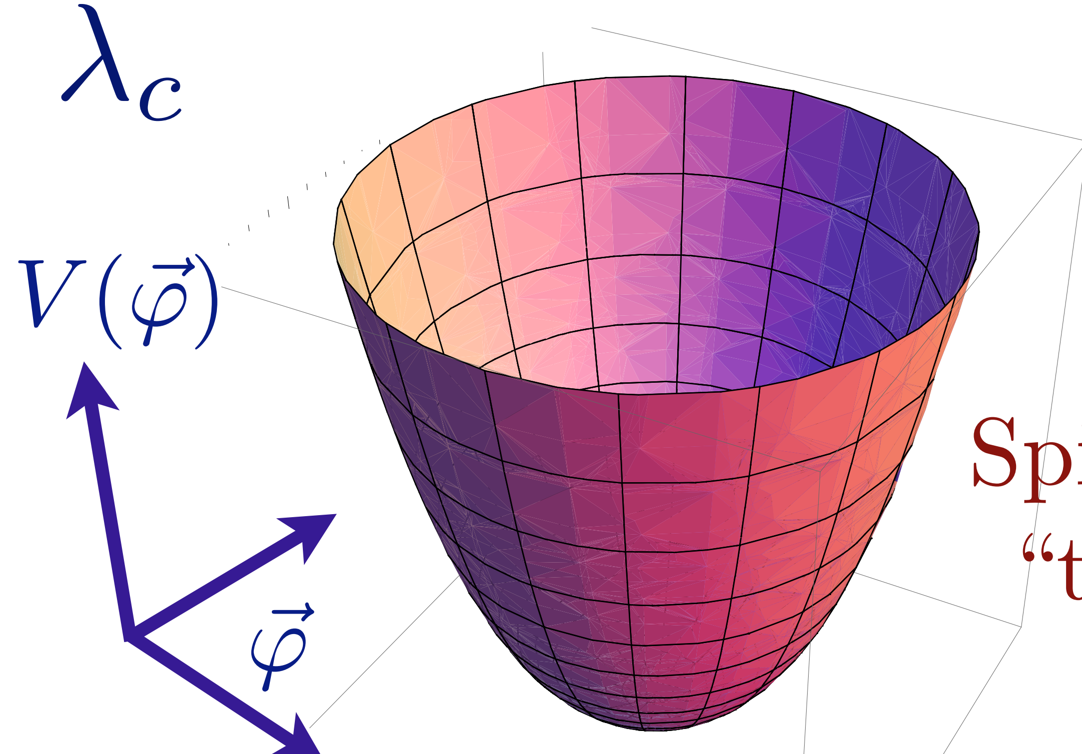

Spin $S = 1$
"triplon"

Excitation spectrum in the paramagnetic phase

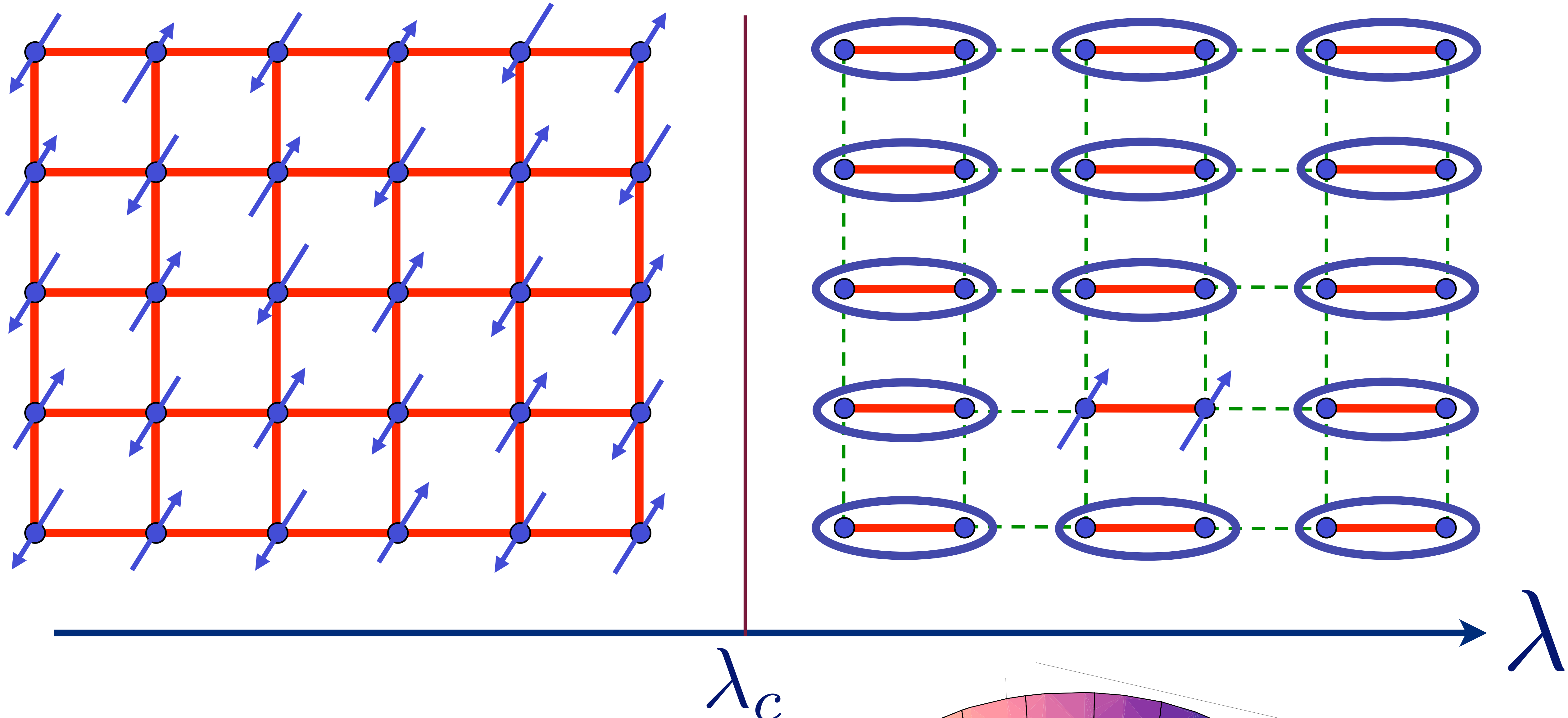

$$V(\vec{\varphi}) = (\lambda - \lambda_c)\vec{\varphi}^2 + u\left(\vec{\varphi}^2\right)^2$$

$$\lambda > \lambda_c$$

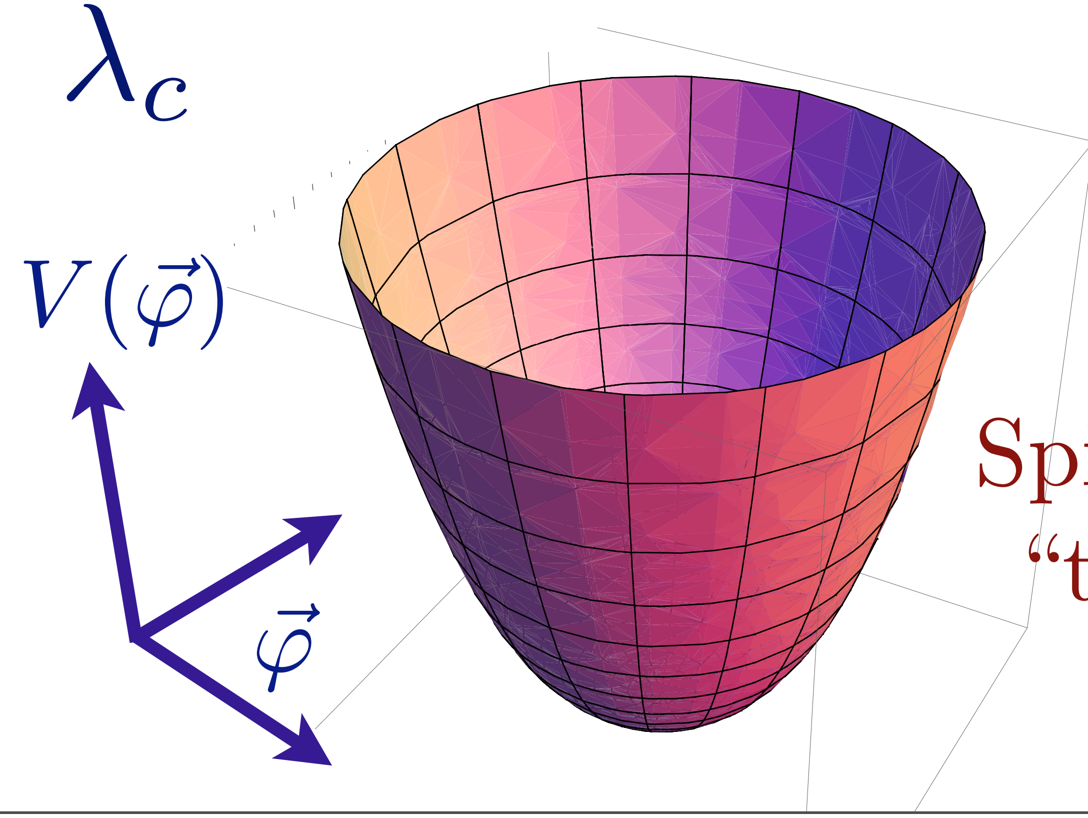

Spin $S = 1$
"triplon"

Excitation spectrum in the paramagnetic phase

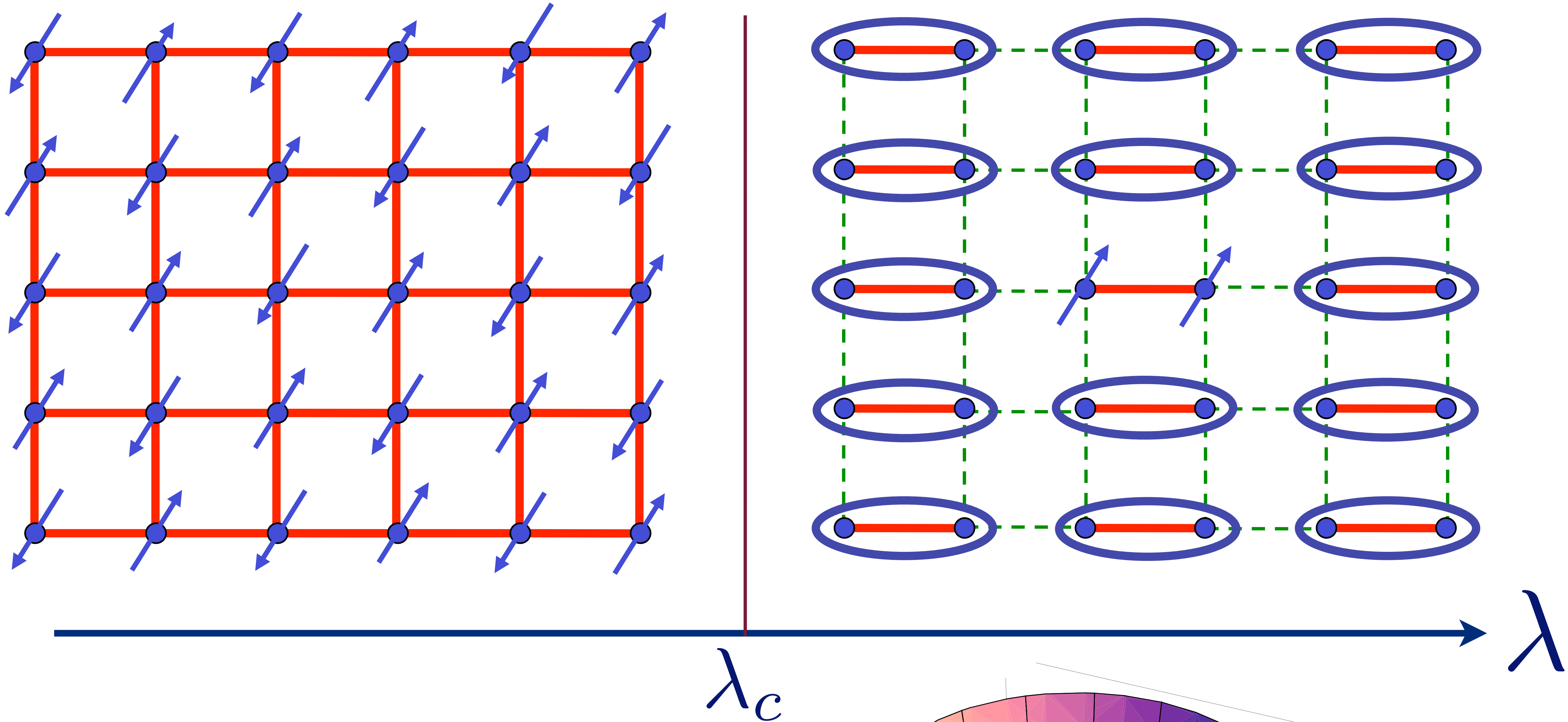

$$V(\vec{\varphi}) = (\lambda - \lambda_c)\vec{\varphi}^2 + u\left(\vec{\varphi}^2\right)^2$$

$$\lambda > \lambda_c$$

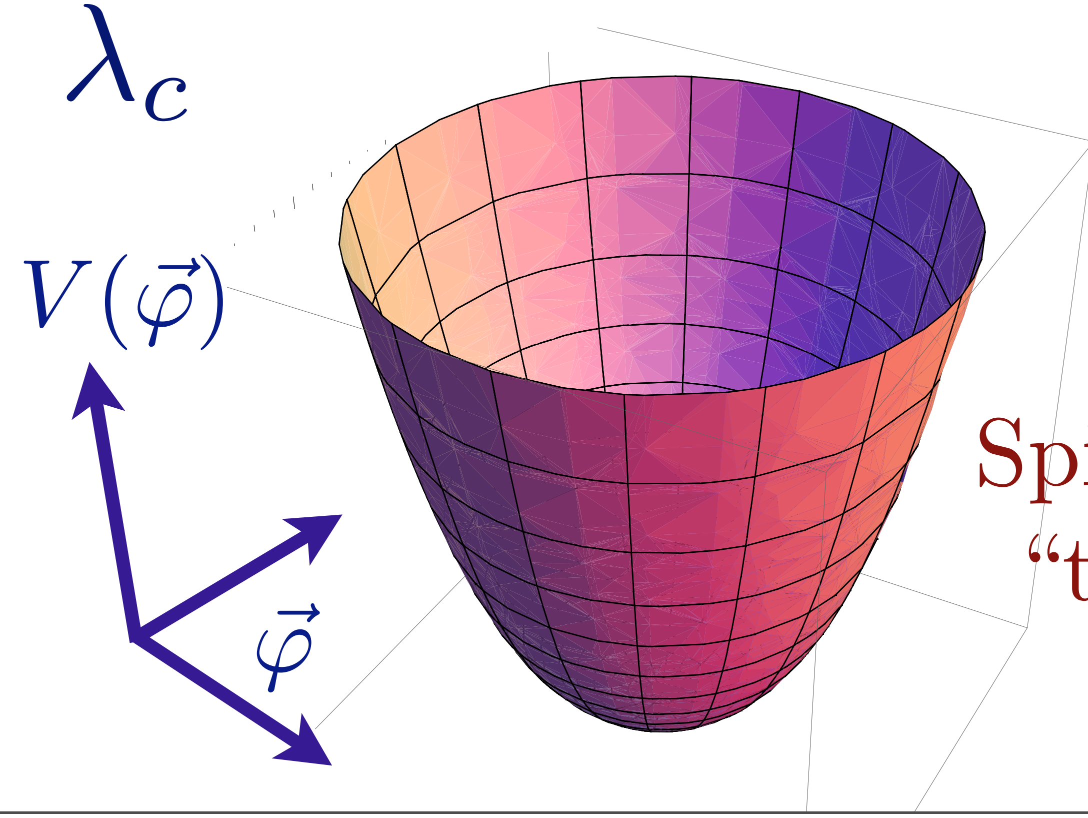

Spin $S = 1$
"triplon"

Excitation spectrum in the paramagnetic phase

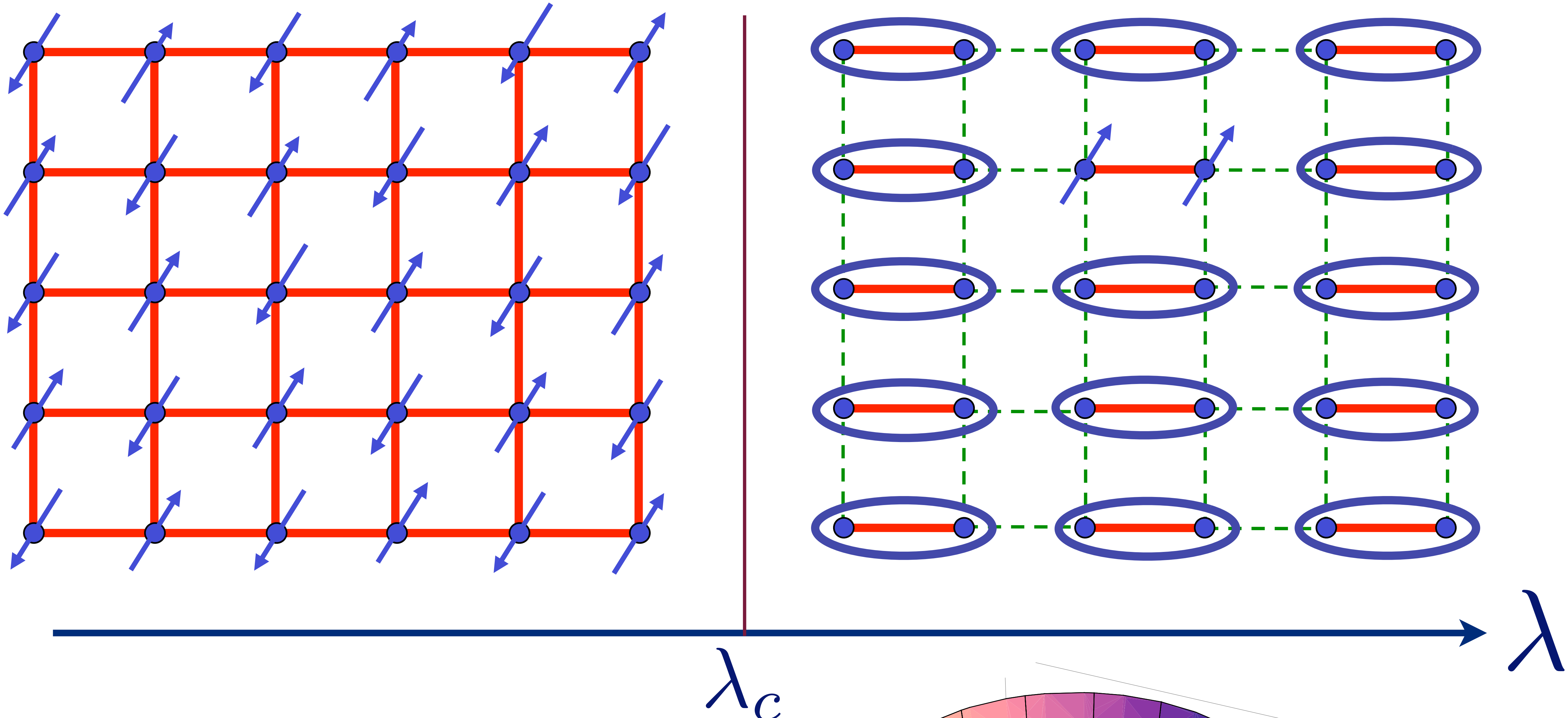

$$V(\vec{\varphi}) = (\lambda - \lambda_c)\vec{\varphi}^2 + u\left(\vec{\varphi}^2\right)^2$$

$$\lambda > \lambda_c$$

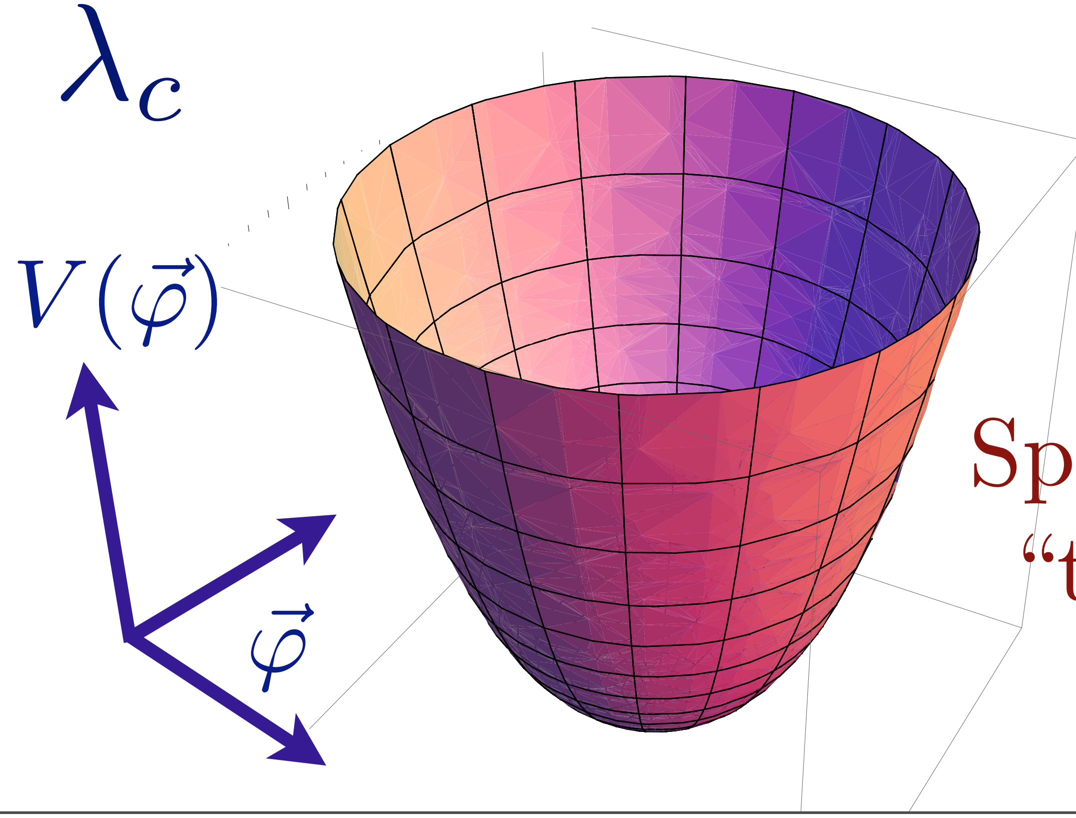

Spin $S = 1$
"triplon"

Excitation spectrum in the paramagnetic phase

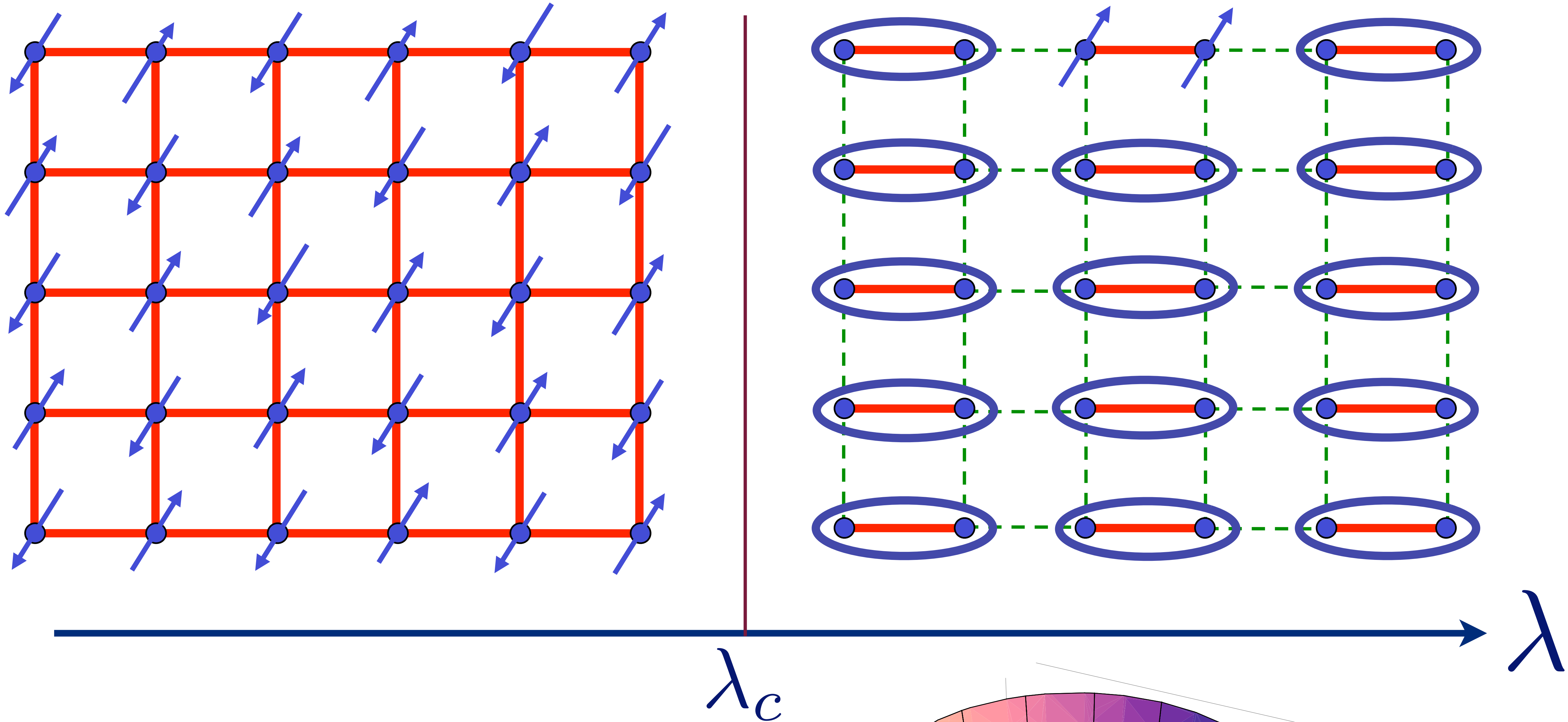

$$V(\vec{\varphi}) = (\lambda - \lambda_c)\vec{\varphi}^2 + u\left(\vec{\varphi}^2\right)^2$$

$$\lambda > \lambda_c$$

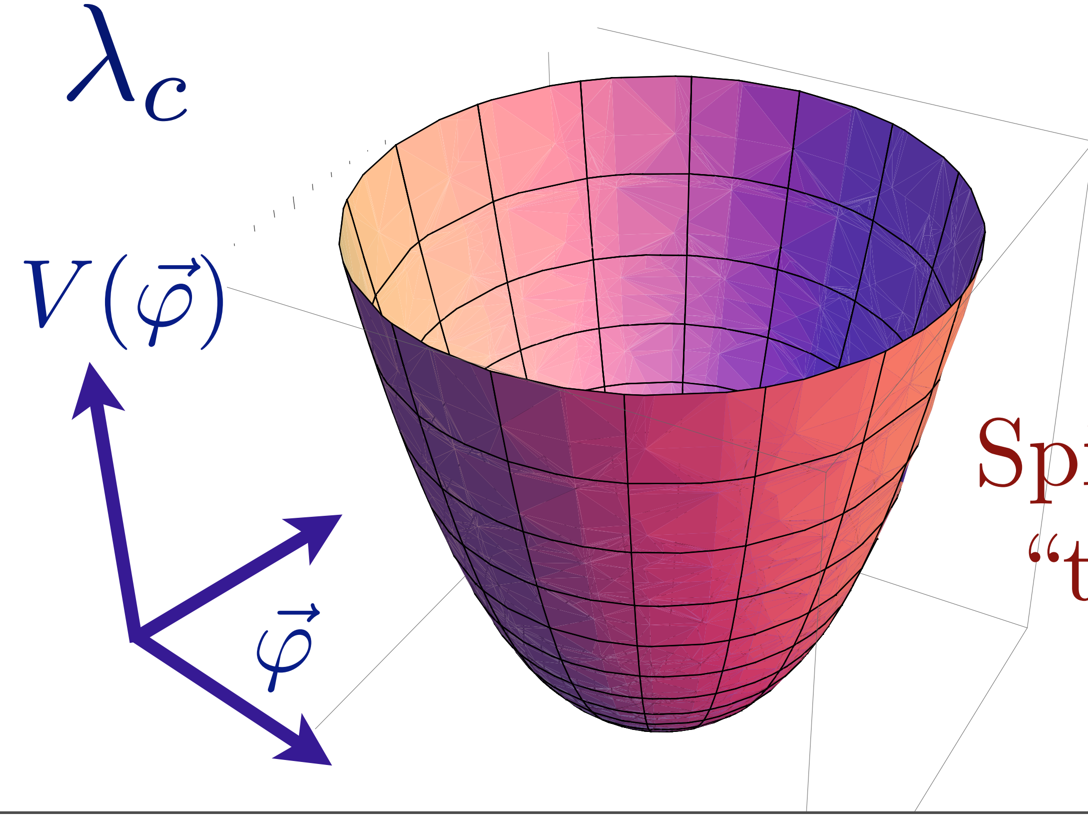

Spin $S = 1$
"triplon"

$TlCuCl_3$ at ambient pressure

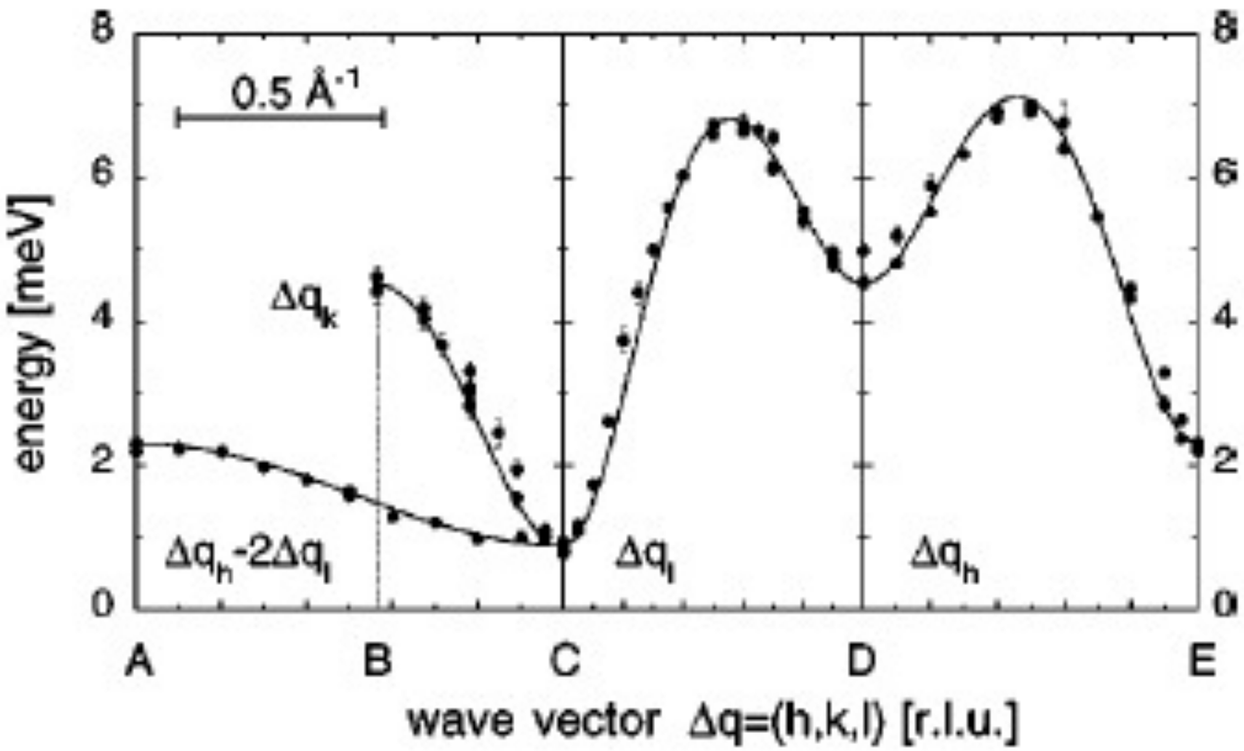

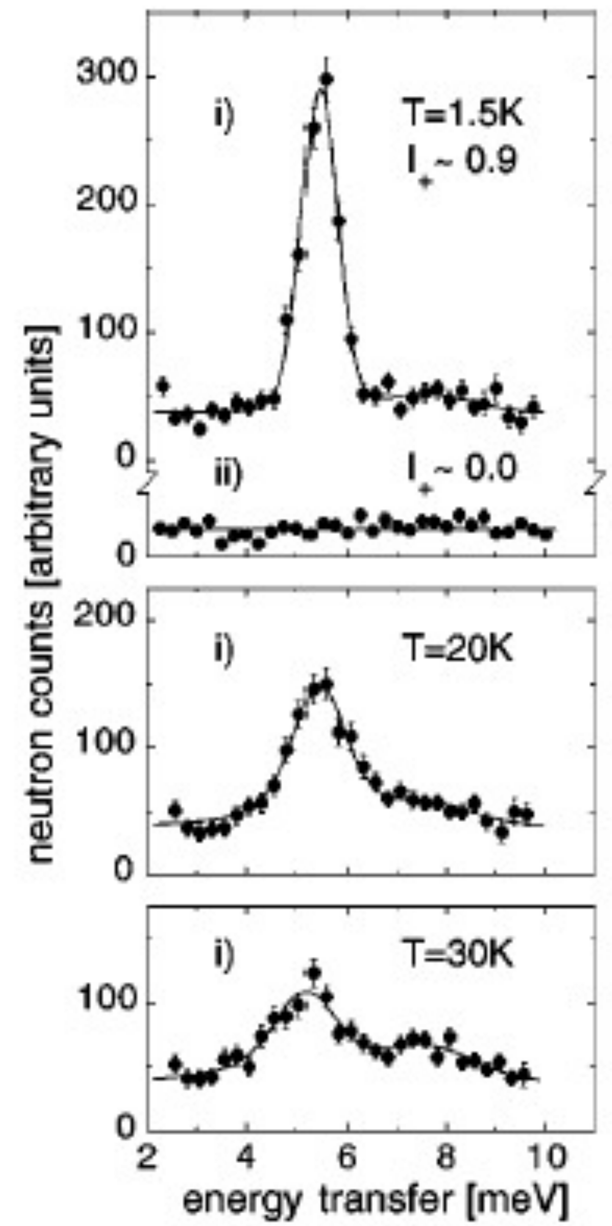

FIG. 1. Measured neutron profiles in the $a^* c^*$ plane of $TlCuCl_3$ for $i=(1.35,0,0)$, $ii=(0,0,3.15)$ [r.l.u]. The spectrum at $T=1.5$ K

N. Cavadini, G. Heigold, W. Henggeler, A. Furrer, H.-U. Güdel, K. Krämer and H. Mutka, *Phys. Rev.* B 63 172414 (2001).

$TlCuCl_3$ at ambient pressure

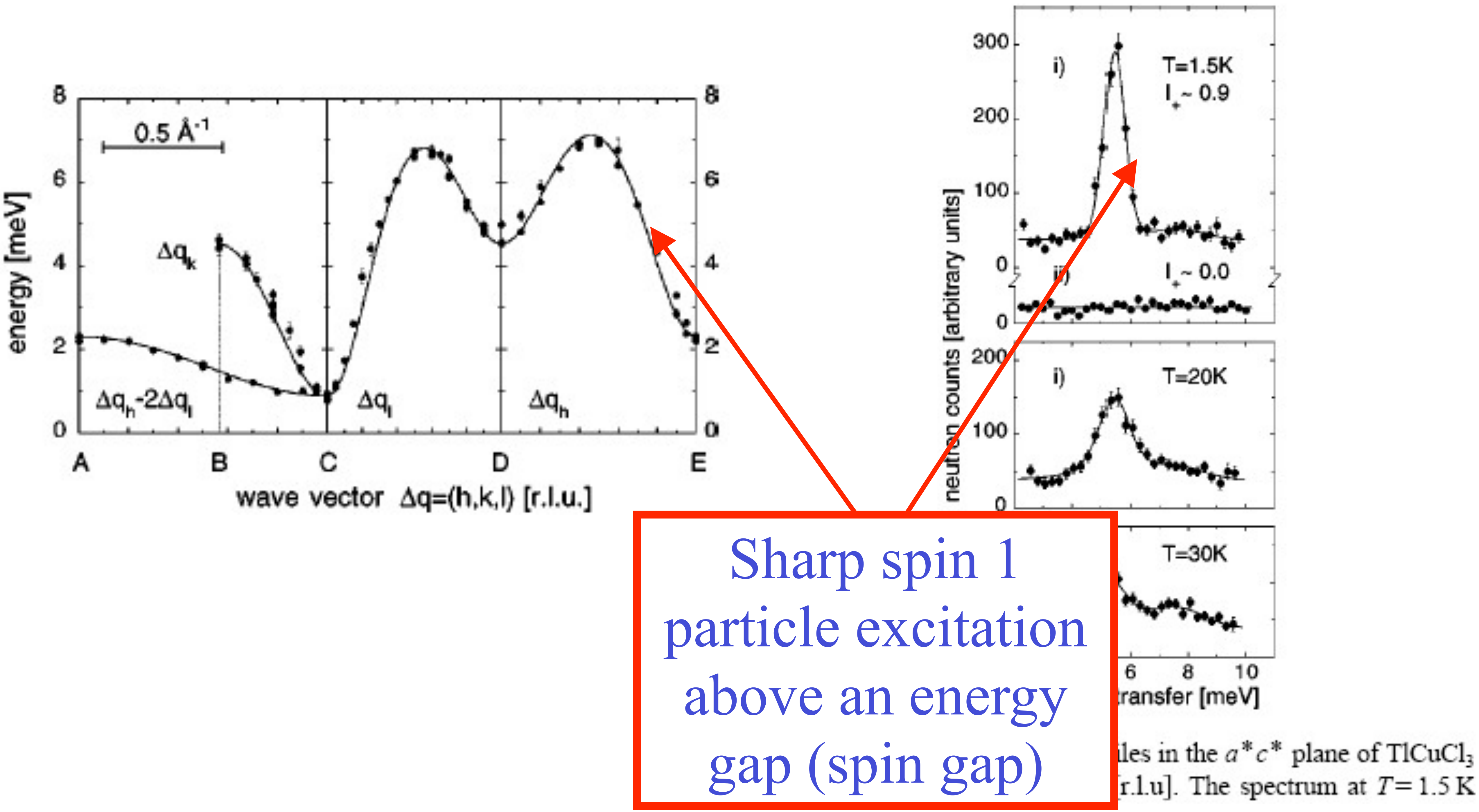

N. Cavadini, G. Heigold, W. Henggeler, A. Furrer, H.-U. Güdel, K. Krämer and H. Mutka, *Phys. Rev.* B 63 172414 (2001).

Excitation spectrum in the Néel phase

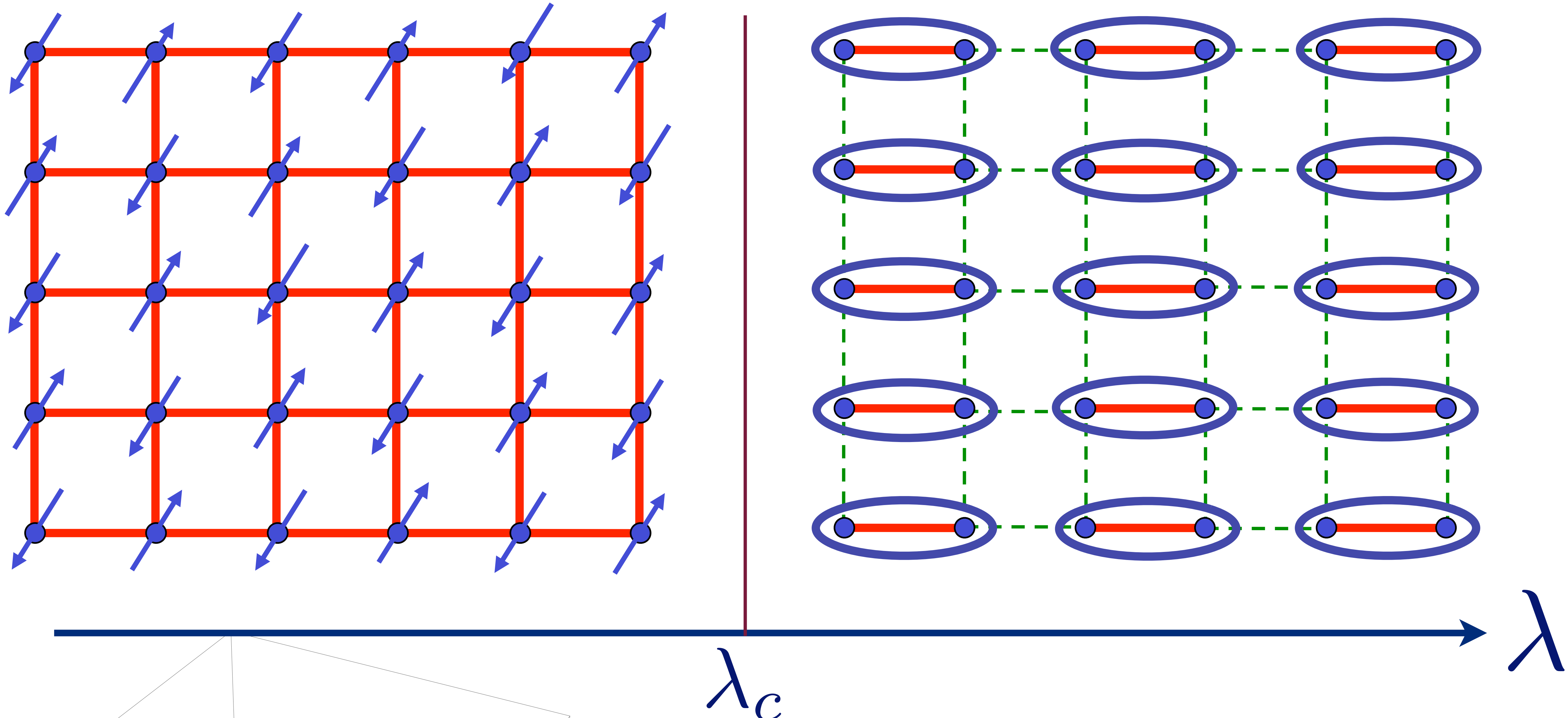

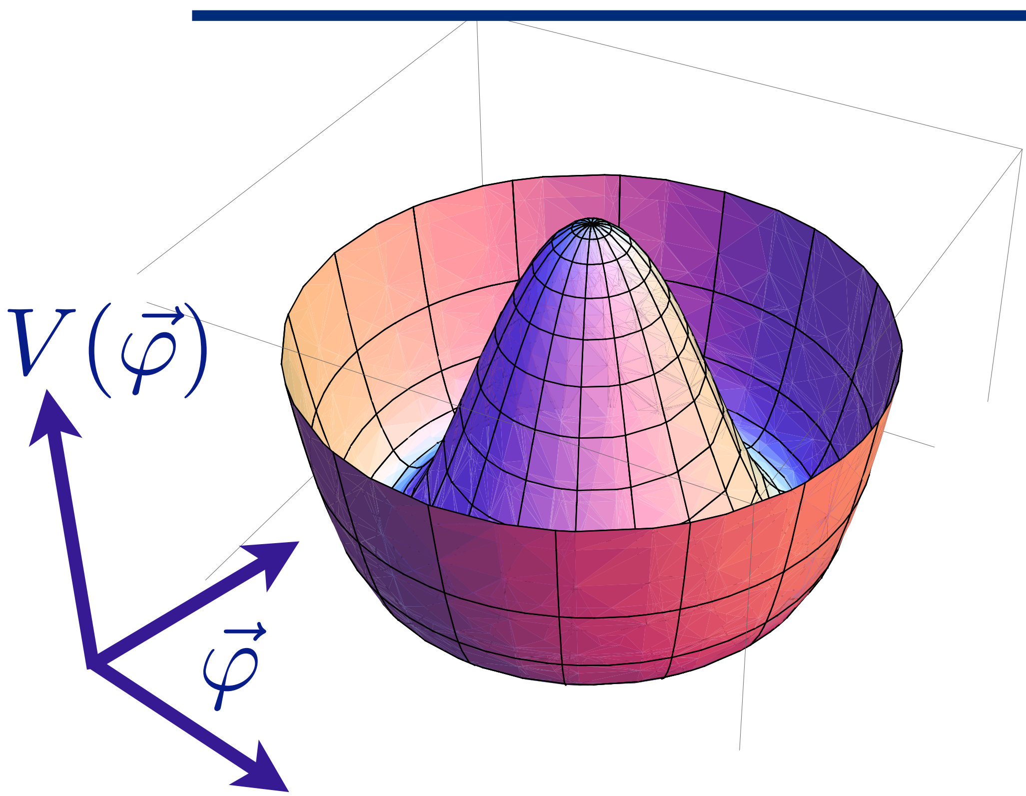

$$V(\vec{\varphi}) = (\lambda - \lambda_c)\vec{\varphi}^2 + u\left(\vec{\varphi}^2\right)^2$$

$$\lambda < \lambda_c$$

Excitation spectrum in the Néel phase

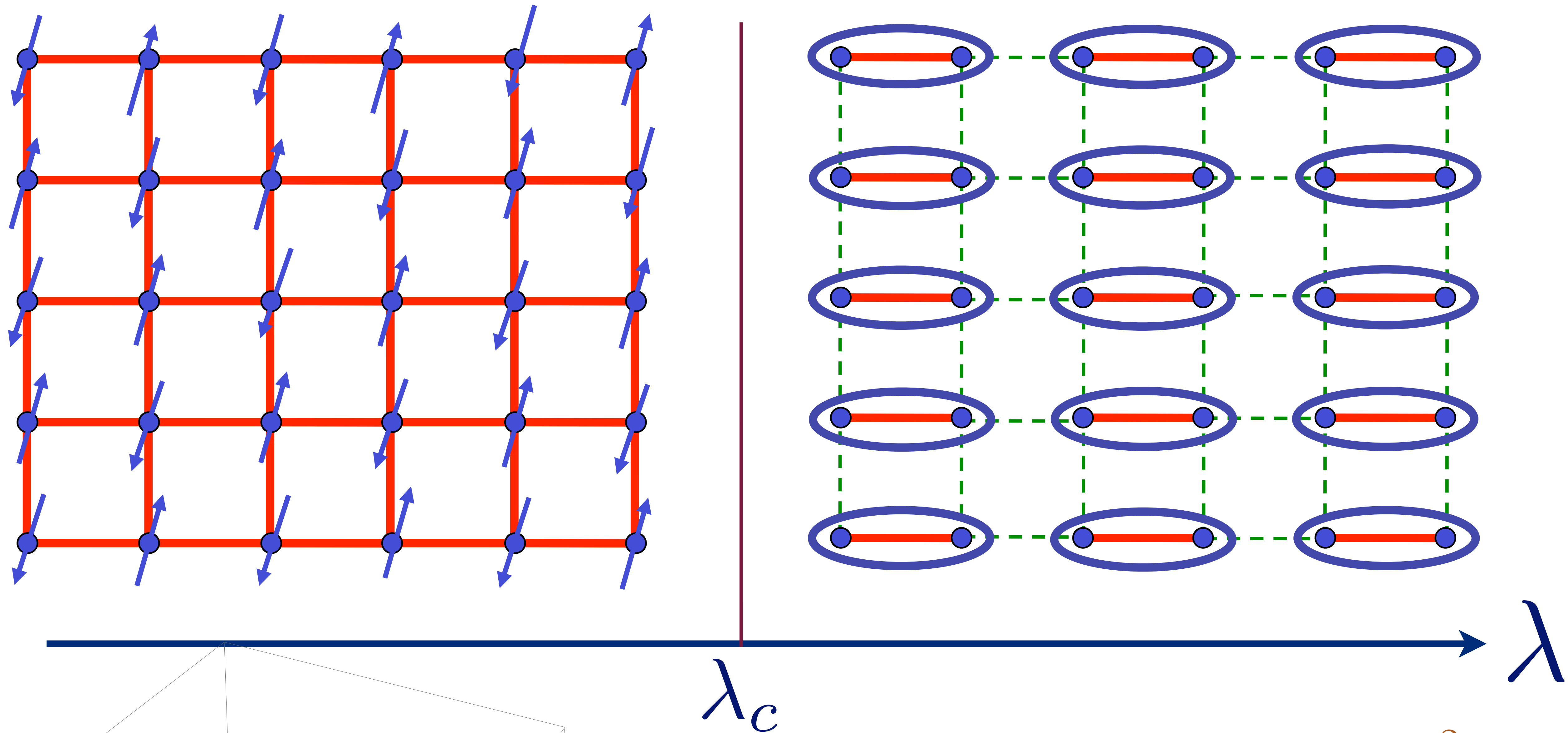

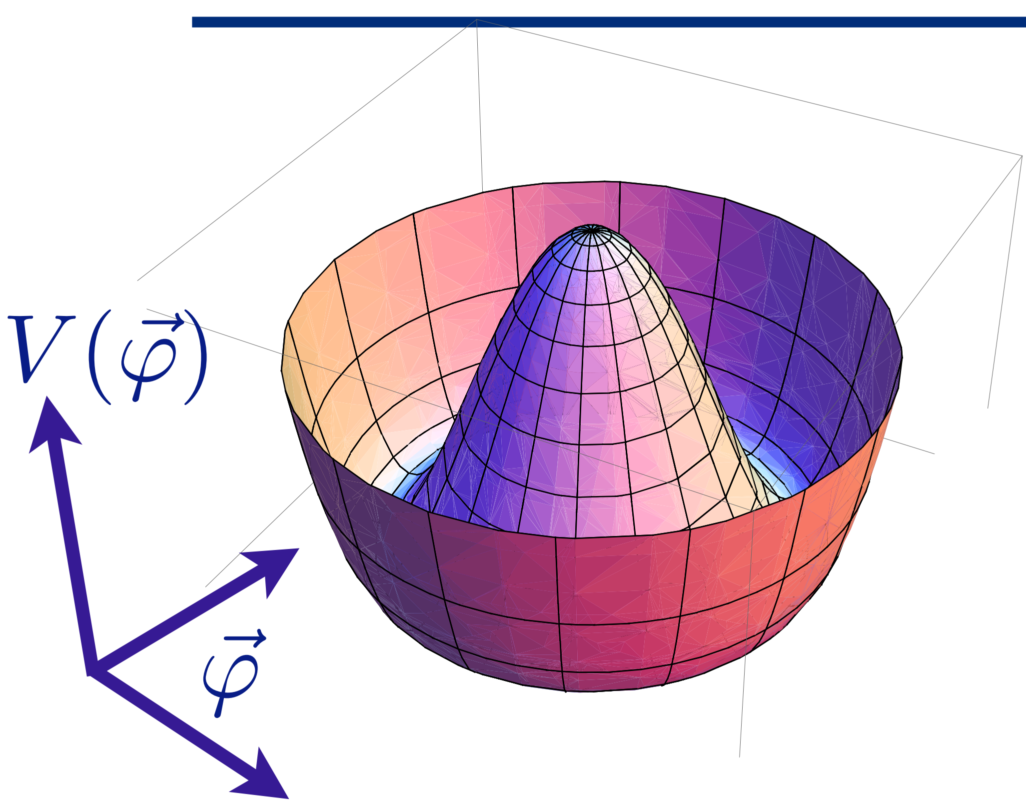

$$V(\vec{\varphi}) = (\lambda - \lambda_c)\vec{\varphi}^2 + u\left(\vec{\varphi}^2\right)^2$$

$$\lambda < \lambda_c$$

Spin waves

Excitation spectrum in the Néel phase

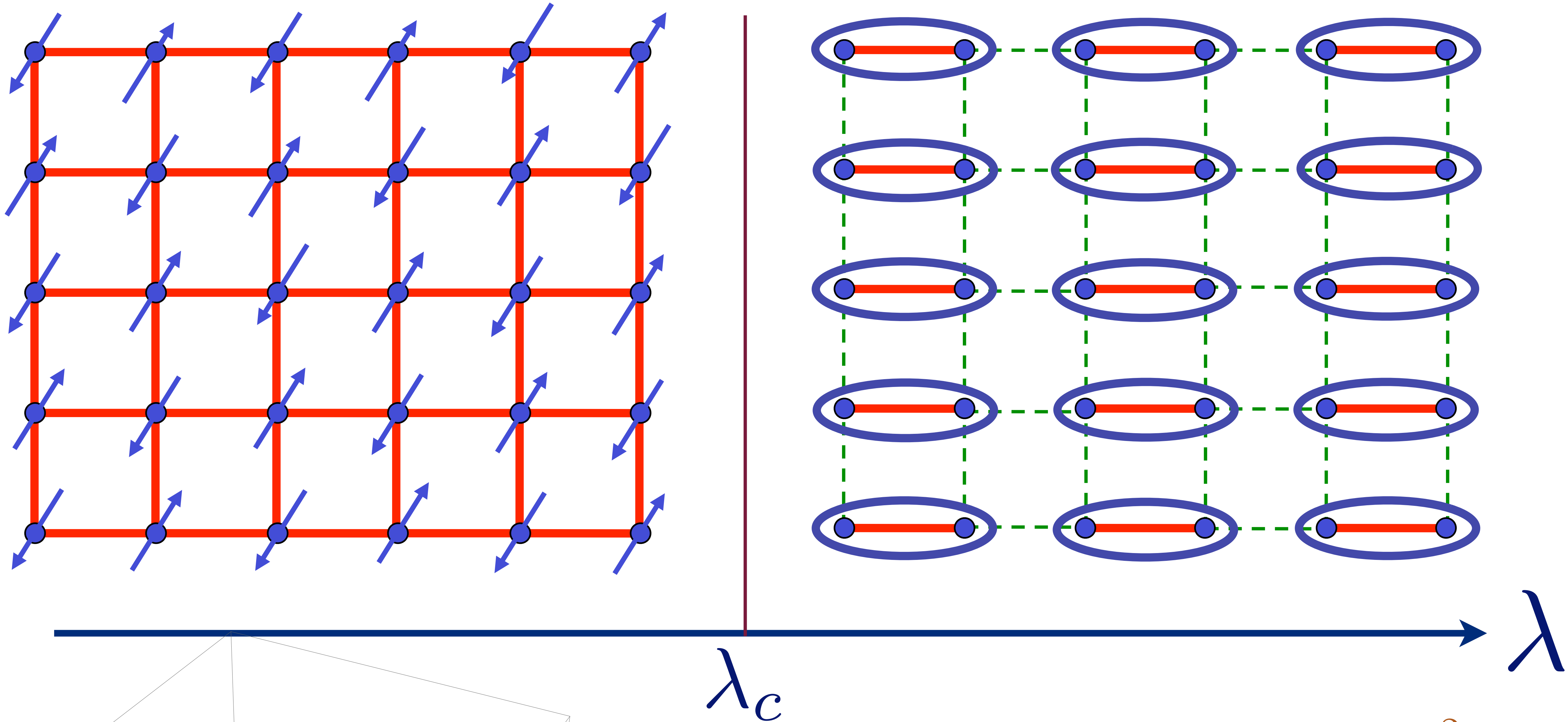

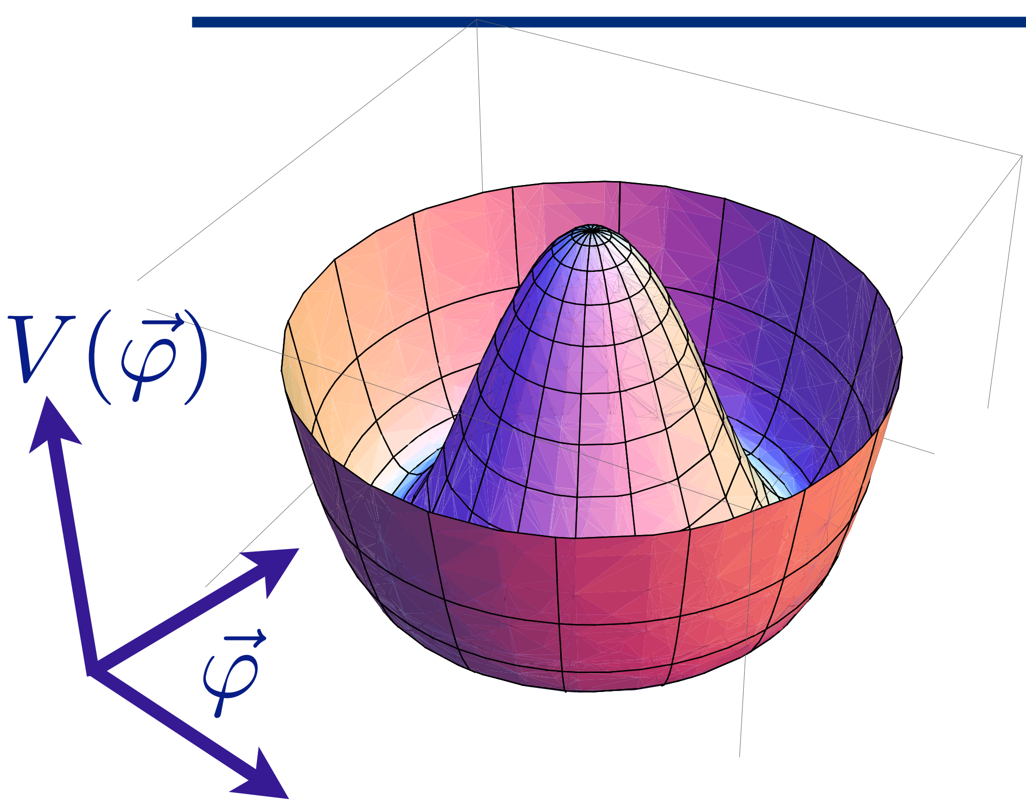

$$V(\vec{\varphi}) = (\lambda - \lambda_c)\vec{\varphi}^2 + u\left(\vec{\varphi}^2\right)^2$$

$$\lambda < \lambda_c$$

Spin waves

Excitation spectrum in the Néel phase

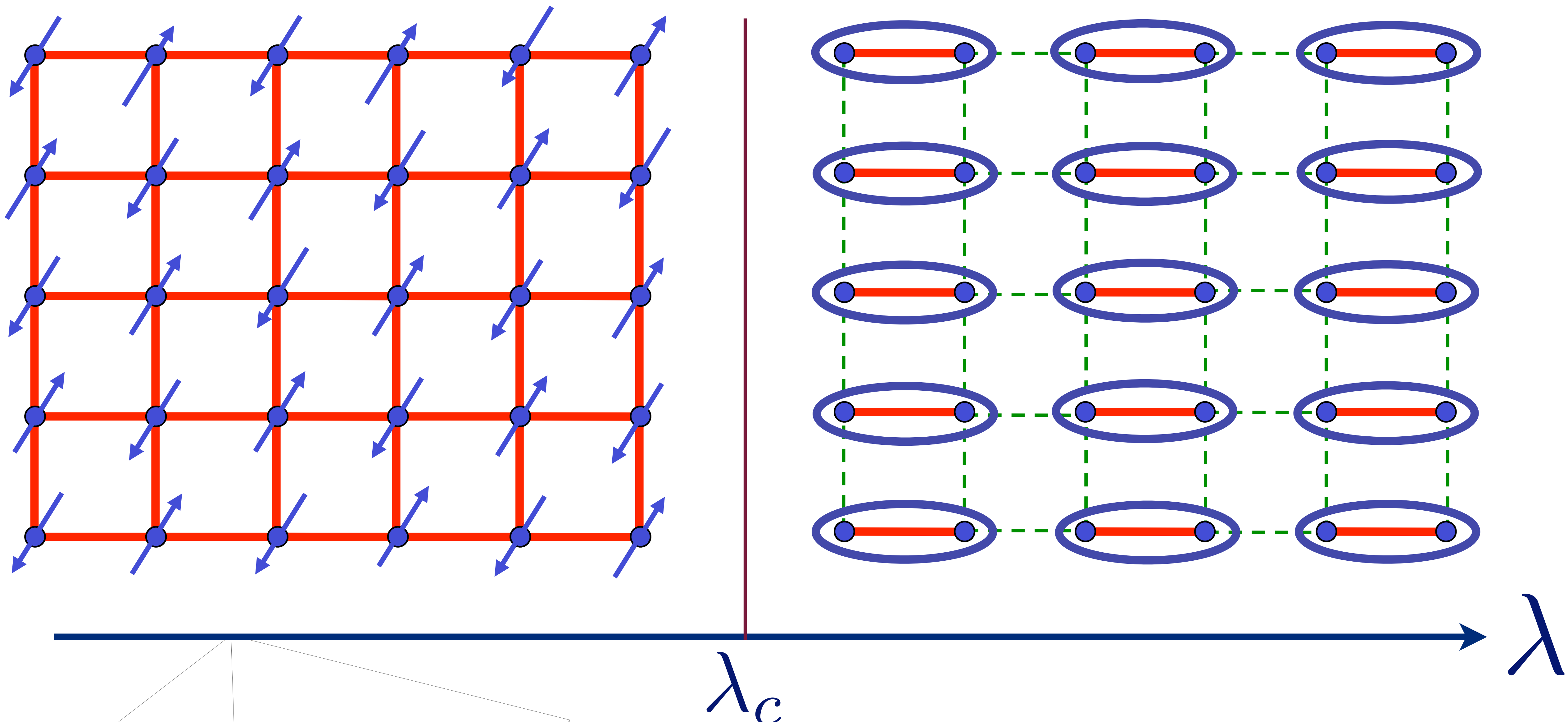

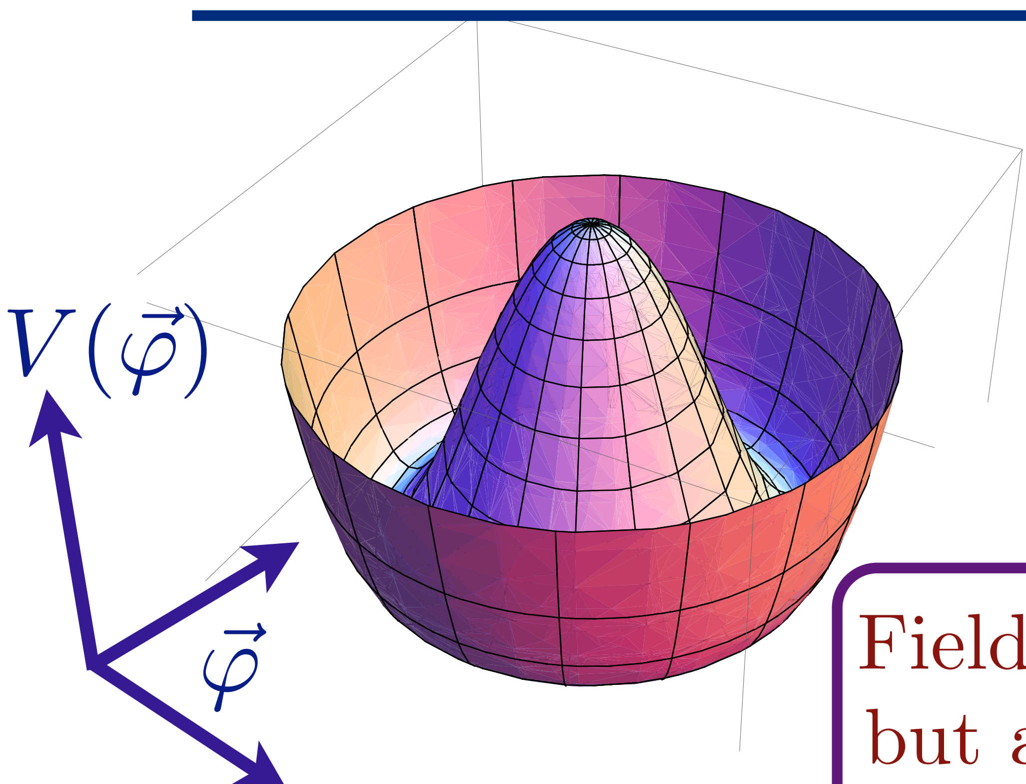

$$V(\vec{\varphi}) = (\lambda - \lambda_c)\vec{\varphi}^2 + u\left(\vec{\varphi}^2\right)^2$$

$$\lambda < \lambda_c$$

Field theory yields spin waves ("Goldstone" modes) but also an additional longitudinal "Higgs" particle

$TlCuCl_3$ with varying pressure

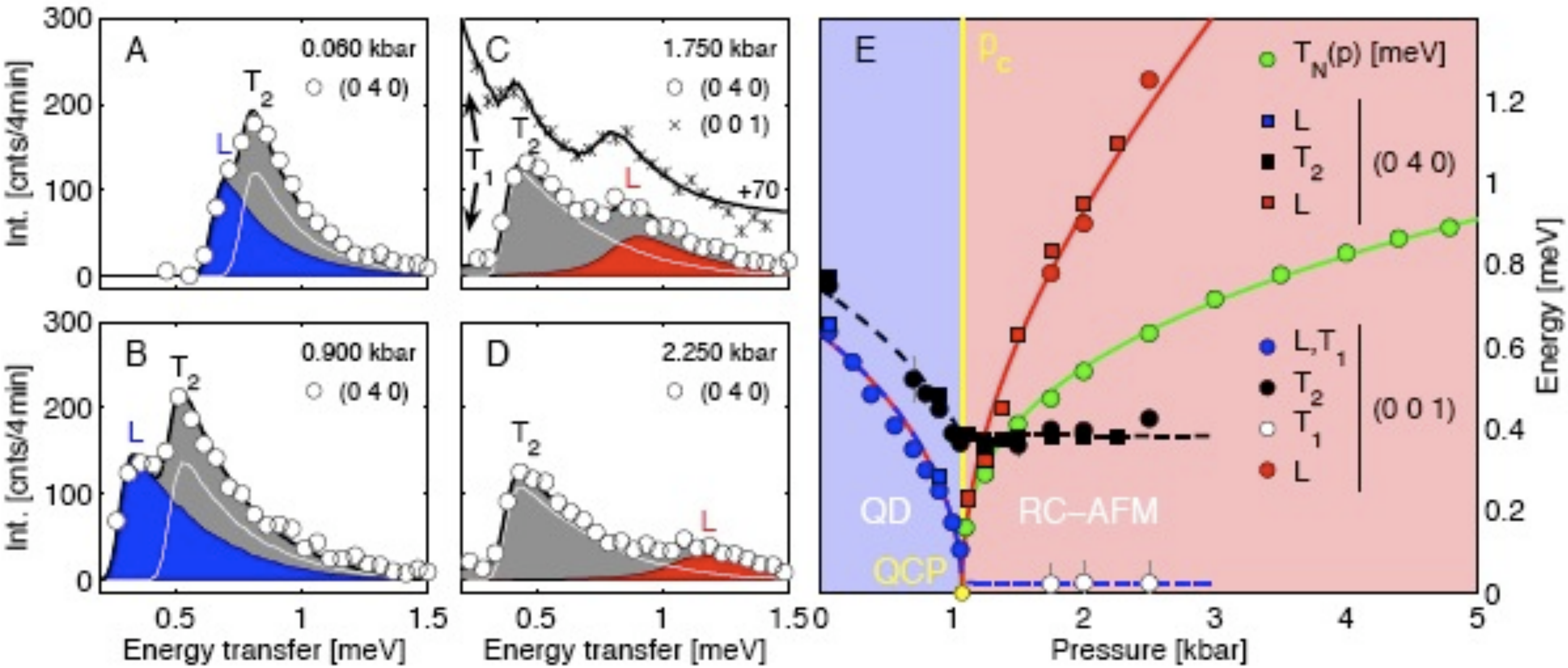

Observation of $3 \to 2$ low energy modes,
emergence of new Higgs particle in the Néel phase,
and vanishing of Néel temperature at the quantum critical point

Christian Ruegg, Bruce Normand, Masashige Matsumoto, Albert Furrer, Desmond McMorrow, Karl Kramer, Hans-Ulrich Gudel, Severian Gvasaliya, Hannu Mutka, and Martin Boehm, *Phys. Rev. Lett.* **100**, 205701 (2008)

Prediction of quantum field theory

Potential for $\vec{\varphi}$ fluctuations: $V(\vec{\varphi}) = (\lambda - \lambda_c)\vec{\varphi}^2 + u\left(\vec{\varphi}^2\right)^2$

Paramagnetic phase, $\lambda > \lambda_c$

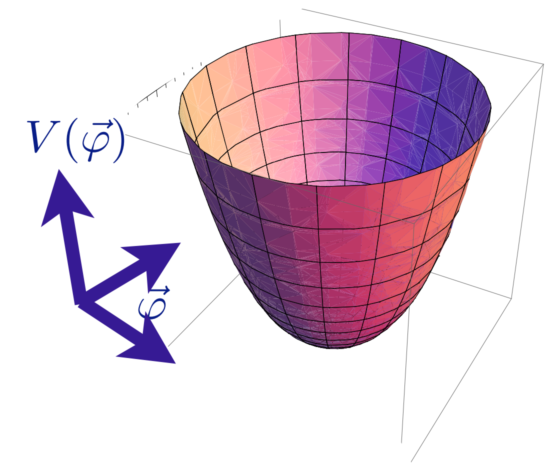

Expand about $\vec{\varphi} = 0$:

$$V(\vec{\varphi}) \approx (\lambda - \lambda_c)\vec{\varphi}^2$$

Yields 3 particles with energy gap $\sim \sqrt{(\lambda - \lambda_c)}$

Prediction of quantum field theory

Potential for $\vec{\varphi}$ fluctuations: $V(\vec{\varphi}) = (\lambda - \lambda_c)\vec{\varphi}^2 + u\left(\vec{\varphi}^2\right)^2$

Paramagnetic phase, $\lambda > \lambda_c$

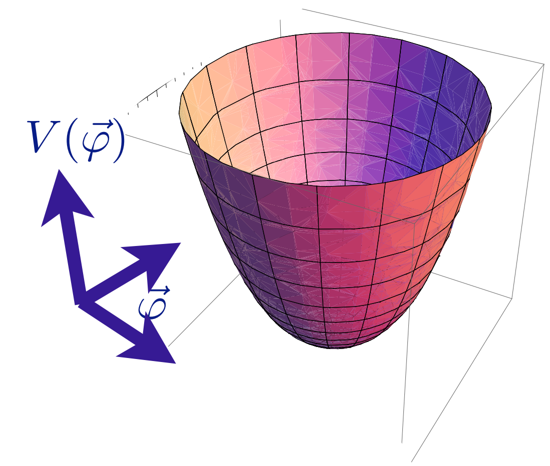

Expand about $\vec{\varphi} = 0$:

$$V(\vec{\varphi}) \approx (\lambda - \lambda_c)\vec{\varphi}^2$$

Yields 3 particles with energy gap $\sim \sqrt{(\lambda - \lambda_c)}$

Néel phase, $\lambda < \lambda_c$

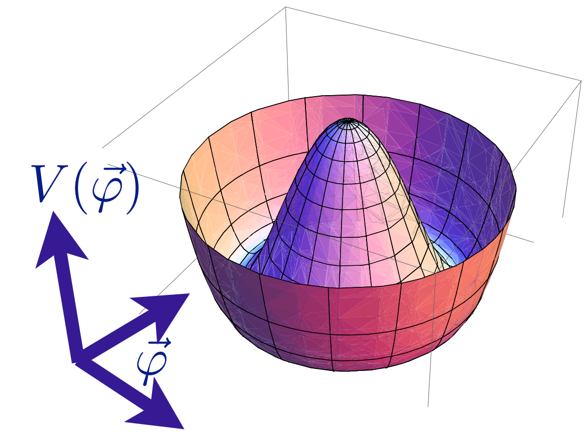

Expand $\vec{\varphi} = \left(0, 0, \sqrt{(\lambda_c - \lambda)/(2u)}\right) + \vec{\varphi}_1$:

$$V(\vec{\varphi}) \approx 2(\lambda_c - \lambda)\varphi_{1z}^2$$

Yields 2 gapless spin waves and one Higgs particle with energy gap $\sim \sqrt{2(\lambda_c - \lambda)}$

Prediction of quantum field theory

$$\frac{\text{Energy of Higgs particle}}{\text{Energy of triplon}} = \sqrt{2}$$

$$V(\vec{\varphi}) = (\lambda - \lambda_c)\vec{\varphi}^2 + u\left(\vec{\varphi}^2\right)^2$$

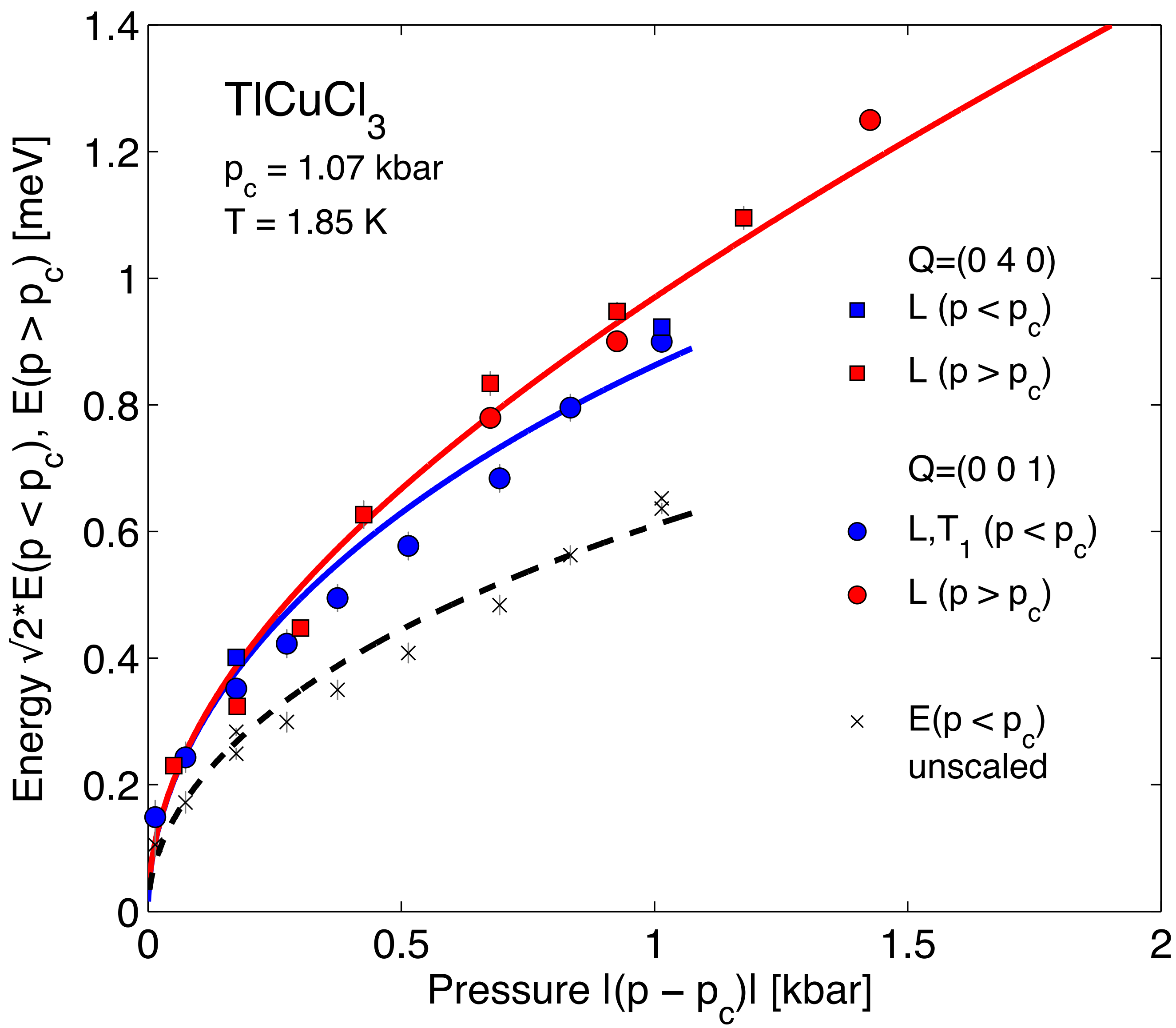

S. Sachdev, arXiv:0901.4103

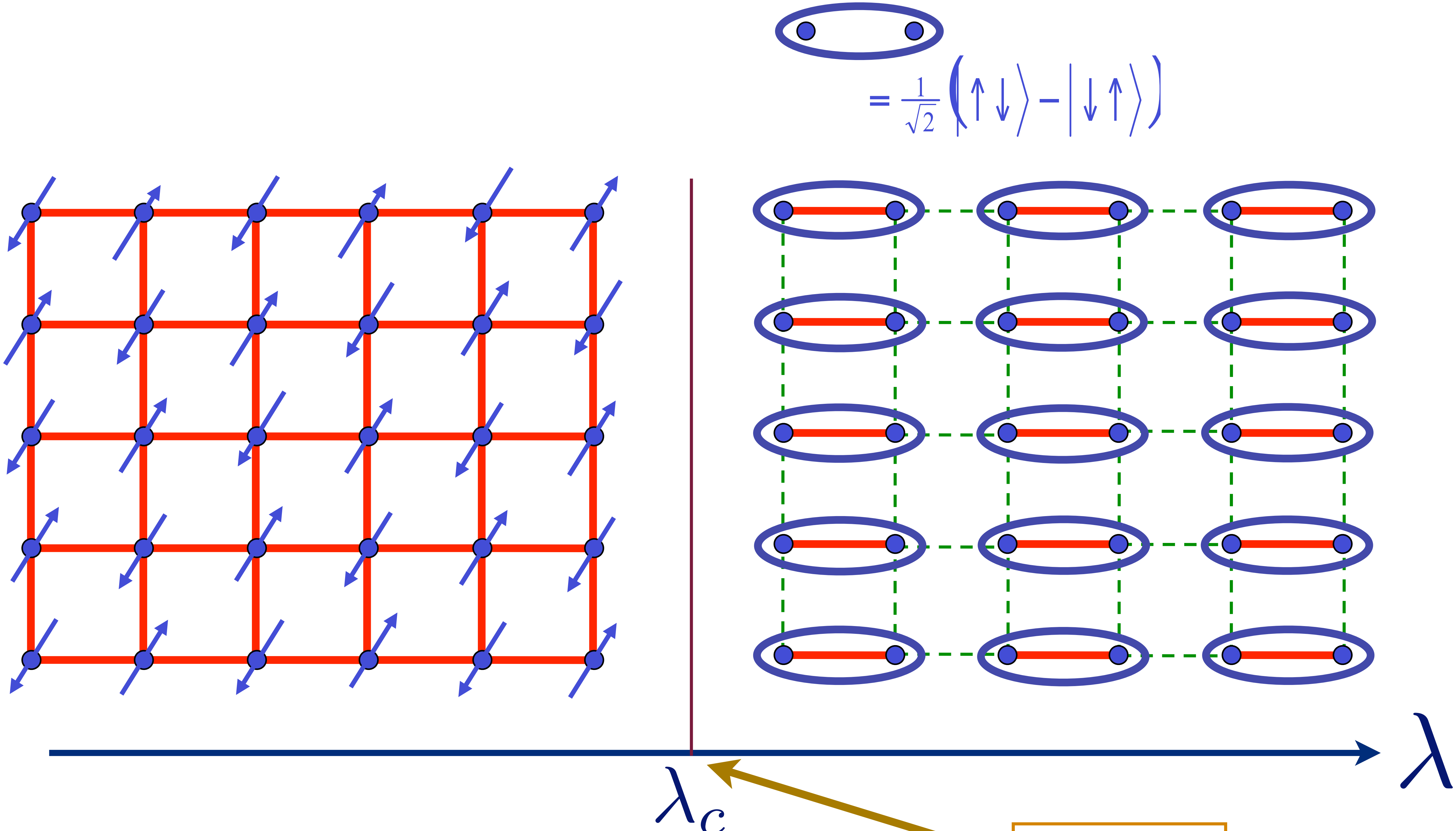

O(3) order parameter $\vec{\varphi}$

$$\mathcal{S} = \int d^2r d\tau \left[(\partial_\tau \varphi)^2 + c^2 (\nabla_r \vec{\varphi})^2 + s\vec{\varphi}^2 + u\left(\vec{\varphi}^2\right)^2 \right]$$

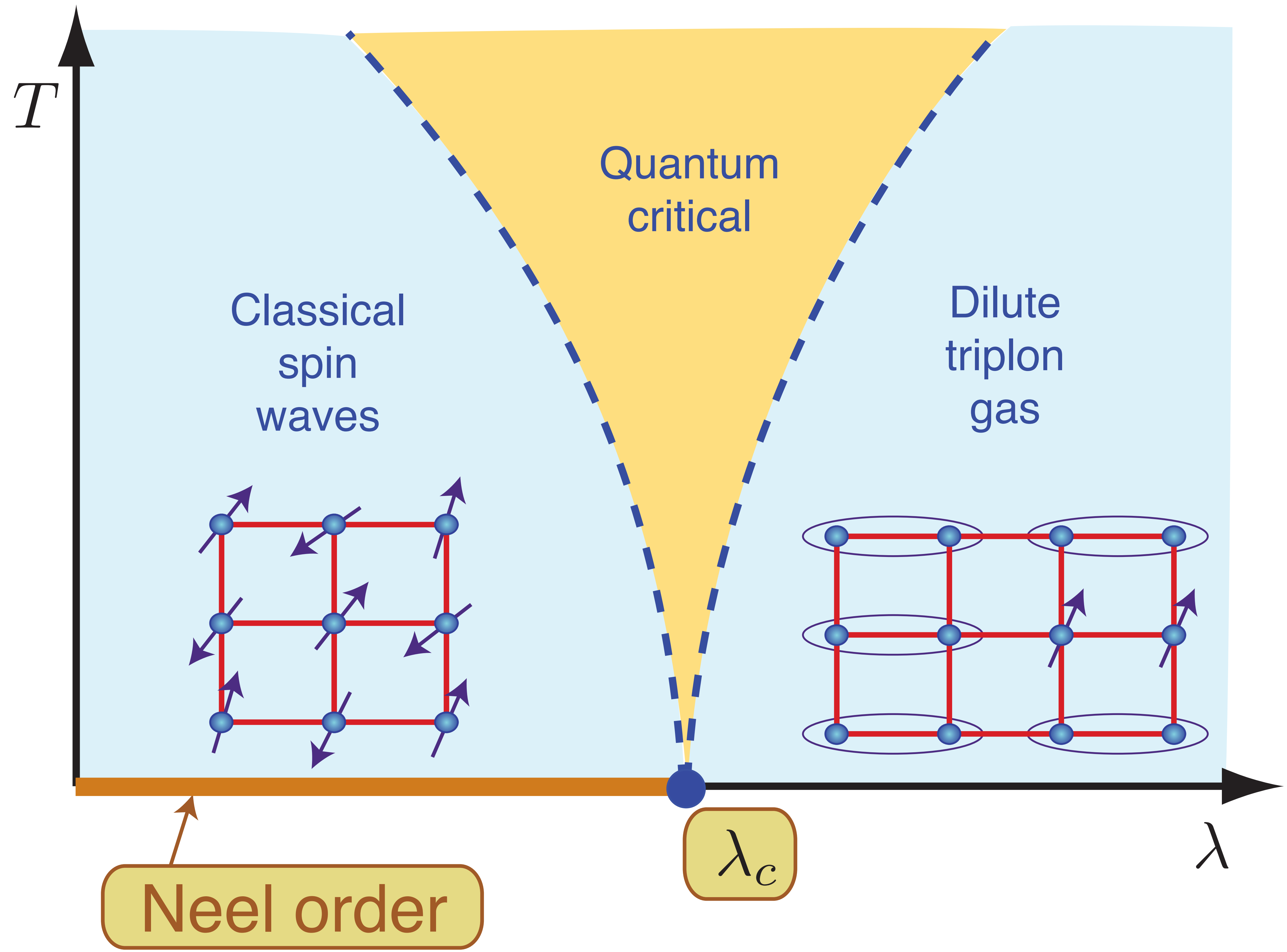

Pressure in $TlCuCl_3$

S. Sachdev and J. Ye, *Phys. Rev. Lett.* **69**, 2411 (1992).

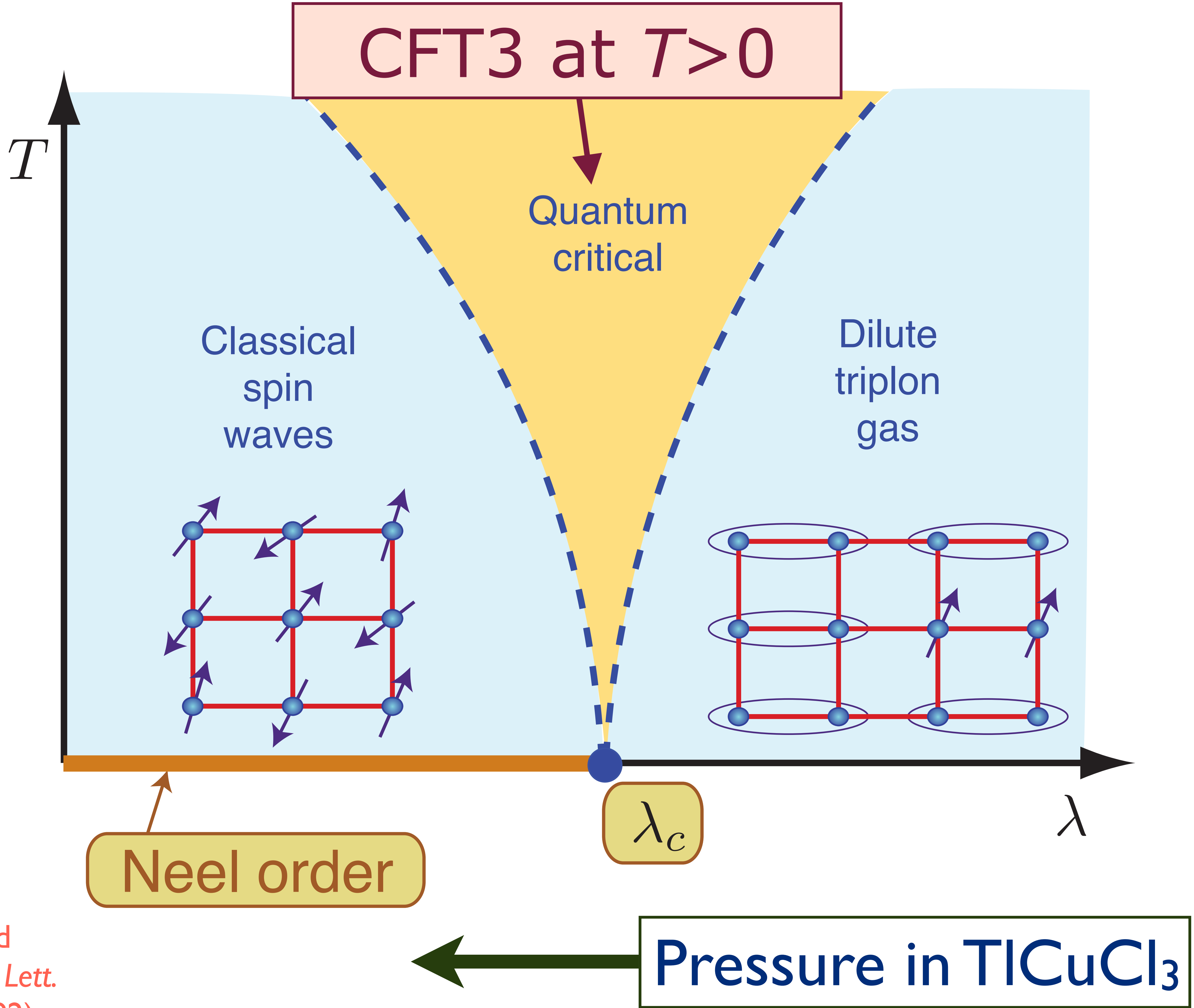

S. Sachdev and J. Ye, *Phys. Rev. Lett.* **69**, 2411 (1992).

Crossovers in transport properties of hole-doped cuprates

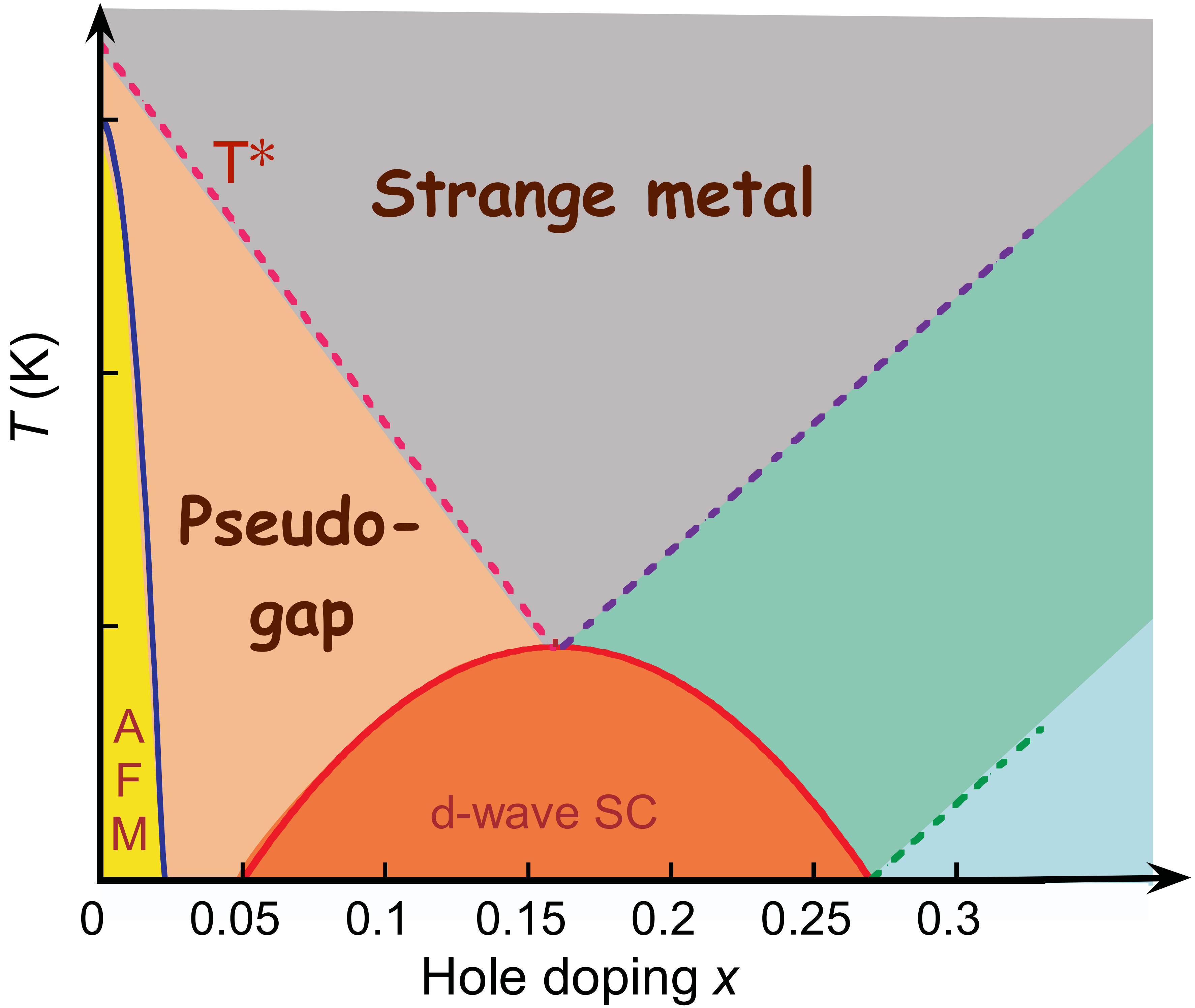

Crossovers in transport properties of hole-doped cuprates

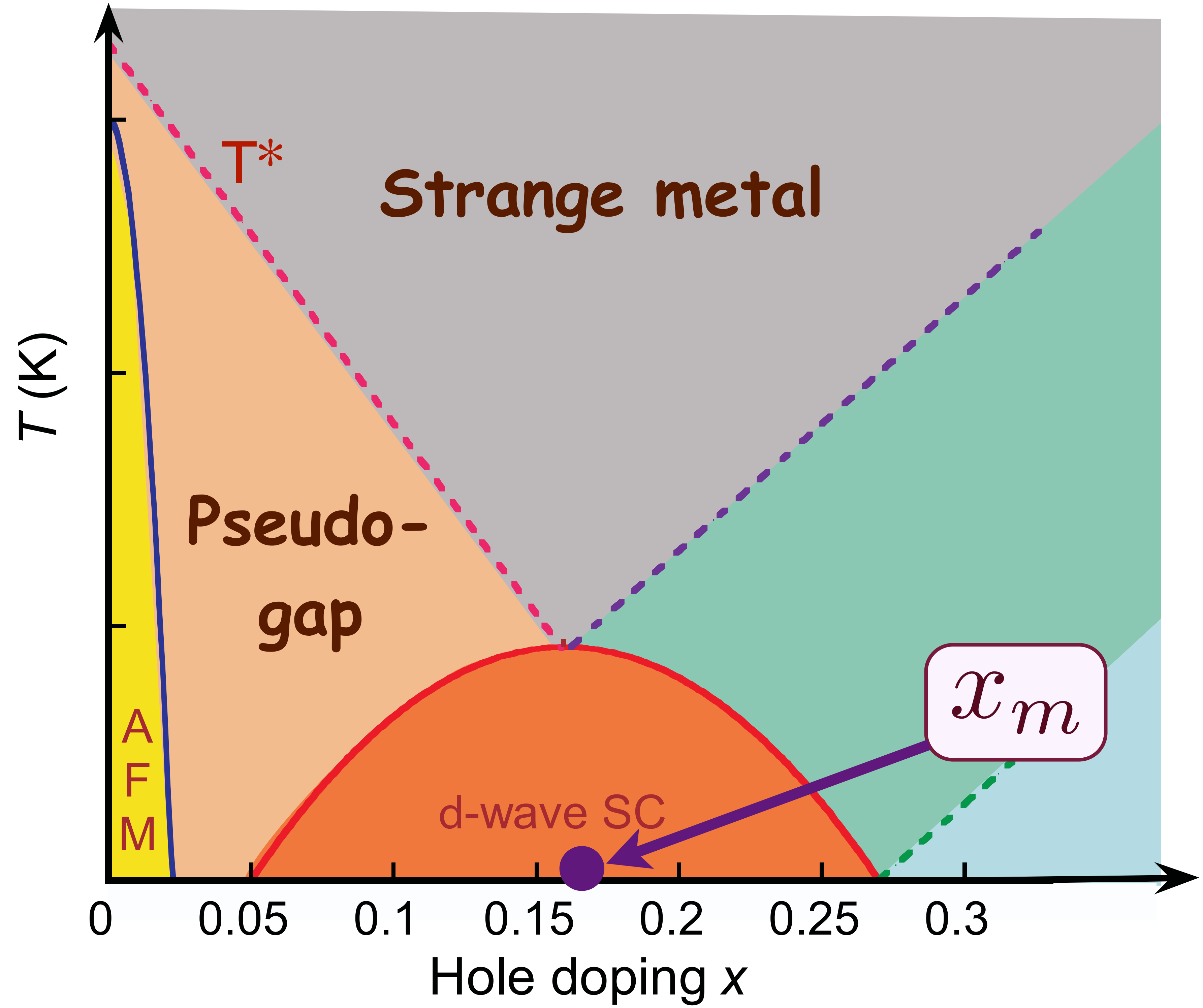

S. Sachdev and J. Ye, *Phys. Rev. Lett.* **69**, 2411 (1992).

A. J. Millis, *Phys. Rev.* B **48**, 7183 (1993).

C. M. Varma, *Phys. Rev. Lett.* **83**, 3538 (1999).

Strange metal: quantum criticality of optimal doping critical point at $x = x_m$?

Only candidate quantum critical point observed at low *T*

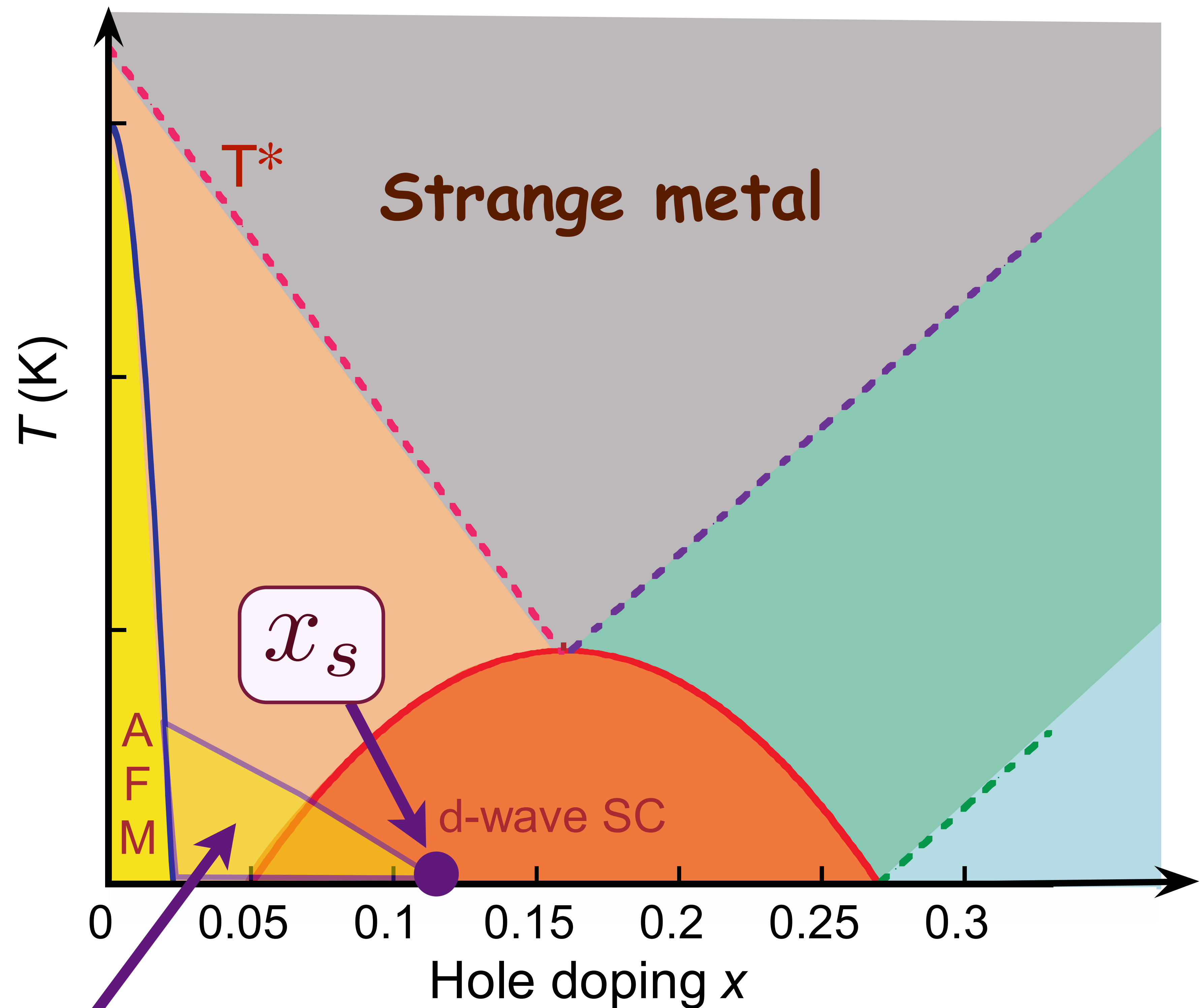

Spin density wave order present
below a quantum critical point at $x = x_s$
with $x_s \approx 0.12$ in the La series of cuprates

Outline

1. Coupled dimer antiferromagnets
   Introduction to quantum criticality

2. Phase diagram of the cuprates
   Quantum criticality of the competition between antiferromagnetism and superconductivity

3. Theory of Ising-nematic ordering in a metal
   Strongly-coupled field theory

4. The AdS/CFT correspondence
   Phases of finite density quantum matter at strong coupling

Outline

1. Coupled dimer antiferromagnets
   Introduction to quantum criticality

2. Phase diagram of the cuprates
   Quantum criticality of the competition between antiferromagnetism and superconductivity

3. Theory of Ising-nematic ordering in a metal
   Strongly-coupled field theory

4. The AdS/CFT correspondence
   Phases of finite density quantum matter at strong coupling

Antiferro-
magnetism

d-wave
supercon-
ductivity

Fermi
surface

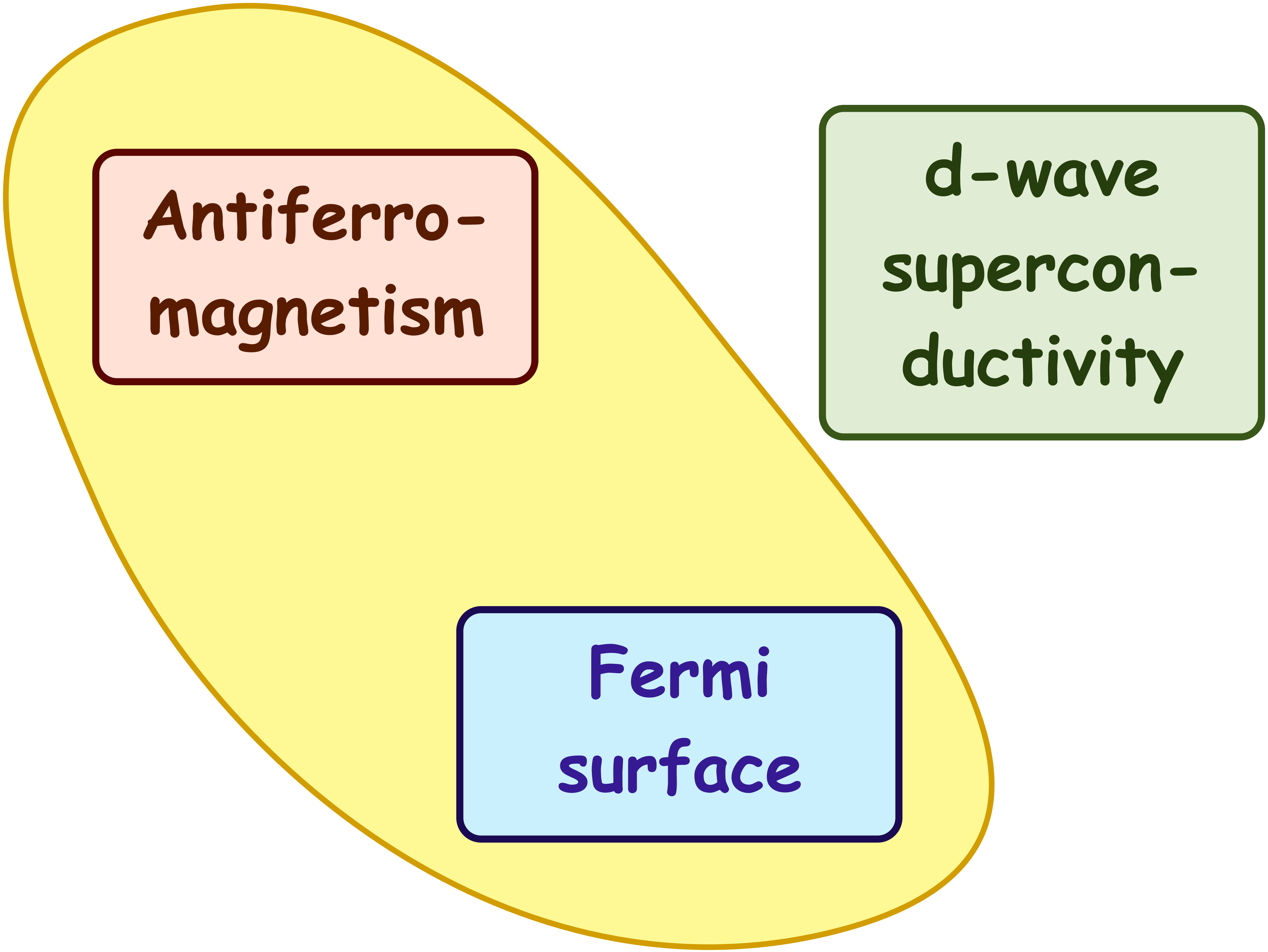
Antiferro-
magnetism
d-wave
supercon-
ductivity
Fermi
surface

Fermi surface+antiferromagnetism

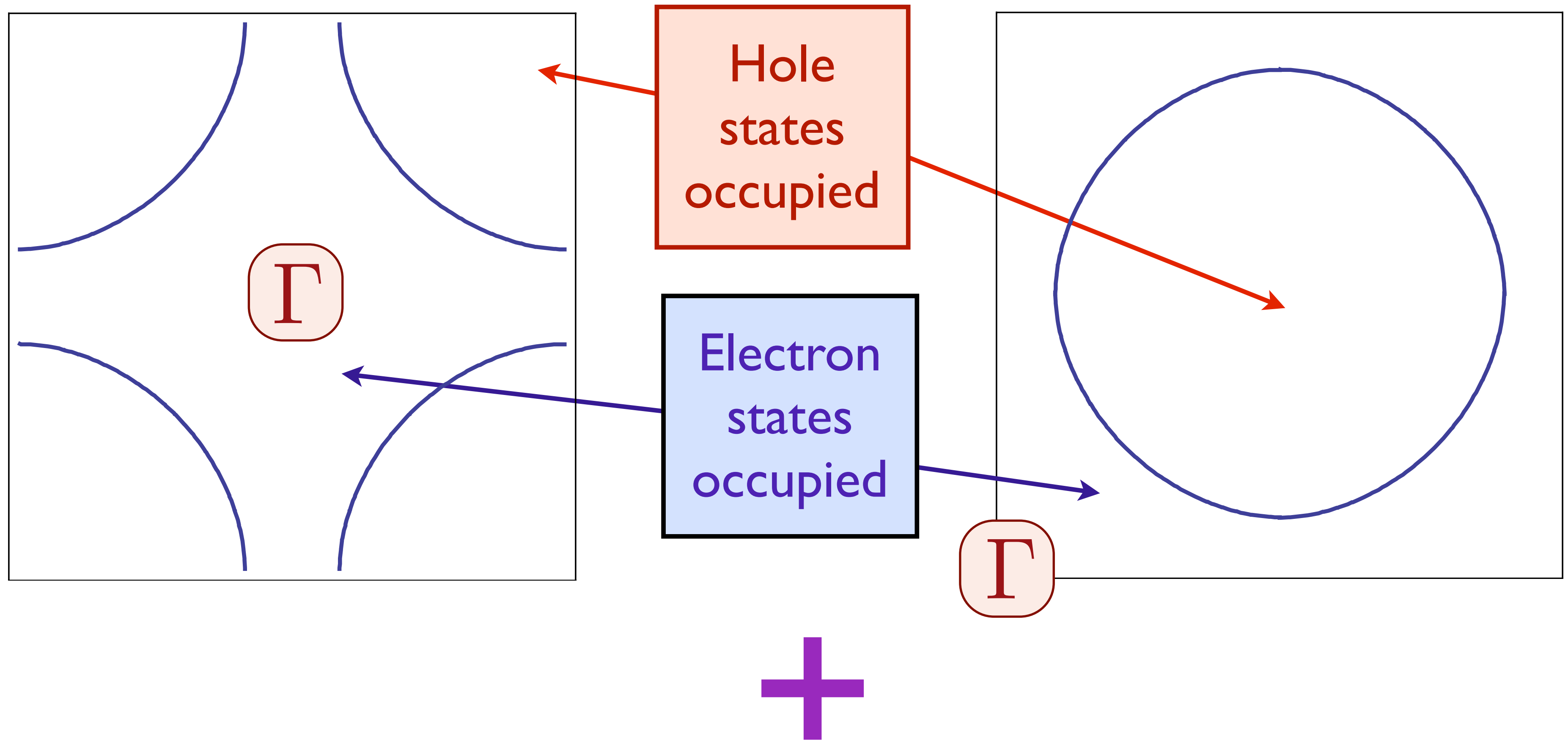

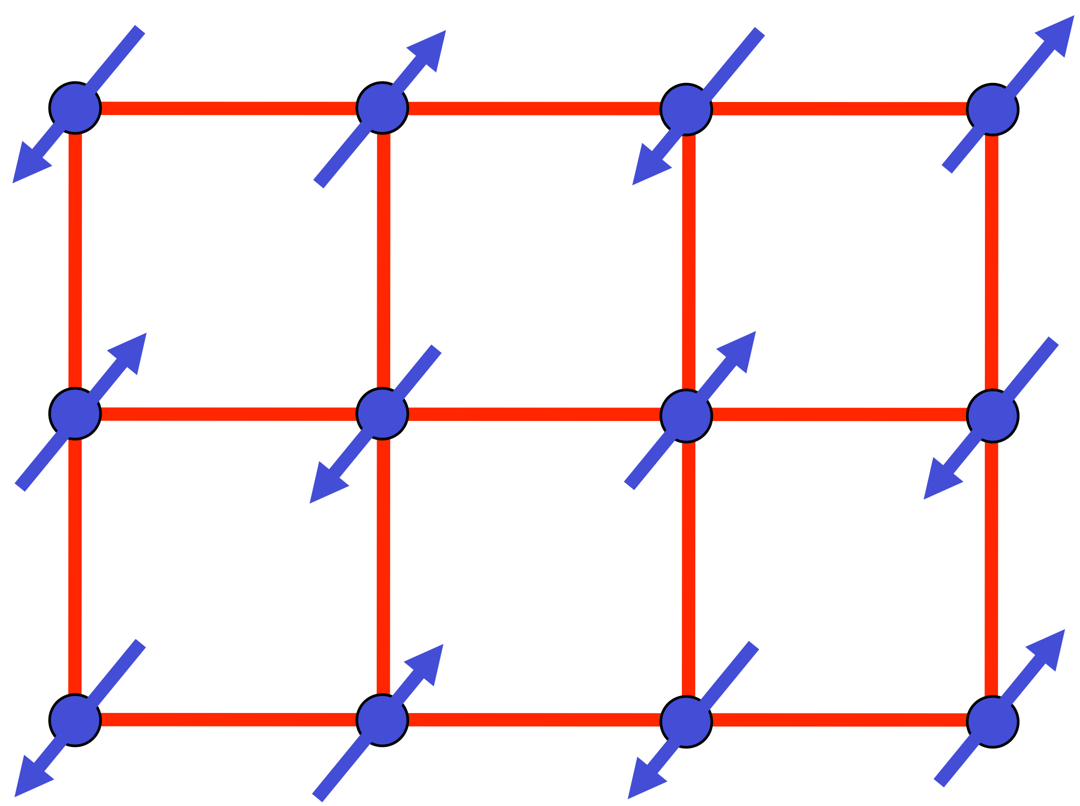

The electron spin polarization obeys

$$\left\langle \vec{S}(\mathbf{r},\tau) \right\rangle = \vec{\varphi}(\mathbf{r},\tau) e^{i\mathbf{K}\cdot\mathbf{r}}$$

where $\mathbf{K}$ is the ordering wavevector.

Hole-doped cuprates

Increasing SDW order

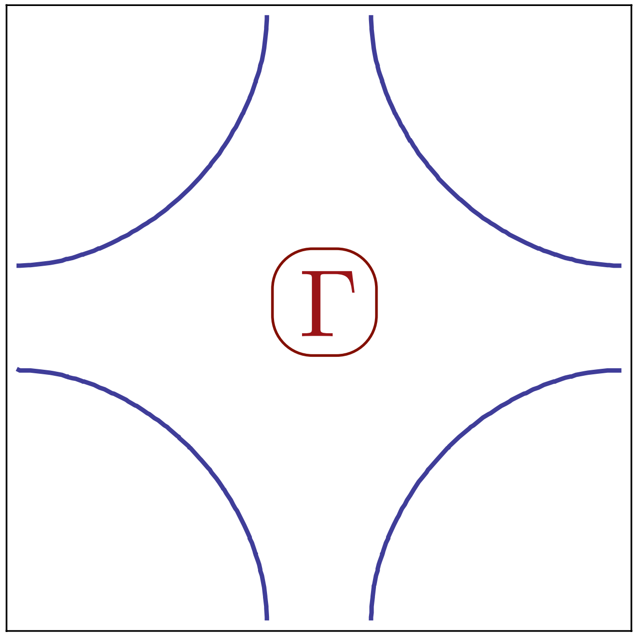

S. Sachdev, A. V. Chubukov, and A. Sokol, *Phys. Rev. B* **51**, 14874 (1995).
A. V. Chubukov and D. K. Morr, *Physics Reports* **288**, 355 (1997).

Hole-doped cuprates

Increasing SDW order

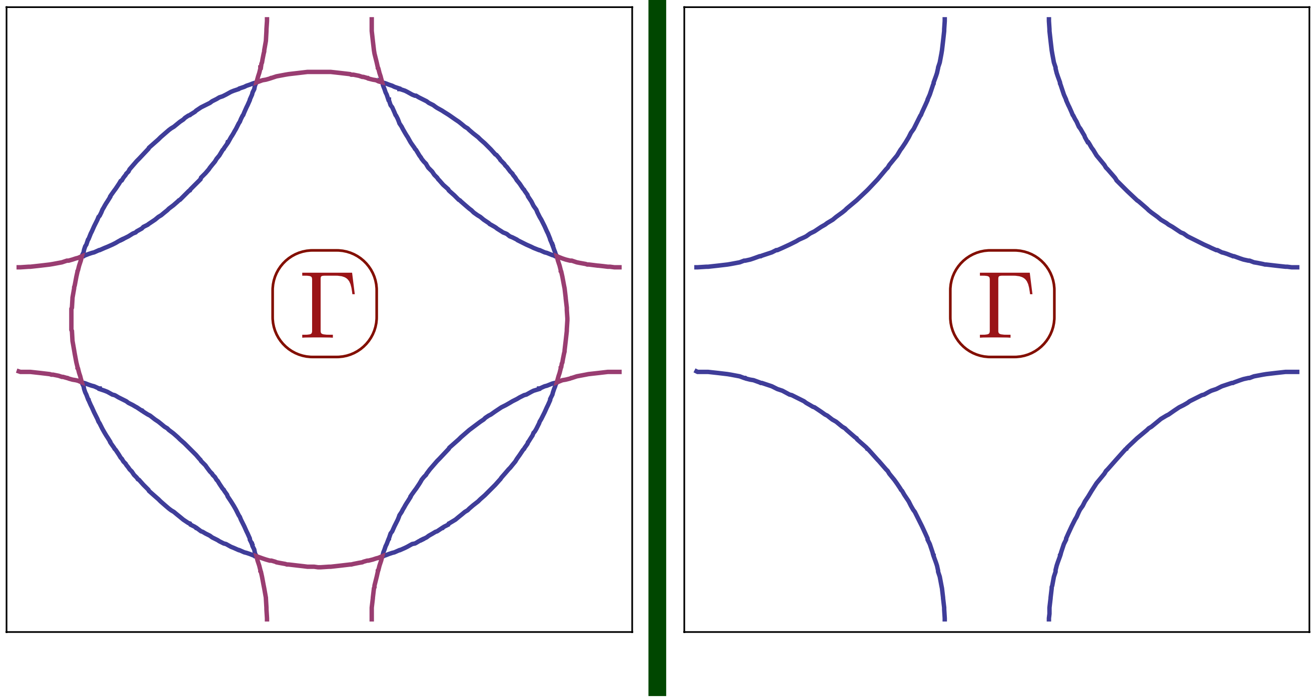

S. Sachdev, A. V. Chubukov, and A. Sokol, *Phys. Rev. B* **51**, 14874 (1995).
A. V. Chubukov and D. K. Morr, *Physics Reports* **288**, 355 (1997).

Hole-doped cuprates

Increasing SDW order

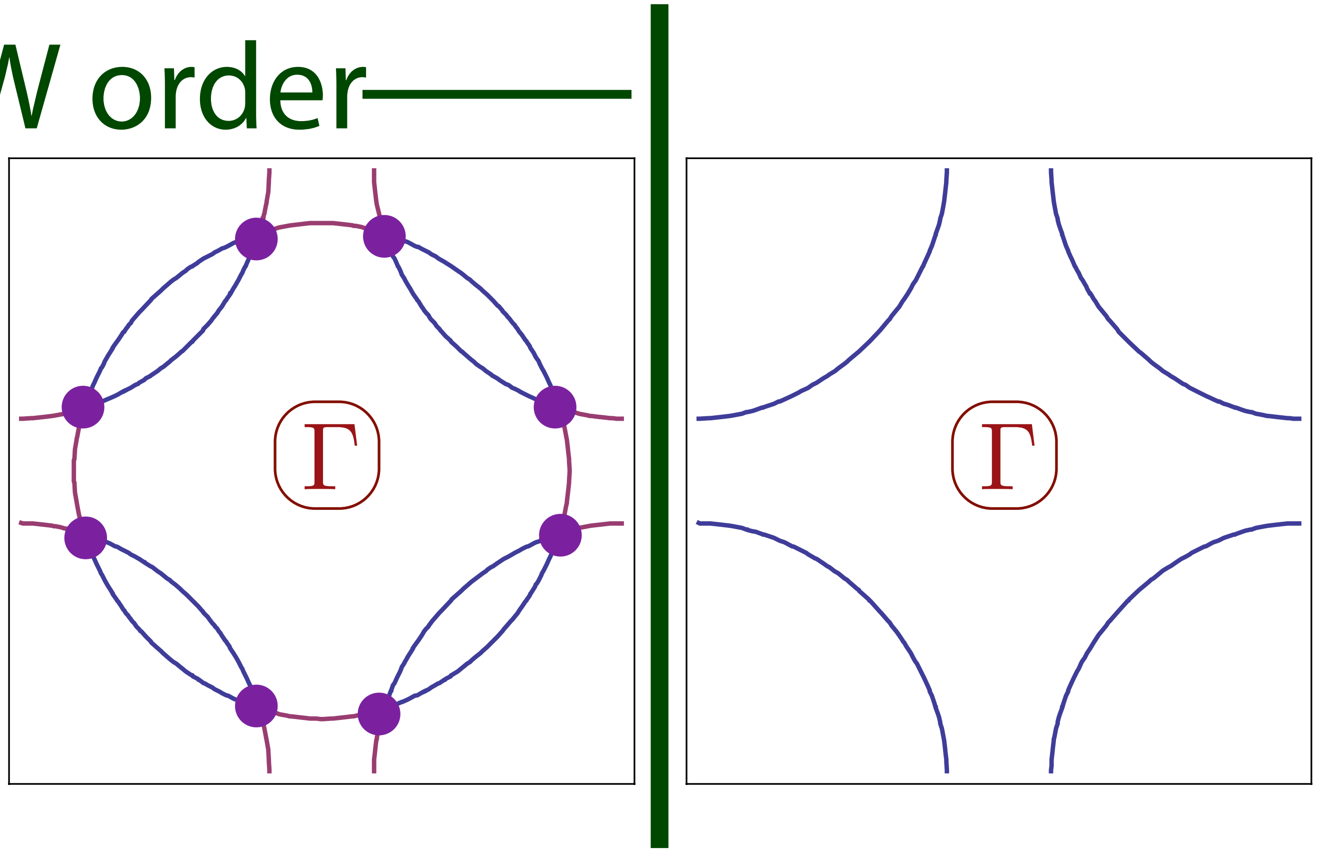

Hot spots

S. Sachdev, A. V. Chubukov, and A. Sokol, *Phys. Rev. B* **51**, 14874 (1995).
A. V. Chubukov and D. K. Morr, *Physics Reports* **288**, 355 (1997).

Hole-doped cuprates

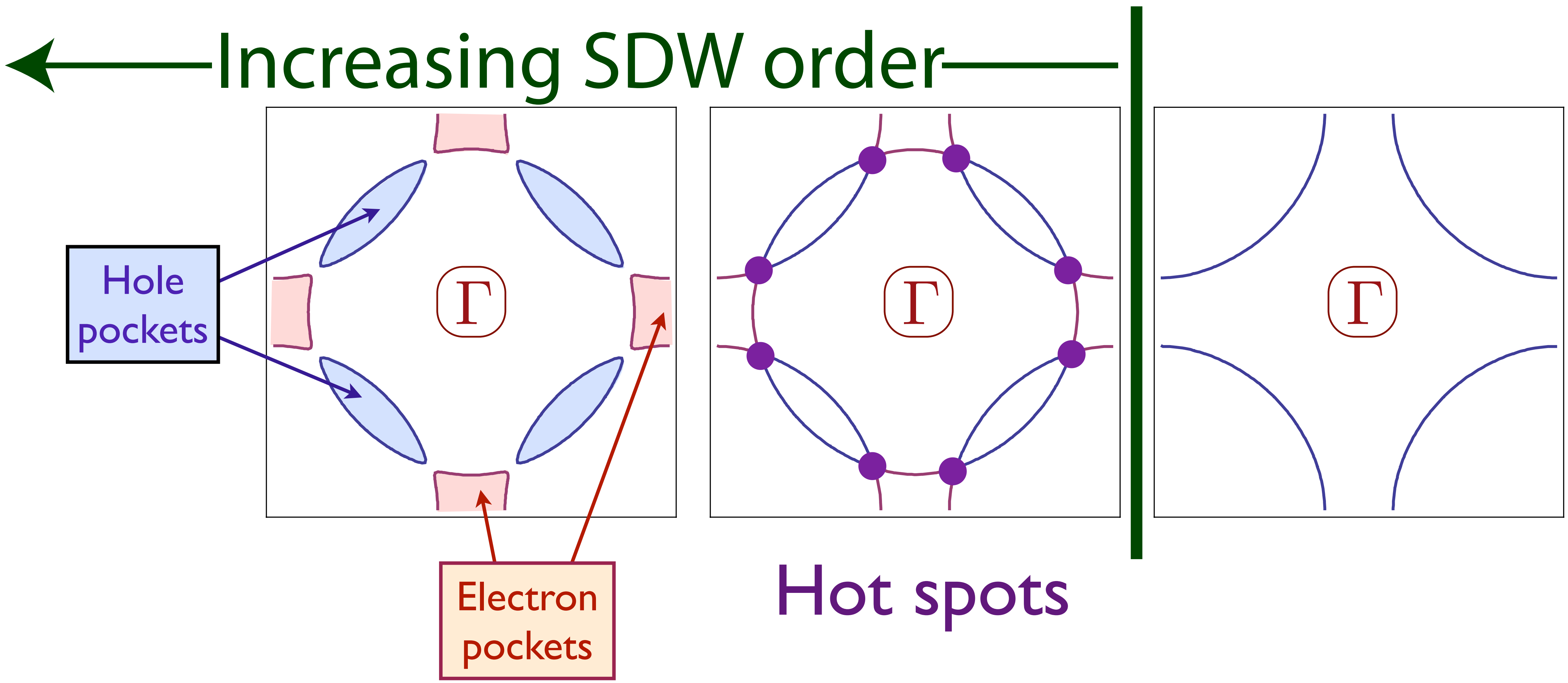

Fermi surface breaks up at hot spots into electron and hole "pockets"

S. Sachdev, A. V. Chubukov, and A. Sokol, *Phys. Rev. B* **51**, 14874 (1995).
A. V. Chubukov and D. K. Morr, *Physics Reports* **288**, 355 (1997).

Hole-doped cuprates

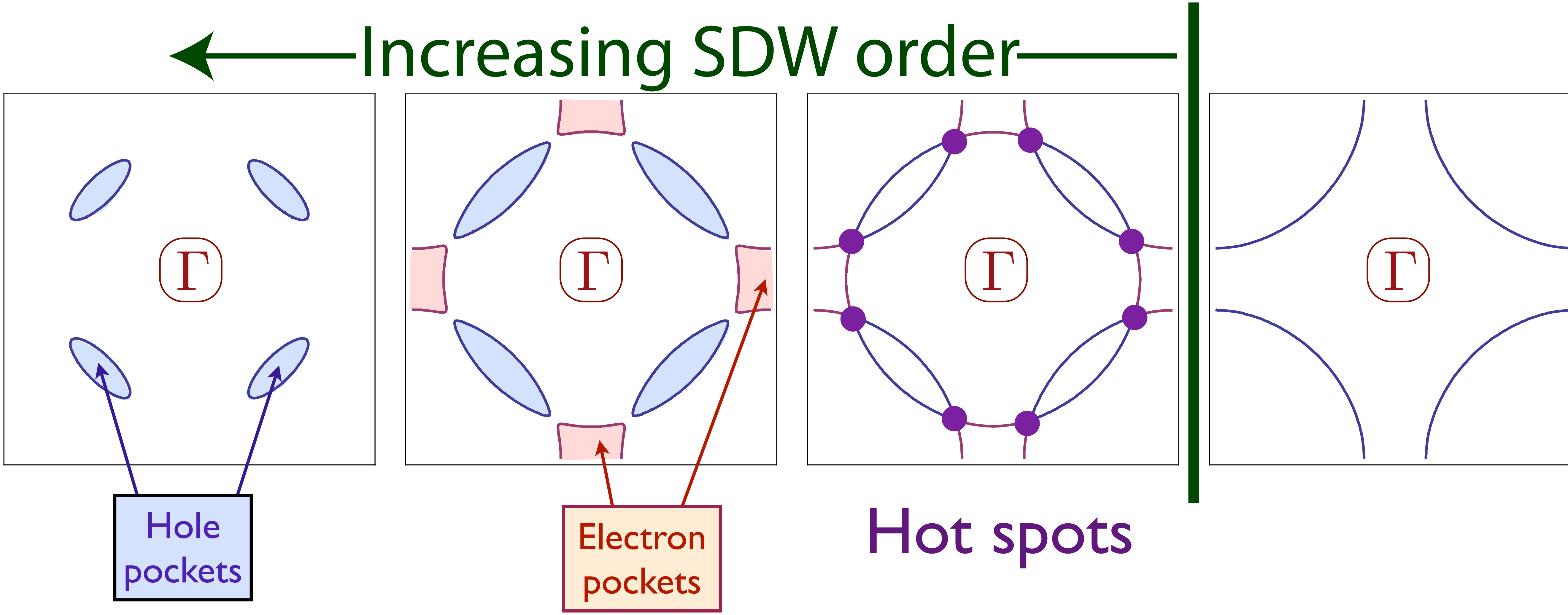

Fermi surface breaks up at hot spots into electron and hole "pockets"

S. Sachdev, A.V. Chubukov, and A. Sokol, *Phys. Rev. B* **51**, 14874 (1995).
A.V. Chubukov and D. K. Morr, *Physics Reports* **288**, 355 (1997).

Hole-doped cuprates

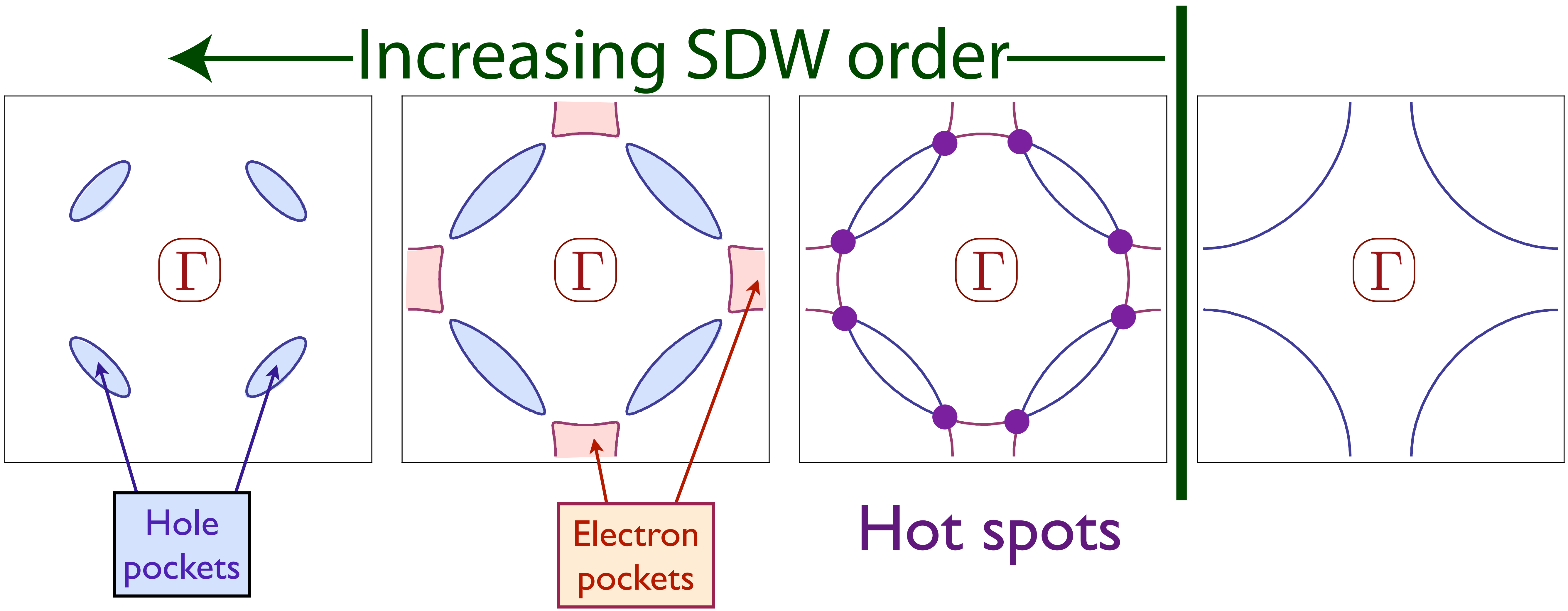

Fermi surface breaks up at hot spots into electron and hole "pockets"

S. Sachdev, A. V. Chubukov, and A. Sokol, *Phys. Rev. B* **51**, 14874 (1995).
A. V. Chubukov and D. K. Morr, *Physics Reports* **288**, 355 (1997).

Quantum oscillations

Electron pockets in the Fermi surface of hole-doped high-T_c superconductors

David LeBoeuf[1], Nicolas Doiron-Leyraud[1], Julien Levallois[2], R. Daou[1], J.-B. Bonnemaison[1], N. E. Hussey[3], L. Balicas[4], B. J. Ramshaw[5], Ruixing Liang[5,6], D. A. Bonn[5,6], W. N. Hardy[5,6], S. Adachi[7], Cyril Proust[2] & Louis Taillefer[1,6]

Nature **450**, 533 (2007)

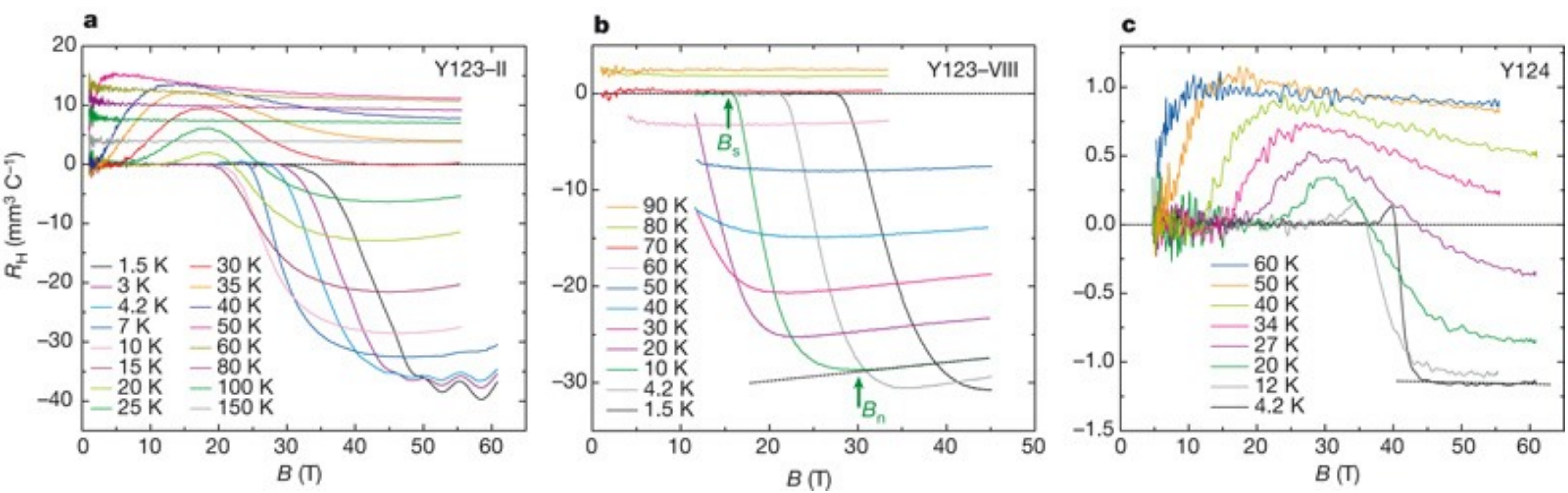

Quantum oscillations

Electron pockets in the Fermi surface of hole-doped high-T_c superconductors

David LeBoeuf[1], Nicolas Doiron-Leyraud[1], Julien Levallois[2], R. Daou[1], J.-B. Bonnemaison[1], N. E. Hussey[3], L. Balicas[4], B. J. Ramshaw[5], Ruixing Liang[5,6], D. A. Bonn[5,6], W. N. Hardy[5,6], S. Adachi[7], Cyril Proust[2] & Louis Taillefer[1,6]

Nature **450**, 533 (2007)

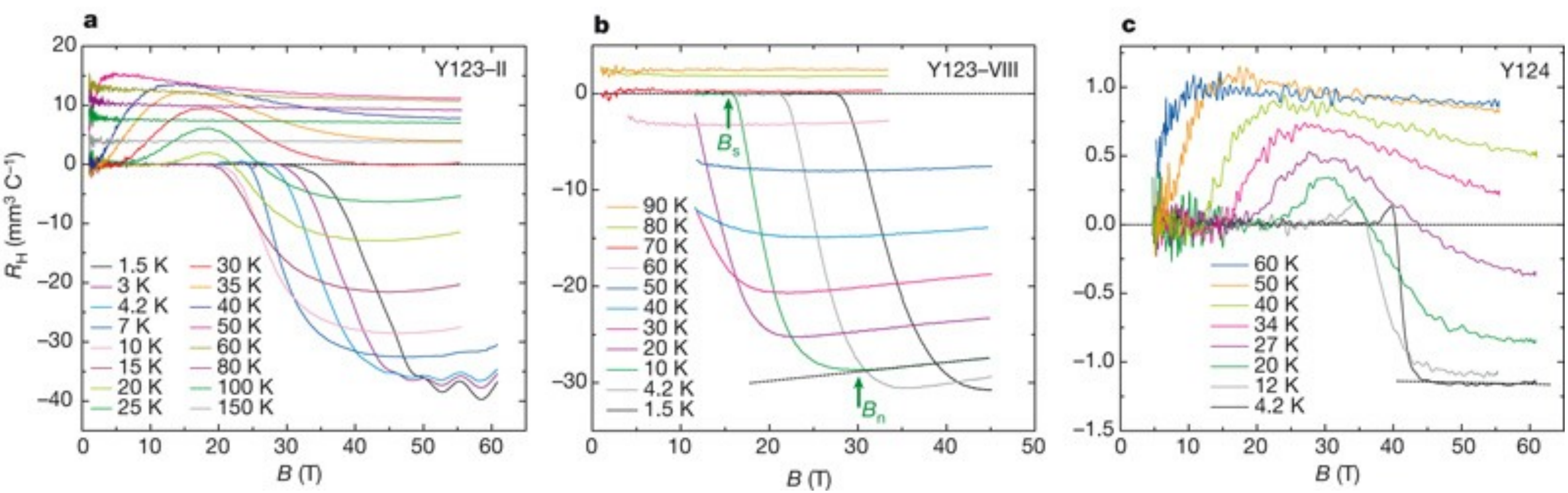

Evidence for small Fermi pockets

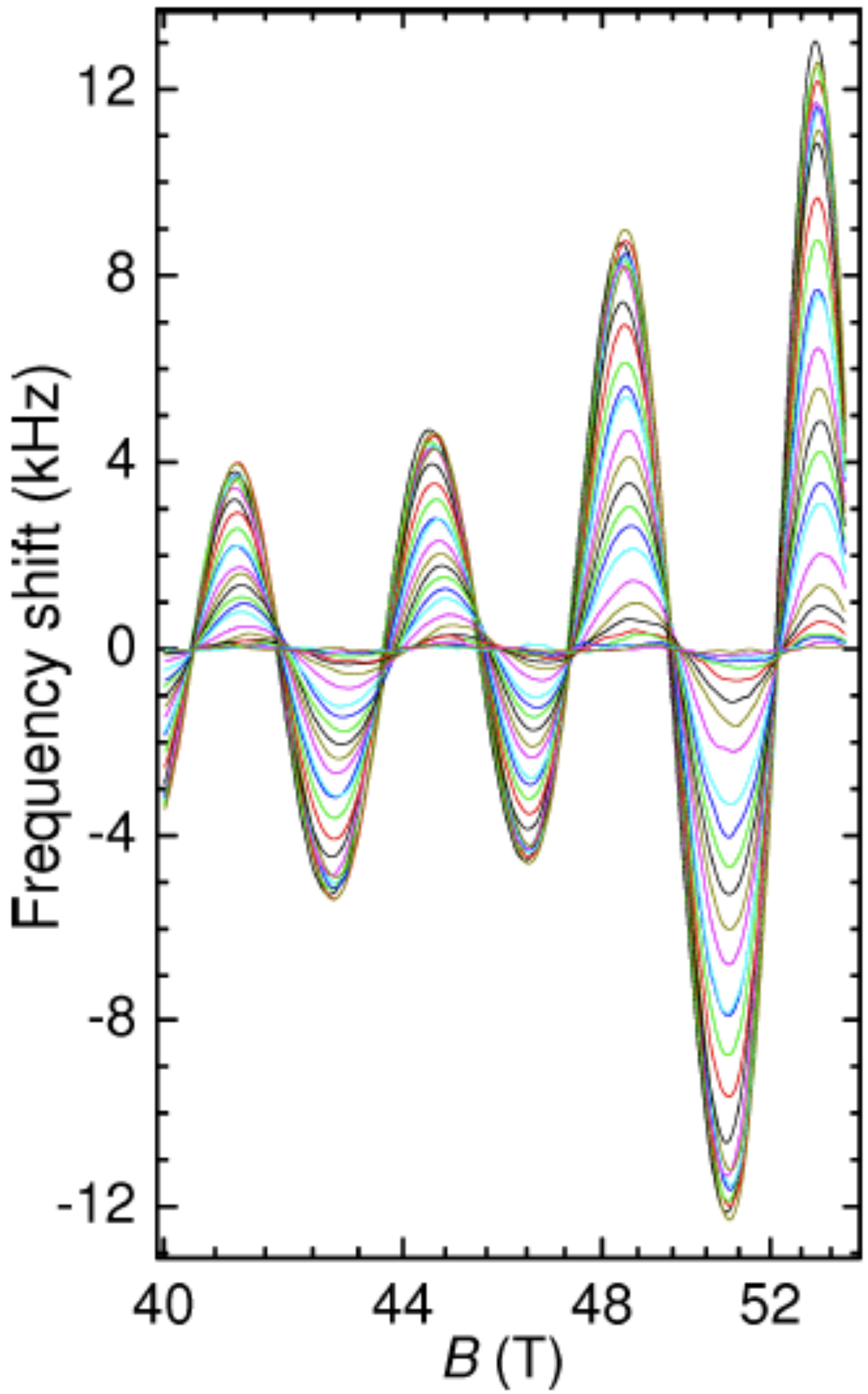

FIG. 2: Magnetic quantum oscillations measured in $YBa_2Cu_3O_{6+x}$ with $x \approx 0.56$ (after background polynomial subtraction). This restricted interval in $B = |\mathbf{B}|$ furnishes a dynamic range of ~ 50 dB between $T = 1$ and 18 K. The actual T values are provided in Fig. 3.

Fermi liquid behaviour in an underdoped high Tc superconductor

Suchitra E. Sebastian, N. Harrison,
M. M. Altarawneh, Ruixing Liang, D. A. Bonn,
W. N. Hardy, and G. G. Lonzarich

arXiv:0912.3022

Theory of quantum criticality in the cuprates

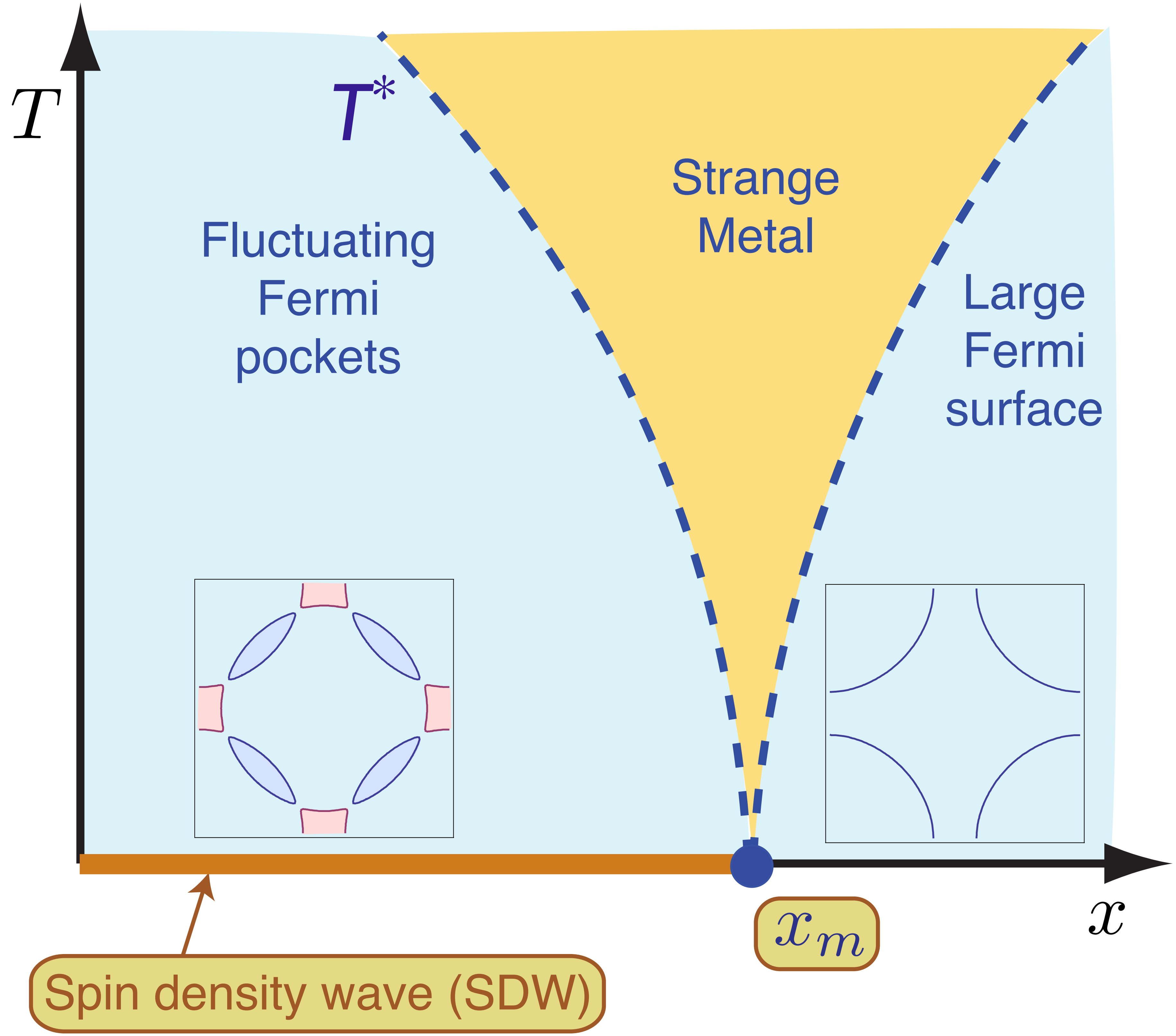

Underlying SDW ordering quantum critical point in **metal** at $x = x_m$

Evidence for connection between linear resistivity and stripe-ordering in a cuprate with a low T_c

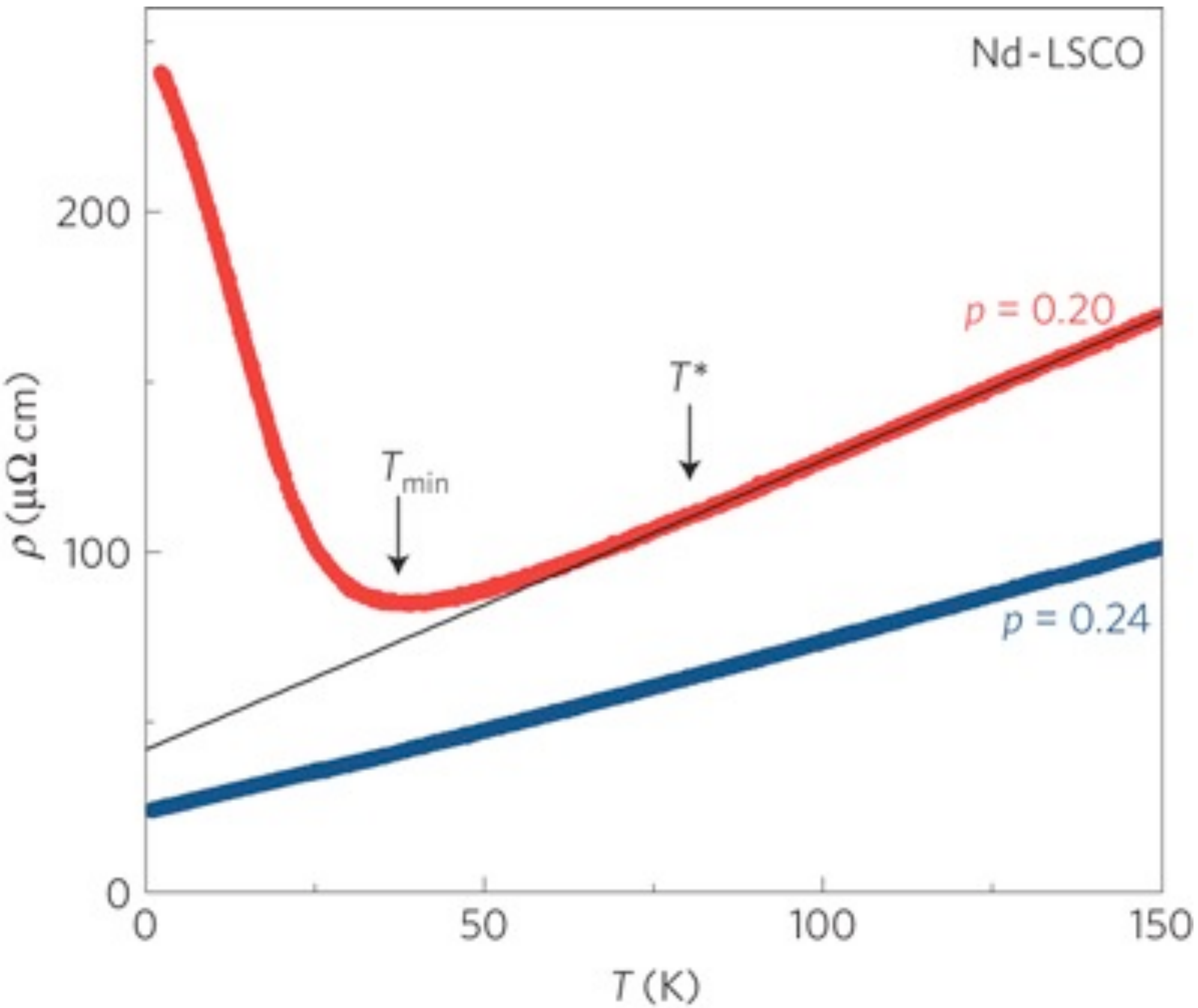

- Magnetic field of upto 35 T used to suppress superconductivity
- Identifies $x_m \approx 0.24$

Linear temperature dependence of resistivity and change in the Fermi surface at the pseudogap critical point of a high-T_c superconductor

R. Daou, Nicolas Doiron-Leyraud, David LeBoeuf, S. Y. Li, Francis Laliberté, Olivier Cyr-Choinière, Y. J. Jo, L. Balicas, J.-Q. Yan, J.-S. Zhou, J. B. Goodenough & Louis Taillefer, *Nature Physics* **5**, 31 - 34 (2009)

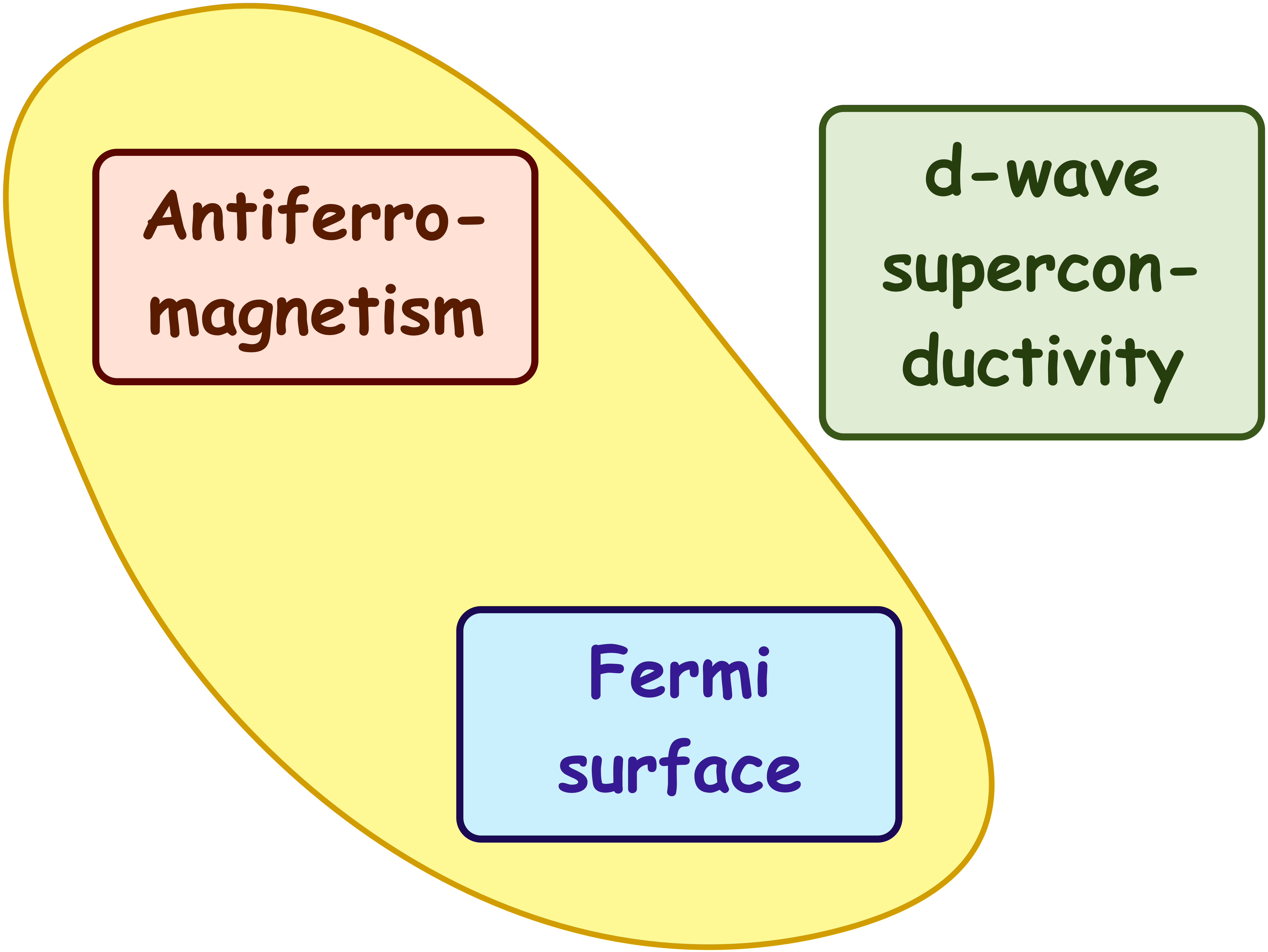
Antiferro-
magnetism
d-wave
supercon-
ductivity
Fermi
surface

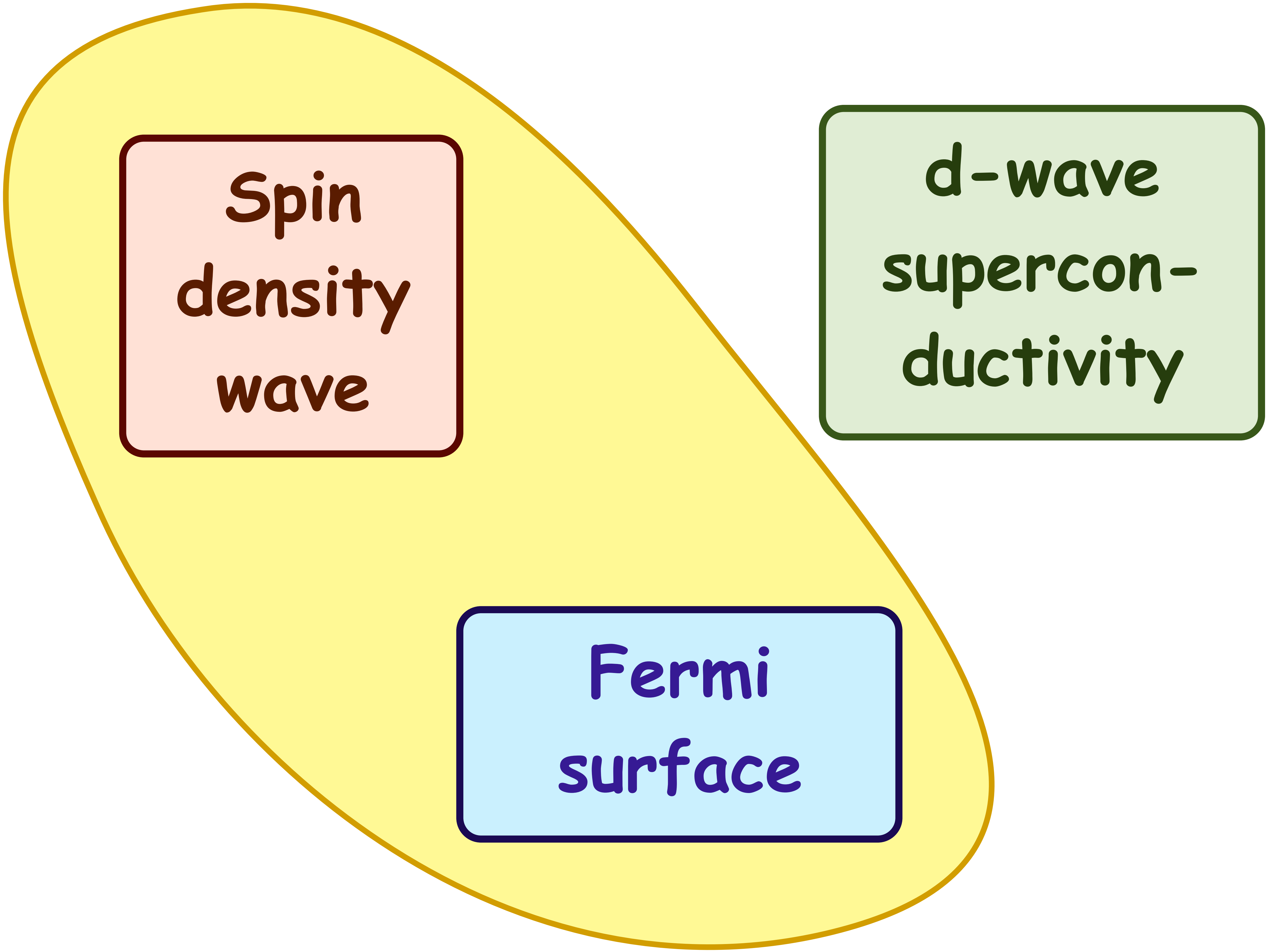
Spin density wave
d-wave supercon-ductivity
Fermi surface

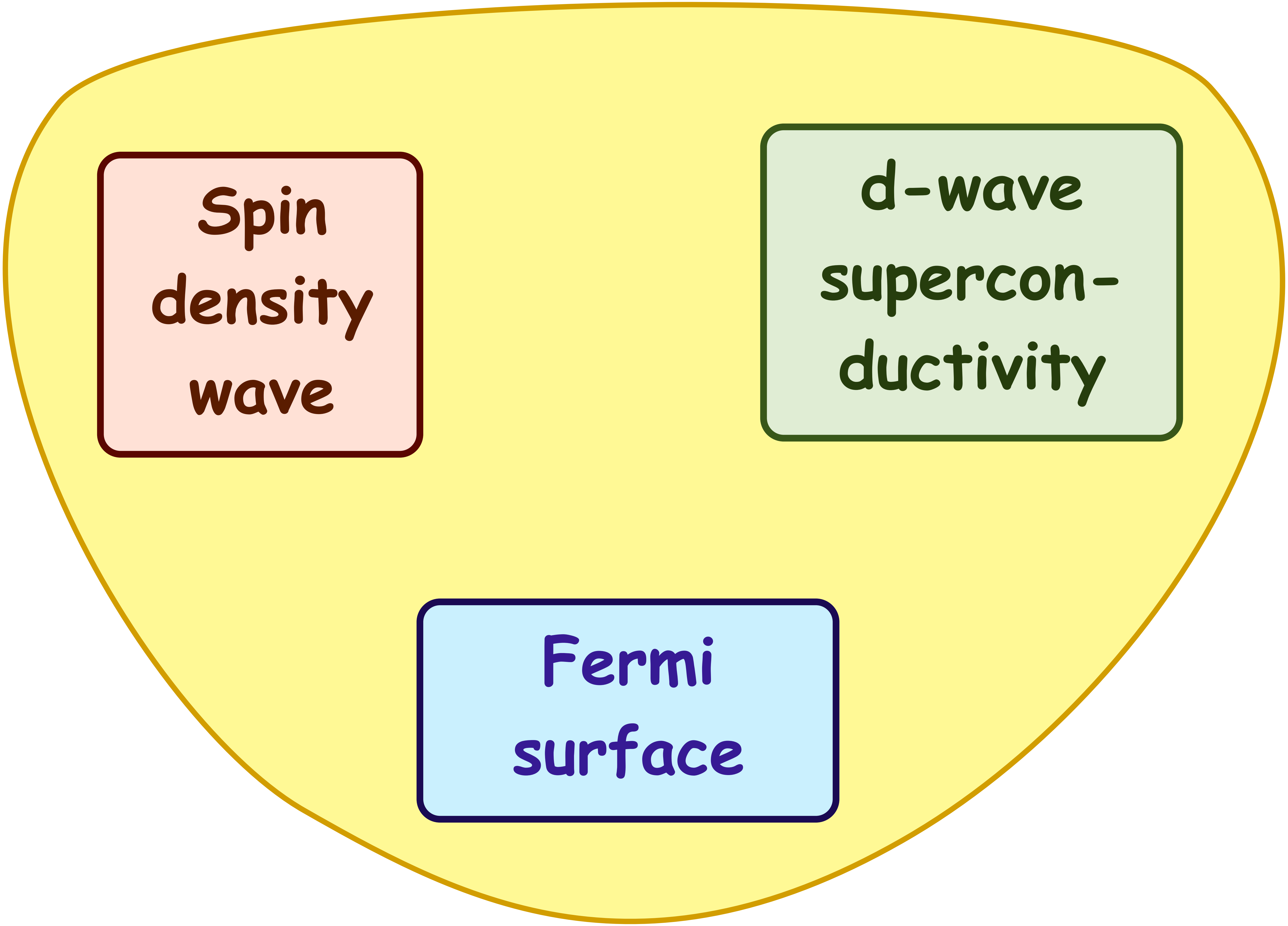
Spin density wave
d-wave supercon-ductivity
Fermi surface

Theory of quantum criticality in the cuprates

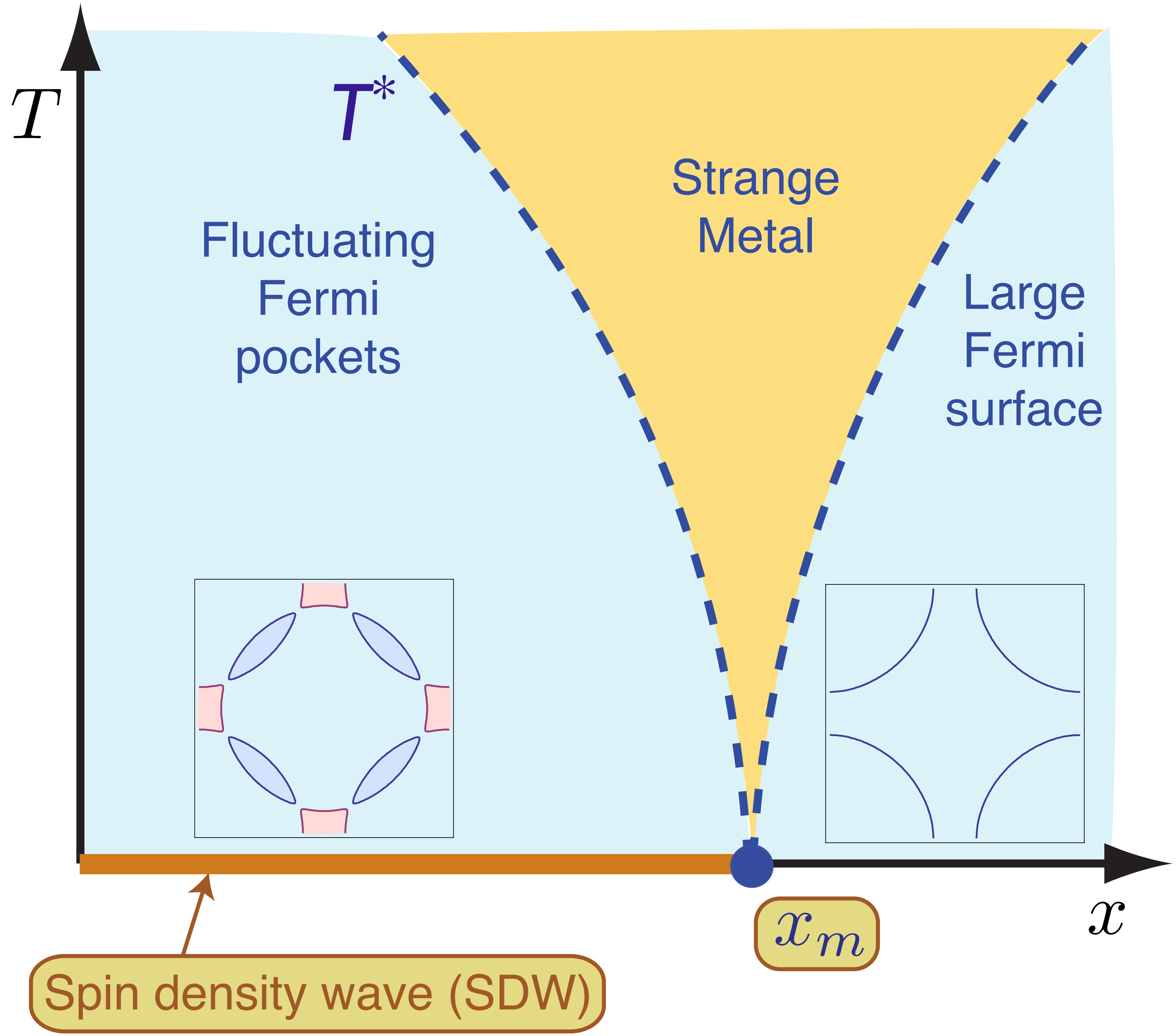

Underlying SDW ordering quantum critical point in **metal** at $x = x_m$

Theory of quantum criticality in the cuprates

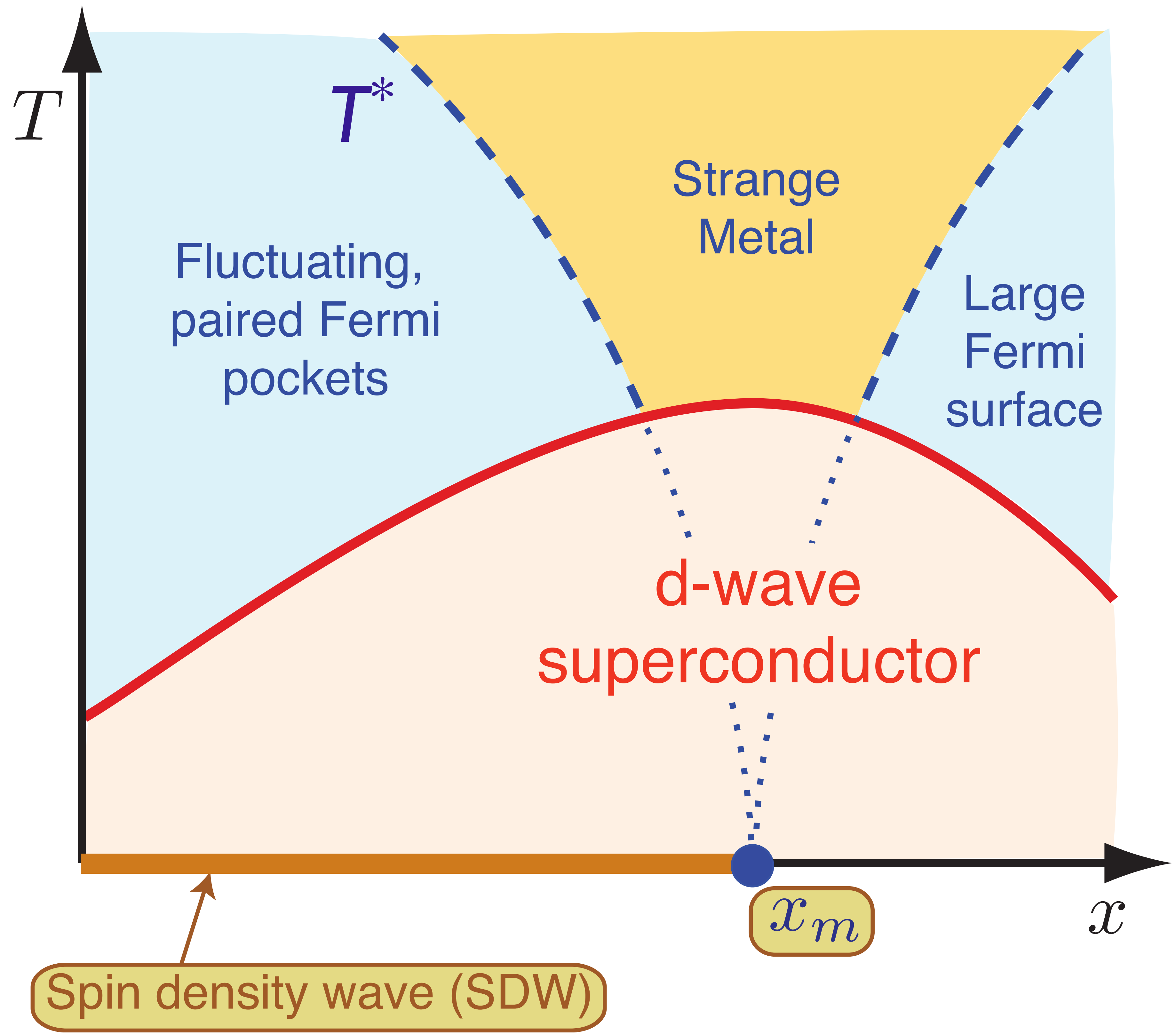

Onset of d-wave superconductivity hides the critical point $x = x_m$

Theory of quantum criticality in the cuprates

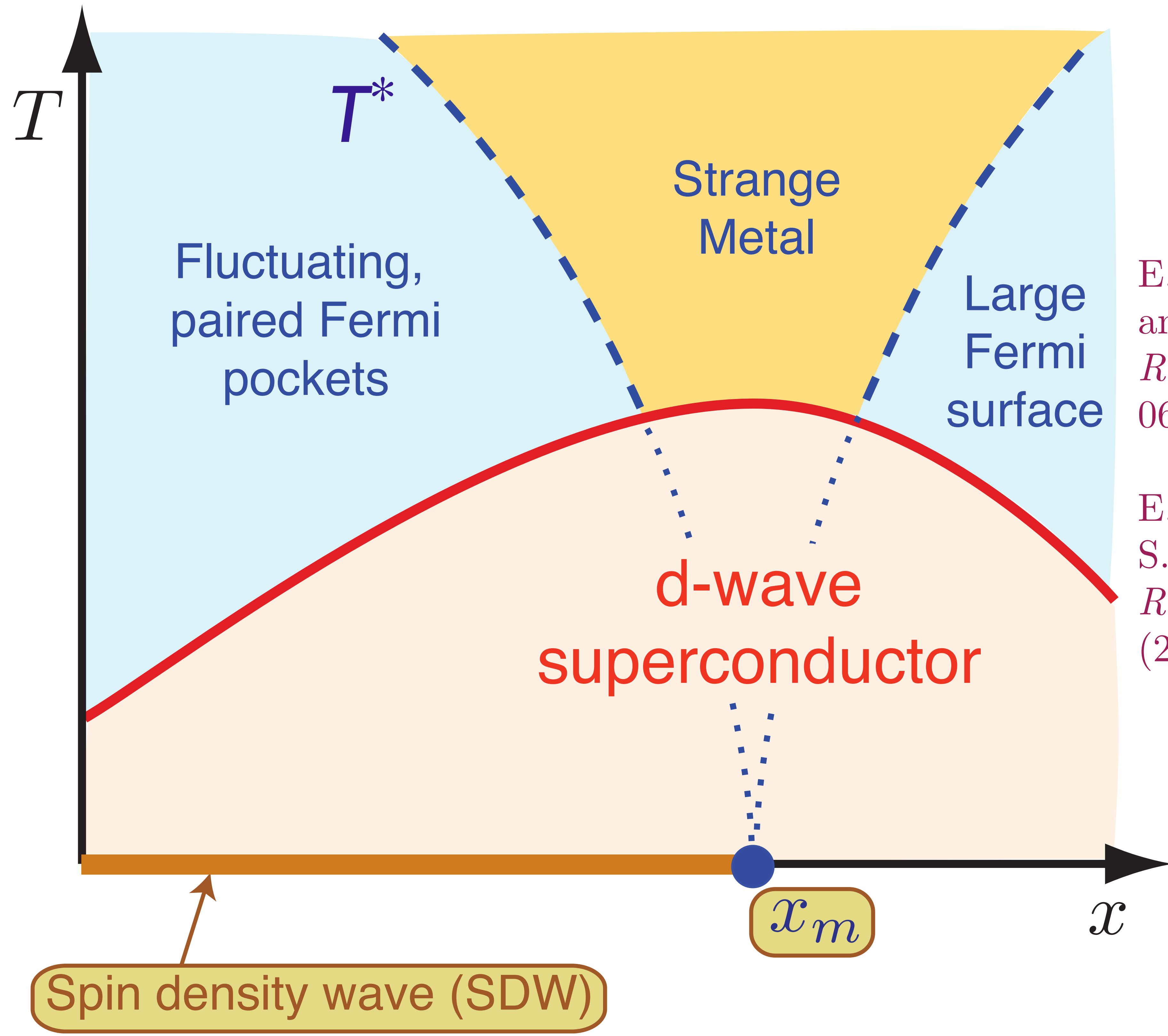

E. Demler, S. Sachdev and Y. Zhang, *Phys. Rev. Lett.* **87**, 067202 (2001).

E. G. Moon and S. Sachdev, *Phy. Rev. B* **80**, 035117 (2009)

Competition between SDW order and superconductivity moves the actual quantum critical point to $x = x_s < x_m$.

Theory of quantum criticality in the cuprates

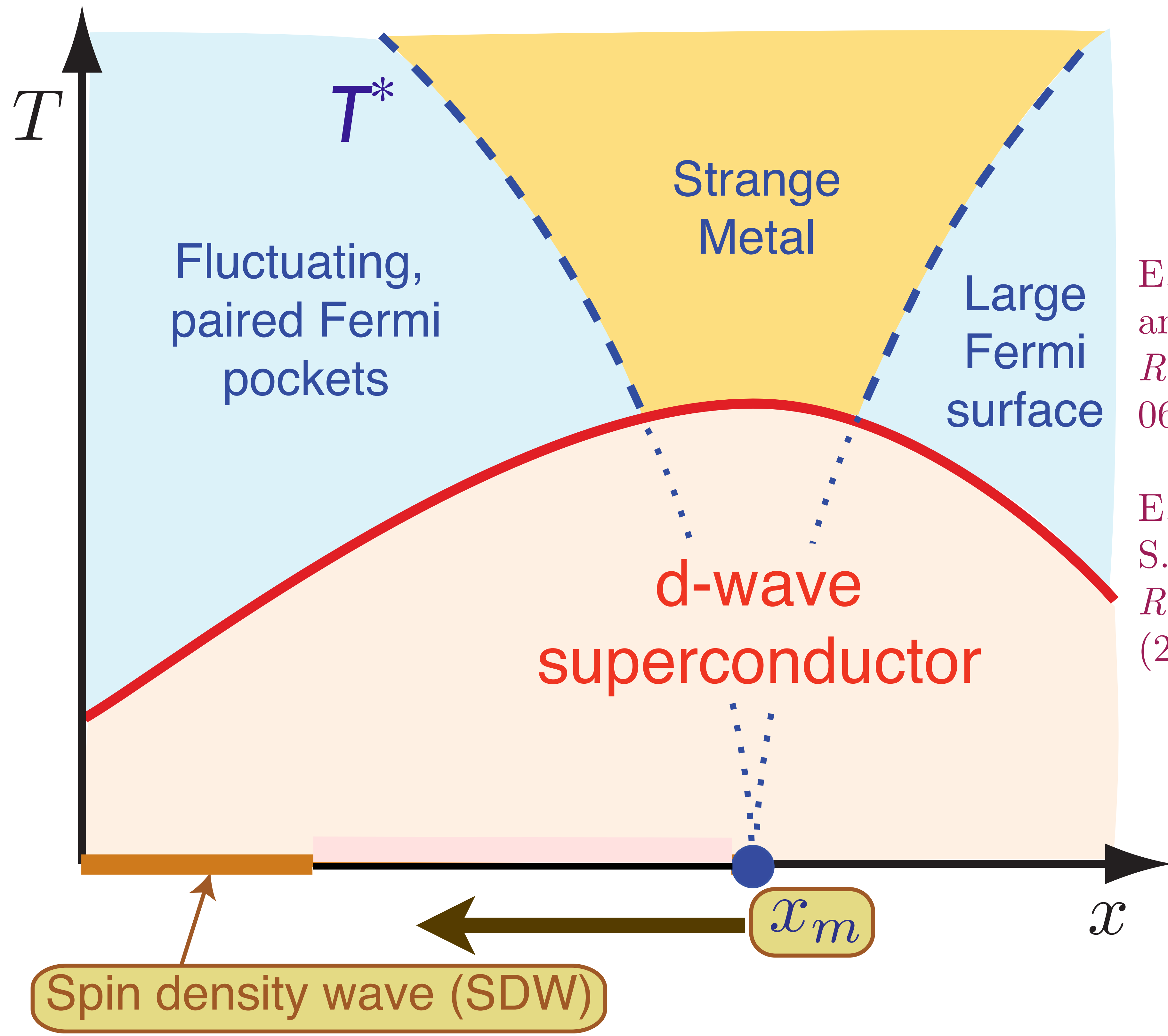

E. Demler, S. Sachdev and Y. Zhang, *Phys. Rev. Lett.* **87**, 067202 (2001).

E. G. Moon and S. Sachdev, *Phy. Rev. B* **80**, 035117 (2009)

Competition between SDW order and superconductivity moves the actual quantum critical point to $x = x_s < x_m$.

Theory of quantum criticality in the cuprates

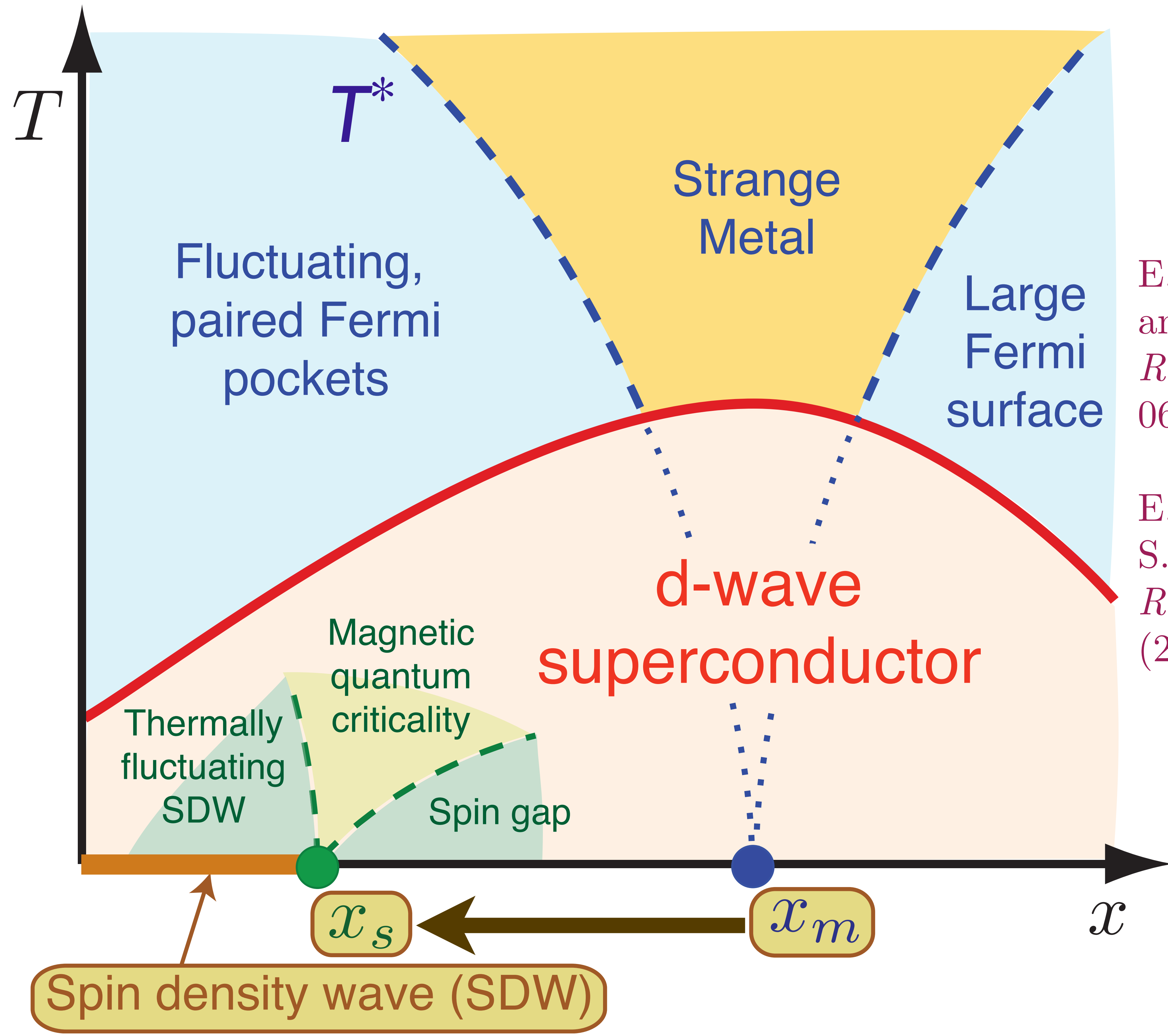

E. Demler, S. Sachdev and Y. Zhang, *Phys. Rev. Lett.* **87**, 067202 (2001).

E. G. Moon and S. Sachdev, *Phy. Rev. B* **80**, 035117 (2009)

Competition between SDW order and superconductivity moves the actual quantum critical point to $x = x_s < x_m$.

Theory of quantum criticality in the cuprates

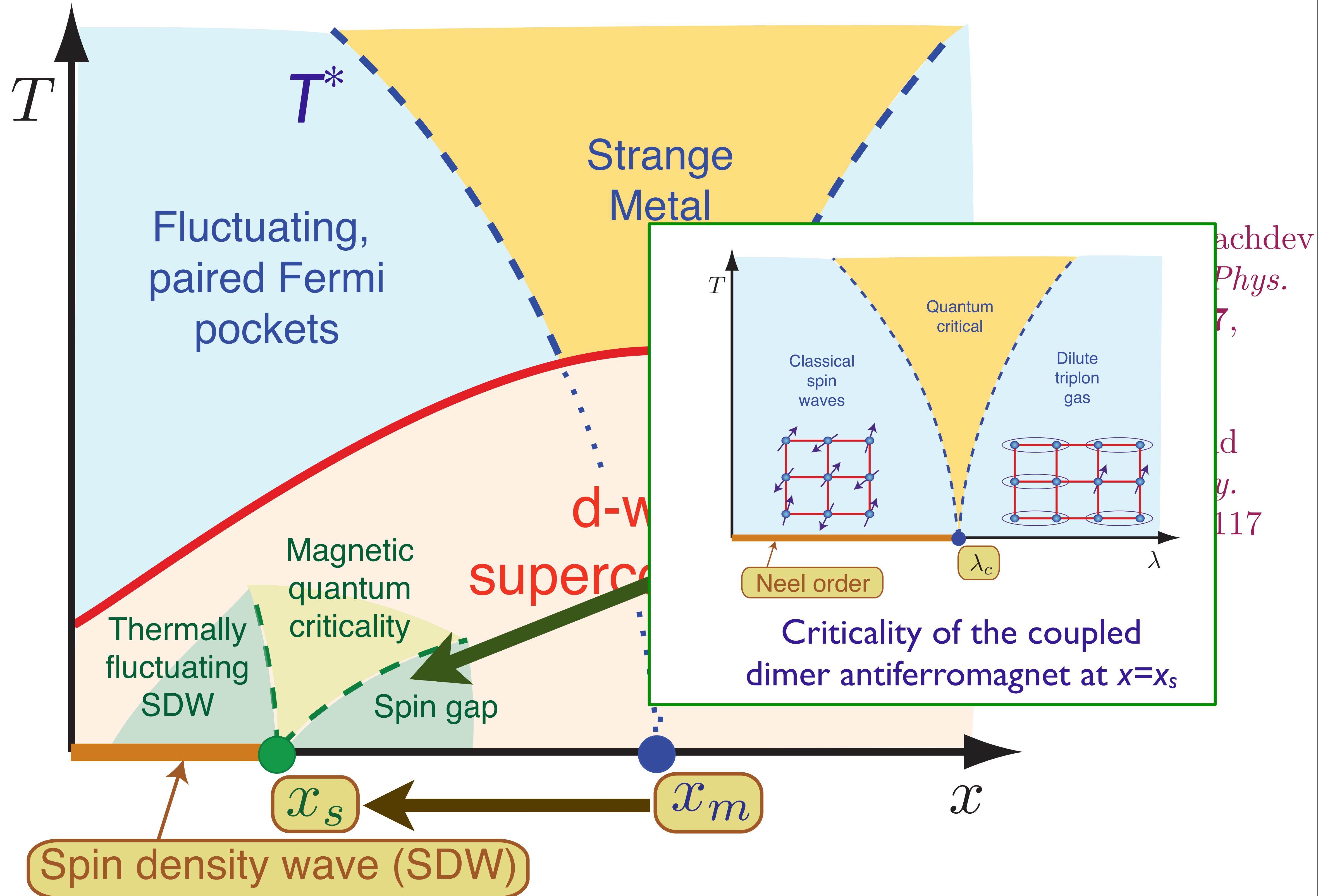

Competition between SDW order and superconductivity moves the actual quantum critical point to $x = x_s < x_m$.

Theory of quantum criticality in the cuprates

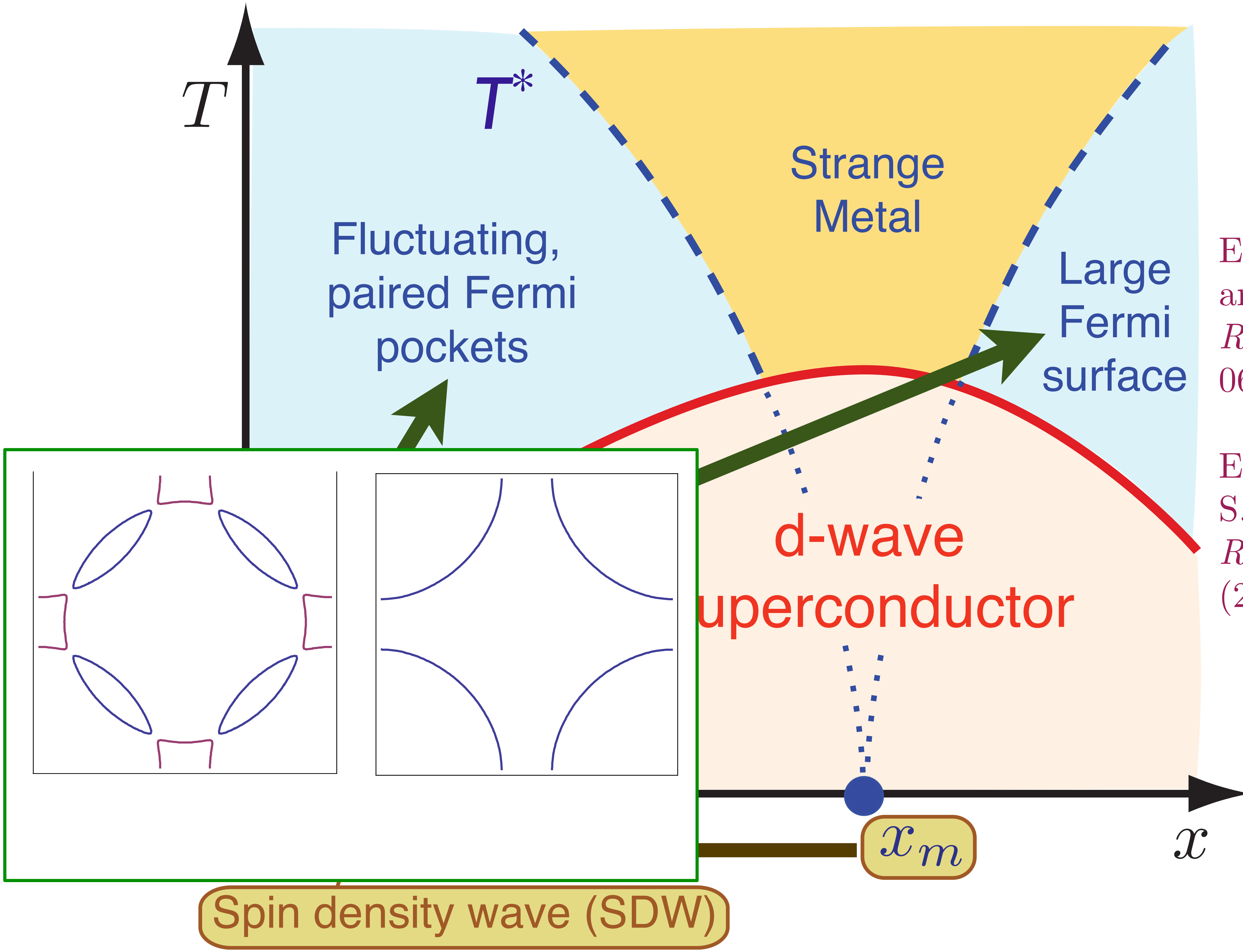

E. Demler, S. Sachdev and Y. Zhang, *Phys. Rev. Lett.* **87**, 067202 (2001).

E. G. Moon and S. Sachdev, *Phy. Rev. B* **80**, 035117 (2009)

Competition between SDW order and superconductivity moves the actual quantum critical point to $x = x_s < x_m$.

Theory of quantum criticality in the cuprates

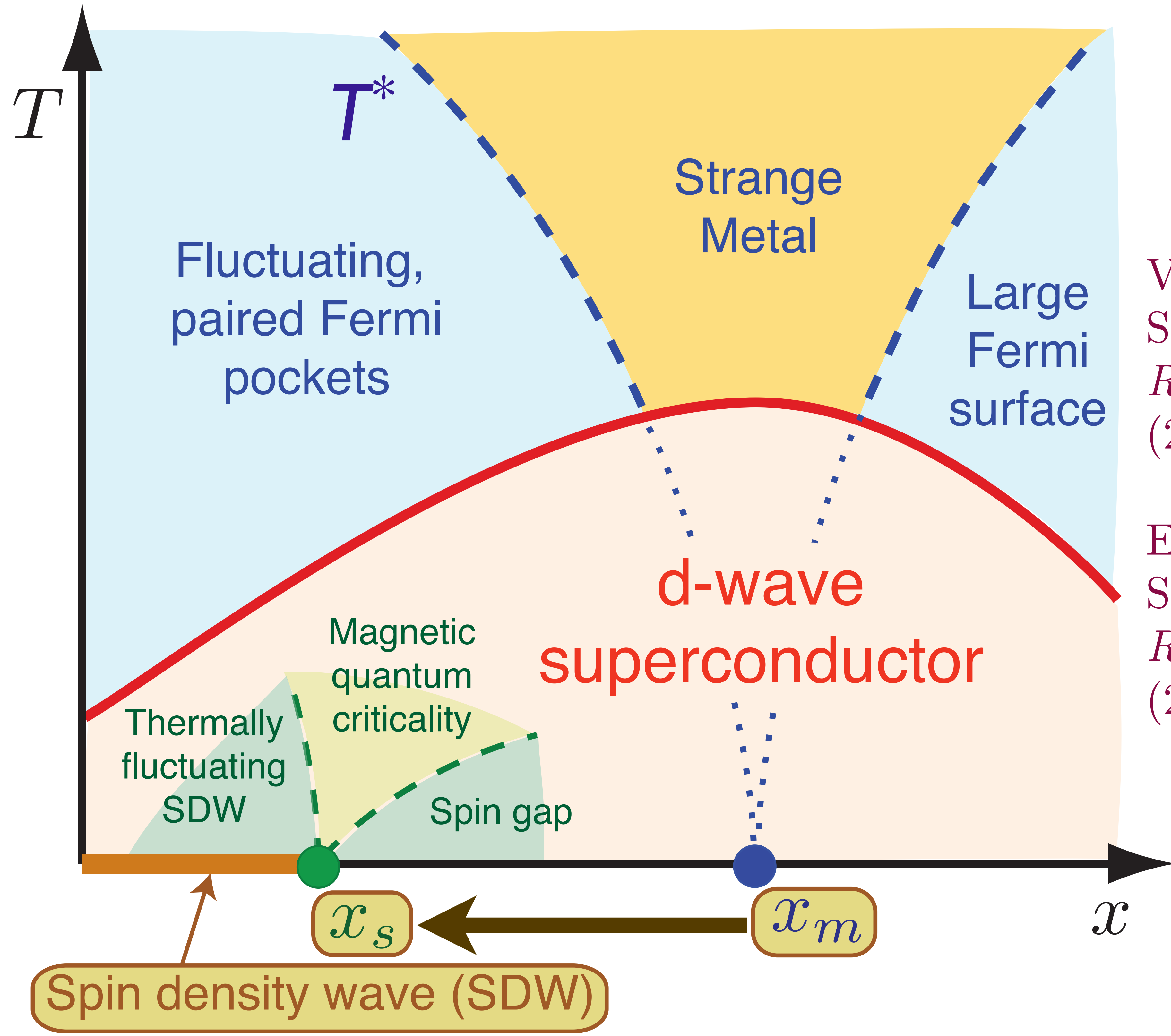

V. Galitski and S. Sachdev, *Phys. Rev.* B **79**, 134512 (2009).

E. G. Moon and S. Sachdev, *Phys. Rev. B* **80**, 035117 (2009)

Physics of competition: d-wave SC and SDW "eat up" same pieces of the large Fermi surface.

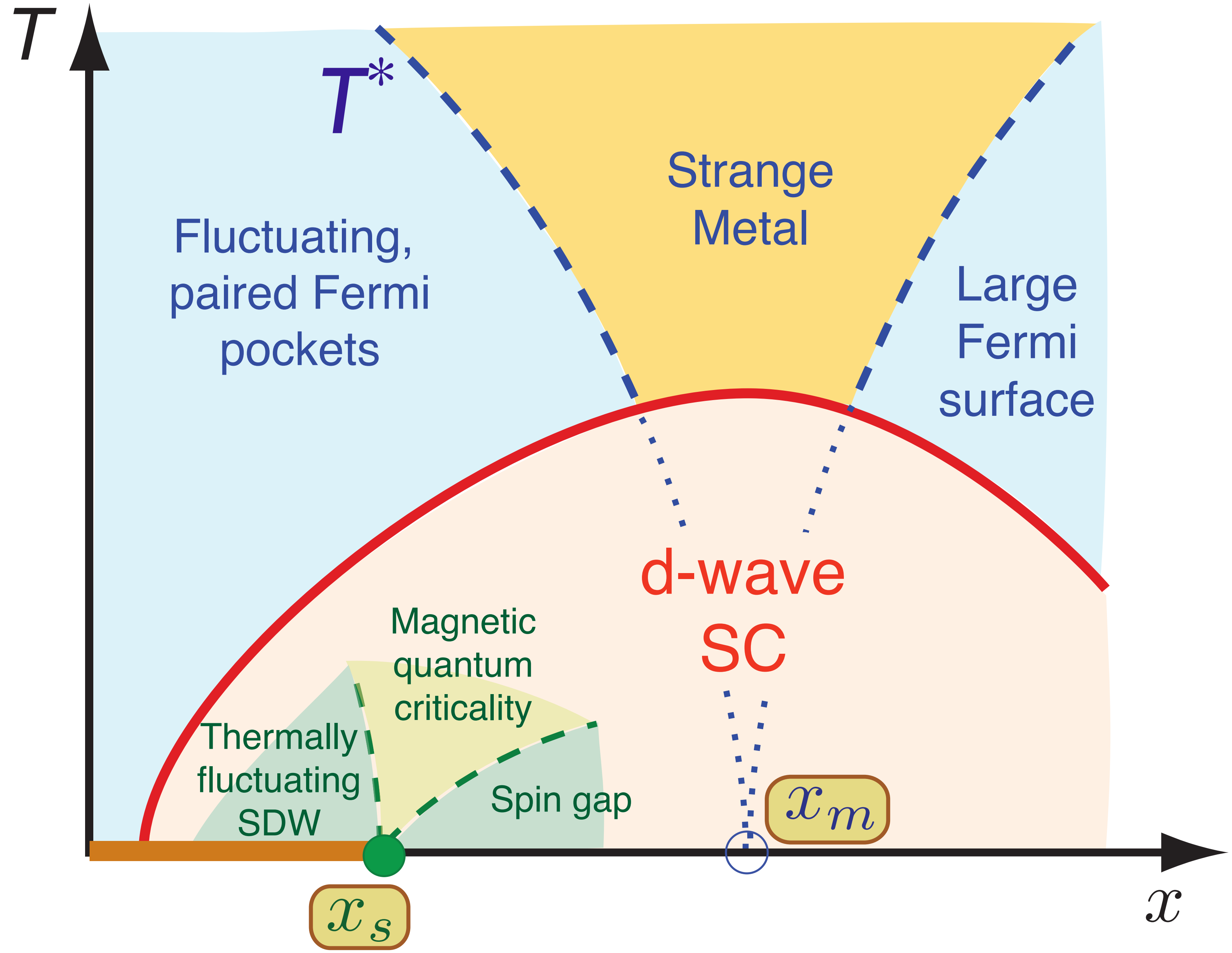
T
T*
Fluctuating,
paired Fermi
pockets
Strange
Metal
Large
Fermi
surface
d-wave
SC
Magnetic
quantum
criticality
Thermally
fluctuating
SDW
Spin gap
x_m
x_s
x

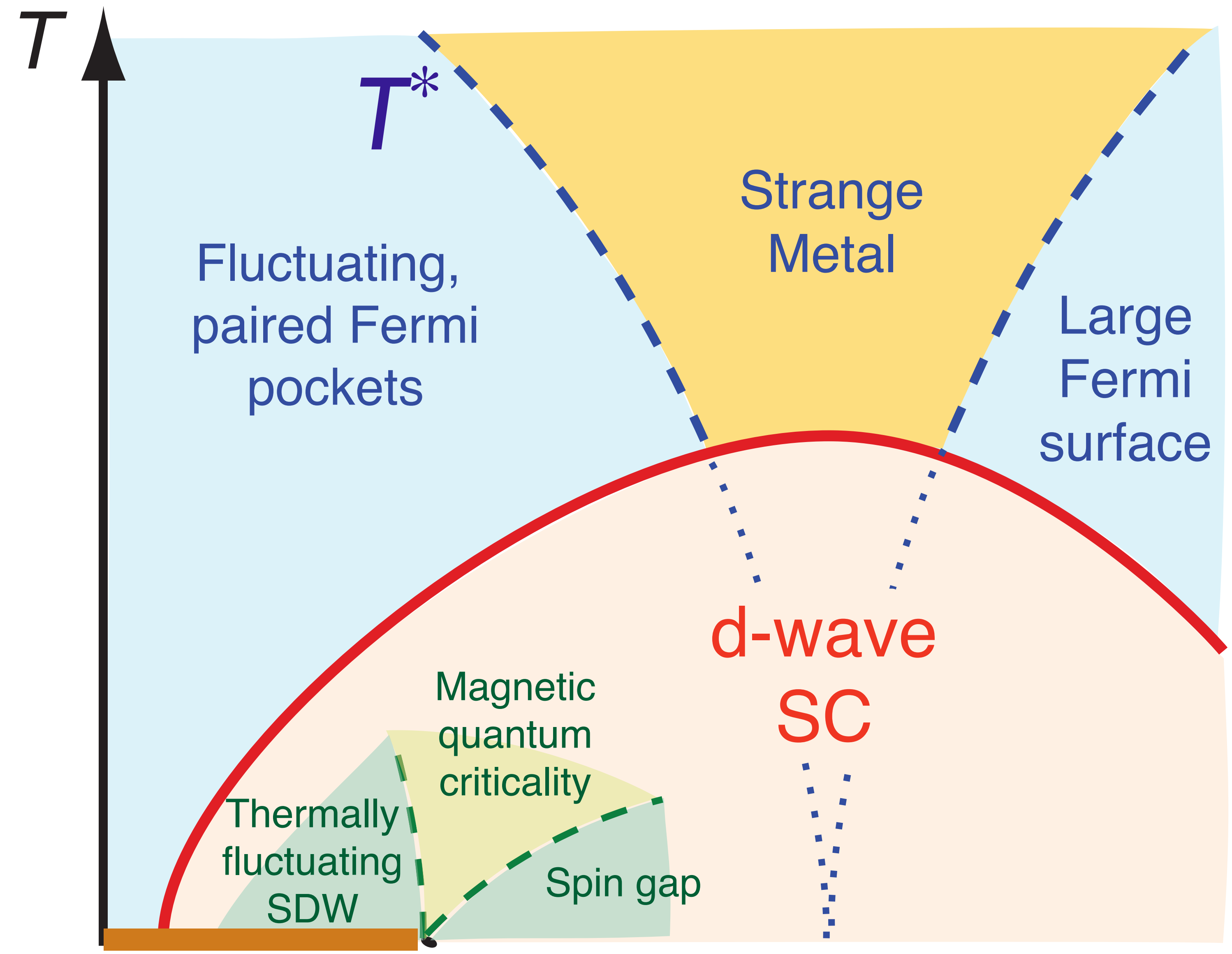

E. Demler, S. Sachdev and Y. Zhang, *Phys. Rev. Lett.* **87**, 067202 (2001).

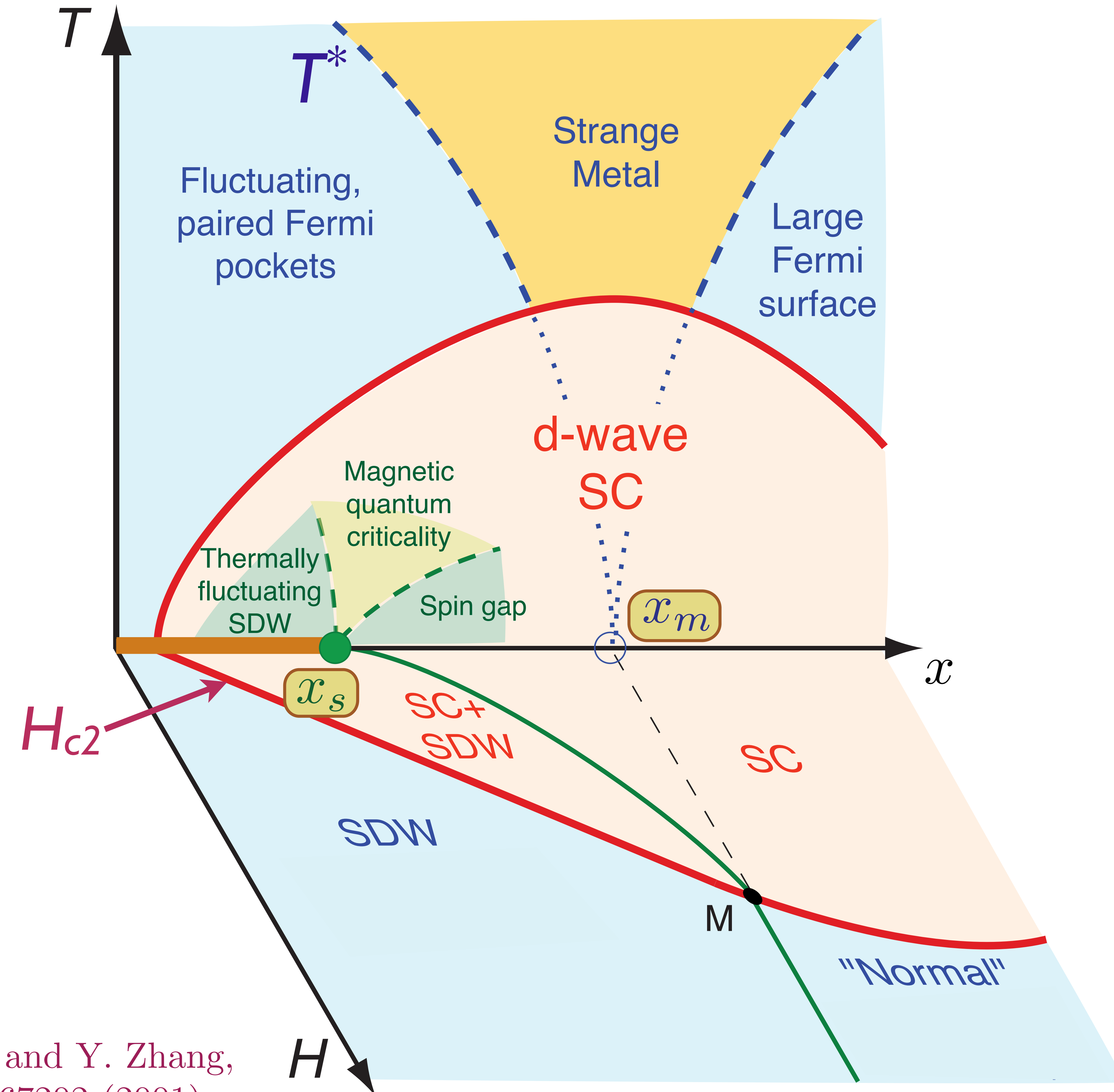

E. Demler, S. Sachdev and Y. Zhang, *Phys. Rev. Lett.* **87**, 067202 (2001).

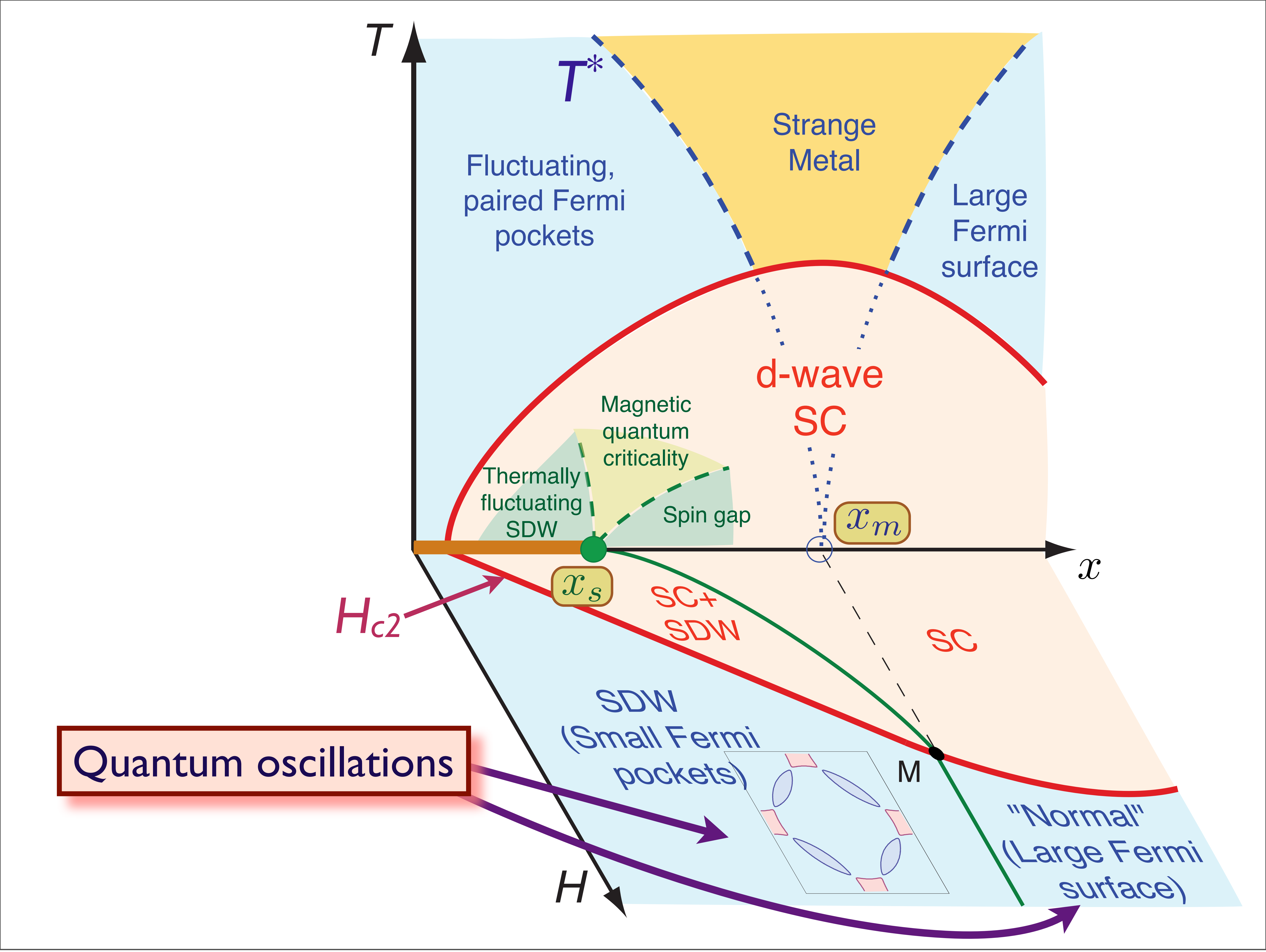
T
T^*
Strange Metal
Fluctuating, paired Fermi pockets
Large Fermi surface
d-wave SC
Magnetic quantum criticality
Thermally fluctuating SDW
Spin gap
x_m
x_s
x
H_{c2}
SC+ SDW
SC
SDW (Small Fermi pockets)
M
"Normal" (Large Fermi surface)
Quantum oscillations
H

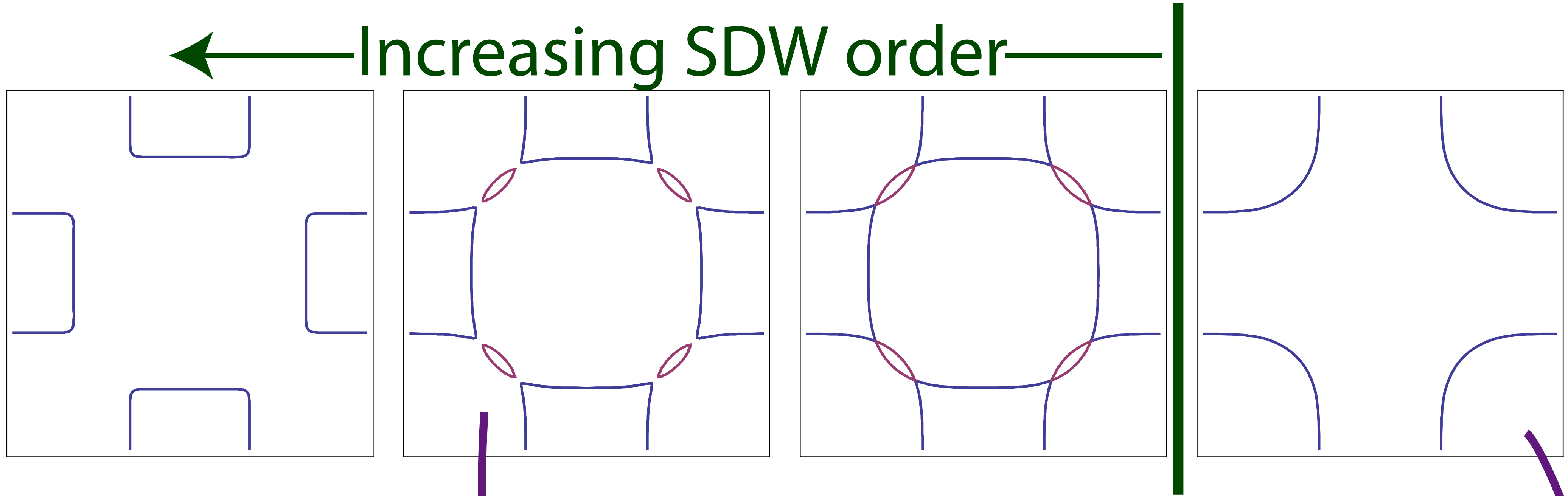

Quantum oscillations

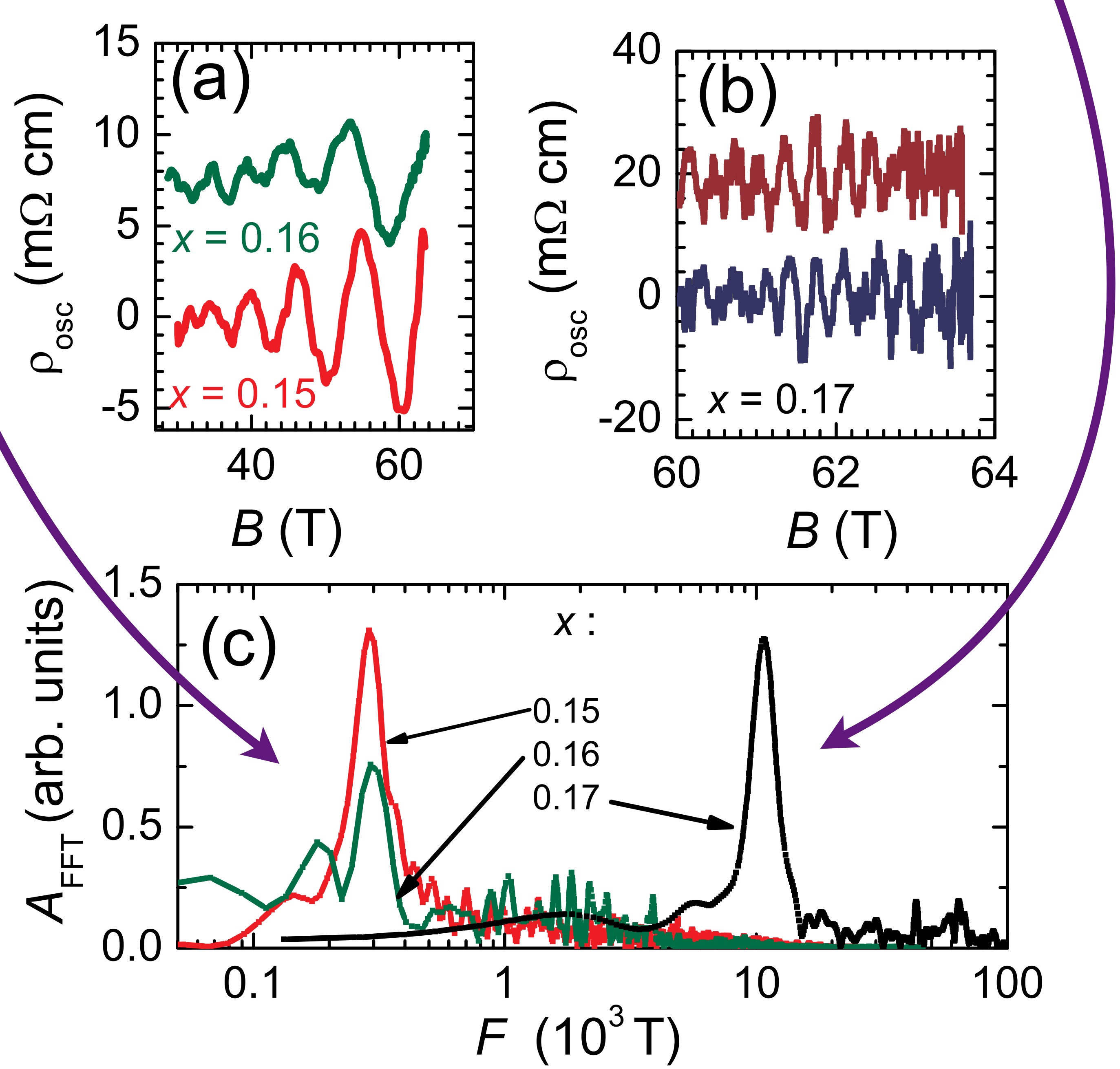

$Nd_{2-x}Ce_xCuO_4$

T. Helm, M.V. Kartsovnik, M. Bartkowiak, N. Bittner, M. Lambacher, A. Erb, J. Wosnitza, and R. Gross, *Phys. Rev. Lett.* **103**, 157002 (2009).

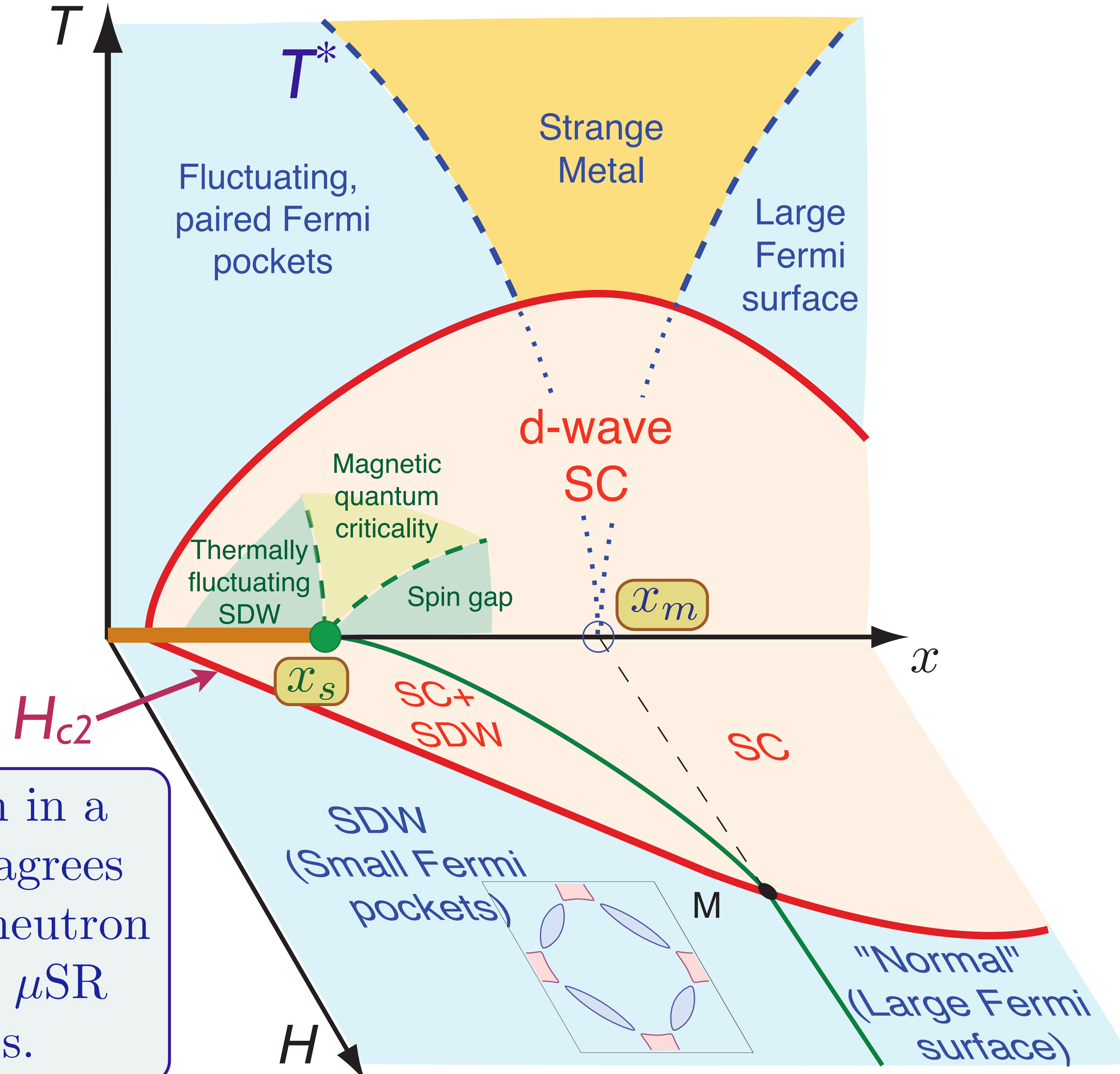

Phase diagram in a magnetic field agrees with numerous neutron scattering and μSR experiments.

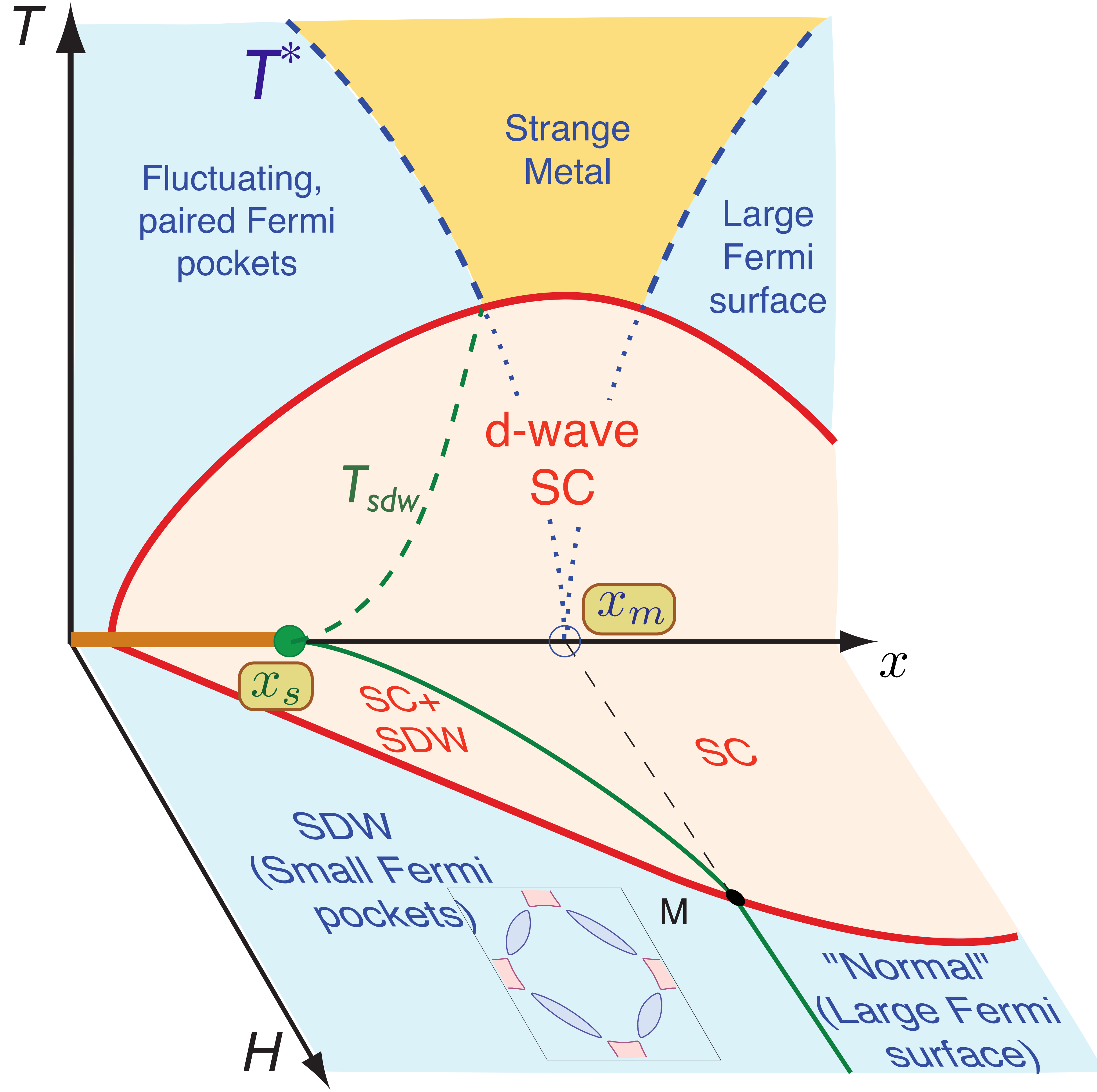

T
T^*
Fluctuating, paired Fermi pockets
Strange Metal
Large Fermi surface
d-wave SC
T_{sdw}
x_m
x
x_s
SC+ SDW
SC
SDW (Small Fermi pockets)
M
"Normal" (Large Fermi surface)
H

Similar phase diagram for $CeRhIn_5$

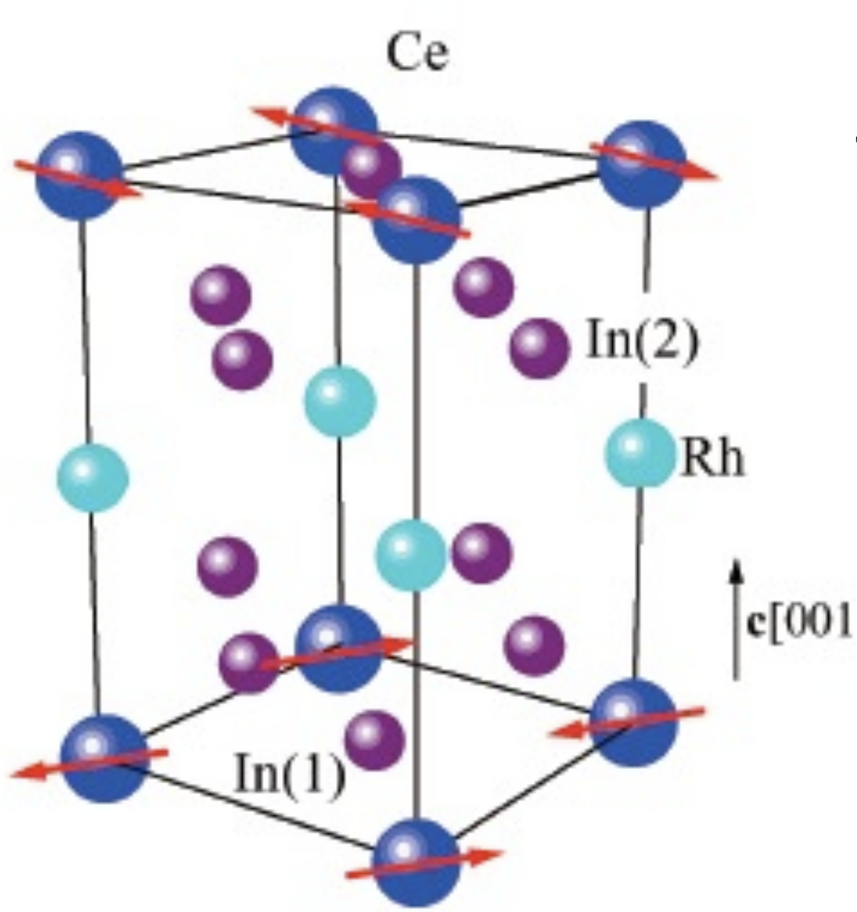

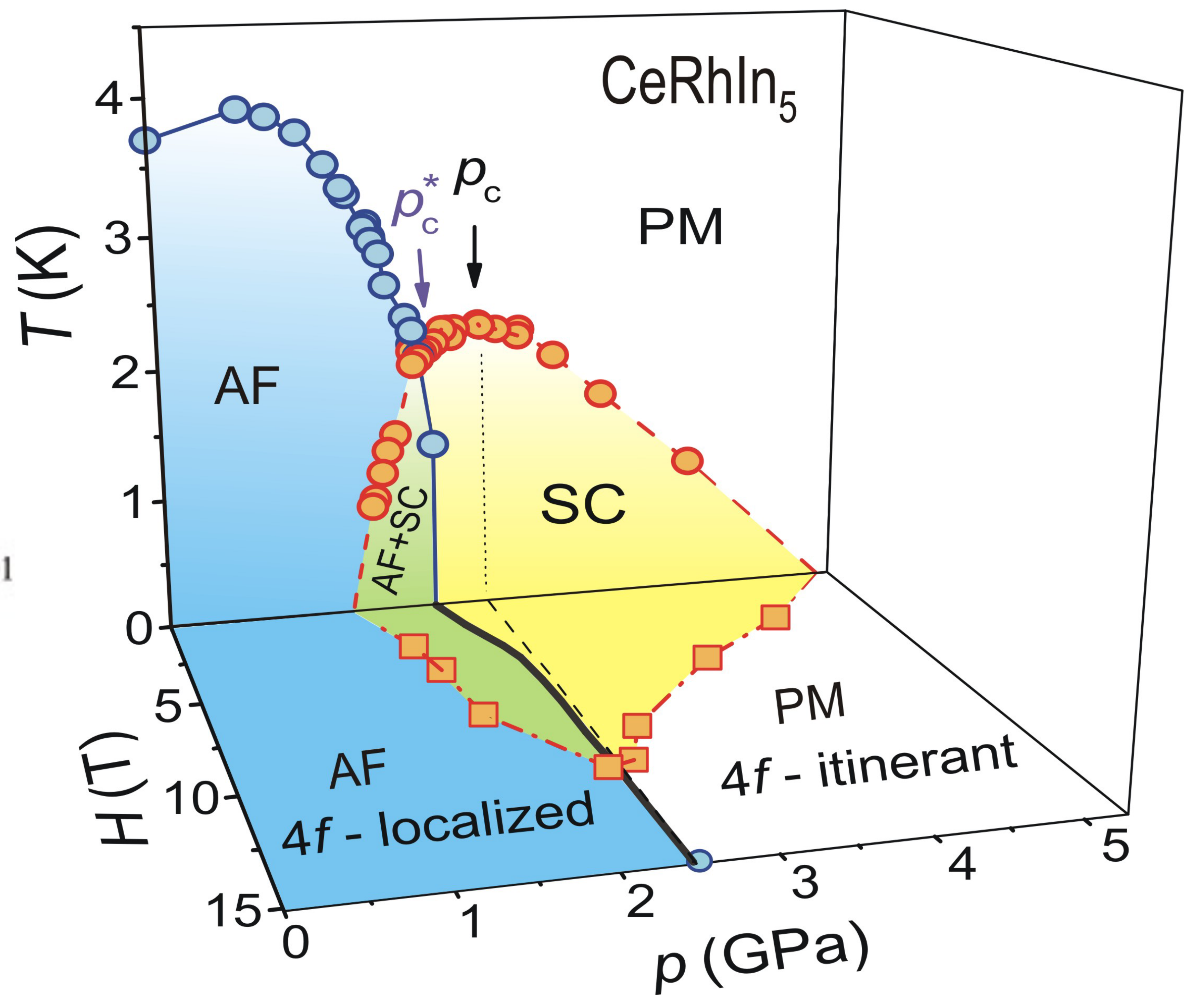

G. Knebel, D. Aoki, and J. Flouquet, arXiv:0911.5223

Similar phase diagram for the pnictides

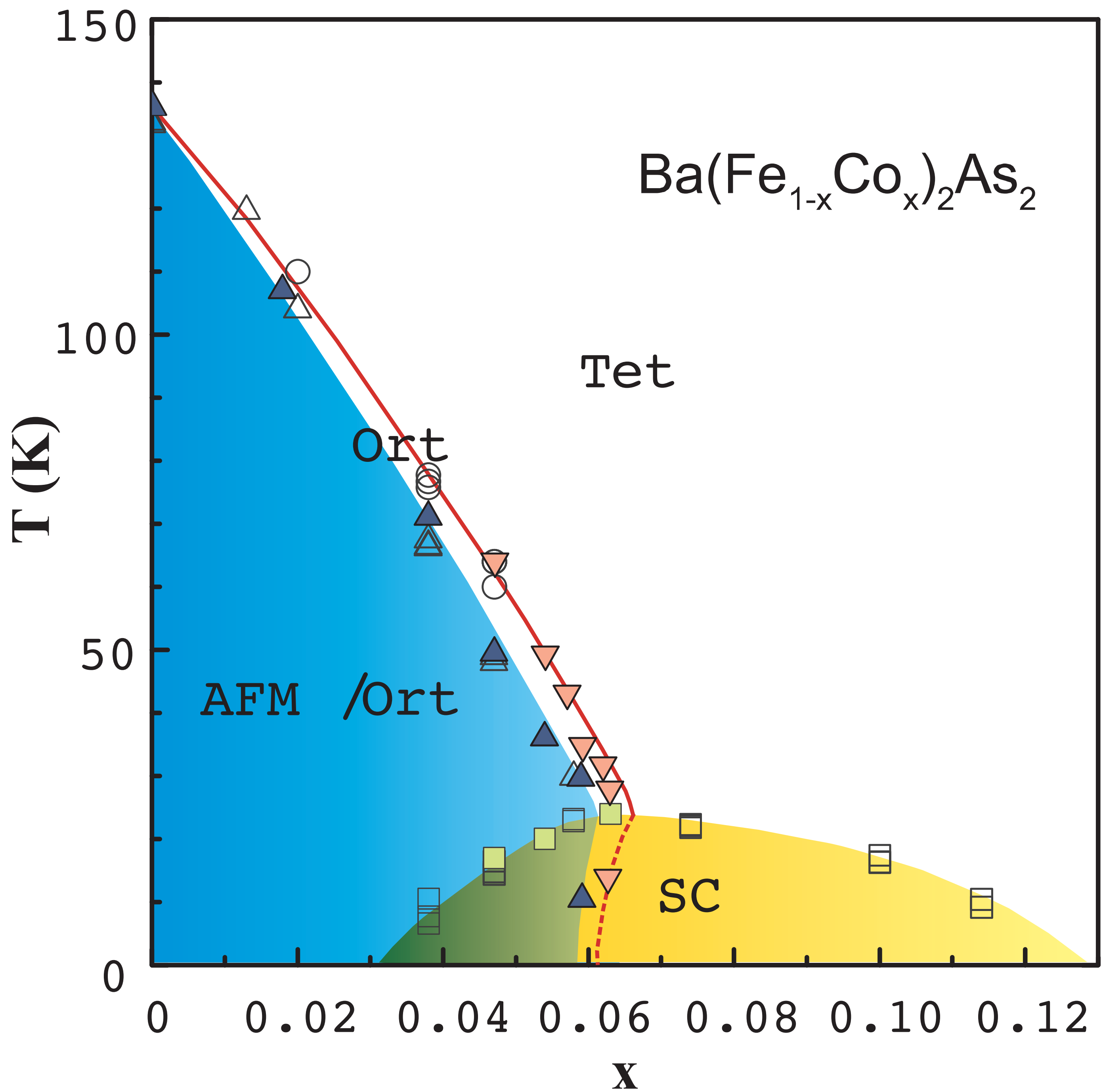

S. Nandi, M. G. Kim, A. Kreyssig, R. M. Fernandes, D. K. Pratt, A. Thaler, N. Ni, S. L. Bud'ko, P. C. Canfield, J. Schmalian, R. J. McQueeney, A. I. Goldman, arXiv:0911.3136.

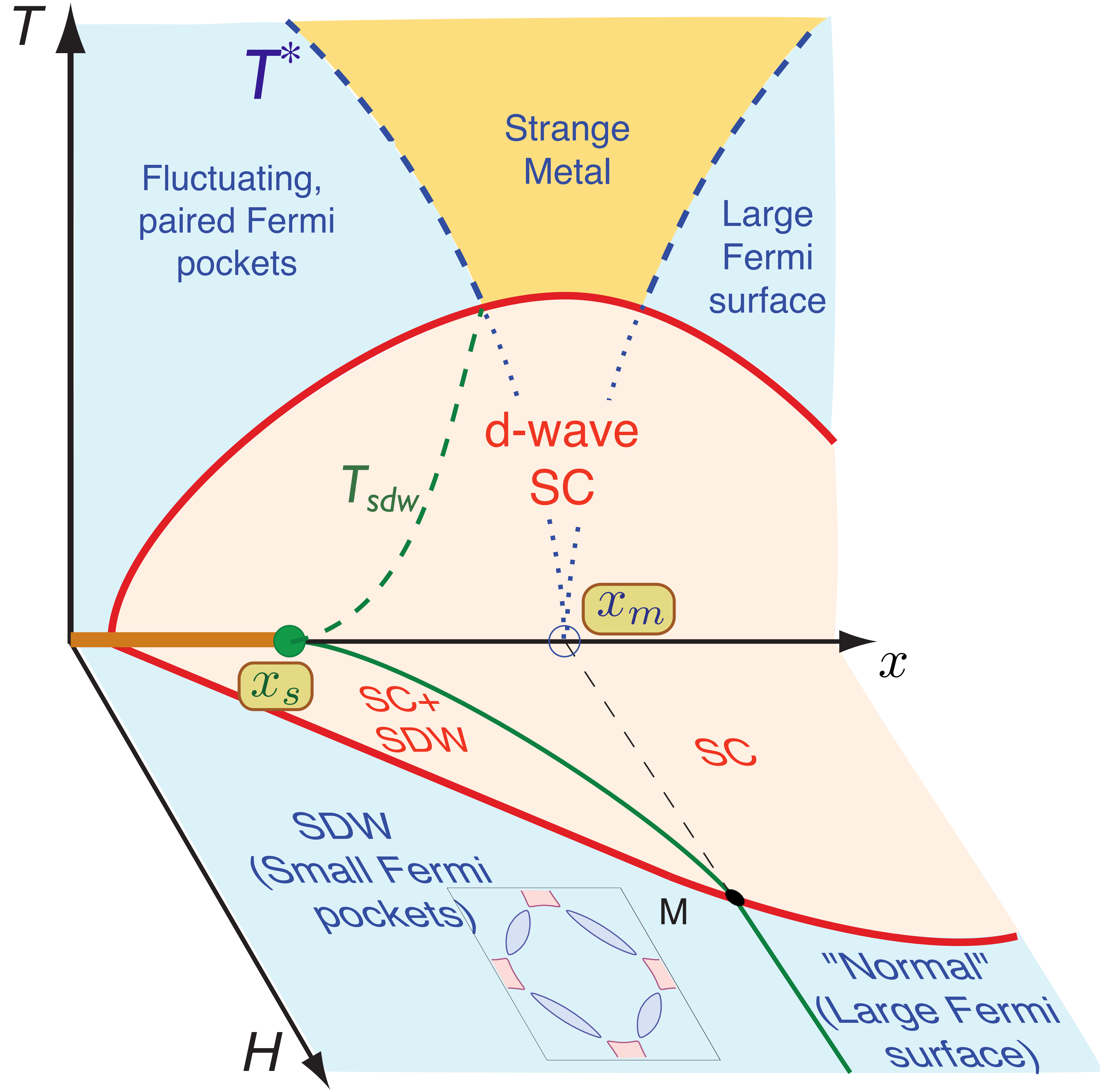

T
T*
Strange Metal
Fluctuating, paired Fermi pockets
Large Fermi surface
d-wave SC
T_{sdw}
x_m
x_s
x
SC+ SDW
SC
SDW (Small Fermi pockets)
M
"Normal" (Large Fermi surface)
H

Onset of superconductivity disrupts SDW order, but valence bond solid (VBS) and/or Ising-nematic ordering can survive

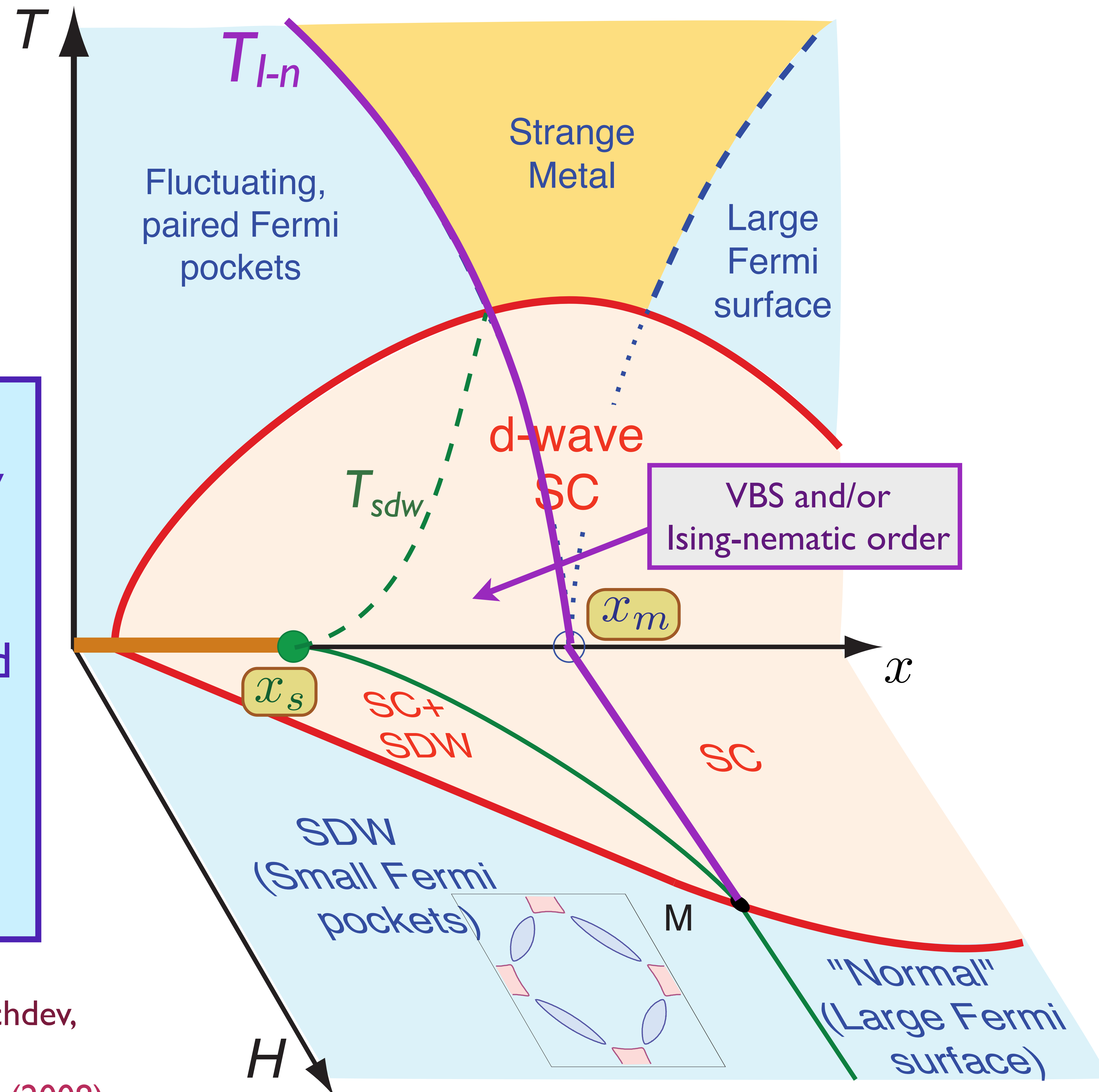

R. K. Kaul, M. Metlitksi, S. Sachdev, and Cenke Xu, *Physical Review B* **78**, 045110 (2008).

Outline

1. Coupled dimer antiferromagnets
   Introduction to quantum criticality

2. Phase diagram of the cuprates
   Quantum criticality of the competition between antiferromagnetism and superconductivity

3. Theory of Ising-nematic ordering in a metal
   Strongly-coupled field theory

4. The AdS/CFT correspondence
   Phases of finite density quantum matter at strong coupling

Outline

1. Coupled dimer antiferromagnets

   Introduction to quantum criticality

2. Phase diagram of the cuprates

   Quantum criticality of the competition between antiferromagnetism and superconductivity

3. Theory of Ising-nematic ordering in a metal

   Strongly-coupled field theory

4. The AdS/CFT correspondence

   Phases of finite density quantum matter at strong coupling

Max Metlitski, Harvard

arXiv:1001.1153

PHYSICS

VE RI TAS

HARVARD

Quantum criticality of Pomeranchuk instability

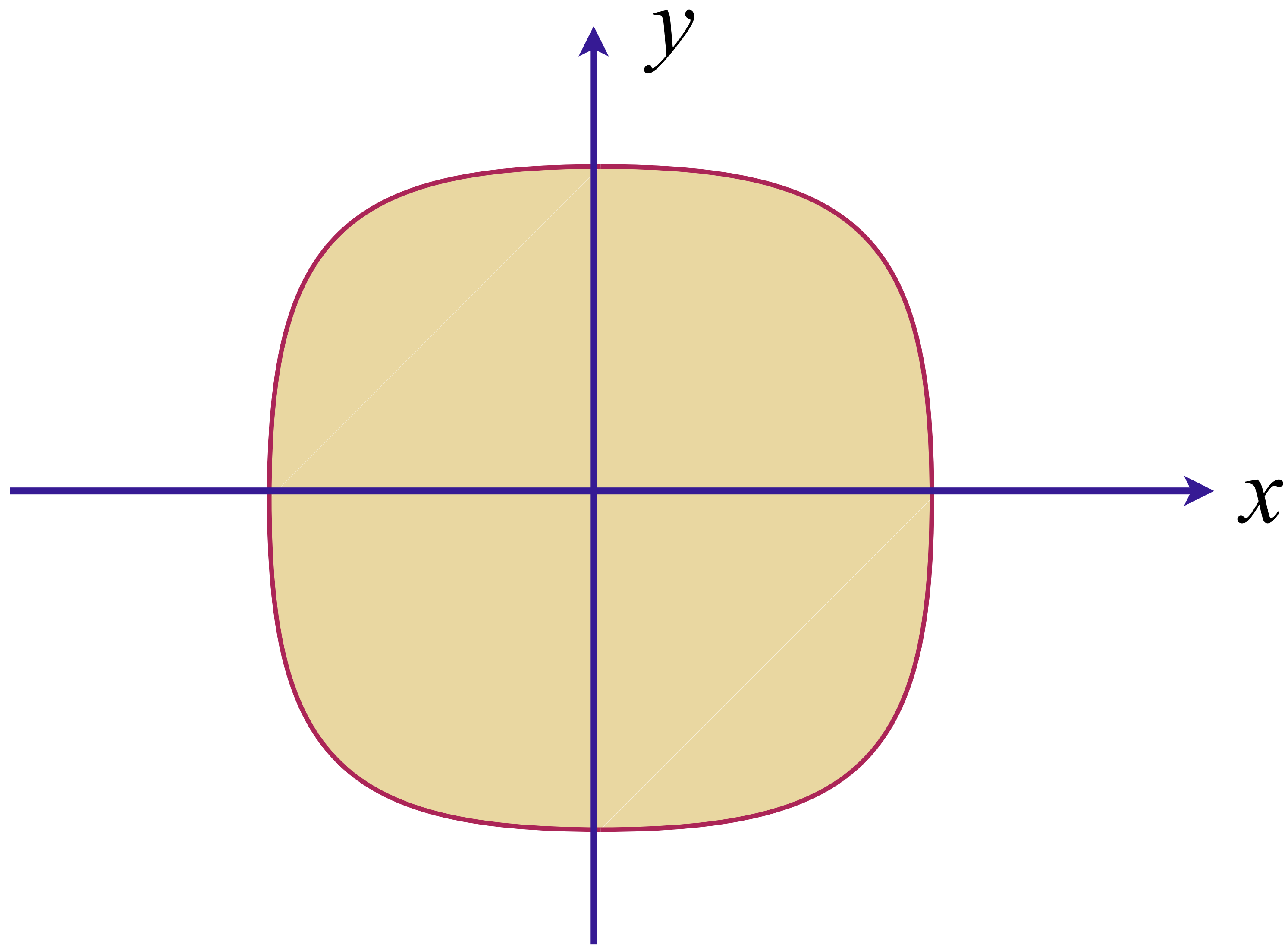

Fermi surface with full square lattice symmetry

Quantum criticality of Pomeranchuk instability

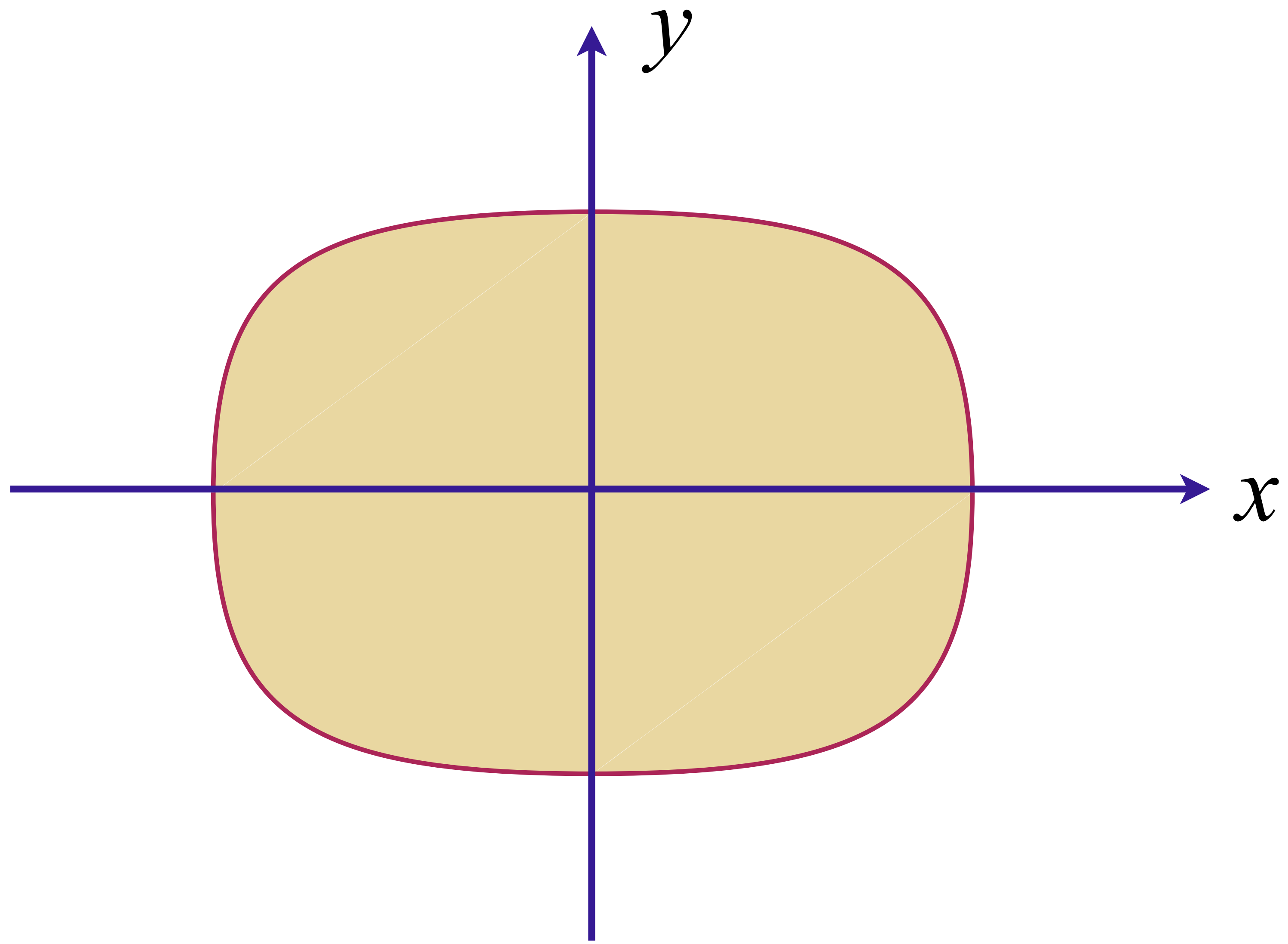

Spontaneous elongation along x direction:

H. Yamase and H. Kohno, J. Phys. Soc. Jpn. **69**, 2151 (2000).
C. J. Halboth and W. Metzner, Phys. Rev. Lett. **85**, 5162 (2000).

Quantum criticality of Pomeranchuk instability

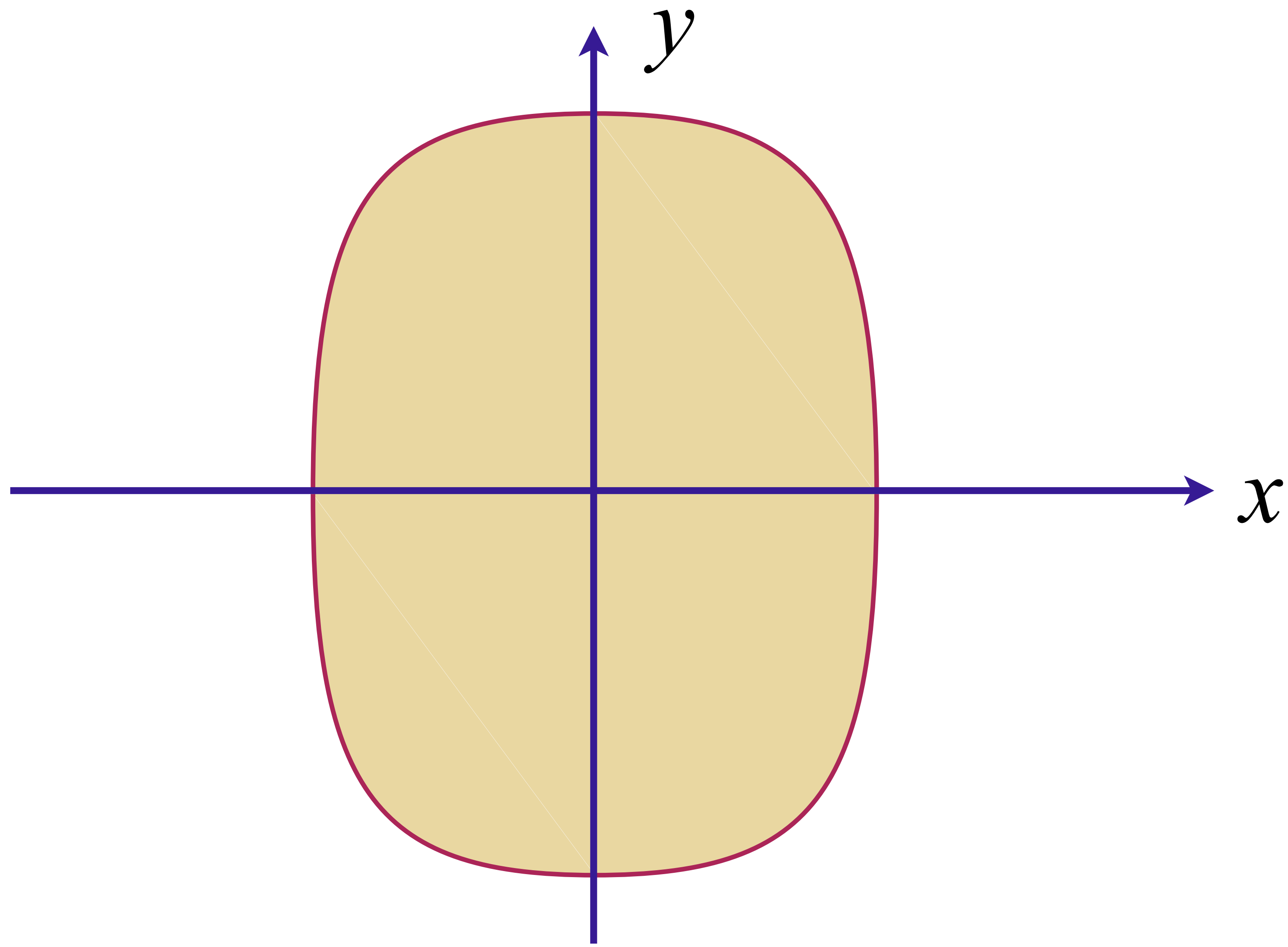

Spontaneous elongation along y direction:

H. Yamase and H. Kohno, J. Phys. Soc. Jpn. **69**, 2151 (2000).
C. J. Halboth and W. Metzner, Phys. Rev. Lett. **85**, 5162 (2000).

Ising-nematic order parameter

$$\phi \sim \int d^2k \, (\cos k_x - \cos k_y) \, c^\dagger_{\mathbf{k}\sigma} c_{\mathbf{k}\sigma}$$

Measures spontaneous breaking of square lattice point-group symmetry of underlying Hamiltonian

Quantum criticality of Pomeranchuk instability

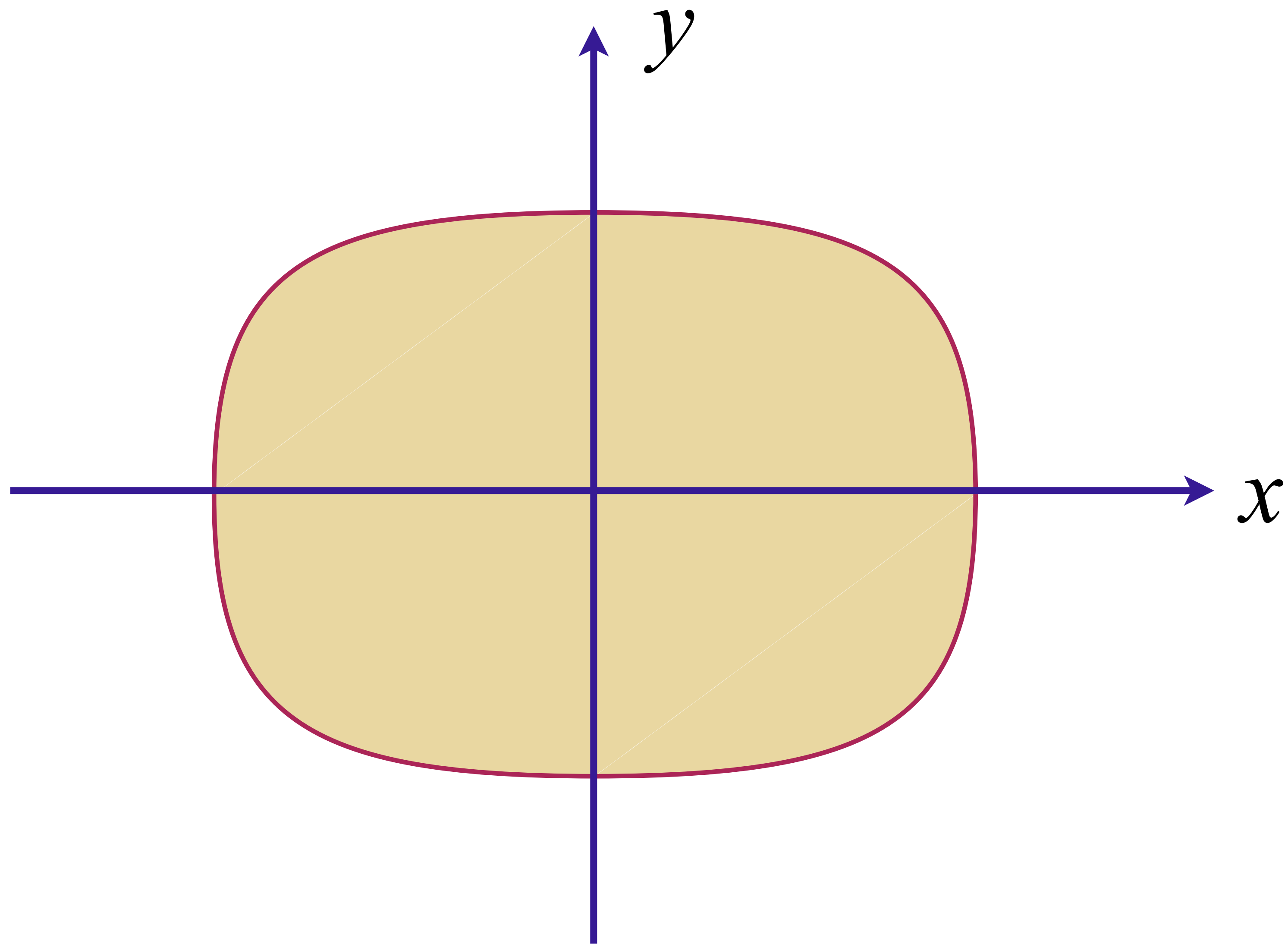

Spontaneous elongation along x direction:
Ising order parameter $\phi > 0$.

H. Yamase and H. Kohno, J. Phys. Soc. Jpn. **69**, 2151 (2000).
C. J. Halboth and W. Metzner, Phys. Rev. Lett. **85**, 5162 (2000).

Quantum criticality of Pomeranchuk instability

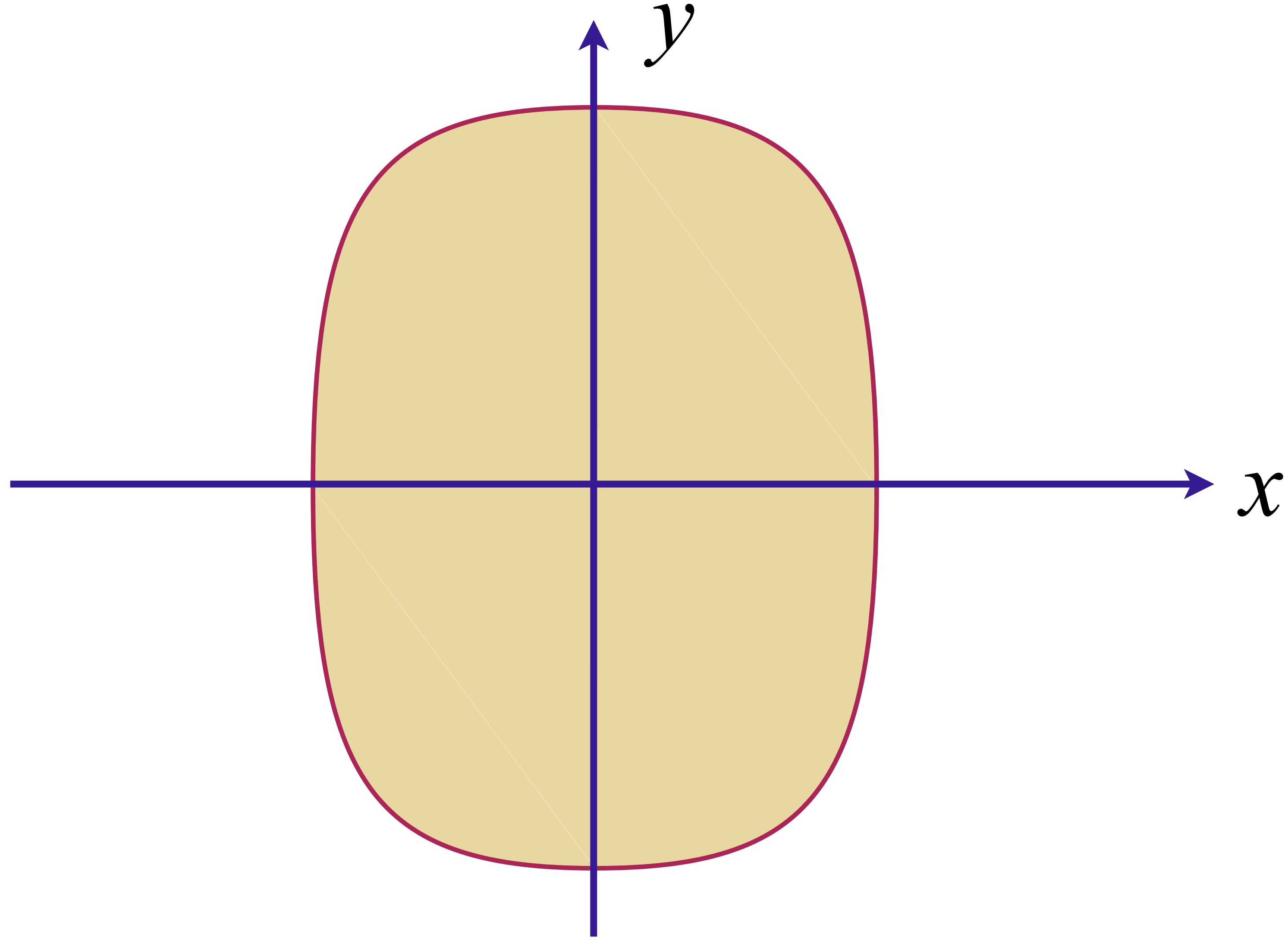

Spontaneous elongation along y direction:
Ising order parameter $\phi < 0$.

H. Yamase and H. Kohno, J. Phys. Soc. Jpn. **69**, 2151 (2000).
C. J. Halboth and W. Metzner, Phys. Rev. Lett. **85**, 5162 (2000).

Quantum criticality of Pomeranchuk instability

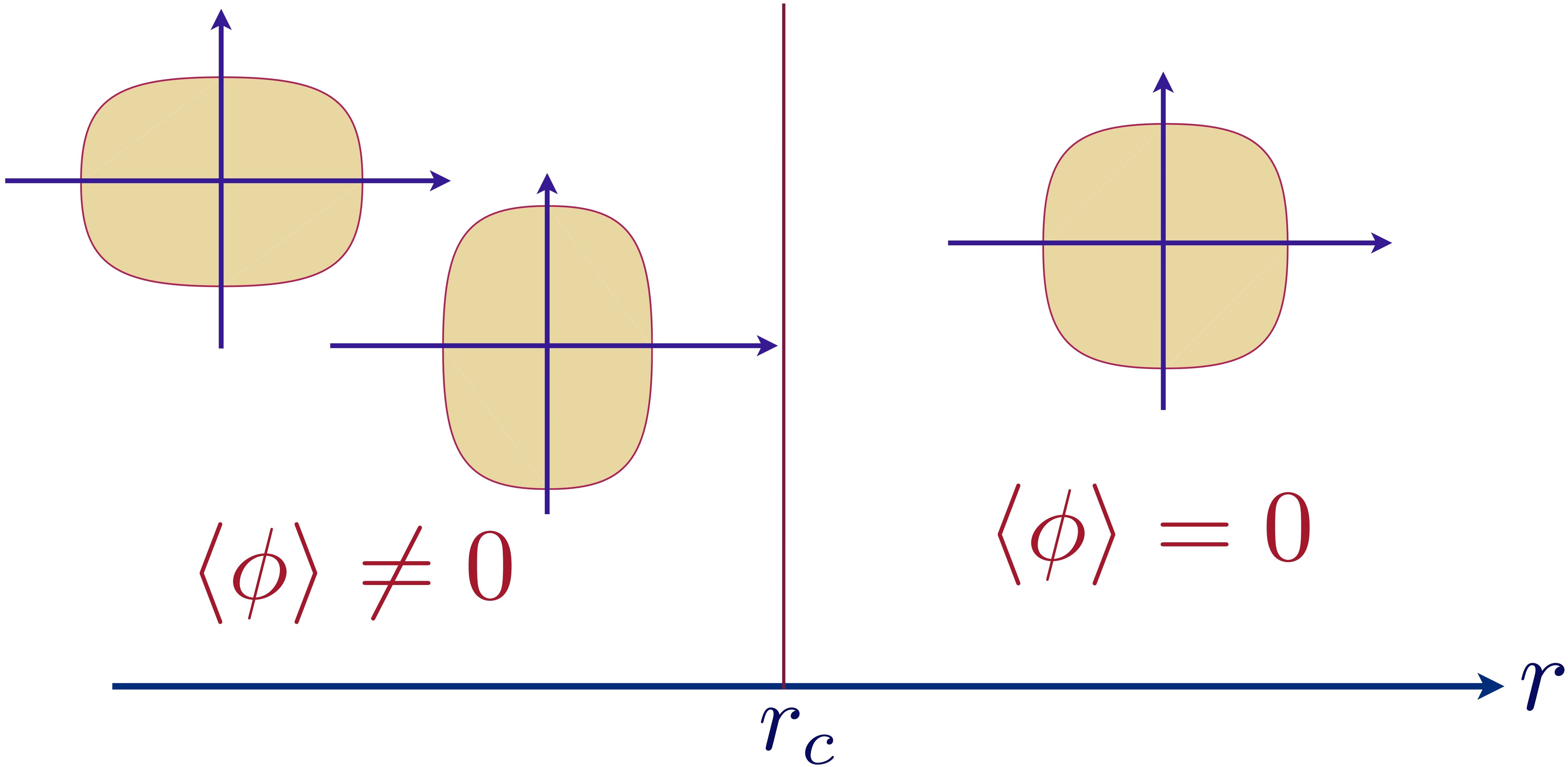

Pomeranchuk instability as a function of coupling r

H. Yamase and H. Kohno, J. Phys. Soc. Jpn. **69**, 2151 (2000).
C. J. Halboth and W. Metzner, Phys. Rev. Lett. **85**, 5162 (2000).

Quantum criticality of Pomeranchuk instability

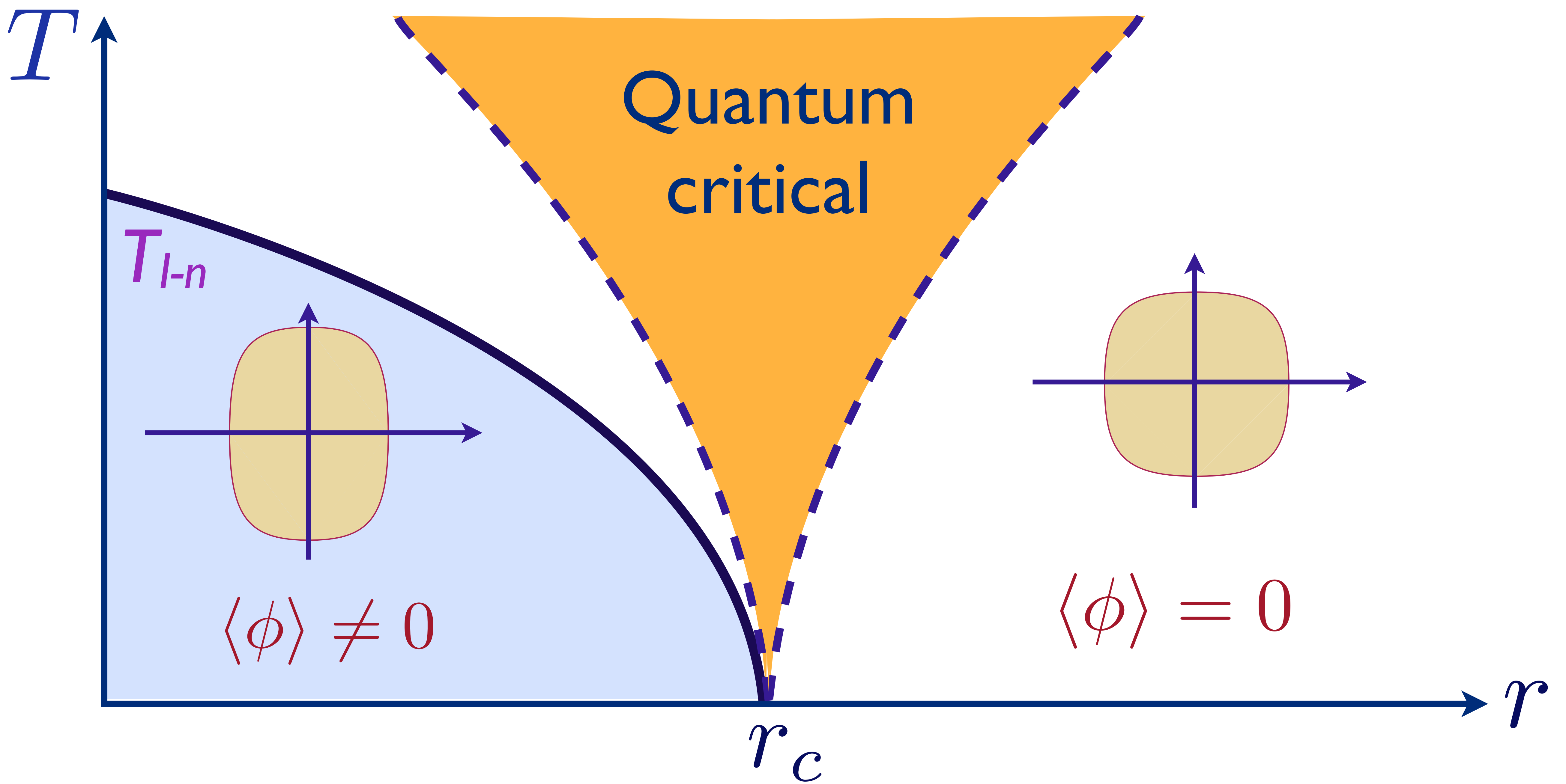

Phase diagram as a function of T and r

Quantum criticality of Pomeranchuk instability

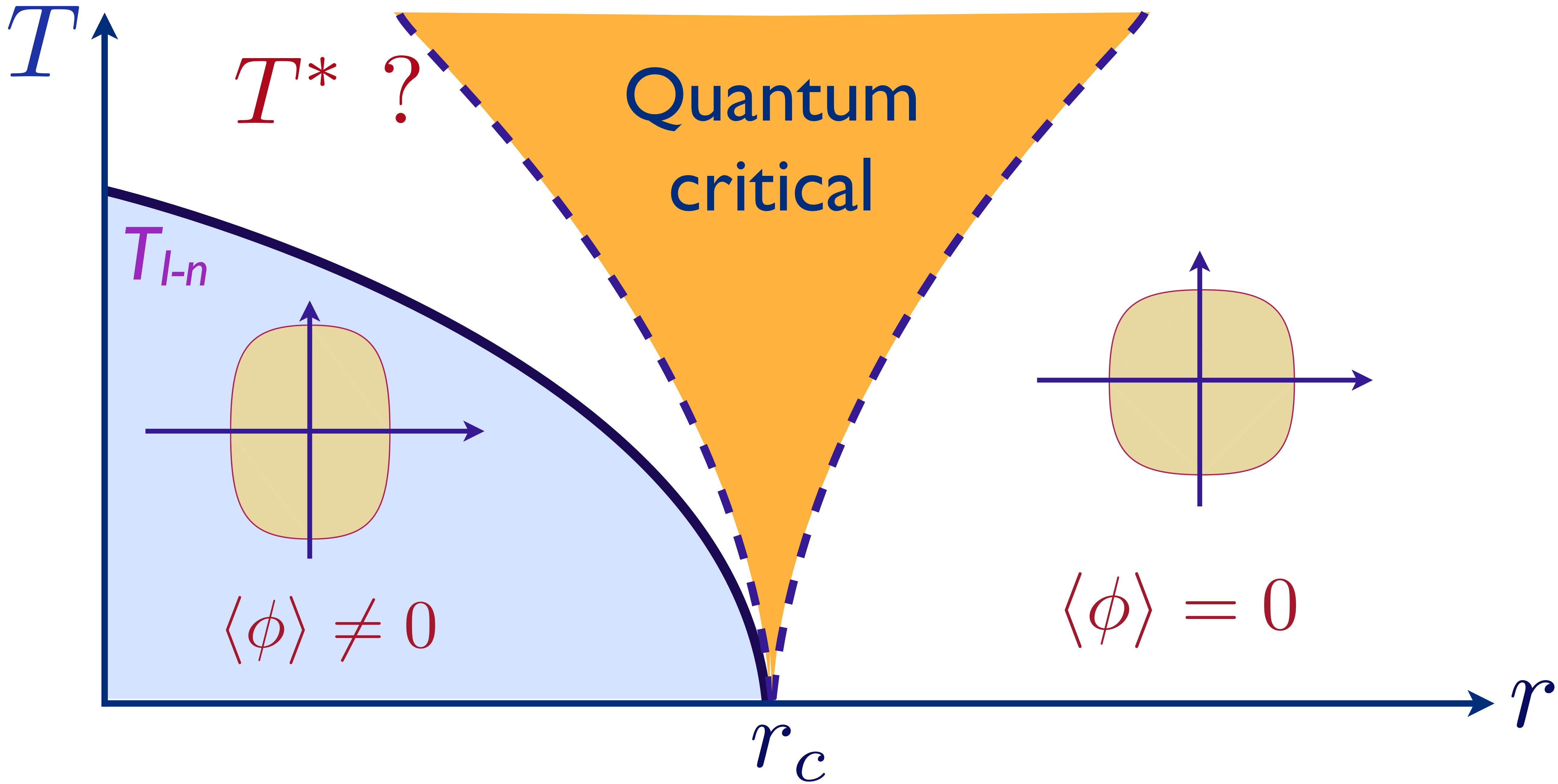

Phase diagram as a function of T and r

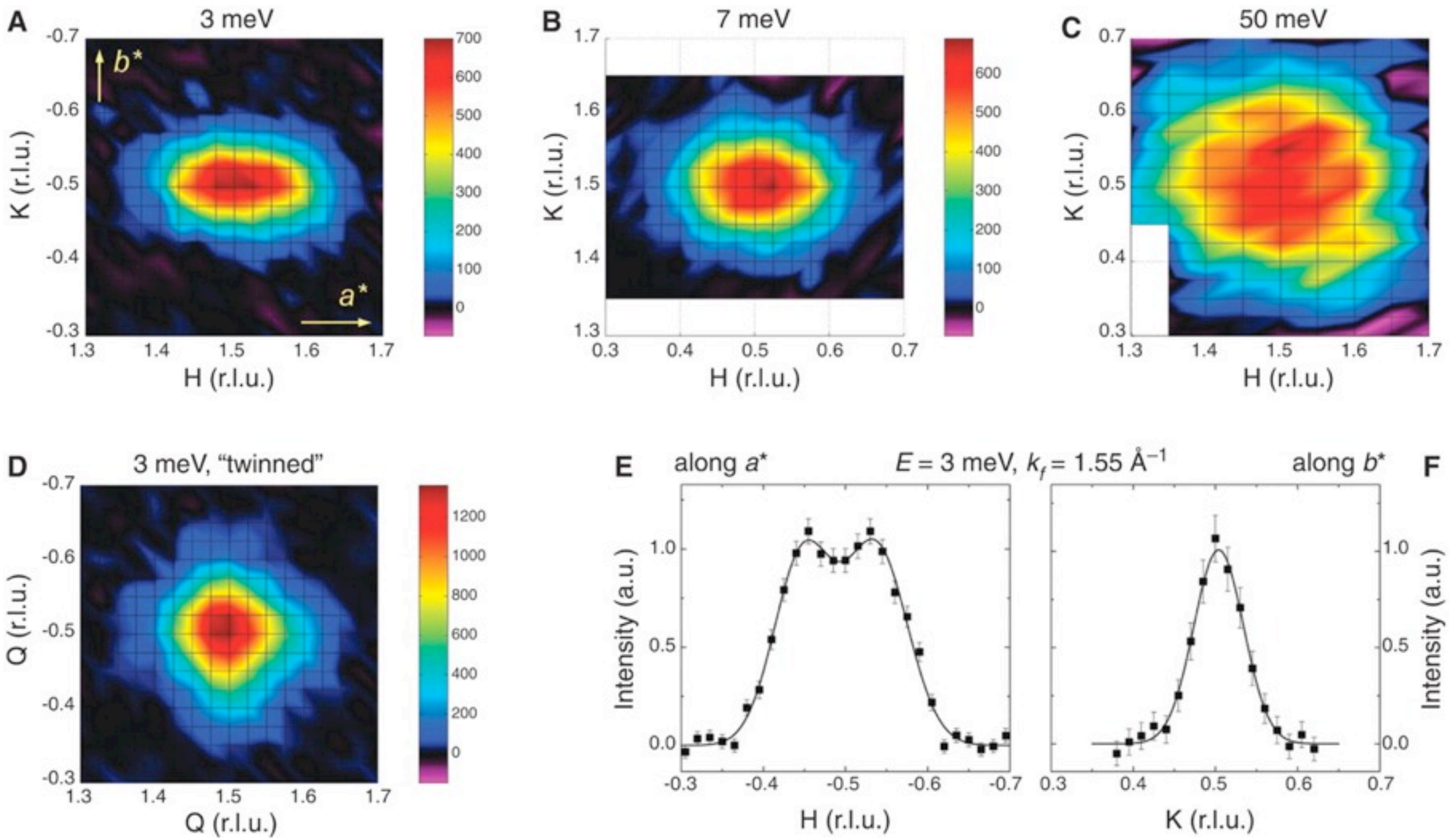

Nematic order in YBCO

V. Hinkov, D. Haug, B. Fauqué, P. Bourges, Y. Sidis, A. Ivanov, C. Bernhard, C. T. Lin, and B. Keimer , *Science* **319**, 597 (2008)

Broken rotational symmetry in the pseudogap phase of a high-Tc superconductor

R. Daou, J. Chang, David LeBoeuf, Olivier Cyr-Choiniere, Francis Laliberte, Nicolas Doiron-Leyraud, B. J. Ramshaw, Ruixing Liang, D.A. Bonn, W. N. Hardy, and Louis Taillefer
arXiv: 0909.4430, Nature, in press.

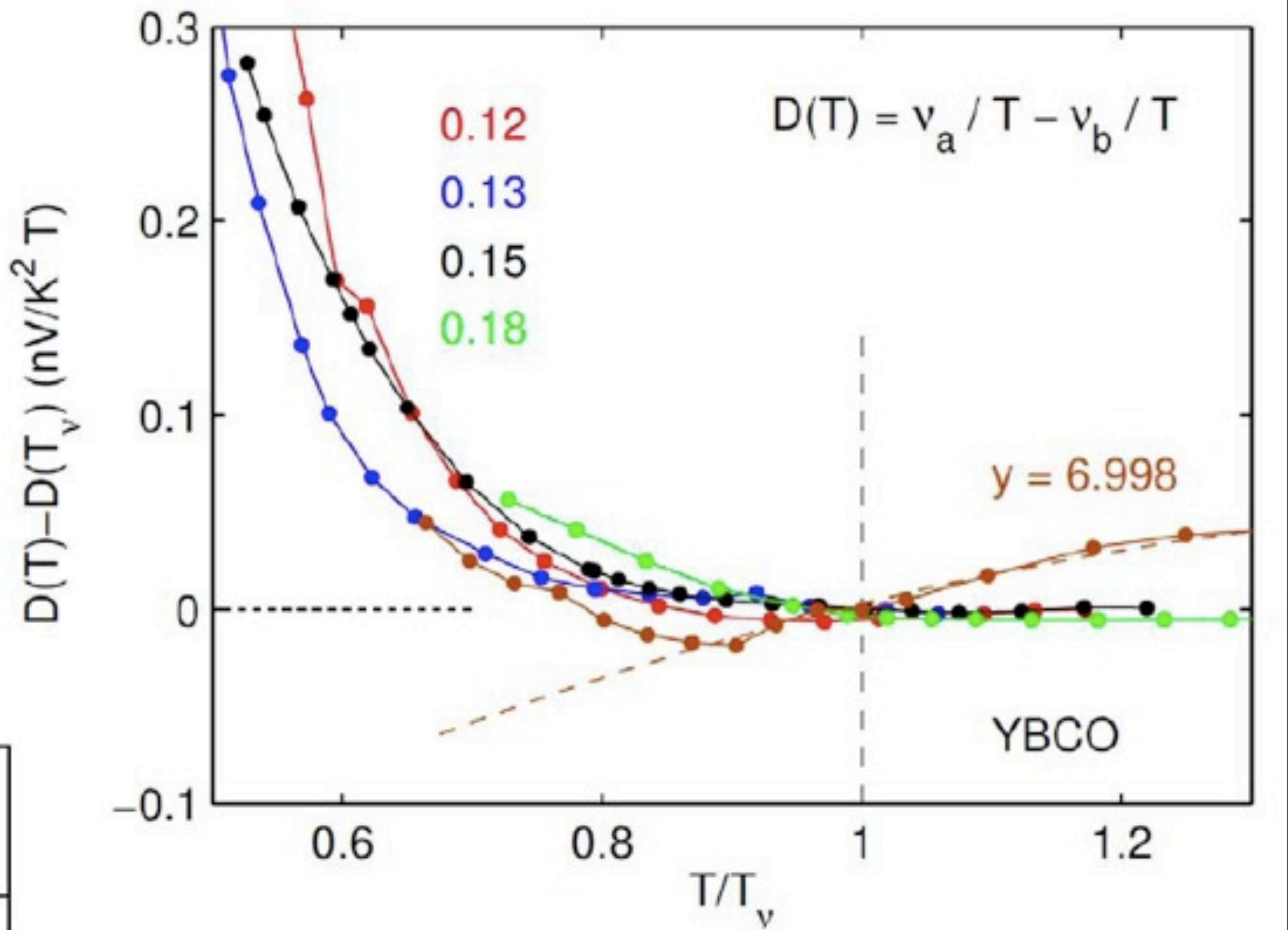

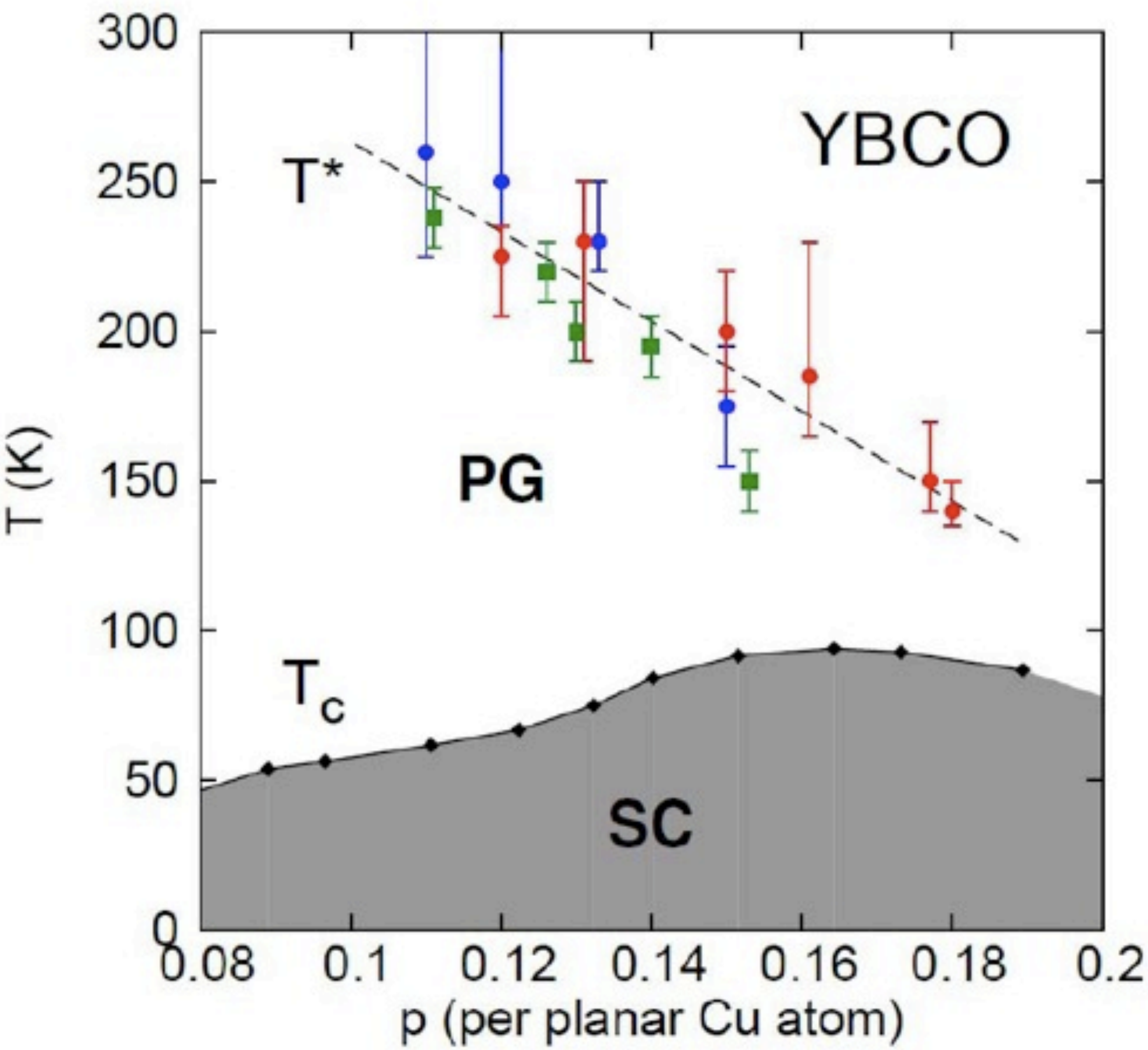

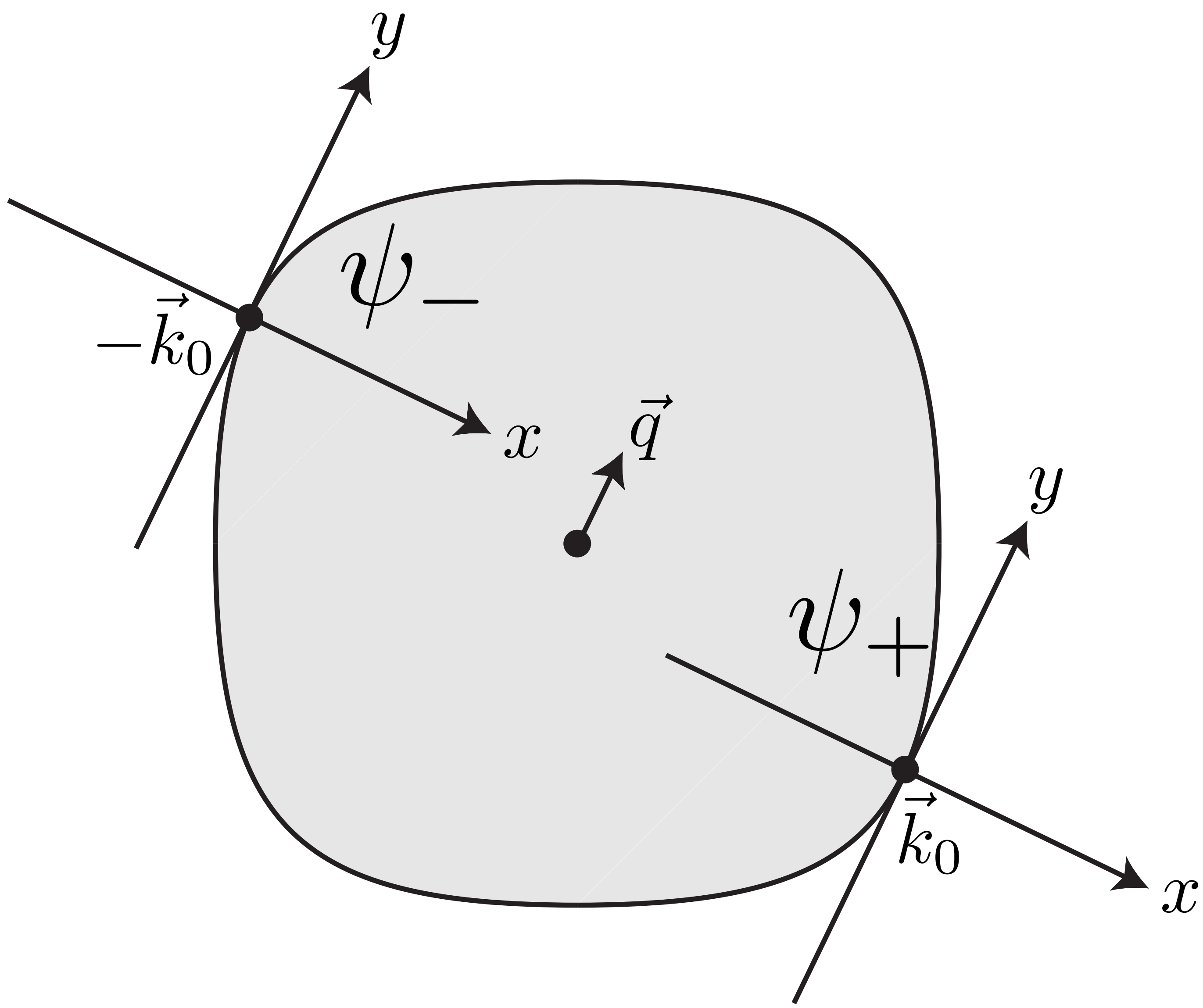

A ϕ fluctuation at wavevector $\vec{q}$ couples most efficiently to fermions near $\pm\vec{k}_0$.

Expand fermion kinetic energy at wavevectors about $\vec{k}_0$

- Critical point is described by an *infinite* set of 2+1 dimensional field theories, one for each direction $\hat{q}$.

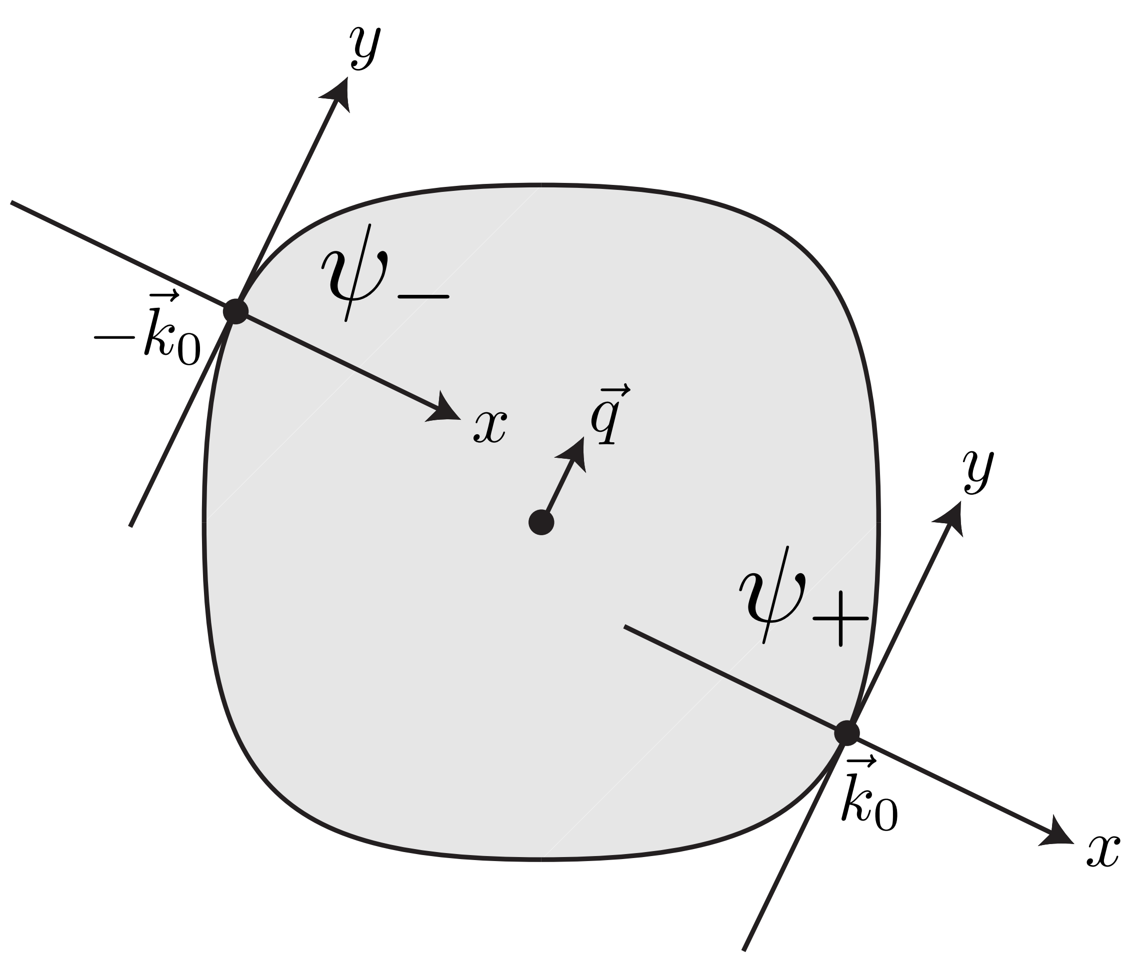

- Critical point is described by an *infinite* set of 2+1 dimensional field theories, one for each direction $\hat{q}$.

- Contrast with "Fermi surface bosonization" methods where there are an infinite set of 1+1 dimensional field theories, one for each direction $\hat{q}$.

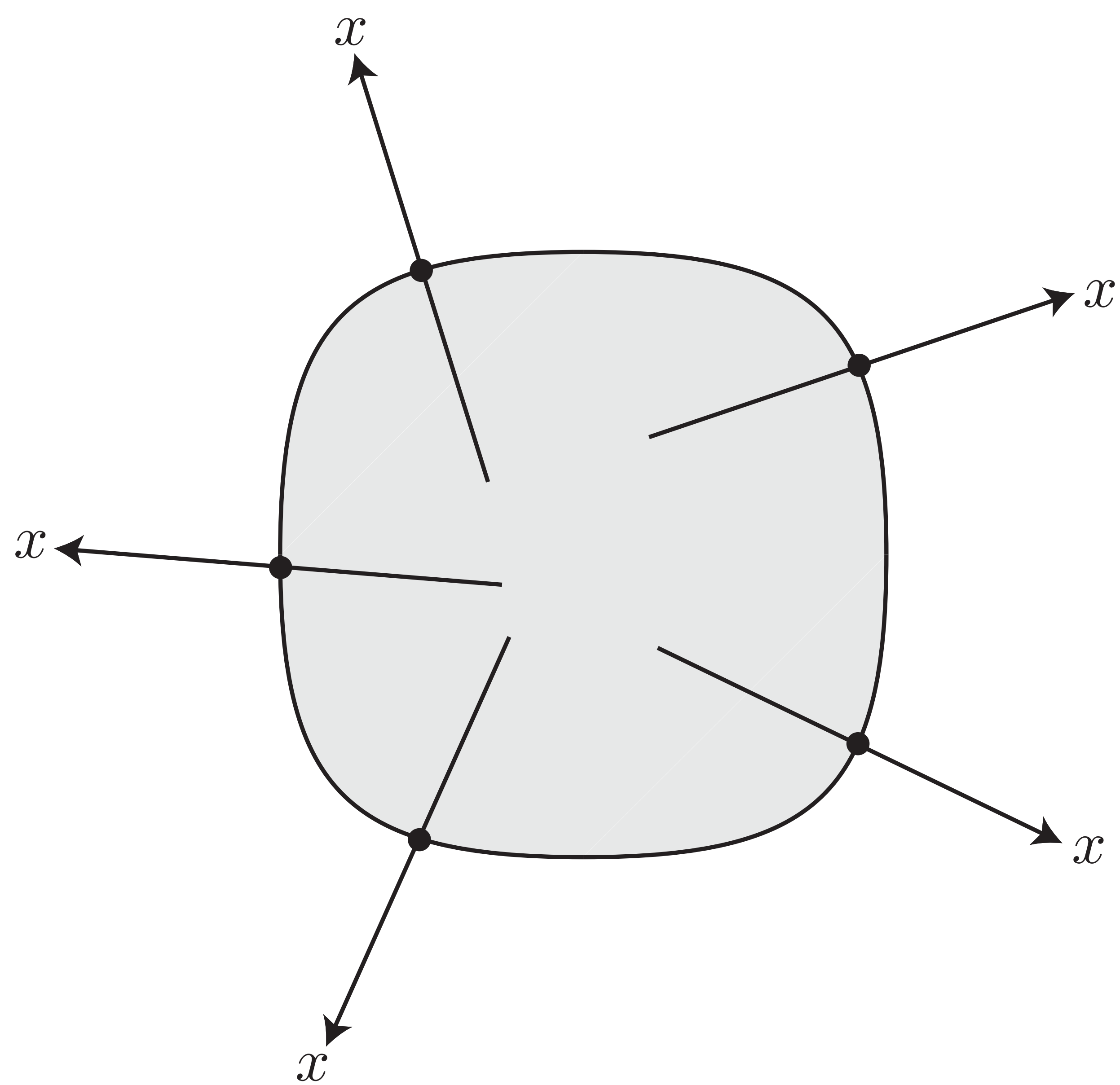

- Critical point is described by an *infinite* set of 2+1 dimensional field theories, one for each direction $\hat{q}$.
- Contrast with "Fermi surface bosonization" methods where there are an infinite set of 1+1 dimensional field theories, one for each direction $\hat{q}$.
- Our approach leads to a redundant description of underlying degrees of freedom. A "Galilean symmetry" ensures consistency of redundant description.

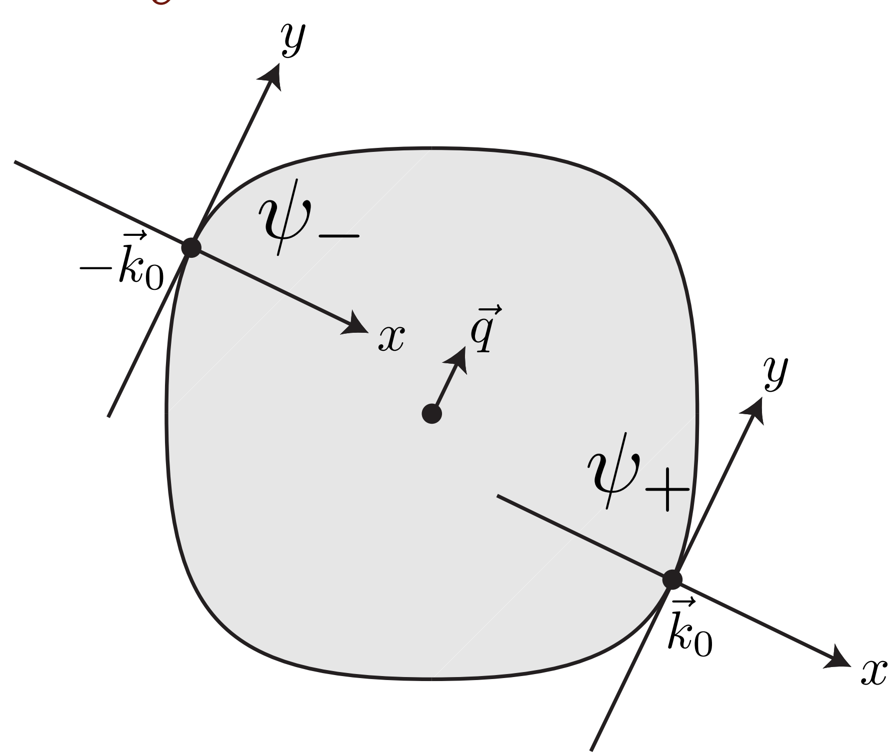

- Critical point is described by an *infinite* set of 2+1 dimensional field theories, one for each direction $\hat{q}$.

- Contrast with "Fermi surface bosonization" methods where there are an infinite set of 1+1 dimensional field theories, one for each direction $\hat{q}$.

- Our approach leads to a redundant description of underlying degrees of freedom. A "Galilean symmetry" ensures consistency of redundant description.

- <u>Infinite set of 2+1 dimensional field theories</u>: implies an emergent dimension of spacetime, and suggests a string-theoretic description and application of the AdS/CFT correspondence.

Outline

1. Coupled dimer antiferromagnets

   Introduction to quantum criticality

2. Phase diagram of the cuprates

   Quantum criticality of the competition between antiferromagnetism and superconductivity

3. Theory of Ising-nematic ordering in a metal

   Strongly-coupled field theory

4. The AdS/CFT correspondence

   Phases of finite density quantum matter at strong coupling

Outline

1. Coupled dimer antiferromagnets

   Introduction to quantum criticality

2. Phase diagram of the cuprates

   Quantum criticality of the competition between antiferromagnetism and superconductivity

3. Theory of Ising-nematic ordering in a metal

   Strongly-coupled field theory

4. The AdS/CFT correspondence

   Phases of finite density quantum matter at strong coupling

Conformal field theory
in 2+1 dimensions at $T = 0$

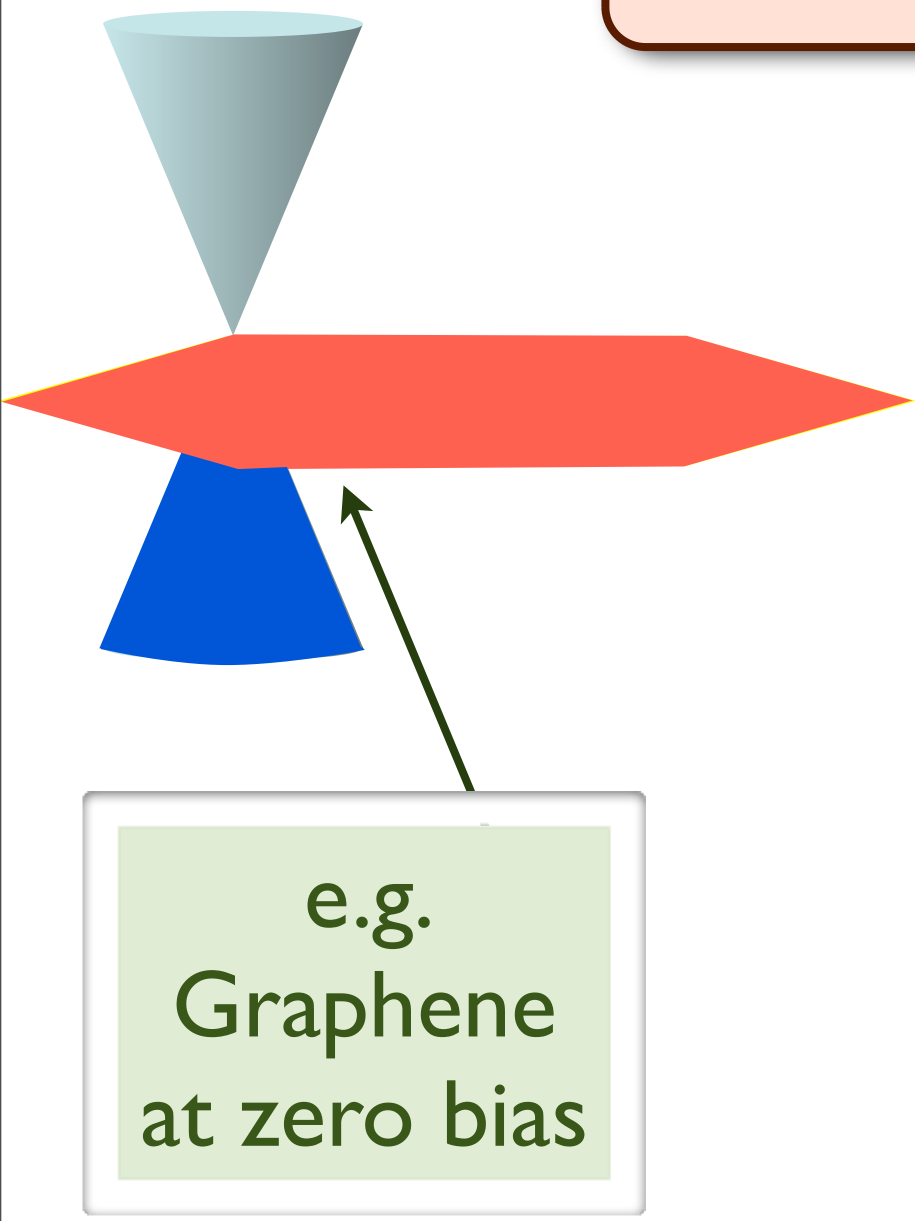

$\updownarrow$

Einstein gravity
on AdS_4

Conformal field theory
in 2+1 dimensions at $T > 0$

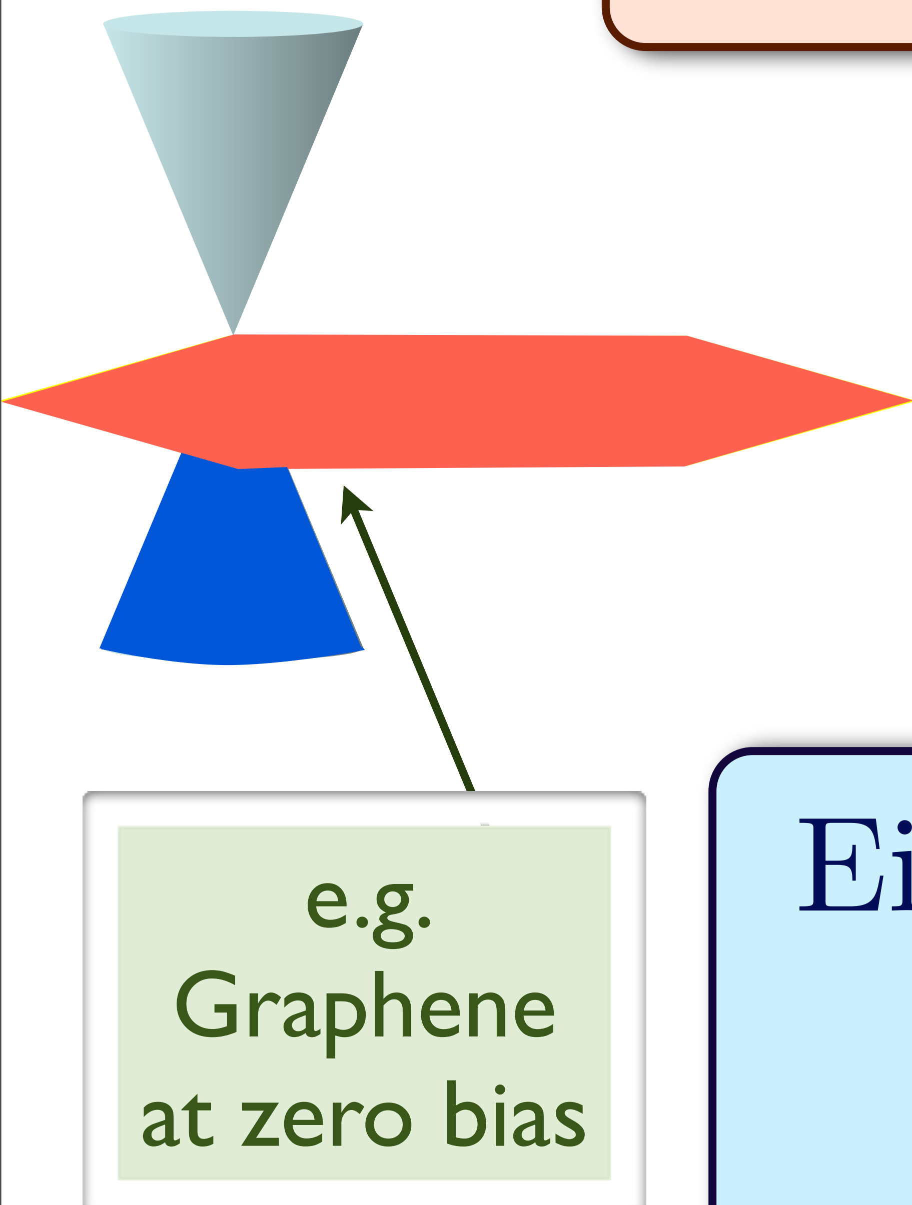

$\Updownarrow$

Einstein gravity on AdS_4
with a Schwarzschild
black hole

Conformal field theory
in 2+1 dimensions at $T > 0$,
with a non-zero chemical potential, μ
and applied magnetic field, B

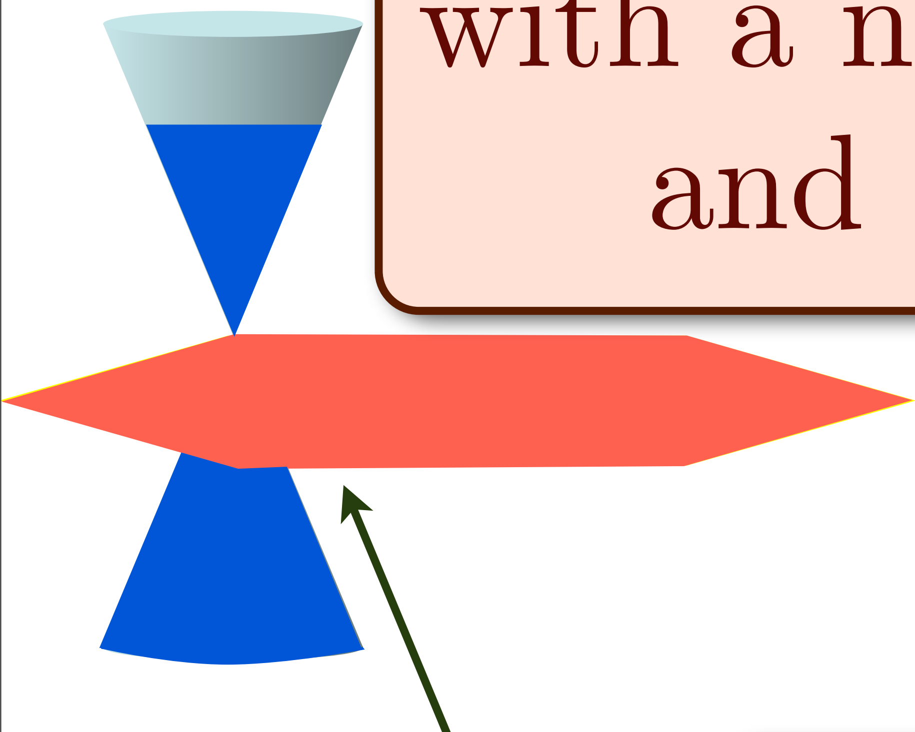

e.g.
Graphene
at non-zero
bias

Einstein gravity on AdS_4
with a Reissner-Nordstrom
black hole carrying electric
and magnetic charges

AdS/CFT correspondence

The quantum theory of a black hole in a 3+1-dimensional negatively curved AdS universe is holographically represented by a CFT (the theory of a quantum critical point) in 2+1 dimensions

3+1 dimensional AdS space

Maldacena, Gubser, Klebanov, Polyakov, Witten

AdS/CFT correspondence

The quantum theory of a black hole in a 3+1-dimensional negatively curved AdS universe is holographically represented by a CFT (the theory of a quantum critical point) in 2+1 dimensions

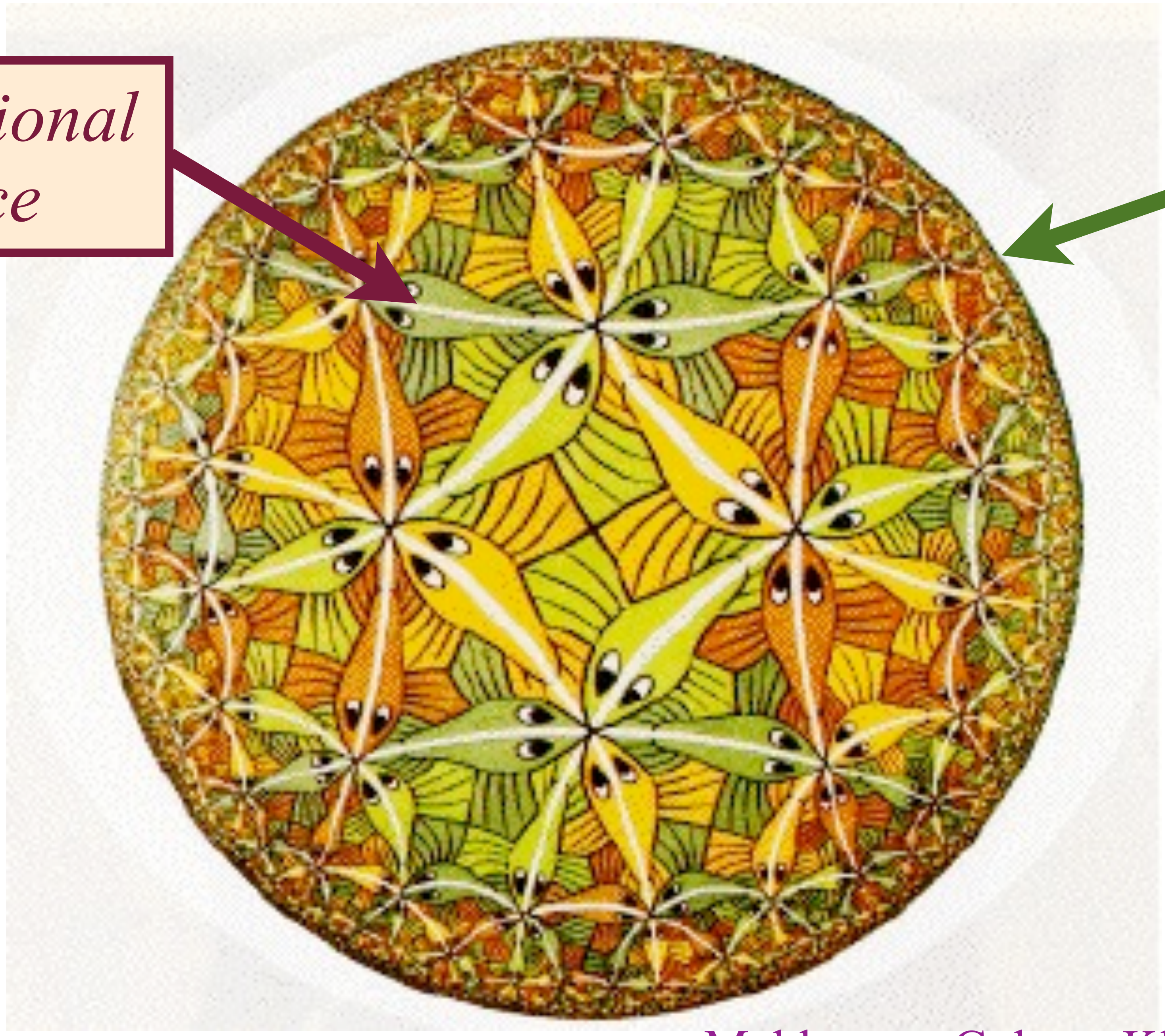

Maldacena, Gubser, Klebanov, Polyakov, Witten

AdS/CFT correspondence

The quantum theory of a black hole in a 3+1-dimensional negatively curved AdS universe is holographically represented by a CFT (the theory of a quantum critical point) in 2+1 dimensions

3+1 dimensional AdS space

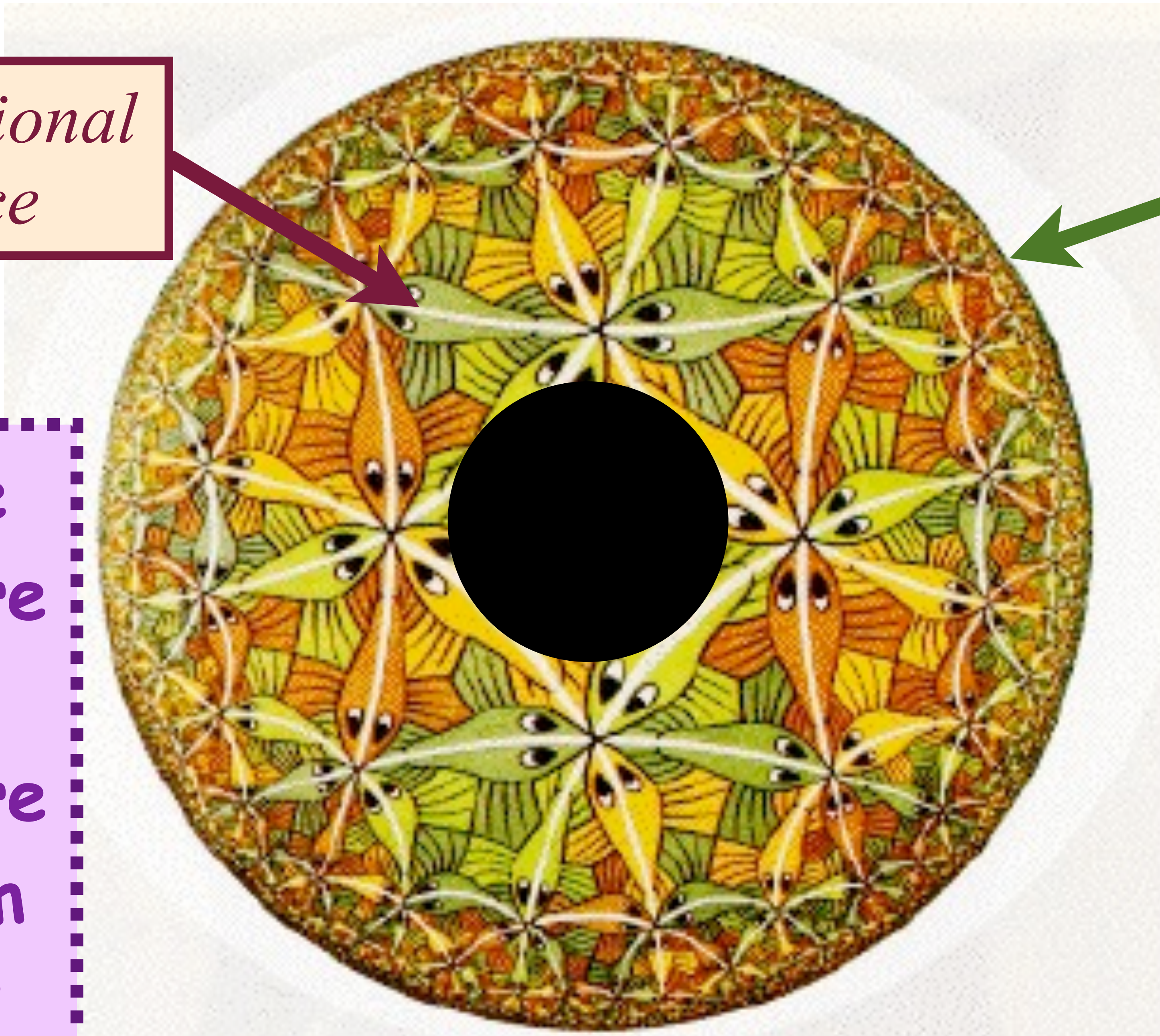

Quantum criticality in 2+1 dimensions

Black hole temperature = temperature of quantum criticality

Maldacena, Gubser, Klebanov, Polyakov, Witten

AdS/CFT correspondence

The quantum theory of a black hole in a 3+1-dimensional negatively curved AdS universe is holographically represented by a CFT (the theory of a quantum critical point) in 2+1 dimensions

3+1 dimensional AdS space

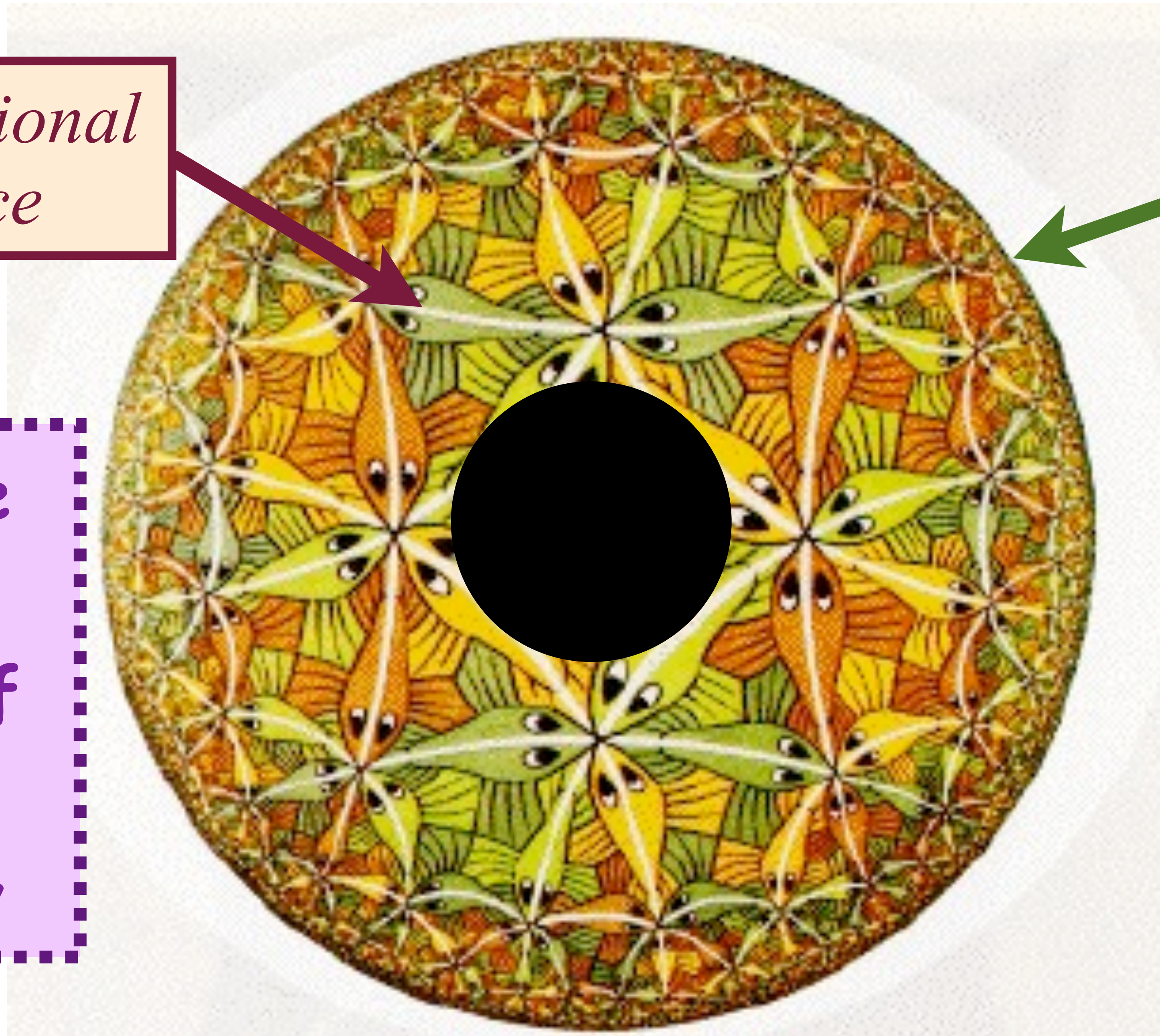

Quantum criticality in 2+1 dimensions

Black hole entropy = entropy of quantum criticality

Strominger, Vafa

AdS/CFT correspondence

The quantum theory of a black hole in a 3+1-dimensional negatively curved AdS universe is holographically represented by a CFT (the theory of a quantum critical point) in 2+1 dimensions

3+1 dimensional AdS space

Quantum criticality in 2+1 dimensions

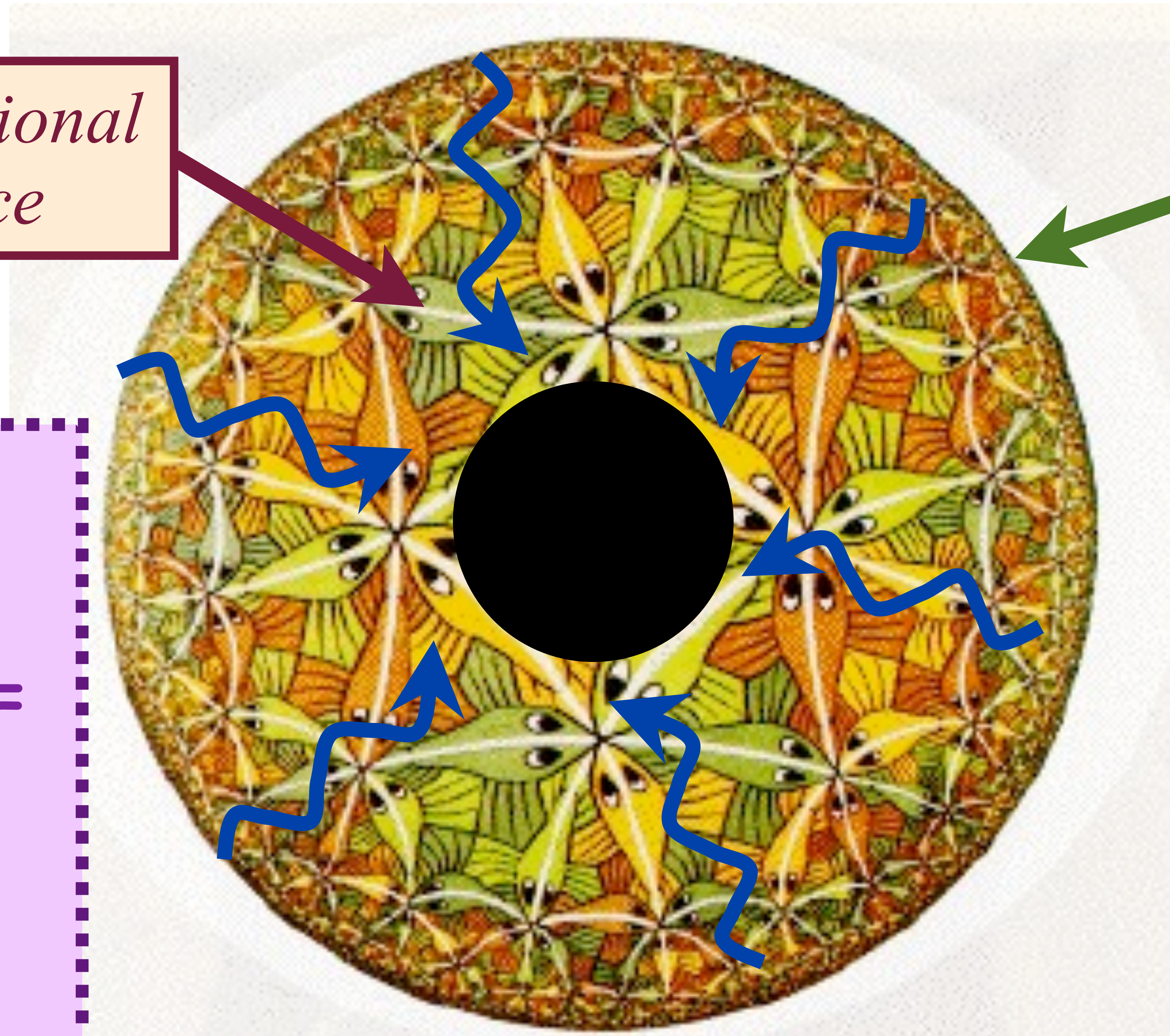

Quantum critical dynamics = waves in curved space

Maldacena, Gubser, Klebanov, Polyakov, Witten

AdS/CFT correspondence

The quantum theory of a black hole in a 3+1-dimensional negatively curved AdS universe is holographically represented by a CFT (the theory of a quantum critical point) in 2+1 dimensions

3+1 dimensional AdS space

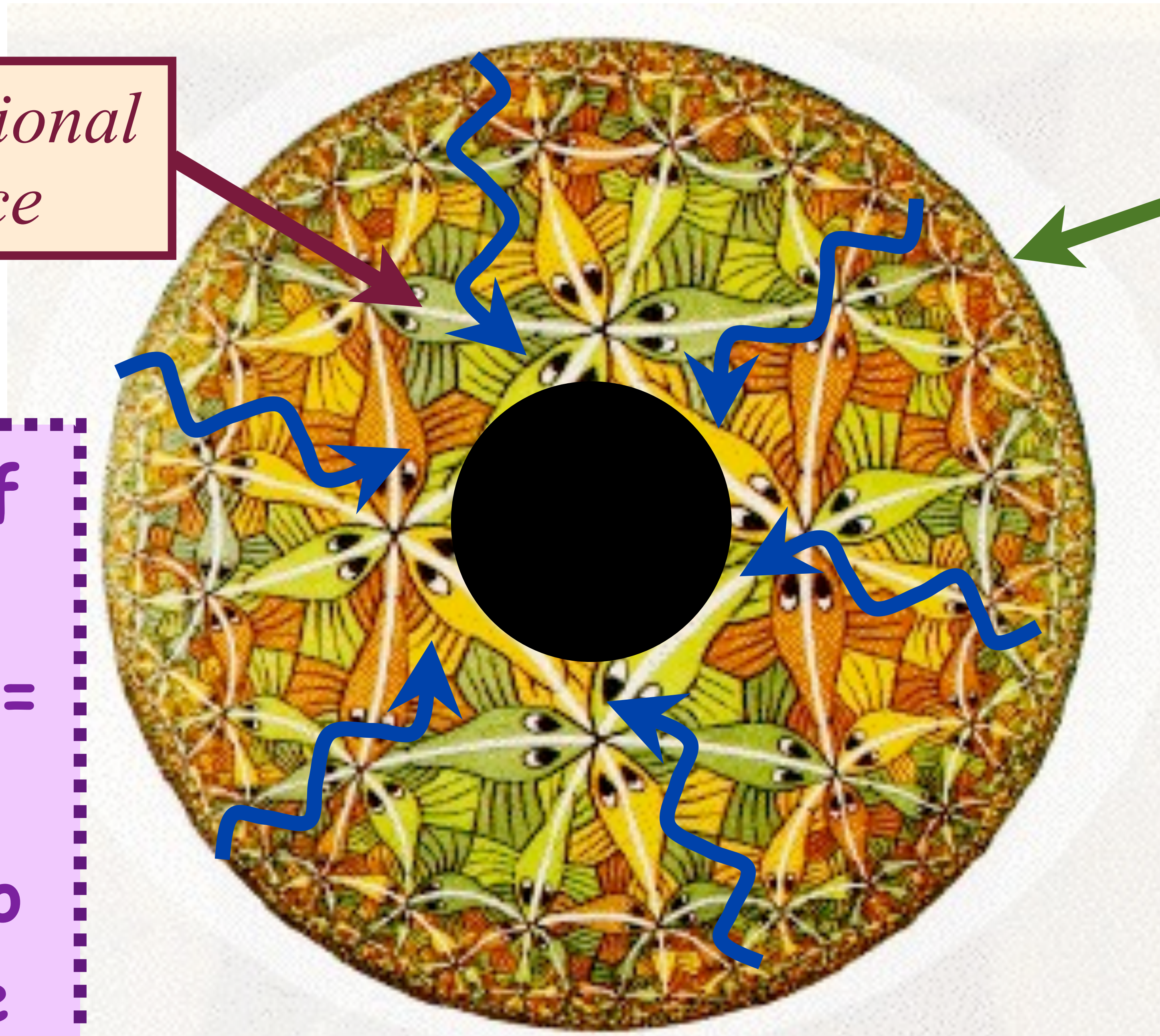

Quantum criticality in 2+1 dimensions

Friction of quantum criticality = waves falling into black hole

Kovtun, Policastro, Son

Magneto-thermo-electric dynamics of graphene obtained using insights from the dynamics of a Reissner-Nordstorm black hole in AdS_4.

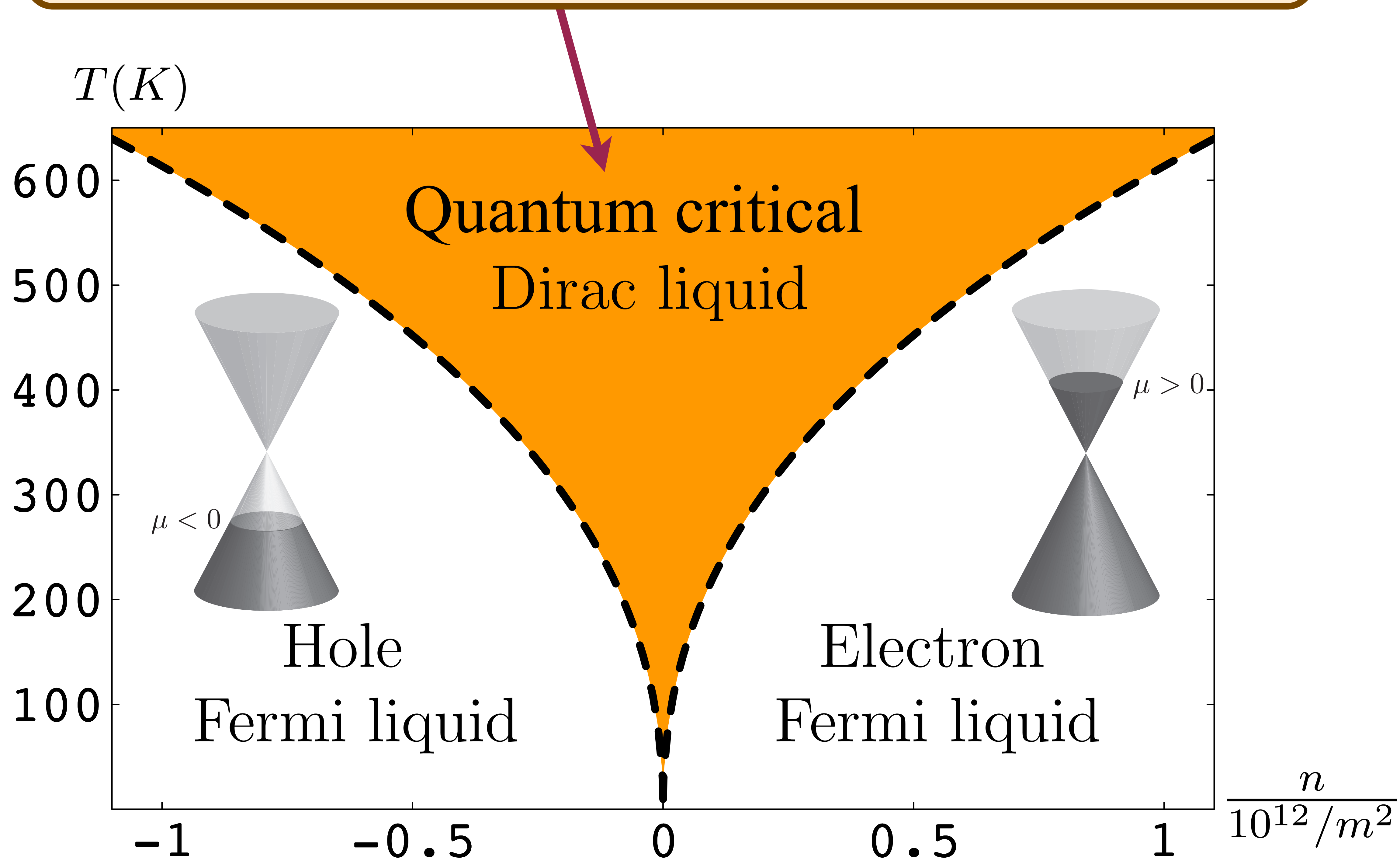

S.A. Hartnoll, P.K. Kovtun, M. Müller, and S. Sachdev, *Phys. Rev.* B **76** 144502 (2007)

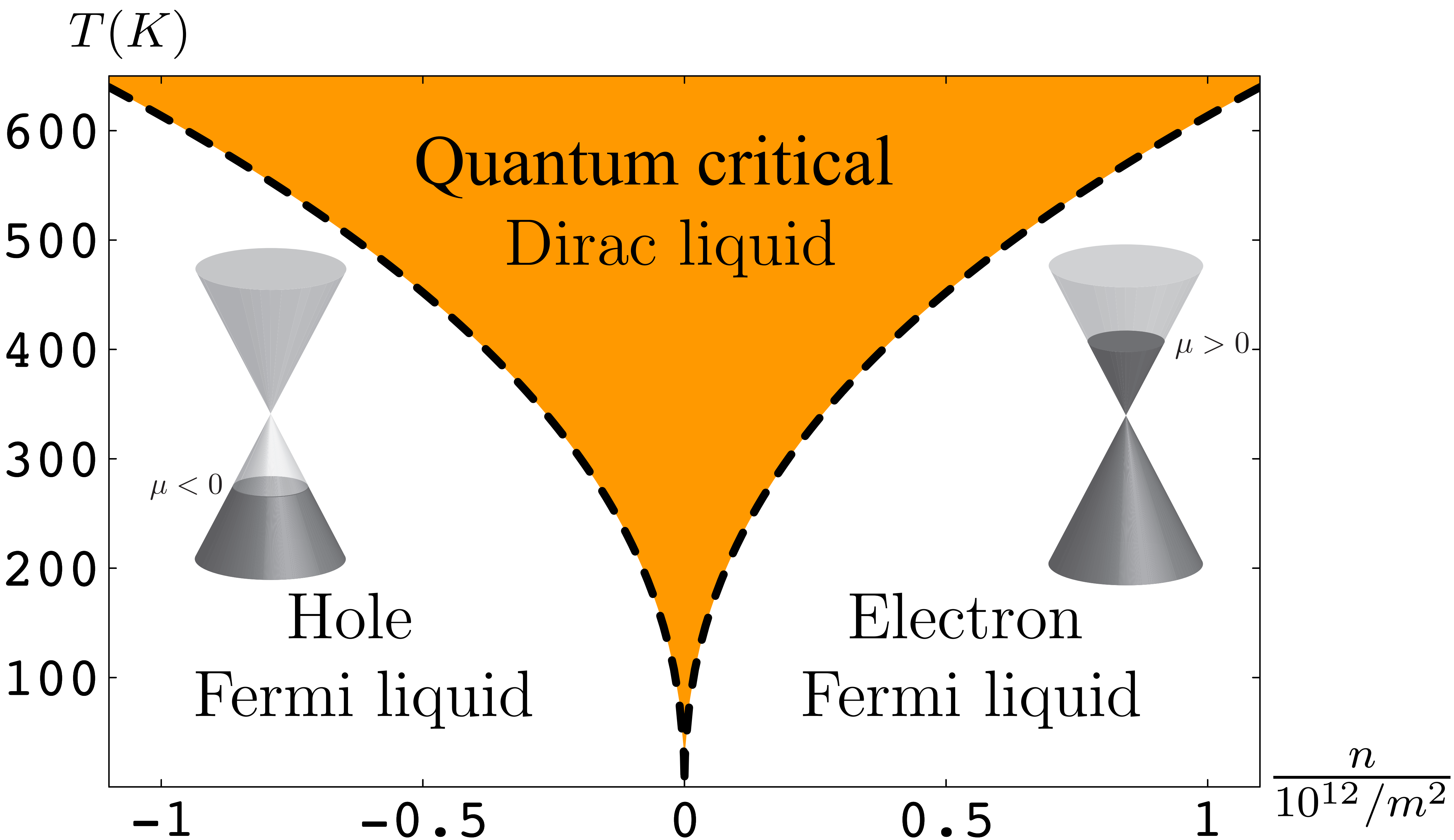

S.A. Hartnoll, P.K. Kovtun, M. Müller, and S. Sachdev, *Phys. Rev.* B **76** 144502 (2007)

At low T graphene is a Fermi liquid

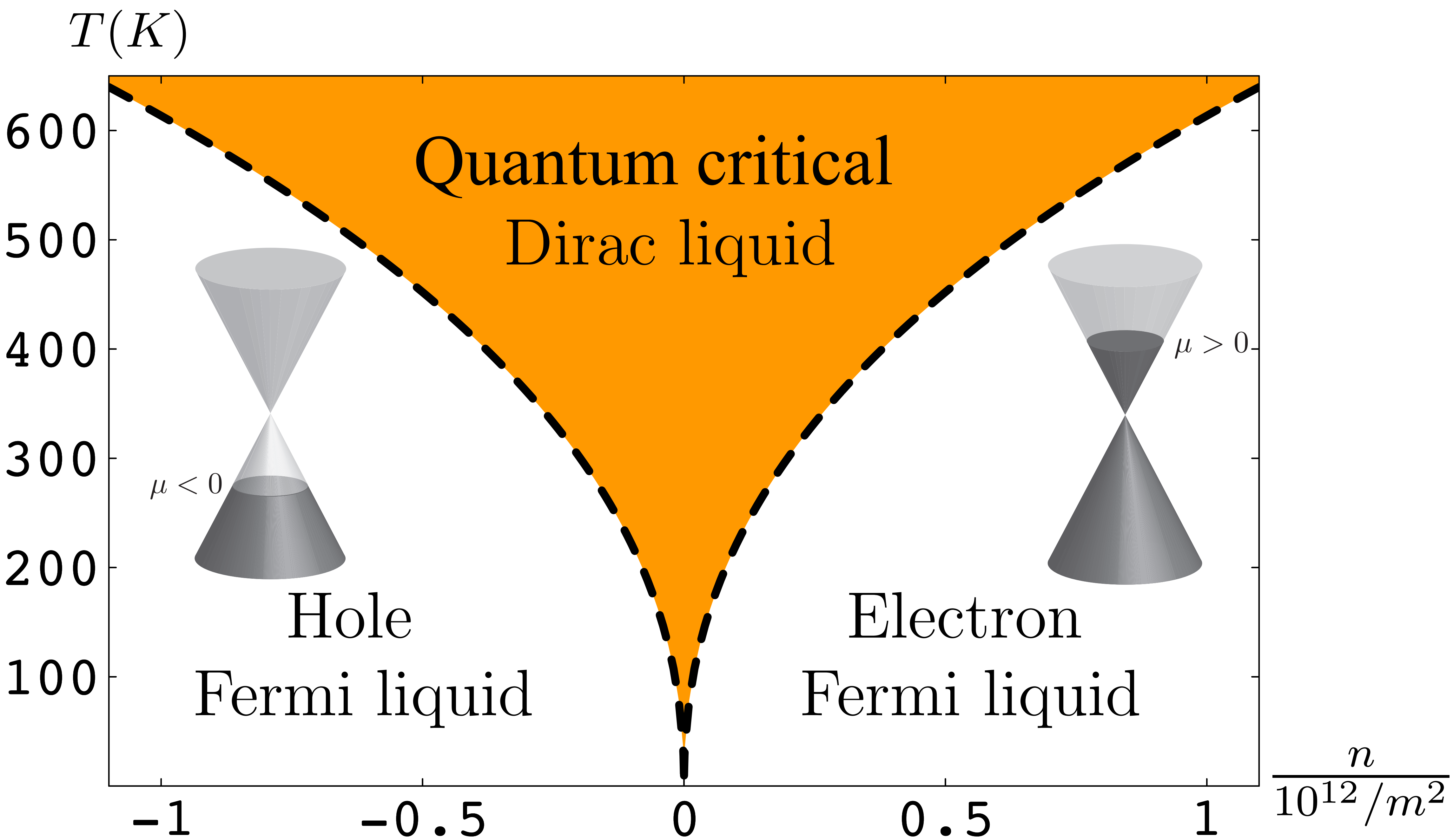

S.A. Hartnoll, P.K. Kovtun, M. Müller, and S. Sachdev, *Phys. Rev.* B **76** 144502 (2007)

At low T graphene is a Fermi liquid

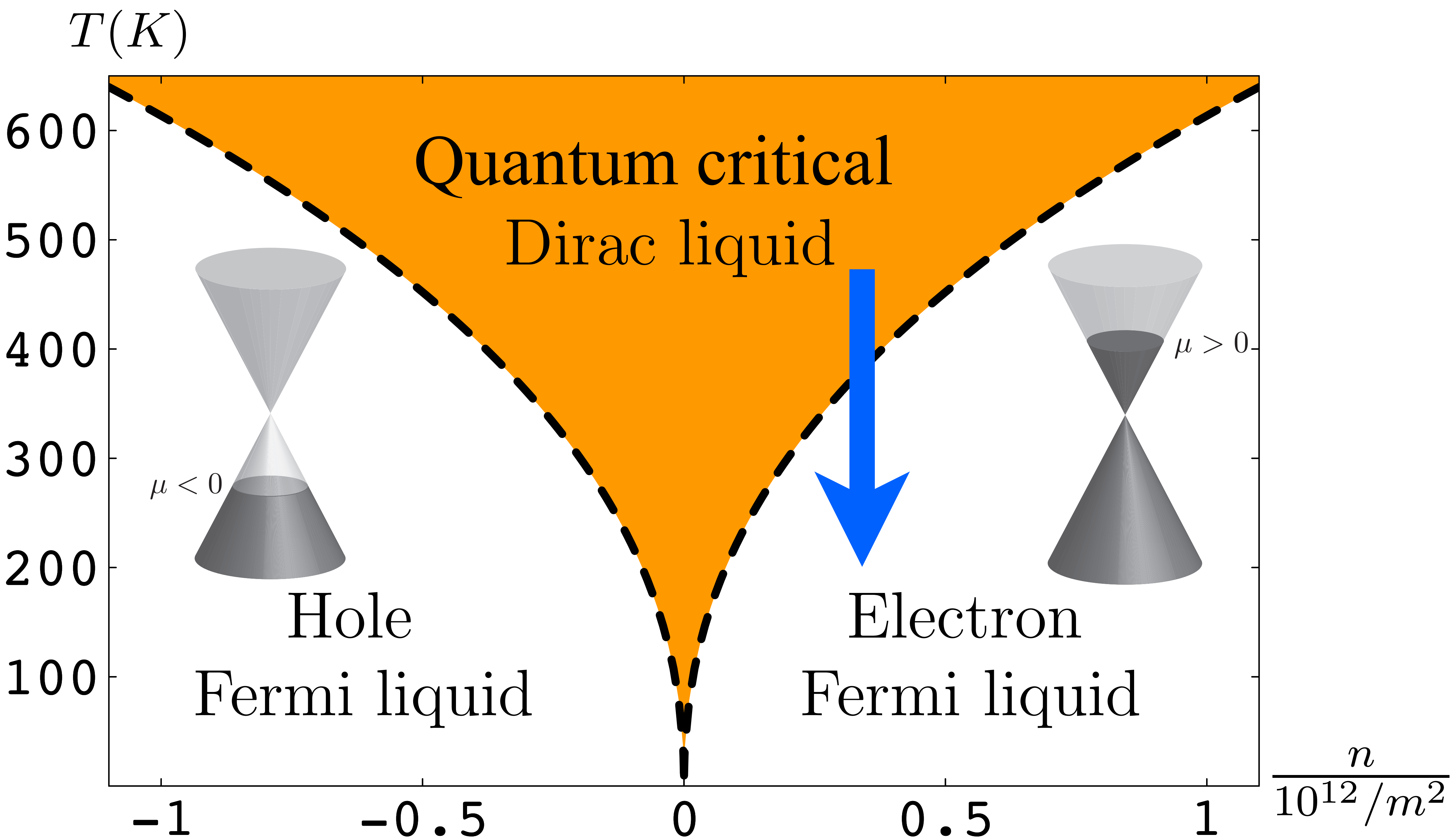

S.A. Hartnoll, P.K. Kovtun, M. Müller, and S. Sachdev, *Phys. Rev.* B **76** 144502 (2007)

At low T graphene is a Fermi liquid

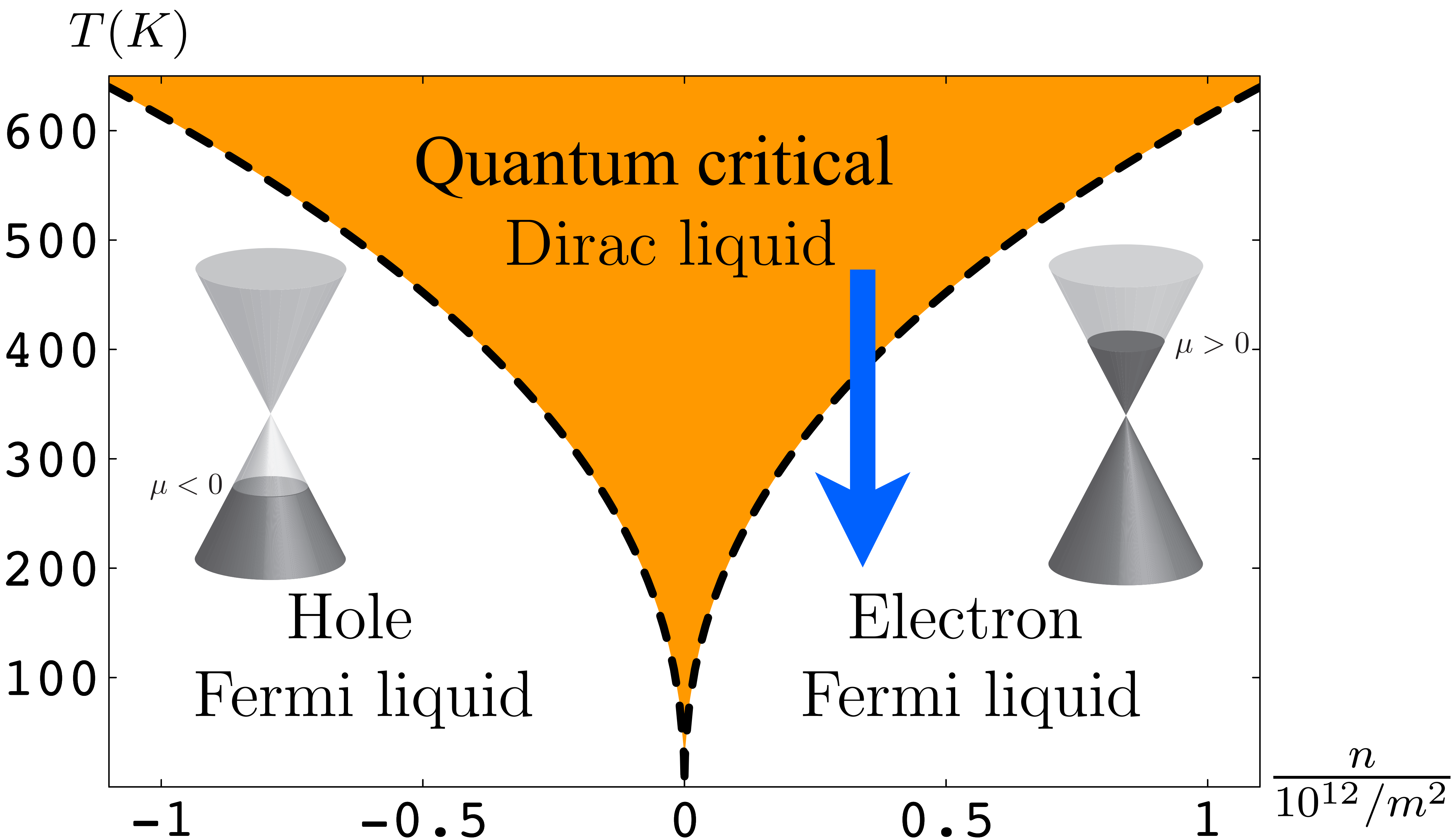

S.A. Hartnoll, P.K. Kovtun, M. Müller, and S. Sachdev, *Phys. Rev.* B **76** 144502 (2007)

At low T graphene is a Fermi liquid

What is the dual of the black hole theory at low T ?

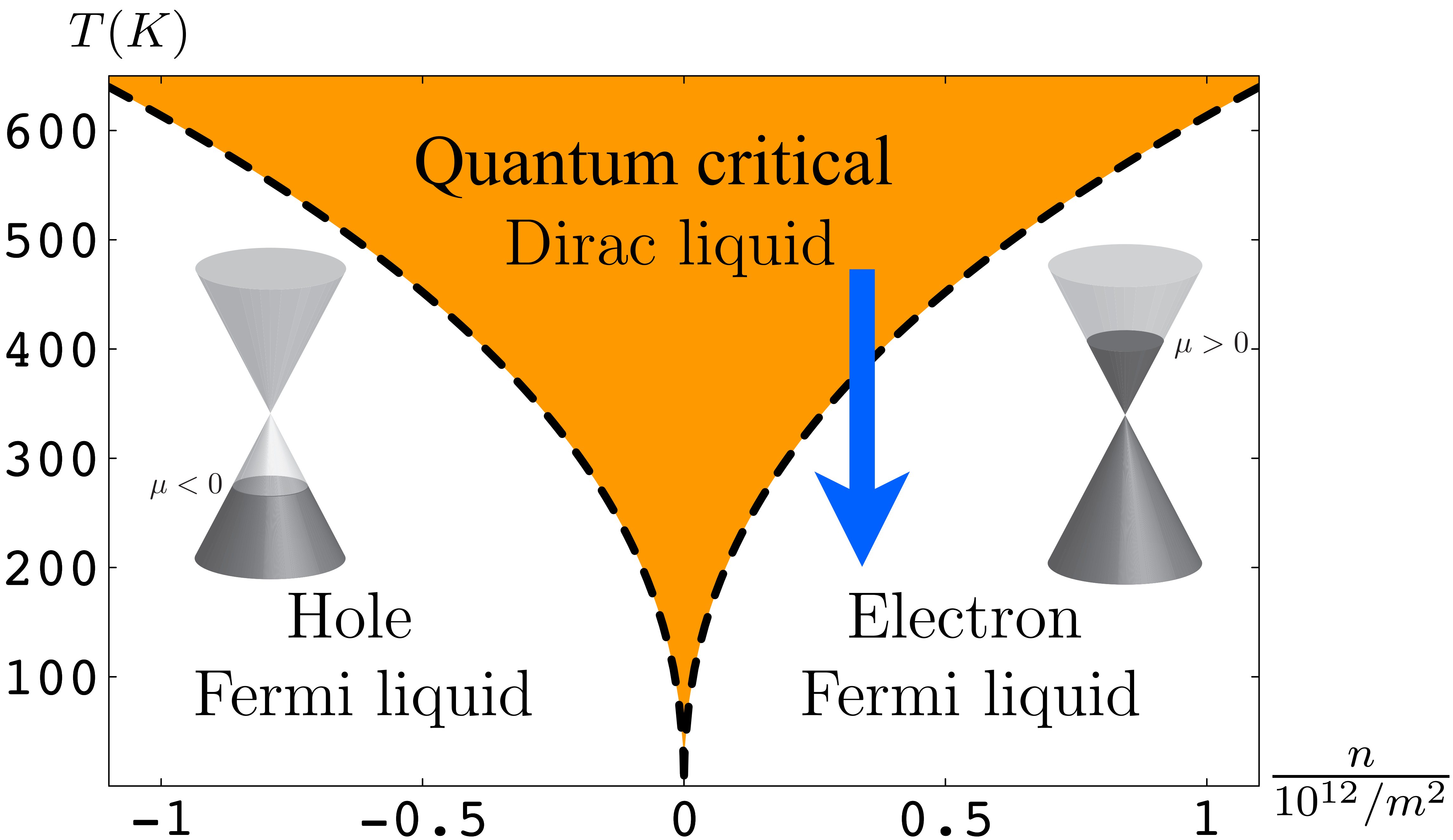

S.A. Hartnoll, P.K. Kovtun, M. Müller, and S. Sachdev, *Phys. Rev.* B **76** 144502 (2007)

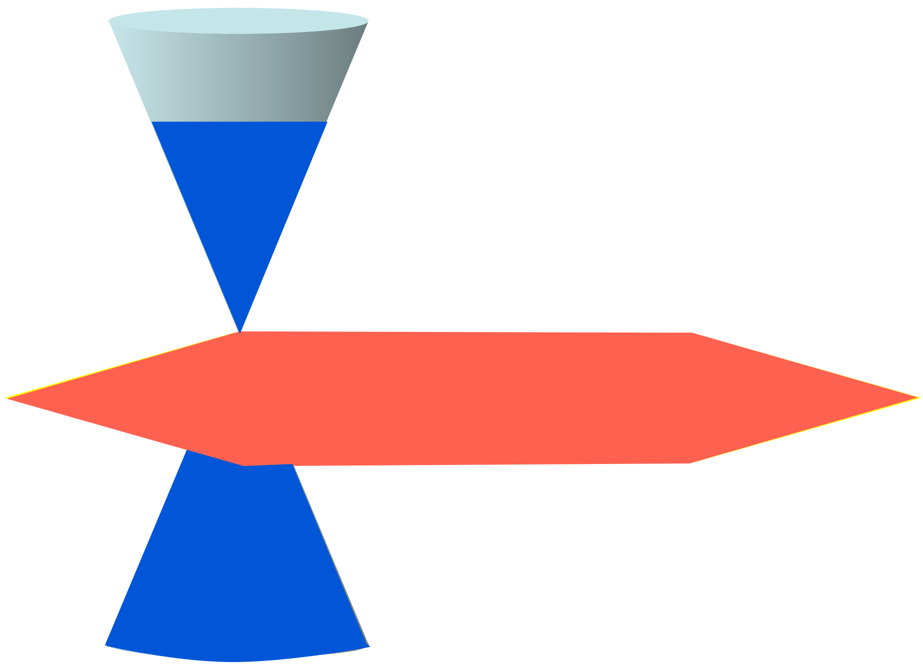

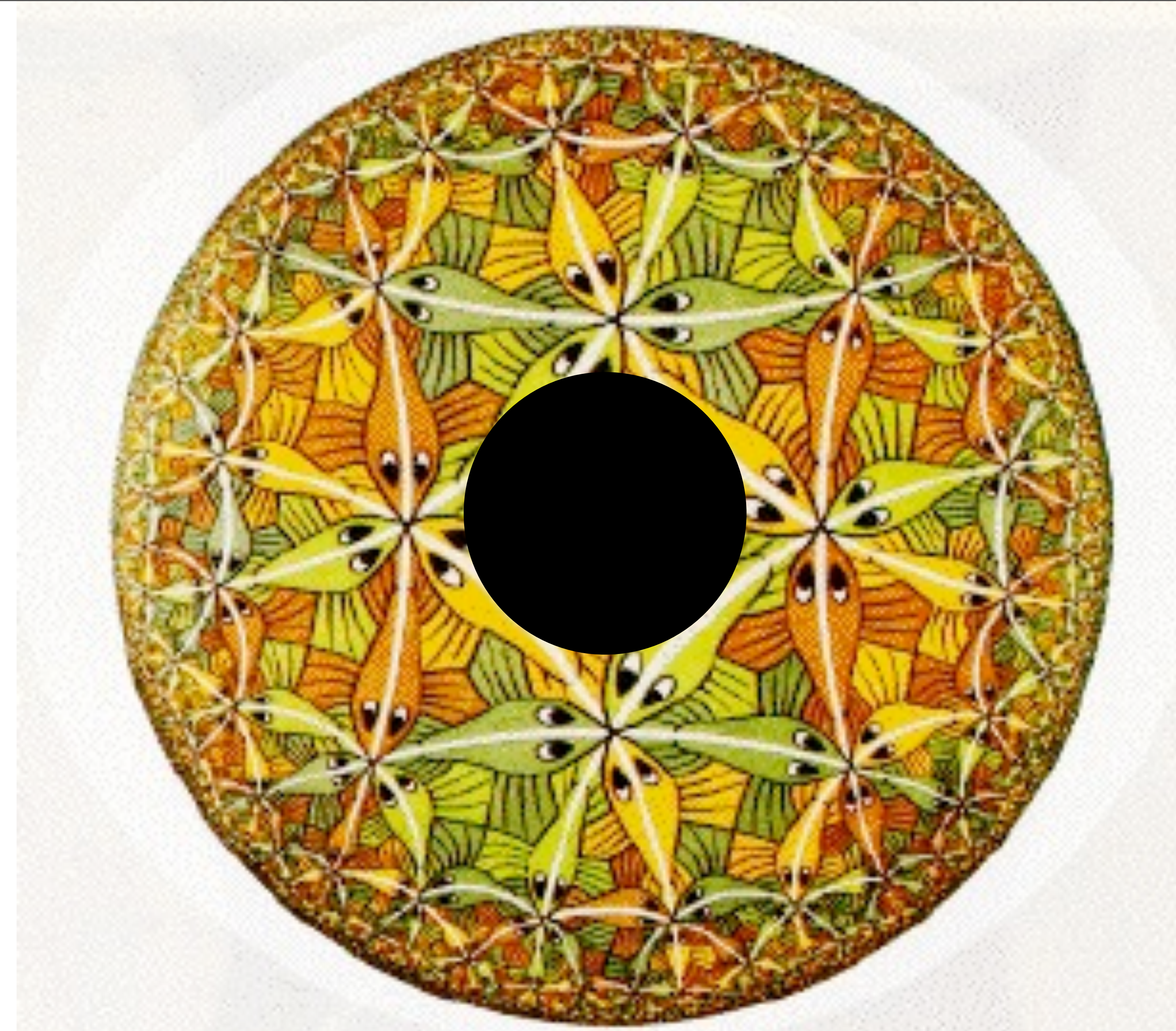

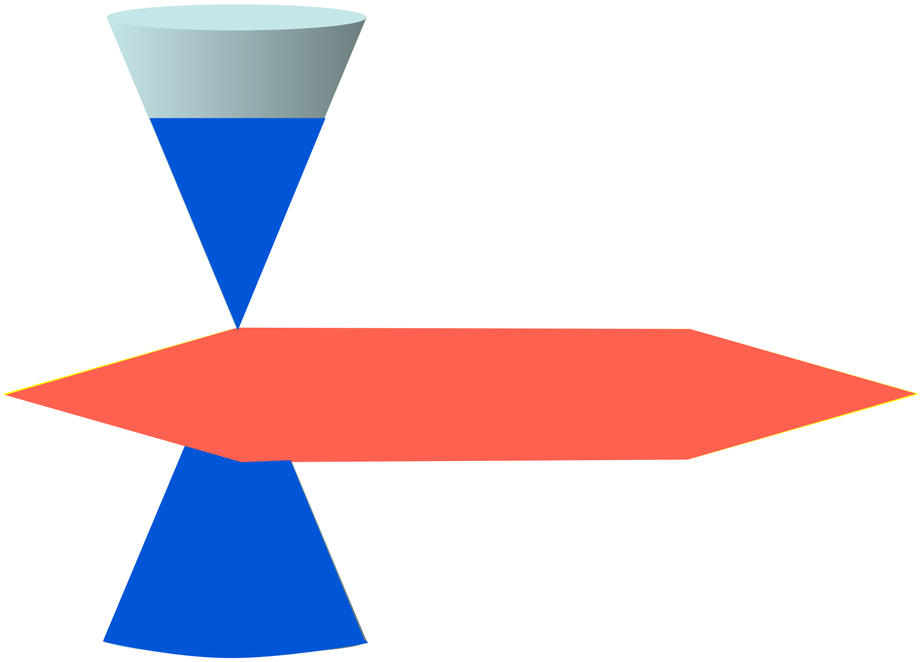

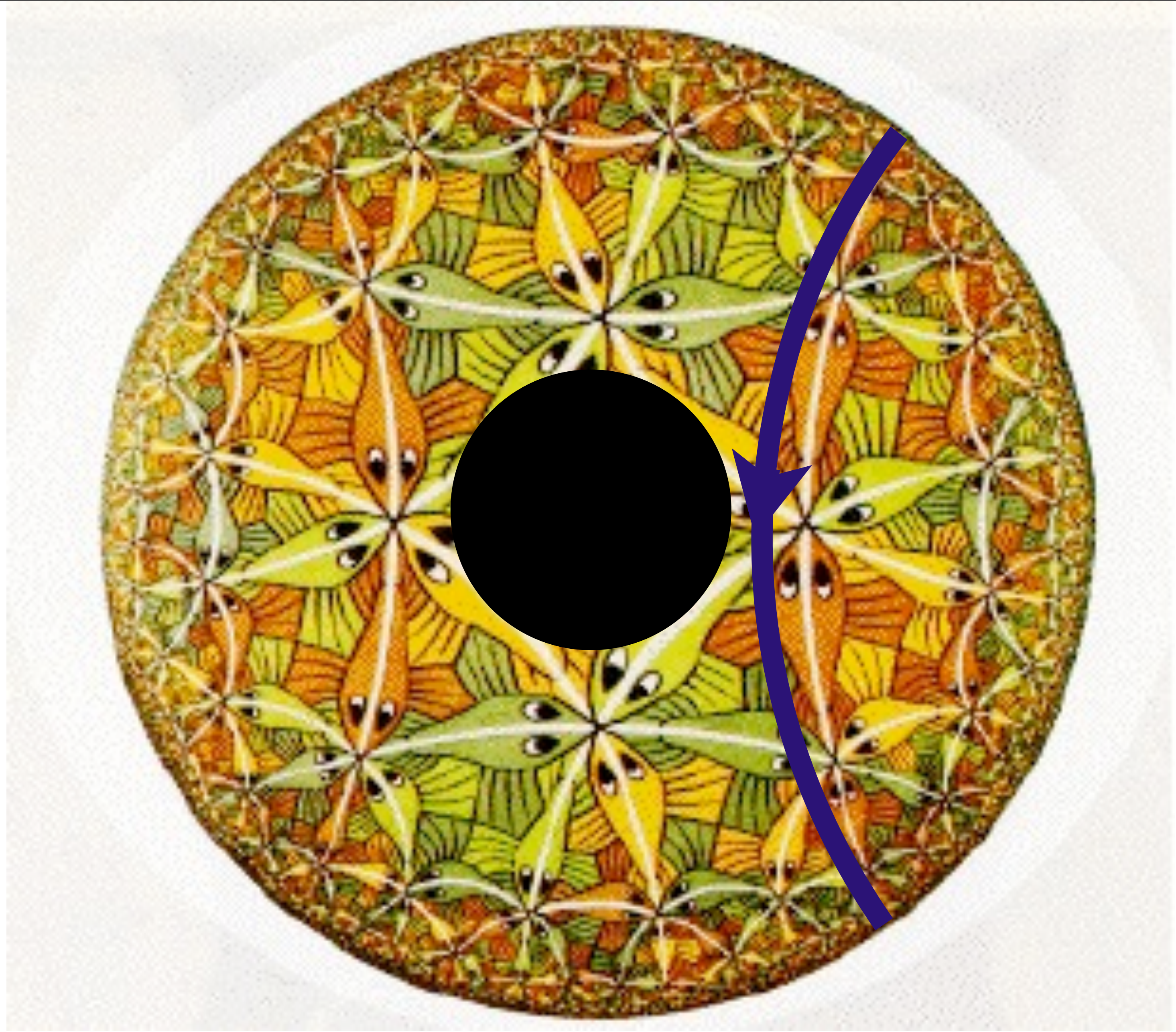

Examine free energy and Green's function of a probe particle

T. Faulkner, H. Liu, J. McGreevy, and D. Vegh, arXiv:0907.2694
F. Denef, S. Hartnoll, and S. Sachdev, arXiv:0908.1788

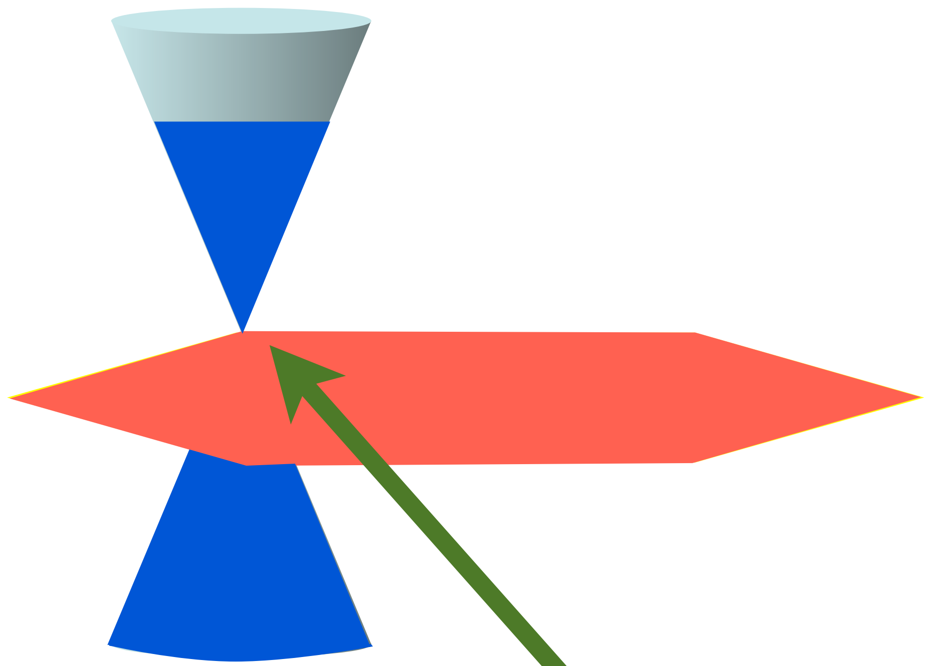

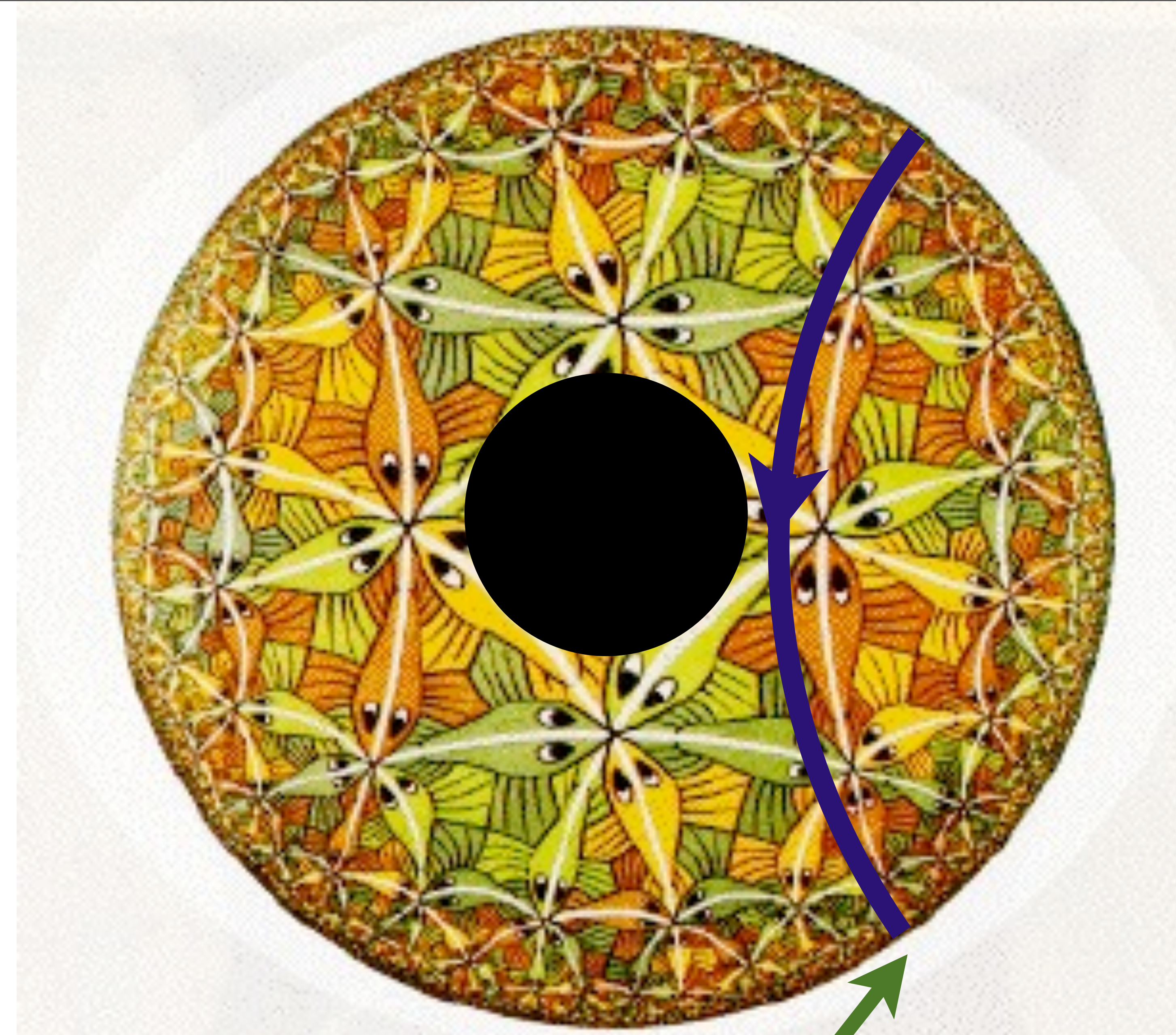

Short time behavior depends upon conformal AdS_4 geometry near boundary

T. Faulkner, H. Liu, J. McGreevy, and D. Vegh, arXiv:0907.2694
F. Denef, S. Hartnoll, and S. Sachdev, arXiv:0908.1788

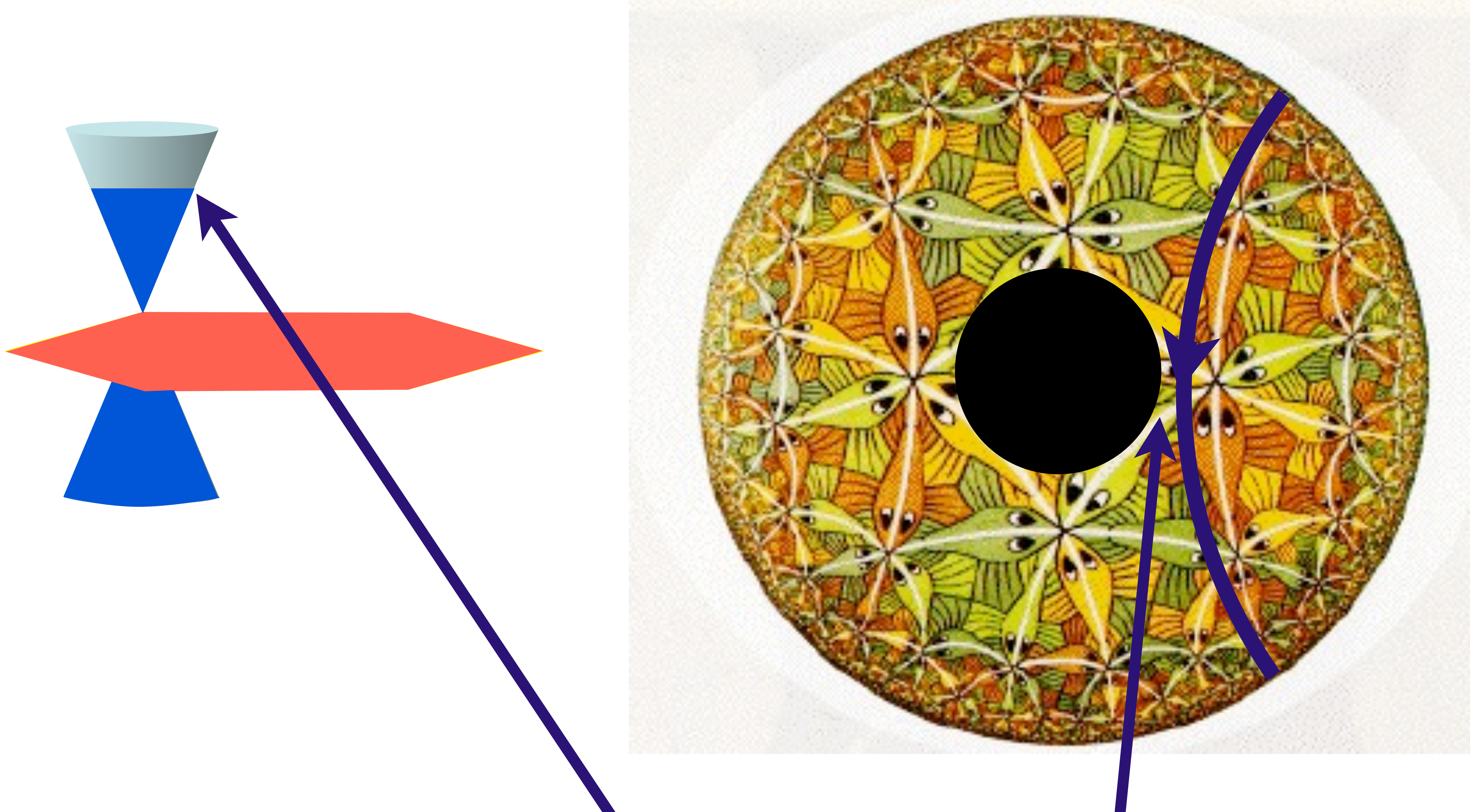

Long time behavior depends upon near-horizon geometry of black hole

T. Faulkner, H. Liu, J. McGreevy, and D. Vegh, arXiv:0907.2694
F. Denef, S. Hartnoll, and S. Sachdev, arXiv:0908.1788

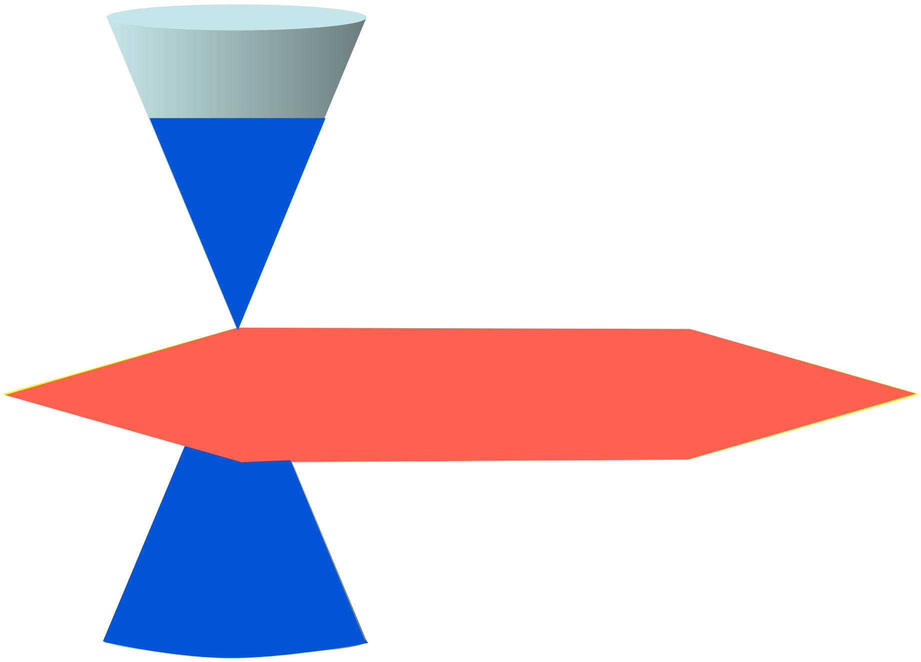

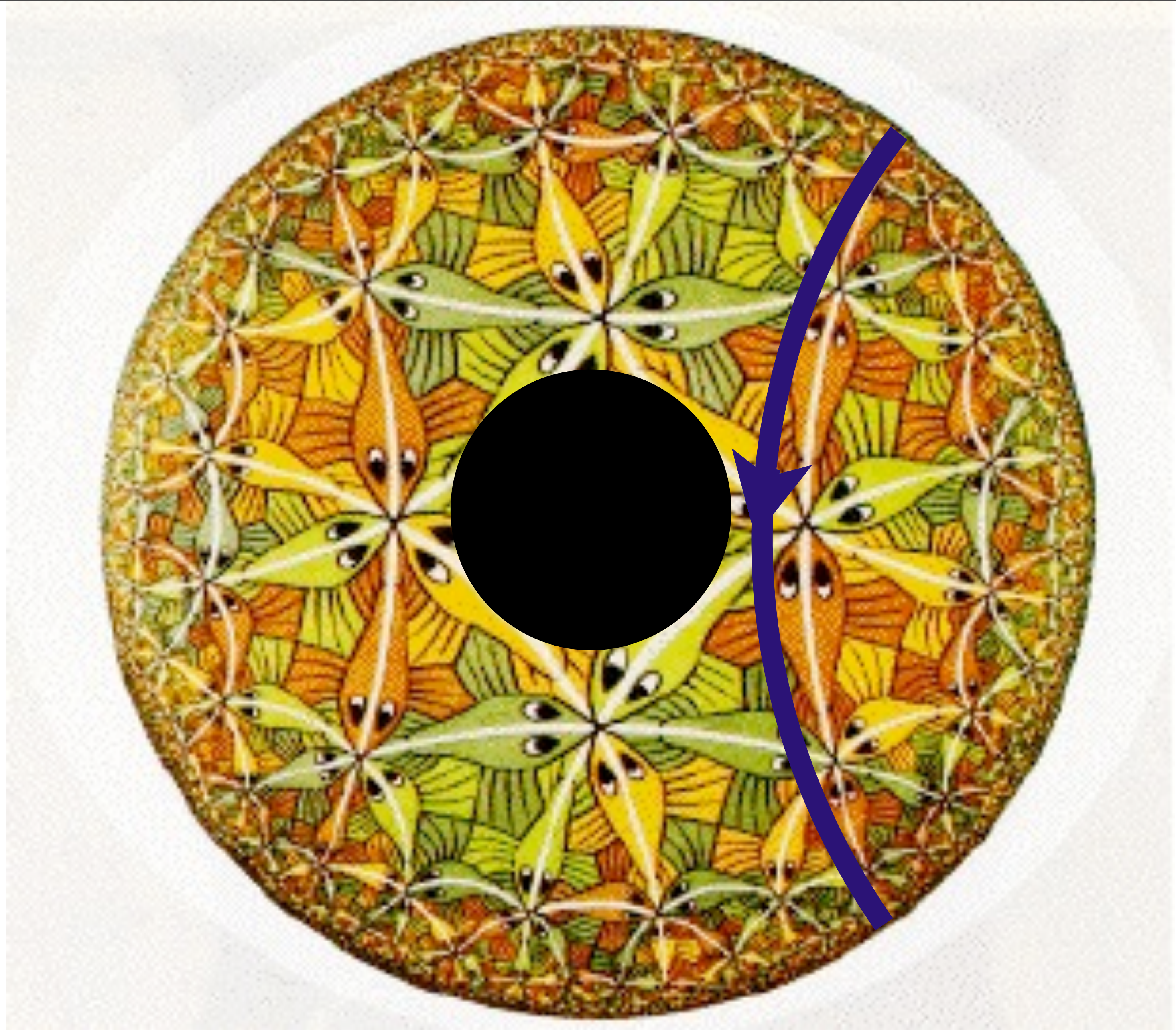

Radial direction of gravity theory is measure of energy scale in CFT

T. Faulkner, H. Liu, J. McGreevy, and D. Vegh, arXiv:0907.2694
F. Denef, S. Hartnoll, and S. Sachdev, arXiv:0908.1788

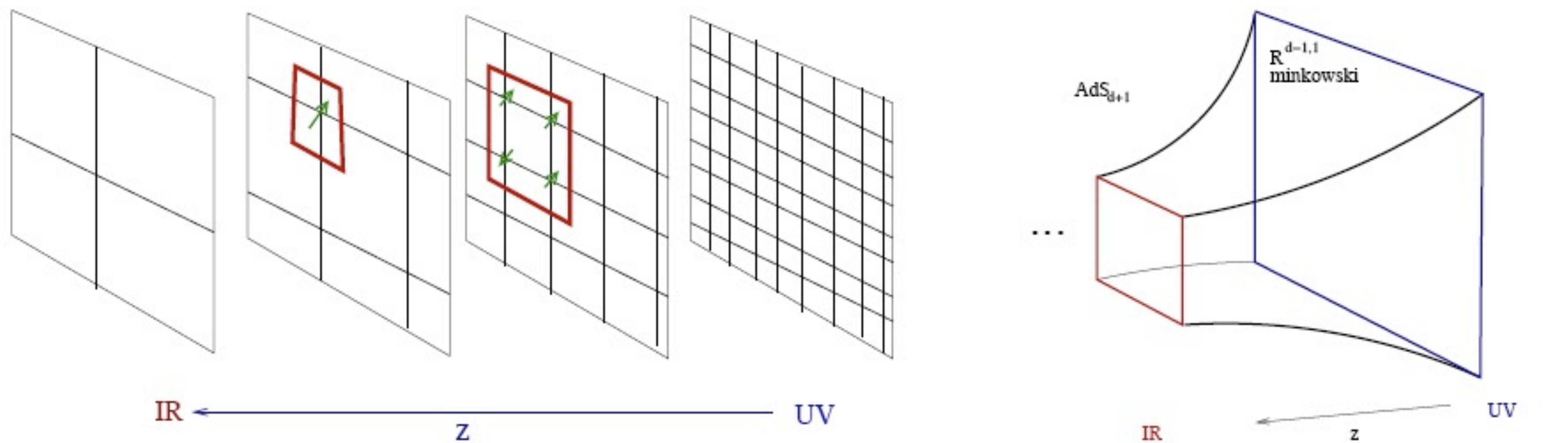

Figure 1: The extra ('radial') dimension of the bulk is the resolution scale of the field theory. The left figure indicates a series of block spin transformations labelled by a parameter z. The right figure is a cartoon of AdS space, which organizes the field theory information in the same way. In this sense, the bulk picture is a hologram: excitations with different wavelengths get put in different places in the bulk image.

J. McGreevy, arXiv0909.0518

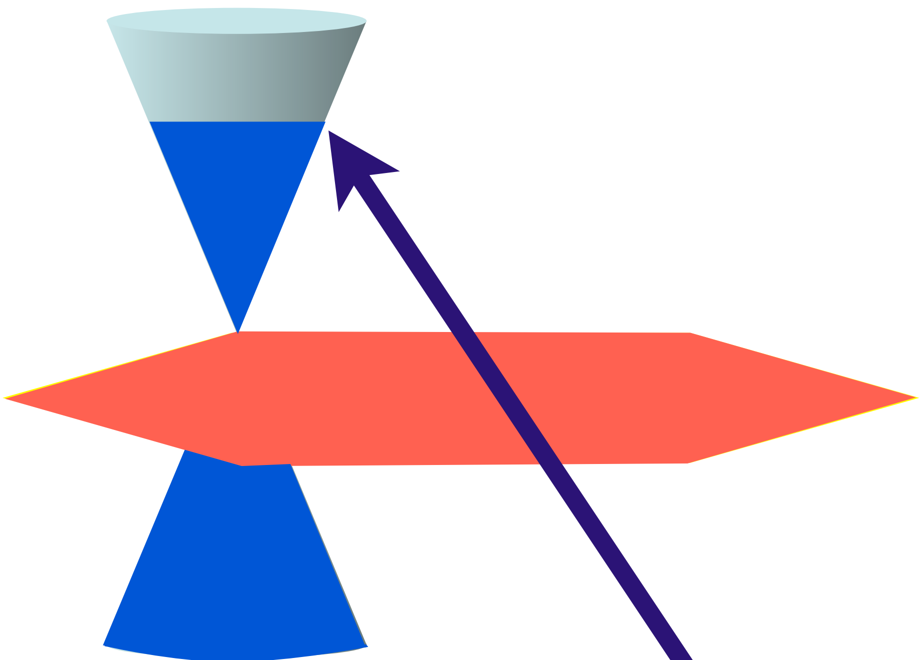

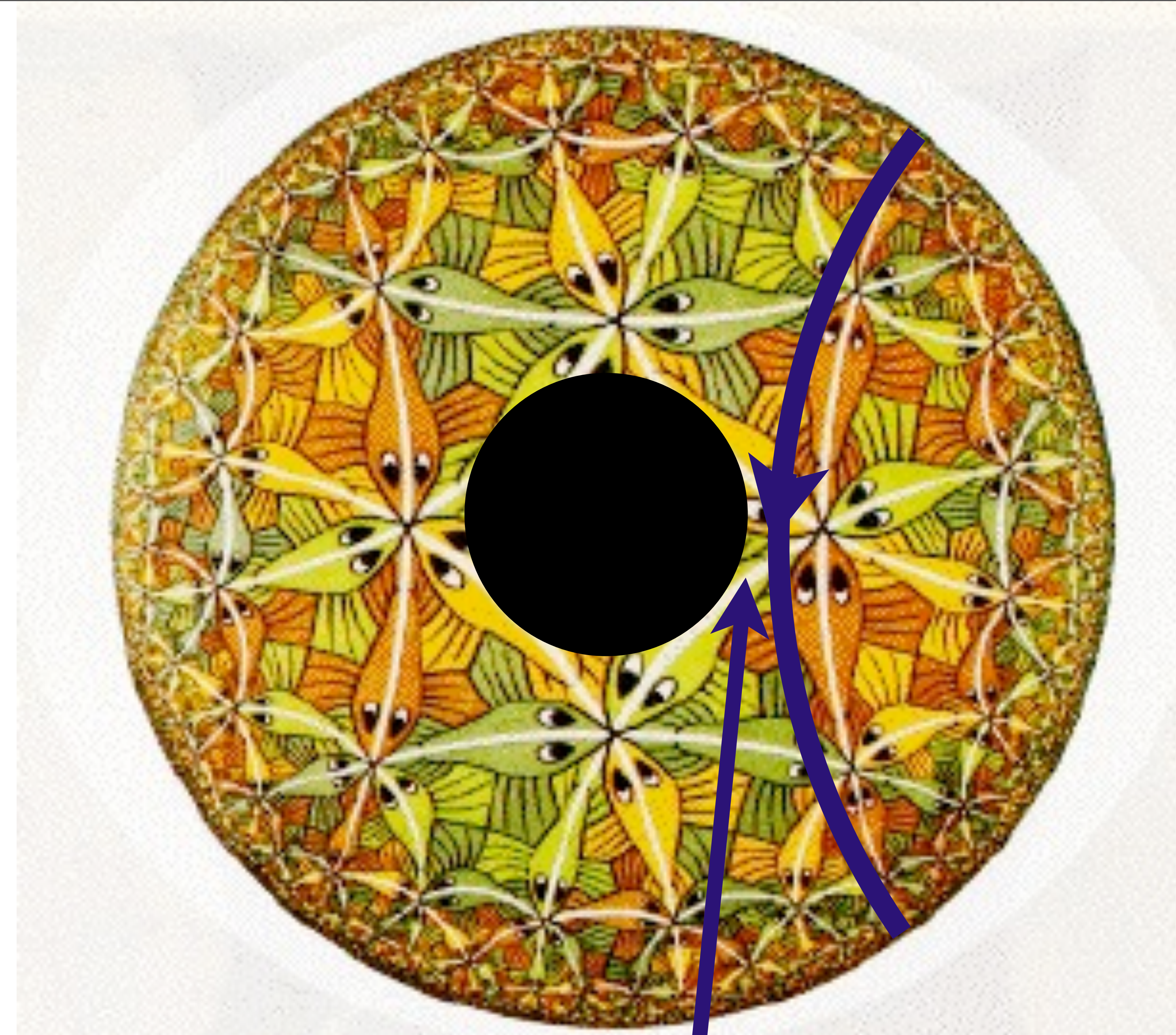

Infrared physics of Fermi surface is linked to the near horizon AdS_2 geometry of Reissner-Nordstrom black hole

T. Faulkner, H. Liu, J. McGreevy, and D. Vegh, arXiv:0907.2694

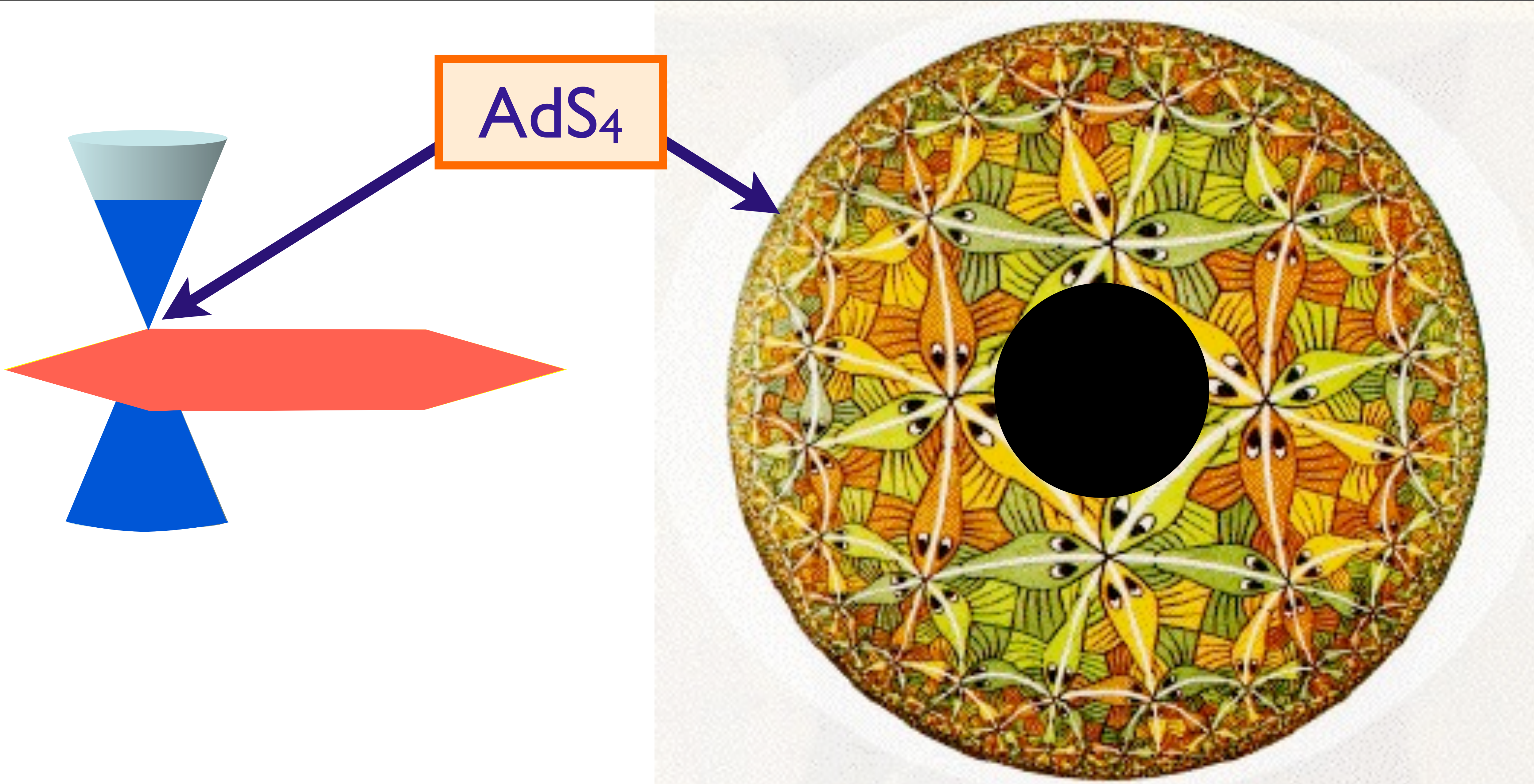

Geometric interpretation of RG flow

T. Faulkner, H. Liu, J. McGreevy, and D. Vegh, arXiv:0907.2694

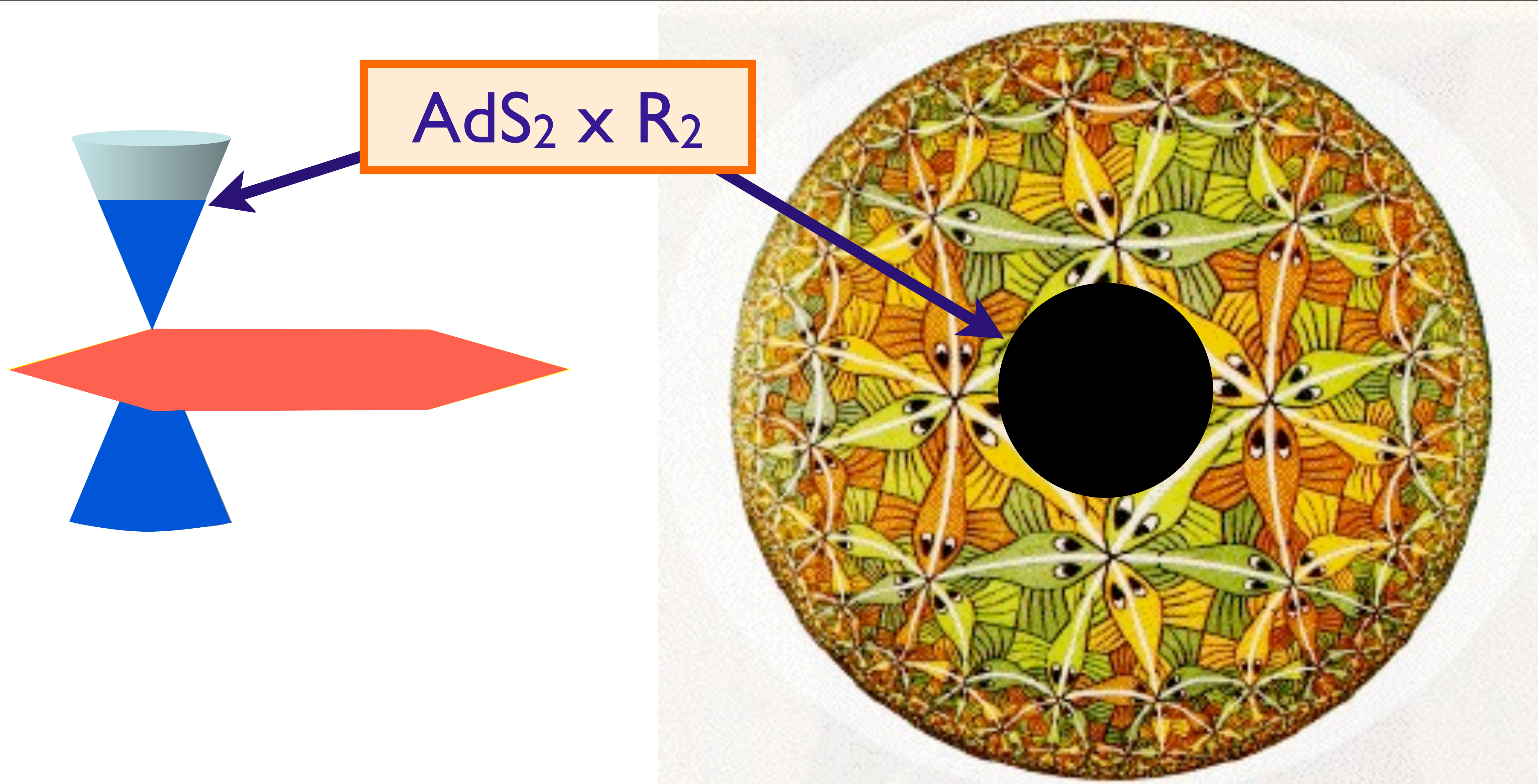

Geometric interpretation of RG flow

T. Faulkner, H. Liu, J. McGreevy, and D. Vegh, arXiv:0907.2694

Green's function of a fermion

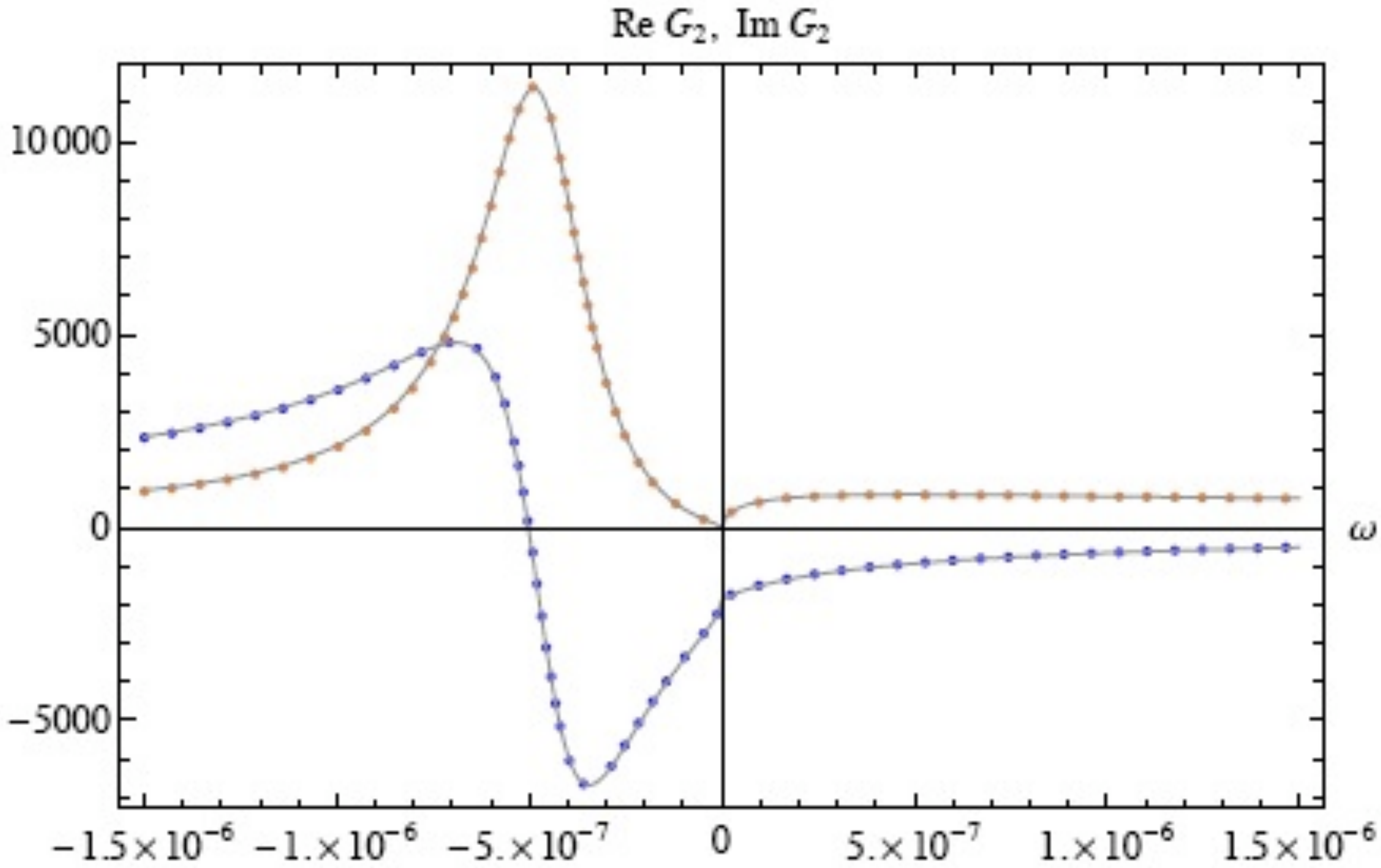

T. Faulkner, H. Liu, J. McGreevy, and D. Vegh, arXiv:0907.2694

$$G(k,\omega) \approx \frac{1}{\omega - v_F(k-k_F) - i\omega^{\theta(k)}}$$

See also S.-S. Lee, *Phys. Rev. D* **79**, 086006 (2009);
M. Cubrovic, J. Zaanen, and K. Schalm, *Science* **325**, 439 (2009);
F. Denef, S. A. Hartnoll, and S. Sachdev, *Phys. Rev. D* **80**, 126016 (2009)

Green's function of a fermion

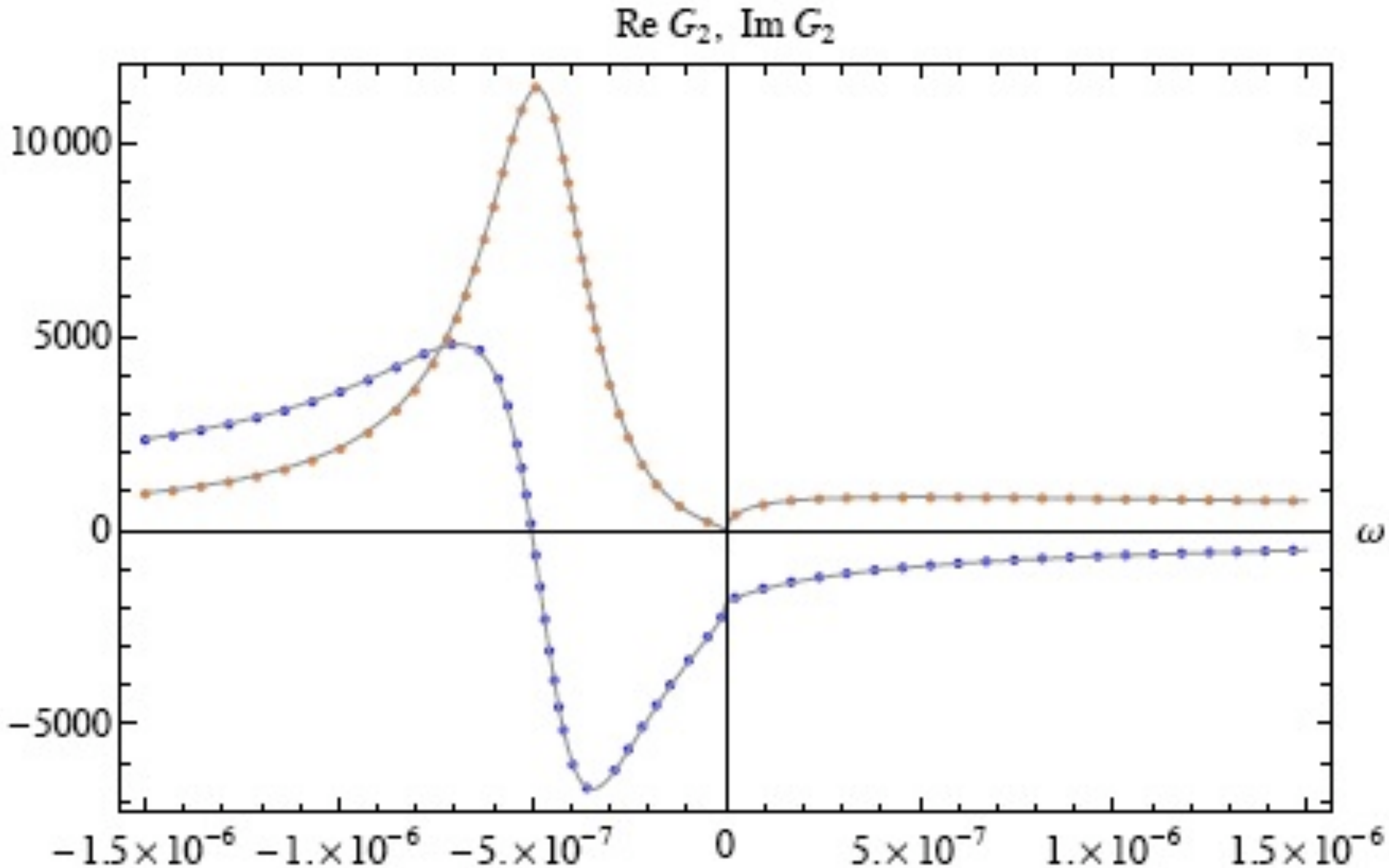

T. Faulkner, H. Liu, J. McGreevy, and D. Vegh, arXiv:0907.2694

$$G(k,\omega) \approx \frac{1}{\omega - v_F(k-k_F) - i\omega^{\theta(k)}}$$

Similar to our theory of the singular Fermi surface near the Ising-nematic quantum critical point

Conclusions

Identified quantum criticality in cuprate superconductors with a critical point at optimal doping associated with onset of spin density wave order in a metal

Elusive optimal doping quantum critical point has been "hiding in plain sight".

It is shifted to lower doping by the onset of superconductivity

Conclusions

Theories for the onset of spin density wave and Ising-nematic order in metals are *strongly* coupled in two dimensions